Delineation of molecular mechanisms of intestinal calcium absorption during postnatal development

by

Megan Rachele Beggs

A thesis submitted in partial fulfillment of the requirements for the degree of

Doctor of Philosophy

Department of Physiology
University of Alberta

Abstract

Infants and children must maintain a positive calcium balance for appropriate growth. Evidence suggests that adaptations in intestinal absorption of calcium are the major determinant of this net balance. However, the molecular details of the pathways mediating this increased absorption at a young age and in different segments have not been delineated. The aim of this thesis work was, therefore, to delineate the molecular details of intestinal absorption contributing to a positive calcium balance during postnatal development. Using mice from birth through adult ages, we initially examined gene expression and protein abundance of known contributors to calcium absorption pathways in the duodenum, jejunum, and ileum of the small intestine as well as the proximal colon. The results of these studies implicated weaning as an age of alterations in the expression of these pathways. We, therefore, employed *ex vivo* and *in vitro* Ussing chamber functional studies, micro-CT of bones and gene expression to test our specific hypotheses that specific patterns of intestinal absorption maximize uptake of calcium during postnatal development. Transient receptor potential vanilloid 6 (TRPV6) mediated transcellular calcium absorption was only observed after weaning in the duodenum. However, we identified transcellular calcium absorption mediated by TRPV6 and $Ca_v1.3$ across the jejunum and nifedipine inhibitable absorption across the ileum in suckling mice which was absent after weaning. We also observed 2-fold greater intestinal calcium permeability, which contributed increased paracellular calcium absorption across the jejunum and ileum in the suckling mice. This permeability is conferred by increased claudin-2 expression in young animals, which is the result of upregulation by epidermal growth factor contained in breast milk.

Despite identifying significant transcellular calcium absorption and paracellular calcium permeability in the proximal colon of older animals, as has been previously reported, our results did not implicate these pathways in younger animals. Specifically, the genetic or

pharmacological loss of TRPV6, L-type calcium channels, claudin-2 and claudin-12 did not alter proximal colon calcium absorption or permeability. However, these studies led to our discovery that claudin-2 and claudin-12 form independent Ca^{2+} permeable pores in the proximal colon and proximal renal tubule. Loss of both of these claudins results in an inability to maintain a normal serum calcium level in adult mice, due to decreased calcium permeability across the colon, decreased net intestinal calcium absorption and decreased renal calcium reabsorption. These alterations in transepithelial calcium absorption contributed to reduced bone mineralization and to altered bone microarchitecture. Thus, this work highlights the role the colon plays in overall calcium balance.

This thesis has ultimately identified novel pathways mediating calcium absorption during postnatal development when requirements for this mineral are greatest and discovered a potential therapeutic modality for infants and adults at risk of poor bone mineralization.

Preface

This thesis is an original work by Megan Beggs. The research project, of which this thesis is a part, received research ethics approval from the University of Alberta Research Ethics Board, animal Project Name "The role of transport proteins in Epithelial Sodium, Bicarbonate and Calcium Transport and Breeding Colonies", AUP00000213 and human ethics project name "Regulation of intestinal calcium absorption by breast milk", Pro00100603.

Excerpts of chapter one have been published as Beggs MR, Alexander RT. "Intestinal absorption and renal reabsorption of calcium throughout postnatal development", *Exp Biol Med (Maywood)*, 2017 Apr;242(8):840-849. I was responsible for the first draft of this review paper and RTA was the supervisory author and was involved with concept formation and manuscript revisions.

Chapter two of this thesis has been published as Beggs MR, Lee JJ, Busch K, Raza A, Dimke H, Weissgerber P, Engel J, Flockerzi V, Alexander RT, "TRPV6 and Cav1.3 Mediate Distal Small Intestine Calcium Absorption Before Weaning", *Cell Mol Gastroenterol Hepatol*, 2019;8(4):625-642. I designed or contributed to the design with RTA to all experiments and performed or supervised learners in conducting experiments for figures 2.2, 2.3, 2.5, 2.6, 2.7, 2.9. I performed all data analysis and drafted the manuscript. JJL, KB, and AR also conducted experiments and contributed to data analysis; HD, PW, JE, VF, and RTA provided reagents; PW, JE, and VF bred and provided mice; and all authors approved the final version of the manuscript.

Chapter three of this thesis is prepared for submission to *Gastroenterology* as Megan R. Beggs, Kennedi Young, Allen Plain, Ahsan Raza, Justin J. Lee, Matthew Saurette, Petra Weissgerber, Veit Flockerzi, Henrik Dimke, R. Todd Alexander, "Epidermal growth factor in breast milk increases calcium permeability across murine small intestine via claudin-2". I designed or contributed to the design with RTA to all experiments and performed or supervised learners in conducting experiments for figures 3S.1, 3.1, gene expression in 3.2, 3.3, gene expression and immunoblots in 3.4, 3S.2, 3S.3, and 3.5 and tables 3.2, 3S.1 – 3S.9. I performed data analysis and drafted the manuscript.

Chapter four of this thesis is prepared for submission to *PNAS* as Megan R. Beggs, Kennedi Young, Wanling Pan, Debbie O'Neill, Matthew Saurette, Allein Plain, Juraj Rievaj, Michael R. Doschak, Emmanuelle Cordat, Henrik Dimke, R. Todd Alexander, "Claudin-2 or claudin -12 is required to maintain calcium homeostasis". I designed or contributed to the design with RTA to all experiments and performed or supervised learners in conducting experiments for figures 4S.1, functional studies in 4.1, 4.2, low calcium diet study in 4S.2, 4S.3, 4S.4, Ussing chamber studies in 4.4, and tables 4S.1 – 4S.5. I performed data analysis and drafted the manuscript.

Experiments in Appendix A were designed by myself and Dr. Alexander and performed by myself.

Acknowledgements

It might be appropriate to first acknowledge Mary-Ann McMaster who convinced Dr. Todd Alexander to consider taking on her clinical dietitian colleague as a PhD student. Todd, I am so glad you were convinced. I can truly say that I have enjoyed my PhD in your lab. Your support for my career goals has, quite literally, changed my life. You are so generous with your time while also allowing independent growth. Your style of mentorship builds confidence in students and lets them always feel supported and I hope to one day follow in your lead.

To everyone in Todd's lab, I could not have done this without you. Wanling, your skills and patience to teach people is extraordinary. I have told you this before, but you one of the reasons I joined the Alexander lab. Deb, you are like a secret weapon for the lab. I owe you much gratitude to the long hours you spent helping me, especially the many repeats of Ussing chamber studies and for the lunch chats. Dr. Allen Plain, I should probably be most thankful for your patience with my poor math skills, but I am really more thankful for the evening beers and pizza when we were both working late. Justin Lee, thanks for all the laughs, putting up with my bad sense of humor and being a friend. To Kennedi Young, I would never have been able to finish this thesis without your help with experiments and metabolic cage studies.

To my committee members, Dr. Catherine Field and Dr. Eytan Wine. You have both been so positive about my work and my goals. I cannot express how thankful I am for the time you have offered to me with my thesis but also just being available for questions. The support I have received from both of you has given me the confidence to carry on in my career.

Many thanks to the collaborators on this work. Dr. Henrik Dimke, I thank you for accommodating our many requests and for the laughs, even if I am shaking my head while

laughing. To Dr. Viet Flockerzi, I am grateful for the time I spent in your lab in Germany. You and your lab helped to make me feel at home, vielen dank. To Dr. Kai Busch and Dr. Ahsan Raza, so many thanks for your time and help with this work.

Finally, I owe many thanks to the support of my friends and family. You may not have understood what I was trying to do but you supported me anyway. In particular for my mom who said, "well, don't rush it Megan, you want to do a good job". And, to Tom, you have supported me without reservation. There have been many long hours but I cannot promise there will not be more.

Contents

List of Tables

List of Figures

List of Abbreviations

BMD	Bone mineral density
CaBP	Intracellular calcium binding protein, calbindin
CaSR	Calcium sensing receptor
Cldn	Claudin
EGF	Epidermal growth factor
EGFR	Epidermal growth factor receptor
FECa	Fractional excretion of calcium
FHH	Familial hypocalciuric hypercalcemia
IBD	Inflammatory bowel disease
J_{Ca}^{2+}	Calcium flux
KO	Knockout
MDCK	Madin-Darby Canine Kidney
Ncx	Na^+/Ca^{2+} exchanger
NEC	Necrotizing enterocolitis
Nhe	Na^+/H^+-exchanger
NSHPT	Neonatal severe hyperparathyroidism
Pmca1	Plasma membrane Ca^{2+}-ATPase
PTH	Parathyroid hormone
PTHR	Parathyroid hormone receptor
P_X	Permeability to ion "X"
SBS	Short bowel syndrome
SGLT1	Sodium glucose transporter 1
TER	Transepithelial resistance
TPN	Total parenteral nutrition
Trpv5	Transient receptor potential vanilloid 5
Trpv6	Transient receptor potential vanilloid 6
VDR	Vitamin D receptor
VDRE	Vitamin D response element
WT	Wildtype

Chapter 1

Introduction

1.1. Achieving a net positive Ca^{2+} balance early in life is critical to long term health

Calcium is necessary for a multitude of physiological functions, including bone mineralization, blood coagulation, neuronal transmission, muscle contraction, and intracellular signalling.[1] Approximately 99% of total body calcium is found in the skeleton, where it is an essential component of the structural matrix. The remaining 1% of total body calcium is in corporal fluids and soft tissues.[2] Given the essential structural role of calcium in bone, this micronutrient is especially important during periods of growth. Bone calcium deposition rate is highest in the fetus[3] and postnatal deposition greatest in the neonate with a roughly 3-fold decrease from birth to one year of age. A further 50% decrease occurs by age 10, and bone deposition declines to a rate ten-fold less than in the initial neonatal period by early adulthood when peak bone mineral density (BMD) is reached.[4] Infancy and childhood are thus critical years for deposition of calcium into bones for long-term health.[5] Overall, the physiological processes enabling optimal bone growth and mineralization are not fully delineated.

Failure to achieve appropriate calcium deposition into bone during growth confers an increased risk of osteoporosis.[5, 6] Although osteoporosis is traditionally thought of as a problem of ageing populations, an estimated 60% of this risk is attributed to the magnitude of peak bone mass reached in early adulthood.[7] Importantly, after peak bone mineral density is achieved in early adulthood, it remains largely stable while a neutral calcium balance is maintained. Women experience a loss of 2-9% in trabecular bone mass and a more minor loss of cortical bone during lactation.[8, 9] However, this loss is transient. Most women fully recover BMD after weaning through compensatory mechanisms independent of vitamin D and do not appear to require added calcium intake over the recommended dietary reference intake.[10-13] However, there is some debate about the exact calcium requirements during pregnancy and lactation.[14] Women will

experience a permanent loss of BMD around menopause and men lose BMD approximately 10 years post the perimenopausal decline in women.[4, 15] Thus, suboptimal bone mineral accretion in childhood is of particular importance as a failure to achieve a healthy peak bone mineral content predisposes an individual to osteoporosis later in life.

Osteoporosis means "porous bones" and is characterized by low mineral density of bone, which poses a significant risk for fragility and fracture.[6] Fractures, in turn, pose a significant risk for morbidity and mortality where almost one-quarter of people experiencing a hip fracture die within one year.[16] More women over the age of 50 experience a fracture due to osteoporosis than heart disease, breast cancer or stroke, combined.[17] In Canada, someone over the age of 40 experiences a fracture due to osteoporosis every 4 minutes.[16] This amounts to a prevalence of 2.2 million Canadian aged 40 and over living with osteoporosis in 2015-2016.[16] The direct costs of treating osteoporotic fractures are reported to be between 5 and 6.5 trillion USD in Canada, the USA, and Europe alone.[18] Fractures have a bimodal distribution by age with highest prevalence in the elderly and youth. Bone mineral density is associated with fracture risk in children and adolescence as well.[19-21] In children aged 0-16 years, the lifetime risk of experiencing a fracture is 42% - 64% for boys and 27% - 40% for girls.[21] A retrospective review of 2.5 million children in Ontario found that experiencing a fracture increases the risk of future fractures.[22] In addition, poor bone mineral content is associated with prematurity, inflammatory bowel disease, short bowel syndrome, and chronic kidney disease.[7, 23-26] Therefore, an understanding of how healthy infants and children retain optimal calcium for growth has broad implications for health, quality of life, and economic burden contributed to the healthcare system.

1.2. Intestinal Ca^{2+} absorption varies by segment

Calcium transport across epithelia occurs along the length of the small intestine. However, each intestinal segment does not contribute uniformly to overall absorption, which is defined here as the net movement of calcium from the lumen of the intestine into the blood. Intestinal perfusion studies in healthy adults demonstrate that, when normalized to segment length, the duodenum is the site of the highest rate of absorption.[27] The jejunum and ileum also transport calcium in humans, the magnitude and direction of which depends on calcium intake.[28] Colonic perfusion studies in healthy adults did not find significant absorption under conditions of adequate calcium intake; however, this segment appears to contribute net absorption when dietary calcium is low.[29, 30] To date, studies in healthy human infants have not assessed the contribution of individual intestinal segments to calcium absorption.[31-33]

Studies in adult rodents have examined the contribution of intestinal segments to net absorption. In rats, Ussing chamber studies on duodenum revealed net absorption of calcium while net secretion was observed in the jejunum and ileum.[34-36] However, net absorption may occur in the ileum under conditions of low calcium intake.[36, 37] The cecum was found to be the major site of net absorption in rats.[38] Net flux has been observed across the proximal colon and very slight or negligible absorption across the distal colon in rats.[36, 38, 39] Whereas flux refers to the movement of calcium across the intestinal tissue or epithelia, net flux is taken as unidirectional calcium flux of mucosa to serosal minus unidirectional flux of serosal to mucosa so that a positive net flux indicates net absorption. In mice, Ussing chamber studies found net secretion in the jejunum while the cecum contributed significantly to net absorption.[39] Importantly, these studies often employed conditions lacking a transepithelial electrochemical gradient, where calcium flux across duodenum, ileum and colon was not significantly different to

zero.[39] However, it should be recognized that the overall contribution of each segment to calcium absorption will vary based upon intraluminal calcium solubility, calcium concentration, transit time, the transepithelial permeability to calcium and potential difference across the epithelia.[40] Importantly, *in vivo,* after a meal there will be a large lumen to blood calcium gradient and the transepithelial potential difference across the intestine is lumen negative. When all these factors are taken into consideration, due to its length, the sojourn time is greatest in the ileum. Thus, this segment is said to be the site of greatest calcium absorption under physiological conditions of adequate calcium intake.[40]

Absorption from the intestinal lumen can follow one of two pathways. Transcellular absorption occurs via calcium influx into the enterocyte, intracellular shuttling, and finally basolateral extrusion. This pathway can therefore move calcium against a concentration gradient, for example when calcium intake is low. Absorption can also occur via a passive, paracellular route, whereby tight junction proteins facilitate or block the movement of calcium between epithelial cells.[41] Ussing chamber studies in rats demonstrate approximately one-third of net absorption from the duodenum, and half the absorption from the cecum occurs via the transcellular route.[34, 38] Calcium absorption and secretion into the jejunum and ileum occurs via the paracellular pathway.[35, 42, 43]

1.2.1. Transcellular pathway

Studies delineating the proteins involved in intestinal calcium absorption have been largely carried out in animal models, predominantly rodents. A current model of the transcellular pathway through an enterocyte is illustrated in Figure 1.1. The current model of transcellular

calcium absorption involves apical entry into the enterocyte, intracellular binding to a buffering protein, shuttling across the cell, and finally basolateral extrusion. The rate-limiting step in this pathway is suggested to be the apical calcium channel based on studies of knockout mouse models.[44]

Calcium entry into the enterocyte is, at least in part, mediated by the transient receptor potential vanilloid 6 (TRPV6), a very calcium-selective channel that is maximally open under hyperpolarizing conditions.[1, 45] *Trpv6* mRNA has been identified in the duodenum, cecum, and colon of 2- and 3-month old mice.[39, 45, 46] Apical staining of TRPV6 occurs in the villi of duodenum but not ileum of rabbits.[47] In humans, *TPRV6* expression has been detected in the duodenum and colon of adults.[48, 49] *In vitro* studies demonstrate that this channel is highly specific to Ca^{2+}.[45] A *Trpv6* knockout mouse model and a nonfunctioning *Trpv6* knockin have been generated. The global KO model, reported by Bianco et al., was generated by homologous recombination and resulted in the disruption of *EphB6*, a gene adjacent to the *Trvp6* gene.[50] *Trpv6* KO mice weighed less at adult age than WT mice with this difference exaggerated when both genotypes were fed a low (0.25%) calcium diet.[50] Up to 30 minutes after oral gavage of 100 µM $^{45}Ca^{2+}$, *Trpv6* KO mice had 60% and 50% decreased $^{45}Ca^{2+}$ in their serum on a 1% and 0.25% calcium diet, respectively. Thus, the *Trpv6* KO mice displayed decreased calcium absorption across the proximal small intestine compared to wildtype mice.[40] These animals had increased serum PTH and calcitriol on standard and low calcium diets and lower serum calcium when fed a low calcium diet. *Trpv6* KO mice also had increased urine volume and Ca^{2+} (in µmoles per day) suggesting a renal defect as well.[50] In addition, *Trpv6* knockout mice at 95 days of age had lower femoral bone mineral density on a regular or high but not low calcium containing diet, although only male mice were examined.[50] Using the everted sac method and 2-

month-old mice, transcellular calcium transport in the duodenum but not ileum of these *Trpv6* knockout mice was significantly reduced when they were fed 0.02% calcium diet.[51] Of note, there was no difference observed by this method on a 1% calcium diet or on either diet when the mice were over 3 months old suggesting an effect of age on this pathway.[51] Although reduced, the presence of residual net luminal to serosal calcium flux in these *Trpv6* knockout mice in both studies suggests the presence of another apical calcium influx mechanism. The second mouse model was genetically engineered to lack functional TRPV6 by expressing a non-functional channel pore via an aspartate to alanine mutation at residue 541 which blocks the Ca^{2+} conductance (*Trpv6*[mt]).[52] In contrast to the first model, these mutant mice did not have different serum calcium, body weight, or urine calcium compared to WT.[53] After oral gavage of 0.1 μM $^{45}Ca^{2+}$, radioactivity measured in serum was increased in both genotypes fed a 0.02% calcium diet but lower in the *Trpv6*[mt] mice compared to WT.[53] No differences were observed between genotypes on a 1% calcium diet.[53] However, in this model femurs from 6-month-old male mice did not show changes in cortical or trabecular mineralization.[54] Further supporting evidence for the role of TRPV6 in intestinal calcium absorption comes from transgenic mice expressing human *TRPV6* under a villin promoter.[55] The transgenic mice had an almost 3-fold increase in proximal intestinal calcium absorption as measured by oral gavage.[55] These studies had to be conducted on mice fed a lower 0.25% - 0.5% calcium diet due to soft tissue calcification noted in transgenic mice fed a standard chow diet.[55] Transgenic mice had increased serum calcium and 28% increase in femur BMD. Furthermore, transgenic TRPV6 expression was enough to rescue the low serum calcium and low BMD of vitamin D receptor (*Vdr*) KO mice.[55] Nonetheless, that calcium absorption is not completely abolished in *Trpv6* KO models provides evidence of a compensatory role for the paracellular pathway or another apical influx mechanism.[53]

The apical L-type calcium channel, $Ca_v1.3$, has been proposed to contribute intestinal calcium absorption under depolarizing conditions, thereby playing a complementary role to TRPV6.[56] Within this model, it has been proposed that in a fed state when luminal glucose is high, sodium and glucose absorption via sodium glucose transporter 1 (SGLT1) will depolarize the plasma membrane, increase the open probability of $Ca_v1.3$ and thereby facilitate postprandial absorption of calcium.[56] Consistent with this, immunocytochemistry of male rats observed $Ca_v1.3$ in the jejunum and proximal ileum, but not in duodenum, cecum, or colon.[57] Further, perfusion of adult rat jejunal loops confirmed unidirectional lumen to mucosa calcium flux was reduced 72% upon addition of an L-type calcium channel blocker and also reduced after addition of the SGLT1 inhibitor phloridzin.[57] Similarly, in Caco-2 cells, a model of human colonic epithelia, unidirectional calcium flux was increased by prolactin administration and this increase was prevented by pharmacological inhibition or knockdown of $Ca_v1.3$, an effect not observed by the knockdown of *Trpv6*.[58] However, in a mouse model, oral gavage of $^{45}Ca^{2+}$ with either fructose or glucose did not lead to a difference in serum appearance of calcium when mice were fed either a 1% or 0.125% calcium diet.[59] Similarly, early everted sac assays of rabbit jejunum found greater net lumen to mucosal calcium flux in the presence of fructose than glucose.[60] Since fructose absorption is via passive, facilitated diffusion, this process does not lead to membrane depolarization and therefore refutes previous studies. Prior to this thesis, all studies on this subject have been conducted on adult animal models.

The cytoplasmic free calcium concentration is maintained around 0.1 μM to prevent apoptosis.[61] High inorganic phosphate concentrations central to cellular metabolism is only compatible with life if free calcium is kept low.[61] Intracellular buffering and shuttling of calcium in intestinal epithelial cells is mediated by calbindin-D$_{9k}$ (CaBP9K encoded by the gene

S100g).[62] This facilitated diffusion of calcium across the cell prevents apoptosis due to increased cytosolic free calcium.[1, 62] CaBP9K expression has been detected in adult human, rat, and mouse duodenum but not jejunum or ileum of either humans or rodents.[39, 46, 63, 64] Expression is also detected in the cecum and proximal colon of mature mice.[39] Further, CaBP9K colocalizes with TRPV6 in rabbit duodenum.[47] Gene expression and protein abundance are not altered in *Trpv6* the global KO mice reported above.[51] Transgenic mice expressing human *TRPV6* have 6-fold increased intestinal calcium absorption and decreased serum calcitriol, yet have increased *S100g* expression that mirrors the *TRPV6* expression. Thus, calbindin-D$_{9k}$ expression appears to be increased in response to calcium influx in order to buffer it, suggesting that expression is regulated by the intracellular calcium concentration and not vitamin D.[55] In response to a 0.02% calcium diet, increased duodenal *S100g* expression was observed concomitant to greater calcium absorption in the *Trpv6*[mt] mice.[53] This again highlights the potential for another apical channel facilitating calcium entry into the enterocyte. *In vivo* calcium absorption studies in 12-week-old *S100g* knockout mice showed no difference to wildtype mice including no change in serum PTH or calcitriol, suggesting that CaBP9K is not essential for intestinal calcium absorption.[51, 65]

The basolateral extrusion of calcium from the enterocyte is mediated by plasma membrane Ca^{2+}-ATPase 1b (PMCA1b) and the Na^+/Ca^{2+} exchanger (NCX1).[1, 66, 67] *In vitro* studies on vesicles from rat duodenum and jejunum identified an ATP-dependent calcium pump as well as passive calcium efflux coupled to sodium influx.[68] Early intestinal everted sac studies in rats and rabbits revealed that this pathway required energy.[60] PMCAs are ubiquitously expressed and serve to pump Ca^{2+} out of cells.[1] In humans, PMCA1 is expressed in the duodenum, ileum, and colon whereas in the mouse *Pmca1* is expressed along all segments of the small and large intestine.[46] In the duodenum of rabbits, PMCA colocalizes with TRPV6 and

CaBP9K.[47] PMCA1 is necessary for calcium absorption. Duodenal calcium transport, determined by the everted sac method, of intestinal specific *Pmca1* KO mice was reduced by almost 50%. Consequently, this led to decreased total and femoral bone mineral density in the knockout mice compared to wildtype mice.[69] Overall, extrusion of calcium from enterocytes by PMCA1b appears to be the predominant mechanism with NCX1 playing a minor role.[1]
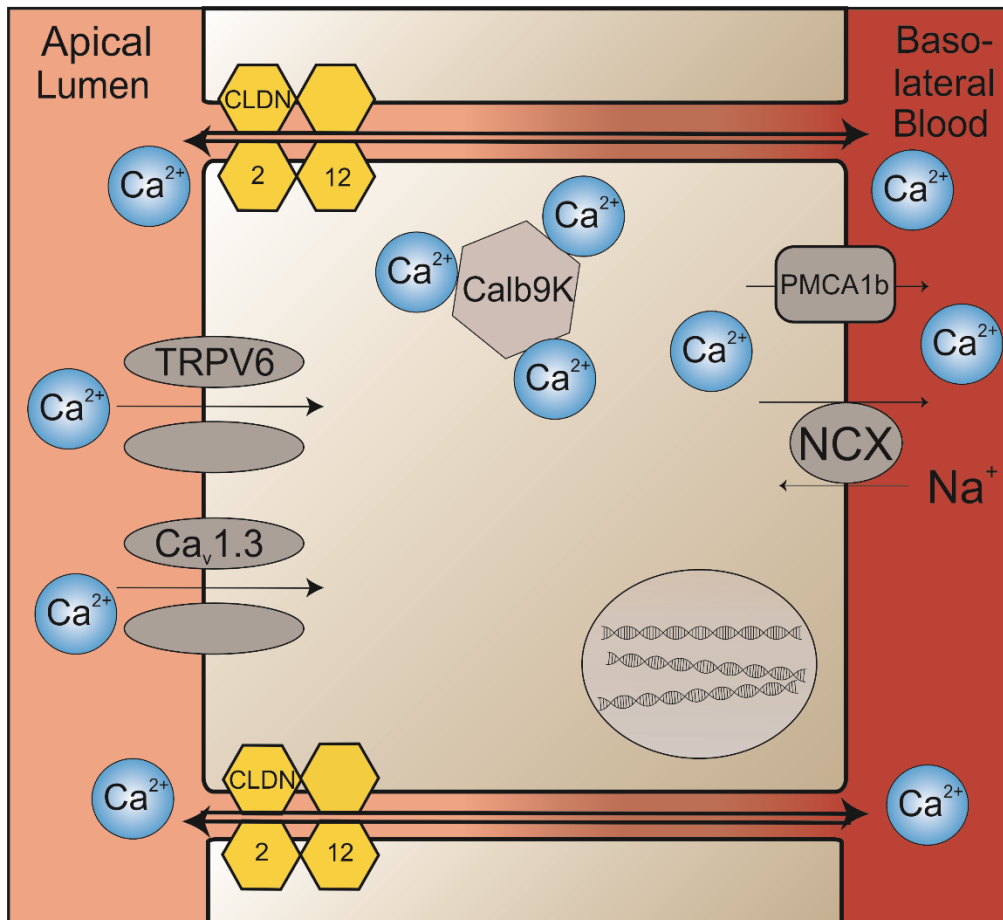
Figure 1.1. Cartoon depicting mediators of transcellular and paracellular calcium absorption and secretion across an enterocyte.

The transcellular pathway involves apical entry into the enterocyte has been proposed to occur via TRPV6 and/or $Ca_v1.3$. Intracellular buffering and shuttling is proposed to occur via calbindin-D_{9k} and basolateral extrusion via PMCA1b and NCX1. The paracellular pathway is characterized by bidirectional diffusion of calcium down an electrochemical gradient and is facilitated by tight junction proteins called claudins. Specifically, claudin-2 and claudin-12 have been implicated in forming calcium permeable pores between enterocytes.

1.2.2. Paracellular pathway

Paracellular calcium absorption is a passive or secondarily active process occurring via diffusion down an electrochemical gradient. Along this pathway, calcium permeates across the epithelia between the cells rather than through the cells. It is considered the major route of absorption when calcium intake is high.[70] A luminal free calcium concentration of at least 1.74 mM is required to overcome the approximately -5 mV transepithelial potential difference present across the small intestine when free calcium concentration in the blood is 1.2 mM.[41] If serum ionized calcium is lower or if the transepithelial potential difference is less negative, a lower luminal calcium concentration would be required to facilitate diffusion. Sodium driven water absorption has been proposed to play a significant role in this process by increasing luminal calcium concentration from proximal to distal segments of the intestine and paracellular water flux itself has been proposed to facilitate paracellular calcium absorption via solvent drag.[35] Consistent with this, mice null for the epithelial Na^+/H^+-exchanger (*Nhe3*), which mediates intestinal sodium and water absorption, have decreased calcium flux across duodenum and cecum.[71]

Paracellular flux requires not only a driving force, but also a paracellular pore. Tight junctions are the apical most cell to cell junction of epithelia.[72] Claudins (gene *Cldn*) are proteins with four transmembrane domains and two extracellular loops that interact between cells to form the "kissing contacts" or tight junctions.[73-75] The extracellular loops of claudins from adjacent cells interact to form pores for or barriers to paracellular movement of solutes by charge and size selectivity.[41, 75, 76] In this manner, claudins confer the permeability properties to epithelia by altering the ability of ions to permeate the cell layer.[74, 75]

Claudins-2 and -12 have been implicated in intestinal calcium absorption as illustrated in Figure 1.1. Claudin-15 has been implicated as forming a monovalent cation permeable pore.[77] These claudins are expressed along the length of the small intestine and colon of adult mice although *Cldn15* has higher expression in the proximal intestine.[39, 78-81] In humans, *CLDN2* and *CLDN15* mRNA are more highly expressed in the proximal segments of the intestine whereas *CLDN12* is expressed throughout the small and large intestine.[82] *Cldn2* and *Cldn12* expression are lower in jejunum than duodenum but *Cldn2* expression increases to 200% of duodenum in ileum in mice.[59] When overexpressed in an epithelial cell culture model, CLDN2 and CLDN12 increase the tight junction selectivity for cations, decrease transepithelial resistance and increase calcium permeability.[78, 83] Overexpression of *Cldn2* but not *Cldn12* also increases relative sodium permeability, suggesting that it forms a more specific cation permeable pore.[78] When a D65N (aspartate to asparagine) mutant of claudin-2 was expressed in MDCK (Madin-Darby Canine Kidney) cells, permeability to calcium was decreased by 22.1-fold compared to expression of the wildtype protein.[84] This mutation represents neutralization of a charged residue in the first extracellular loop of claudin-2 and thus implicates this amino acid charge as contributing the cation selectivity of the pore.[84]

Global *Cldn2* KO mouse models have been created.[85] These mice are grossly normal with no change in serum calcium or bone mineral density at 4, 6, 8, 10, 12 and 16 weeks age.[86] Calcium permeability across the duodenum, ileum, and colon measured by the everted sac method under conditions of 0.25 mM and 5 mM calcium revealed significant decreases in the KO mice across the colon only.[86] These results were confirmed *ex vivo* with bi-ionic diffusion potential experiments in Ussing chambers.[86] Interestingly, these mice had greater net intestinal absorption and increased urinary excretion of calcium. However, the urinary excretion difference

was attenuated on a low calcium diet.[86] To explain these findings, it is proposed that the colon of the adult mouse acts as a site of regulation that can secrete calcium.[86]

A *Cldn12* KO mouse model has also been generated.[87] These mice also have a grossly normal phenotype with no differences in serum or fecal excretion of calcium.[87] Intestinal calcium permeability and expression of other genes or proteins mediating calcium absorption were not investigated in the initial publication with these mice. Thus, it is not clear if there is altered permeability or compensation with the loss of intestinal *Cldn12*. Of note, compensatory increases in *Cldn2* and *Cldn15* were observed in the duodenum of adult *S100g* KO mice, suggesting the possibility of a cooperative interaction between the transcellular and paracellular calcium absorption pathways.[88]

1.2.3. Postnatal Developmental Changes of the Intestine

The small and large intestine function as a barrier to the external environment and to absorb nutrients ingested in the diet. At birth, these functions are not fully mature. As such, developmental changes occur during the postnatal period.[89] After birth, the intestines show a pattern of cylindrical growth whereby intestinal length and diameter increases.[90] This growth coincides with the period of greatest crypt fissure, whereby the crypts divide longitudinally, a process partly regulated by the G protein-coupled receptor CD97.[90, 91] This occurs predominantly during the first year of life when babies are milk fed, and is likely regulated by bioactive compounds in breast milk.[90] The human small intestine length is on average 275, 380, 450, and 575 cm at term, one, five and 20 years, respectively.[90] Owing to increased length and diameter with age, the functional, absorptive area of the small intestine increases more than 40-fold from infancy to adulthood.[92] Similarly, in mice, the length of the small intestine increases significantly from 2 to 6 weeks of age and the large intestine increases significantly with age from

approximately 40 mm at 2 weeks, to 77 mm at 4 weeks, to 94 mm at 6 weeks and 111 mm at 12 weeks.[93]

The formation of villi is required to increase the surface area of the intestine for adequate nutrient absorption. Failure to form villi results in intestinal failure. This process begins during embryogenesis driven by mesenchymal cell clusters which induce overlaying epithelial cells to form villi.[94] Villi formation also results in intervilli spaces which are flat sheets of epithelial cells at birth. In mice, from P0 to P10, a myosin II-dependent apical constriction of cells in this space results in invagination and formation of crypts.[94] After weaning, luminal growth predominates and is characterized by increased submucosal folds and villi hyperplasia.[91] A rapid increase of 33 – 90% in villus height and 14 – 51% increase in villus diameter have been observed within days of birth in piglets.[95, 96] In mice, the height of the villi along the small intestine is not reported to change from 2 to 12 weeks in any segment where it measures about 348 – 378 µm in the duodenum, 329 – 365 µm in the jejunum, and 208 – 282 µm in the ileum, although increases with age have been noted in other species including humans.[93] However, the diameter of the villi increases significantly from 2 to 4 weeks in the duodenum and jejunum.[93] Subsequently, the number of villi per mm^2 decreases from 4 to 6 weeks age in the jejunum and ileum.[93]

Epithelial cells localized to the villi are the absorptive cells of the intestine and express enzymes and nutrient transporters. Important changes in the expression of these enzymes and transporters have been established during postnatal development. For example, lactase expression, an enzyme that breaks down lactose into glucose and galactose enabling the absorption of carbohydrates from milk, are 2 to 4-fold greater in the infant than adult.[92, 95] Conversely, sucrase, an enzyme that breaks sucrose into simple sugars is expressed at very low levels until weaning.[95, 97, 98] Similarly, alkaline phosphatase activity is minimal in the neonate

and increases throughout postnatal development.[92] While postnatal changes in macronutrient absorption have been characterized, similar potential alterations in micronutrient handling, including calcium, during development have not been fully delineated and is the aim of this thesis.

1.2.4. Changes in Intestinal Calcium Absorption During Postnatal Development

While most investigations of intestinal calcium absorption are carried out in adult subjects or mature animal models, existing studies highlight clear changes with age in both the absorption of calcium from intestinal segments and the expression of molecules participating in intestinal calcium absorption. Table 1.1 summarizes changes in expression of molecules implicated in intestinal calcium absorption throughout development. Dual isotope studies in very low birth weight infants found that the achievement of a net positive calcium balance was primarily determined by the magnitude of intestinal calcium absorption. The authors observed high variability of calcium balance between subjects, although a large range of birth weights (750-1750 g) lends the possibility that some variability might be due to differences in developmental age.[31] Still, this study highlights that the intestine plays a major role in determining overall calcium balance in infants. Premature infants require higher dietary calcium in order to maintain a positive balance.[32] A similar study found that intestinal calcium absorption was a linear function of intake with an extrapolated intercept of zero and independent of vitamin D intake, suggesting the existence of only the paracellular pathway in premature infants.[99] These findings may be consistent with an inability to upregulate the active, transcellular pathway which permits absorption at lower lumen concentrations.[100] Thus, infants may rely on passive, paracellular absorption to meet their requirements.[32] It is important to note however that

intestinal absorption in preterm infants may be more representative of fetal physiology.[3] Nonetheless, a decline in the predominance of the paracellular pathway is observed from childhood to adulthood as the coefficient of intestinal calcium absorption (a measure of intestinal calcium permeability) measured by dual isotopes, decreased more than 50% between the ages of 12 and 80 years of age.[101] Balance studies in rats found that the fraction of calcium absorption from the intestine was approximately 50% of intake at 3 weeks of age, peaked at 70% at 5 weeks and then declined to about 40% by 7 weeks. It is noteworthy that calcium retention mirrored intake.[102] Very early balance studies in rats starting from weaning noted that total body calcium balance peaked at 6-7 weeks of age and then declined thereafter with an accompanying increase in fecal calcium excretion.[103] The results of these studies demonstrate that intestinal calcium absorption changes with age to meet requirements for bone mineralization during periods of growth. However, the molecular details of these changes have not been fully delineated, nor have mechanisms regulating the changes.

Table 1.1. Expression of molecules implicated in intestinal calcium absorption throughout development.

	Duodenum			Jejunum			Ileum			Cecum			Colon			
Age (weeks)	< 3	3-8	> 8	< 3	3-8	> 8	< 3	3-8	> 8	< 3	3-8	> 8	< 3	3-8	> 8	Ref
Transcellular																
Trpv6	Yes	Yes	Yes*	ND	ND	No	ND	ND	No	ND	ND	Yes	ND	ND	Yes	37, 40, 71, 104, 105
Cav1.3	ND	ND	No	ND	ND	Yes	ND	ND	Yes	ND	ND	No	ND	ND	No	56
CaBP9K	Yes	Yes	Yes*	ND	Yes	No	ND	ND	No	ND	Yes	Yes	ND	ND	Yes	37, 40, 62, 63, 71, 104, 105
Pmca1	Yes	Yes	Yes*	ND	ND	Yes	ND	ND	Yes*	ND	ND	Yes	ND	ND	Yes*	37, 40, 65, 66, 69, 71, 104
Pmca4	ND	ND	Yes	ND	ND	Yes	ND	ND	Yes	ND	ND	Yes	ND	ND	Yes	66
Ncx1	ND	ND	Yes	ND	ND	Yes	ND	ND	Yes	ND	ND	Yes	ND	ND	Yes	37
Paracellular																
Cldn2	ND	Yes	Yes*	Yes	Yes	Yes	ND	ND	Yes*	ND	ND	Yes*	ND	ND	Yes*	37, 69, 71, 80, 86
Cldn12	ND	ND	Yes*	Yes	Yes	Yes	ND	ND	Yes*	ND	ND	Yes*	ND	ND	Yes*	37, 69, 71, 80
Cldn15	ND	ND	Yes*	Yes	Yes	Yes	ND	ND	Yes*	ND	ND	Yes*	ND	ND	Yes*	37, 69, 71, 80
Cldn19	ND	ND	No	Yes	ND	No	ND	ND	No	ND	ND	No	ND	ND	No	80
Nhe3	ND	ND	Yes	ND	ND	Yes	ND	ND	Yes	ND	ND	Yes	ND	ND	Yes	37

Note: Ages refer to age of rodent animal models. ND, no data.

*Expression in adult human and rodent samples.

Functional measures of calcium transport across intestinal segments have been performed on rodents to measure changes with age. Using the everted sac technique in rat duodenum, greater net calcium absorption was observed in 3- and 5-week old pups compared to 8 week and 15-month-old animals.[106] Using *in situ* ligated loops of rat duodenum, no evidence of saturable absorption was found in 3 or 5-day old rats. In this study, the saturable component (which represents transcellular absorption) was first observed at 19 days of age and became proportionally greater with increasing age until maximum flux was observed between 24 and 40 days.[107] Expression of the intracellular calcium binding protein, CaBP followed the same pattern consistent with an increasing contribution of transcellular absorption from the duodenum with age.[107] Similarly, using *in situ* loops of rat duodenum, there is no evidence of transcellular calcium uptake in pups at 14 days while linear regression of absorption at different luminal calcium concentrations suggests a transcellular pathway present in pups only at 18 days old. This is based on plotting absorption as a function of concentration. A straight line of fit that passes through zero at the y-intercept indicates absorption via an entirely non-saturable, paracellular pathway. A biphasic distribution occurs when absorption is via both a saturable, transcellular and non-saturable, paracellular pathway. Under these conditions, a line of regression through only the linear portion of the curve will give an equation where the y-intercept represents the maximal transcellular transport and the slope represents the paracellular portion of absorption.[108] By weaning at 21 days, intestinal calcium absorption had switched from predominantly non-saturable, paracellular diffusion to predominantly saturable, transcellular.[108] At one month of age, both paracellular and transcellular pathways appear to be present in the duodenum along with CaBP expression while in the ileum, only non-saturable absorption seems to occur and

CaBP is not present.[108] Everted sac studies of rat duodenum similarly found active transport, measured as the serosal to mucosal ratio of $^{45}Ca^{2+}$ flux, decreased 4.5-fold from 3 weeks to 3.5 months of age. This was accompanied by a similar decrease in CaBP protein.[65, 109] Active absorption from the duodenum of rats appears to continue to decrease with age.[110] A study of everted duodenum and jejunum from suckling (2 week), weanling (3 week), adolescent (6 week), and adult rats revealed that in the suckling rat, unidirectional lumen to serosal calcium flux is predominantly non-saturable suggesting paracellular absorption. At weaning, a transition to predominantly saturable absorption occurred, suggesting a larger contribution of a transcellular pathway.[111] Concurrently, the calcium permeability of duodenum and jejunum decreases with age.[111] Thus, the results of this study are indicative of a transition from passive diffusion at an early age to a transcellular process in the proximal small intestine later in development, then back to diffusion in adulthood. Consistent with this, using the *in situ* ligated loop technique in 16-day old rat pups, net calcium absorption was found from the duodenum, jejunum, and ileum with net secretion in the colon. In this context, secretion refers to the net loss of calcium from the blood into the intestinal lumen. The jejunum appeared to be the segment of greatest net absorption which increased when luminal sodium decreased, independent of mannitol flux.[104] An early study in mice and rats from P1 to 1 month, incubated excised segments of linearized intestinal tissue in $^{45}Ca^{2+}$ containing buffer for one hour and subsequently measured radioactivity of the homogenized tissue. Prior to weaning, there was greater $^{45}Ca^{2+}$ uptake into the cells of the ileum compared to the duodenum and this quickly changed at weaning.[112] Thus, limited evidence supports transcellular calcium absorption from the distal small intestine prior to weaning. This is in contrast to net secretion from the jejunum and net absorption in the cecum in adult rodents.[35, 38, 39] Together, the current evidence suggests that intestinal calcium absorption is significantly

altered throughout early development, likely to maintain a positive calcium balance. In particular, weaning in rodents appears to be a time of rapid change. Figure 1.2 depicts the current state of evidence supporting net absorption and secretion by intestinal segment before and after weaning.
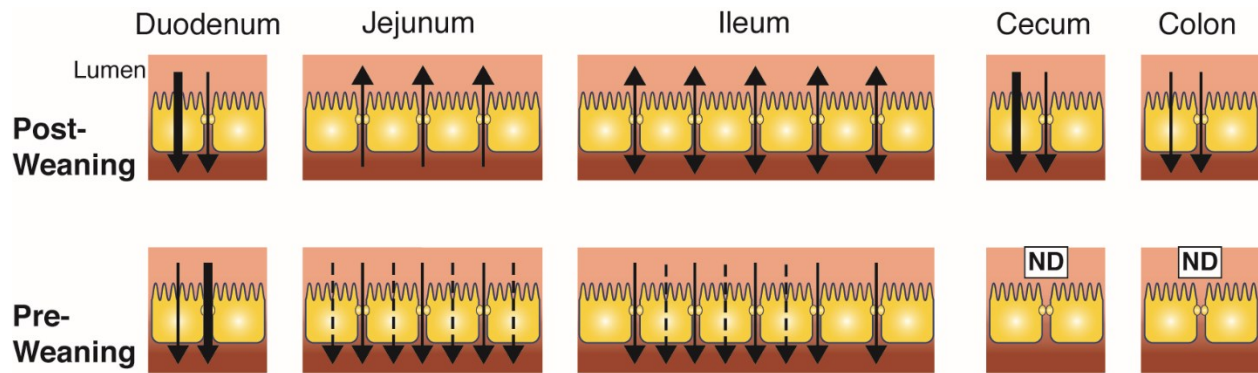
Figure 1.2. Net calcium absorption and secretion by intestinal section during suckling and after weaning: A pictorial representation of evidence prior to thesis studies. Absorption is represented by a downward arrow indicating net movement of calcium from lumen to serosa. When both transcellular and paracellular pathways are present in a segment, a larger arrow indicates the predominant pathway. Note that the transcellular pathway in the duodenum pre-weaning occurs after 1–2 weeks of age in rodents. The dashed line indicates that evidence supporting the pathway is limited. Evidence for calcium absorption in the cecum is from animal models only. Weaning is at 21 days in rodents. ND: no data.

While functional changes in intestinal calcium absorption have been described throughout development, very few studies have examined the molecular details conferring these changes. When expression was examined at 1, 3, 6, and 8 weeks of age in mice, *Trpv6* mRNA was detected only after one week with a peak at 3 weeks. A similar pattern was observed for both the gene and protein expression of CaBP9K. Unfortunately, the authors simply state "intestine" so it is not clear which segment was examined or if a mixture of intestinal segments were employed and thus specific conclusions about changes in specific segments from this work are difficult to make.[113] In a separate study of mice, mRNA expression of *Trpv6*, *S100g* (the gene encoding calbindin-D$_{9k}$), and *Pmca1* in duodenum is first noted at 14 days and peaks at 21 days.[114] At 6 weeks of age, CaBP9K was highly expressed in duodenum with a small amount in jejunum and cecum. At 44 weeks of age, CaBP9K expression is no longer detected in jejunum and cecum but remains in duodenum.[65]

With respect to paracellular transport, a single study has looked at the expression profile of claudins in the jejunum of mice at 1 day, 2 weeks, 1 and 3 months of age. The authors noted a decrease in *Cldn2* but increases in *Cldn12* and *Cldn15* with age. Of note, *Cldn19* (a claudin that mediates calcium transport across the thick ascending limb of the renal tubule) was observed at 1 day and 14 days of age, whereas expression of this gene is not found in intestinal segments of adult mice.[80] Together, expression studies highlight that the molecules mediating intestinal calcium absorption are not constant throughout development. Similar to the results of functional studies, important changes appear to occur around the age of weaning, which are largely consistent with a change from paracellular to transcellular calcium flux in the duodenum and jejunum as well as a transition from net absorption to net secretion in the distal small bowel.

23

Important gaps in the literature exist regarding the potential role of the colon and the molecular details of the paracellular pathway along the small and large intestines during postnatal development.

1.2.5. Potential Mediators of Changes in Intestinal Calcium Absorption During Postnatal Development

Studies in rodents and humans demonstrate alterations in intestinal calcium absorption from neonatal through adult ages. However, what mediates the changes observed in expression of calcium transport genes, that contribute the functional changes in absorption at these ages has not been delineated. Extensive research has been conducted into the role of vitamin D and its active hormone, calcitriol, in mediating intestinal calcium transport.[115] It is well established that decreased serum calcium causes an increased release of parathyroid hormone (PTH), which acts on the kidney to increase transcription of *Cyp27b1*, which then converts vitamin D to its active form, calcitriol, which then acts on the intestine to increase calcium absorption (as reviewed in [2]). In mice with a nonfunctional vitamin D receptor (VDR), the phenotype of poor weight gain and decreased bone mineral density (BMD) is only evident after weaning, highlighting that calcium absorption while suckling is not calcitriol dependent.[3, 116] In adult mice, calcitriol acts to increase intestinal calcium absorption by increasing the transcription of *Trpv6* in the duodenum and cecum.[35, 38, 46, 117] Expression of these genes has not been identified in mice prior to weaning when calcium absorption appears to occur via passive, paracellular diffusion.[118, 119] Further, consistent with calcitriol not participating in intestinal calcium absorption pre-weaning, using the everted sac technique in duodenum, Halloran et al. observed that calcitriol injections increased active and total calcium uptake of 6 week old mice but not 14 day old pups.[120]

Calcitriol has also been proposed to affect the paracellular pathway thereby enhancing calcium absorption.[78] This finding is based on the observation that VDR knockout mice have lower expression of *Cldn2* and *Cldn12* in the small intestine and colon, and that the treatment of a colonic epithelial cell culture model with calcitriol increased *Cldn2* and *Cldn12* expression.[78, 121] Vitamin D exerts its effects in a cell by binding to the VDR which then translocates to the nucleus and binds to the vitamin D response element (VDRE) of a gene to regulate its transcription. Using chromatin immune precipitation assays, VDR was observed to bind to the claudin-2 gene in mouse colon cells and human colonic epithelial cell line (SKCO15 cells) and, using a dual luciferase assay, a functional VDRE was identified in the claudin-2 promoter.[121] Therefore, the authors conclude that claudin-2 is a direct target of vitamin D regulation. This is intriguing given the high levels of *Cldn2* expression identified in the intestine in suckling mice.[80] In children with celiac disease, vitamin D deficiency is associated with decreased expression of claudin-2 in villi and crypts of duodenum samples and correlated with BMD, notably 44% of these patients had osteoporosis.[122] However, the injection of exogenous calcitriol into adult mice, did not effect a change in *Cldn2* or *Cldn12* mRNA expression in duodenum.[123] This apparent discrepancy may be reconciled by the hypothesis that, *in vivo*, there is a maximal effect of calcitriol to upregulate the transcription of these genes. Regardless, the potential role of calcitriol as a regulator of paracellular calcium absorption throughout development has not been fully characterized but given the lack of an apparent role for transcellular absorption early in life, it is unlikely important for the changes in paracellular absorption observed.

It is recognized that lactose present in milk or the diet facilitates increased calcitriol-independent calcium absorption. This is of particular importance during the neonatal period (as reviewed in [118] and [124]). Lactose also facilitates increased calcium absorption from the ileum of

adult rats, a section of the intestine where the paracellular pathway predominates.[125] In addition, ingested lactose augments calcium absorption thereby rescuing the calcium phenotype of VDR mutants.[117, 126] However, whether the absence of lactose after weaning mediates molecular alterations in calcium transport pathways is not known.

Prolactin is a peptide hormone that is present in high amounts in early breast milk but has a declining concentration through lactation.[127, 128] It consists of several isoforms produced via alternative splicing, proteolytic cleavage, and post-translational modifications.[129] Maternal prolactin is absorbed and bioactive in neonatal rats where the prolactin receptor is present on epithelial cells throughout the small and large intestines as well as the duodenum and colon of humans.[128, 130] Prolactin directly alters the expression and activity of mediators of both transcellular and paracellular calcium absorption in the intestine of both sexes via intracellular signaling molecules including PI3K.[58, 105, 131] Provision of exogenous prolactin increases net intestinal calcium absorption at 3 weeks of age in rats but decreases fractional absorption at 5 and 7 weeks. In the same study, inhibition of endogenous prolactin production with bromocriptine decreased fractional absorption at 3 and 5 weeks but increased absorption at 7 weeks of age.[102] Similarly, in suckling rat pups, bromocriptine treatment decreased net calcium absorption from the jejunum while the administration of bromocriptine with exogenous prolactin returned net calcium absorption to baseline. Under conditions where only exogenous prolactin was present, net calcium absorption from the duodenum was absent.[104] This study illustrates the potential for endogenous and exogenous prolactin to confer different effects on intestinal calcium absorption. In adult mice and in human cell culture models, endogenous prolactin appears to increase calcium flux through an L-type calcium channel, presumably $Ca_v1.3$.[58, 105] Moreover, the induction of hyperprolactinemia in mice led to increased femoral total calcium content

whereas bromocriptine treatment lowered total lumbar calcium, suggesting a role for prolactin in mediating mineral accrual into bone.[102] Taken together these results infer that exogenous prolactin in breast milk may stimulate calcium absorption from the intestine by non-traditional mechanisms and its withdrawal may lead to the more typical calcium absorption mechanisms seen in adults.

Another bioactive compound of note in breast milk is epidermal growth factor (EGF).[132] EGF is present in several other biological fluids as well, including amniotic fluid and saliva.[133, 134] EGF has mitogenic effects on cells, promoting epithelial cell growth and repair and is considered vital for the developing gut of the fetus.[132, 135] Importantly, EGF is resistant to digestion and can be administered orally and does not seem affected by pasteurization of human milk.[136-138] In colonic epithelial cell models, EGF or signaling via the EGF receptor (EGFR) leads to decreased transepithelial resistance (TER) and increased claudin-2 protein abundance.[139] EGF has been shown to increase claudin-2 expression in colonic epithelial cells and lung epithelial cell models.[140, 141] This presents an interesting model given that suckling mice have greater claudin-2 gene and protein expression in the jejunum.[80] Whether EGF in breast milk will also increase claudin-2 expression in intestinal cells and, in turn, increase permeability to calcium has not been directly demonstrated. It is important to note, however, that breast milk contains hundreds of bioactive compounds that may alter nutrient absorption or bioavailability and further research into this area is required.[142, 143]

1.3. Renal Ca^{2+} reabsorption

Calcium filtered by the kidney is reabsorbed along the nephron to maintain the serum concentration. The mature nephron efficiently reabsorbs most calcium so that only 1-2% of

filtered calcium is excreted in urine.[144] Similar to the intestine, renal reabsorption can occur via both paracellular and transcellular pathways. Most filtered calcium, about 70% of the total in the proximal tubule and 20% of the total in the thick ascending limb, is reabsorbed via the paracellular pathway.[41] Microperfusion studies and characterization of the *Nhe3* knockout mice highlight the coupling of sodium and water movement to paracellular calcium reabsorption in the proximal tubule and thick ascending limb.[41, 71] The remainder of calcium is reabsorbed in the distal nephron, in particular, the distal convoluted tubule and connecting tubule via an active transcellular process.[1, 145]

1.3.1. Paracellular pathway in the proximal tubule and thick ascending limb

As in the intestine, paracellular calcium reabsorption along the nephron occurs down an electrochemical gradient or via solvent drag.[41] Claudin-2 confers calcium permeability across the proximal tubule. *Cldn2* KO mice have decreased monovalent cation permeability in the proximal tubule and a 3-fold increase in fractional excretion of calcium (FECa).[146] Another *Cldn2* KO model mouse has a 2-fold increase in FECa on standard lab cow that is attenuated when the mice were fed a low calcium diet.[86] These KO mice have increased net intestinal absorption due to decreased colonic secretion, therefore the increased FECa is due to a "spill-over" effect. This poses an increased risk of developing nephrocalcinosis caused by hypercalciuria. Indeed, humans with mutations in *CLDN2* have been identified with a propensity towards developing kidney stones.[86] Schnermann et al. also showed that *Cldn2* knockout mice have a 22.7% decrease in water permeability of the proximal tubule.[147]

Claudin-12 is also expressed in the proximal tubule.[87] Microperfusion of this nephron segment from *Cldn12* KO mice reveals a 50% decreased in calcium permeability.[87] However, these mice do not have altered FECa on standard, high, and low calcium containing diets.[87] Interestingly, these mice also displayed decreased *Cldn2* expression and *Cldn14* expression, the latter which blocks calcium reabsorption as discussed below. Moreover, mice null for the transporter mediating the majority of sodium reabsorption from the proximal tubule, *Nhe3*, have a 2-fold increase in FECa. Together these results highlight how tightly coupled sodium, water, and calcium reabsorption is in the proximal tubule.[71] What other claudins may contribute to paracellular calcium permeability across the proximal tubule is not known.

In the thick ascending limb, claudins-16 and -19 form a cation permeable pore through heteromeric interaction.[148] Loss of function mutations of either claudin-16 or claudin-19 leads to hypomagnesemia and hypercalciuria.[148, 149] Claudin-14 is expressed in this nephron segment under conditions of increased plasma calcium and blocks paracellular reabsorption of cations, including calcium.[150, 151] Microperfusion of the cortical thick ascending limb from 2-month-old mice showed that a high calcium diet results in increased transepithelial resistance (TER), decreased absolute calcium permeability, and a 3-fold increase in *Cldn14* mRNA with no change to *Cldn16* or *Cldn19* expression.[152] Subsequently, a high calcium diet led to a more than 3-fold increase in urinary calcium to creatinine ratio (Ca/Cr) and a 4-fold increase in FECa.[152] In addition, pharmacological downregulation of *Cldn14* expression in wildtype mice decreased total urinary calcium and FECa while microperfusion studies revealed decreased transepithelial resistance and increased cation permeability across the thick ascending limb.[153] Together these studies highlight how paracellular calcium reabsorption can be regulated in the thick ascending limb via altering the permeability of the tight junction.

Expression of the calcium sensing receptor (CaSR) has been reported in all segments of the renal tubule, however expression is greatest in the thick ascending limb (as reviewed in [153]). Activating CaSR mutations increase *Cldn14* transcription via down regulation of microRNAs, which in turn results in decreased calcium reabsorption.[153] Disease causing mutations in the CaSR highlight its important role in the regulation of renal calcium handling. Gain of function mutations result in autosomal dominant hypocalcemia.[154] Conversely, loss of function mutations in the CaSR cause hypercalcemia ranging from benign in familial hypocalciuric hypercalcemia (FHH) to potentially fatal neonatal severe hyperparathyroidism (NSHPT).[154, 155]

1.3.2. Transcellular pathway in the connecting tubule and distal convoluted tubule

Active transcellular calcium reabsorption involves apical entry into the cell, intracellular binding and shuttling, and then basolateral extrusion. The transient receptor potential vanilloid 5 (Trpv5) calcium channel is expressed in the distal convoluted tubule and connecting tubule of rat kidney.[156] In rabbit and rodent kidney, TRPV5 colocalizes with intracellular calcium binding protein, Calbindin-D_{28k} (CaBP28K encoded by gene *Calb1*) as well as PMCA and NCX1.[47, 156, 157] In *Trpv5* knockout mice, CaBP28K is dispersed in the cell whereas in wildtype mice, it is more abundant apically, suggesting an interaction between the proteins.[157] *Trpv5* knockout and *Trpv5*/*Calb1* double knockout mice have increased urinary calcium excretion from the distal nephron and maintain plasma calcium levels via compensatory intestinal hyperabsorption of calcium.[158, 159] The *Trpv5* knockout and double knockout mice compensate with increased expression of *Trpv6* and *S100g* in duodenum, suggesting a complementary regulation which is likely mediated by increased serum vitamin D.[158, 159] *Calb1* knockout mice do not display a phenotype of altered calcium homeostasis.[160] However, *Calb1*/*Vdr* double knockout mice weigh

30

less than half of wildtype mice at 2 months and still significantly less than single *Vdr* KO mice. These double knockout mice also display decreased tibia and femur length and total, trabecular, and cortical bone mineral density compared to *Vdr* single knockout mice. These observations suggest that *Calb1* is not necessary to maintain calcium homeostasis.[161] In human and mouse kidney, PMCA4 is expressed in the distal nephron and, in mice, is most highly expressed in cells with TRPV5.[66] This suggests a role in calcium reabsorption although its expression is not altered by calcium intake and *Pmca4* knockout mice do not display an altered calcium phenotype, thereby inferring compensation by another PMCA or a housekeeping role.[66, 162] An *Ncx1* knockout model is embryonically lethal due to its importance in cardiomyocyte development. However, work in cell culture models support the idea that NCX1 significantly contributes to basolateral calcium extrusion in the distal nephron.[163, 164]

1.3.3. Changes to Renal Calcium Reabsorption During Postnatal Development

Studies in humans and mice highlight the existence of changes in renal calcium handling with age. Table 1.2 summarizes the changes in expression of molecules implicated in renal calcium reabsorption throughout postnatal development. Premature and low birth weight infants have a high incidence of renal calcifications on ultrasound. This is likely due to their urine calcium excretion that can be 3-fold higher than the upper limit of normal for term infants.[165] In healthy children, urine Ca/Cr (calcium normalized to creatinine) declines by 50% between 1 month and 2 years of age, with a further reduction to 30% of neonatal values by 10 years of age.[166] In a Swedish cohort, urine Ca/Cr was significantly higher in children aged 2-6 years compared to 7-18 years and it significantly declined from 2 to 18 years of age. Importantly, urine Ca/Cr values did not correlate to milk intake suggesting inherent underlying differences in tubule

transport physiology.[167] Microperfusion of mouse proximal tubules shows a 36% reduction in relative sodium permeability (P_{Na}/P_{Cl}) and a 200% increase in relative bicarbonate permeability (P_{HCO3}/P_{Cl}) from 10 days of age to adult age in mice.[168] Together, these studies strongly suggest developmental changes in renal tubular calcium handling. Figure 1.3 illustrates current evidence of altered renal calcium reabsorption during suckling and post-weaning.

Table 1.2. Expression of molecules implicated in renal calcium reabsorption throughout development.

Age	< 3 weeks	3-8 weeks	> 8 weeks	Reference
Transcellular				
Trpv5	Yes	Yes	Yes	53, 71, 113, 156-158, 161
CaBP28K	Yes	Yes	Yes	53, 71, 113, 156-159, 161
Pmca1	ND	Yes	Yes	53, 71
Pmca4	ND	Yes	Yes	66, 162
Ncx1	ND	ND	Yes	53, 71, 164
Paracellular				
Cldn2	Yes	Yes	Yes	146, 168
Cldn6	Yes	ND	No	168
Cldn9	Yes	ND	No	168
Cldn12	ND	ND	Yes	87
Cldn14	ND	Yes	Yes	150-152
Cldn16	Yes	Yes	Yes	71, 148, 152, 168
Cldn19	ND	Yes	Yes	71, 148, 152

Note: Ages refer to age of rodent animal models. ND: no data
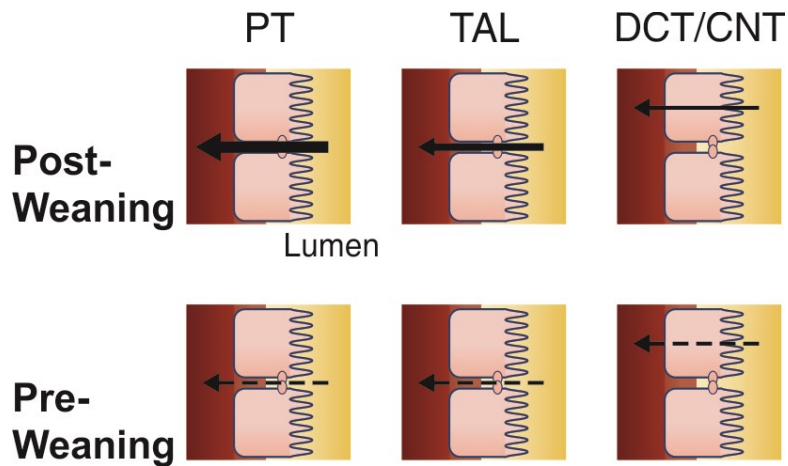
Figure 1.3. Renal calcium reabsorption during suckling and after weaning. An illustrative representation of evidence prior to thesis studies. The leftward arrow indicates net movement of calcium from lumen to serosa represents reabsorption. The thickness of the arrow represents relative reabsorption between tubule segments and ages. The dashed line indicates that reabsorption is inferred from expression studies or limited functional studies. Weaning is at 21 days in rodents. PT: proximal tubule; TAL: thick ascending limb; DCT: distal convoluted tubule; CNT: connecting tubule.

Few studies have investigated the molecular details of how renal calcium reabsorption changes with age. In mice, mRNA of *Trpv6* in the kidney is highest at 1 week and declines 3-fold by 3 weeks. Conversely, *Trpv5*, *S100g*, and *Calb1* mRNA increases by at least 2-fold from 1 week of age to peak at 3 weeks with a subsequent decline of 30% by 6 weeks of age. CaBP9K and CaBP28K protein expression follows a similar pattern.[113] TRPV5 and CaBP28K expression decline further after 10 weeks while *Trpv5* mRNA expression is not different from 3 to 12 months.[169, 170] *Trpv5* knockout mice at 10 weeks have increased intestinal calcium absorption as measured by appearance of $^{45}Ca^{2+}$ in the serum up to 12 minutes after oral gavage of radioisotope-spiked 100 µM dose of calcium.[169] This method assesses duodenal absorption by TRPV6 and is consistent with increased serum calcitriol in the KO mice.[169] It may be that, if the renal tubule is unable to reabsorb calcium in the young, the intestine compensates via hyperabsorption to ensure a positive calcium balance is maintained. Together, these studies suggest that transcellular calcium reabsorption is highest during suckling and then declines through maturation. A higher FECa at early ages suggests that there are also changes to the paracellular pathway. Indeed, at one day of age, expression of *Cldn6*, *Cldn9*, and *Cldn13* is detected in the kidney whereas no expression is detected in adult kidney.[168] When overexpressed in a kidney cell model, CLDN6 and CLDN9 led to increased TER and decreased permeability of chloride, P_{Na}/P_{Cl}, and P_{HCO3}/P_{Cl}.[171] If cation permeability is indeed reduced across the proximal tubule of neonates due to altered claudin expression, this may explain the increased calcium excretion observed at young ages. However, changes that occur in renal tubule calcium transport during postnatal development have not been fully delineated.

1.4. Regulation of Calcium Homeostasis

For over a hundred years, it has been recognized that serum calcium is maintained within a narrow range and that intake of a low calcium diet results in calcium being sacrificed from the bones in order to maintain plasma levels.[172] Serum calcium is tightly regulated by a set of complex interactions between the intestine, kidneys, and bones.[1] Ingested calcium is absorbed from the intestine into blood making it available for its various functional and structural roles. After calcium in plasma is filtered by the renal glomerulus, it is either reabsorbed back into the blood or excreted in the urine. Therefore, net calcium balance is determined by a combination of intestinal absorption or secretion and renal reabsorption or excretion. If intestinal and renal calcium losses are greater than intestinal absorption, a negative balance ensues. Importantly, calcium is sacrificed from bone to maintain blood levels to support vital cellular functions. Conversely, a positive calcium balance is fundamental to ensuring adequate plasma calcium to mineralize bone throughout development. Hormonal regulation of calcium homeostasis is not the primary focus of this thesis however a brief description is provided below.

A decrease in serum calcium causes the parathyroid gland to release parathyroid hormone (PTH). J. B. Collip at the University of Alberta was the first to use an extract from the parathyroid gland to reverse tetany in dogs and restore blood calcium to a normal level.[173] The parathyroid directly senses blood calcium concentration via the plasma membrane calcium sensing receptor (CaSR).[174-177] Binding of extracellular calcium to the CaSR in the parathyroid, prevents release of PTH.[178] PTH exerts its effect on cells by binding to the PTH receptor (PTHR), a G protein-coupled receptor in the target tissue.[179, 180] High PTH levels increase bone resorption to release calcium into the blood.[181, 182] PTH also acts on the kidney to increase transcription of *Cyp27b1* in the proximal tubule encoding 1α-hydroxylase to increase calcitriol

sythesis.[183-187] The primary action of calcitriol is to increase intestinal calcium absorption through binding to VDR (as reviewed in [187]). As reviewed in section 1.2.4 of this chapter, calcitriol increases expression of *Trpv6*, *Pmca1* and *Cldn2*. Calcitriol also suppresses expression of renal *Cyp27b1* in feedback regulation.[186] Similar to its role in the intestines, calcitriol, downstream of PTH, increases active calcium reabsorption in the distal nephron via transcriptional regulation (as reviewed in [1]). In addition, PTH has calcitriol-independent actions on the distal nephron. It increases transcription of *Trpv5*, *Calb1*, and *Ncx* as well as directly increasing the open probability of the TRPV5 channel thereby increasing calcium reabsorption (as reviewed in [2]).

1.5. Rationale for Work

A review of the literature highlights knowledge gaps in understanding the molecular mechanisms allowing infants and children to maintain a positive calcium balance during critical periods of growth. Previous work has addressed calcium homeostasis during fetal development[3], during pregnancy and lactation[15], and in ageing.[188, 189] Complementary regulation of calcium handling in the intestines and kidneys together determines net balance. All calcium must be attained by absorption via the intestines and research to date highlights this organ as likely increasing absorptive capacity to meet increased requirements for growth. This is illustrated by a study in infants where calcium retention in bones mirrors net intestinal absorption.[102] Previous work is limited but highlights important alterations in transcellular and paracellular intestinal calcium absorption pathways early in life.

1.6. Aim and Hypotheses to be Tested

The overall aim of this thesis is to delineate the molecular details contributing to a positive calcium balance in postnatal development.

Specific hypotheses to be tested are:

1. We hypothesize that the paracellular pathway predominates along the small intestine early in life and that a transition to predominantly transcellular absorption across the duodenum and colon occurs after weaning.

2. We hypothesize that paracellular permeability across the intestine is conferred by claudins-2 and -12.

3. We hypothesize that EGF, a bioactive compound in breast milk, increases intestinal claudin-2 expression, thereby enabling increased intestinal calcium transport to maximize uptake of this mineral from the diet.

   Understanding the underlying molecular physiology of how infants and children attain a positive calcium balance will provide insight into how intestinal diseases increase risk of osteoporosis. Additionally, understanding the regulation of optimal intestinal calcium absorption may lead to therapeutic developments for infants or any one at risk of osteoporotic fractures.

Chapter 2

Transcellular Calcium Absorption Across the Small Intestine during Postnatal Development

2.1. Abstract

Background & Aims: Intestinal Ca^{2+} absorption early in life is vital to achieving optimal bone mineralization. The molecular details of intestinal Ca^{2+} absorption have been defined in adults, after peak bone mass is obtained, but are largely unexplored during development. We sought to delineate the molecular details of transcellular Ca^{2+} absorption during this critical period.

Methods: Expression of small intestinal and renal calcium transport genes was assessed using quantitative PCR. Net calcium flux across small intestinal segments was measured in Ussing chambers, including after pharmacological inhibition or genetic manipulation of TRPV6 or $Ca_v1.3$ calcium channels. Femurs were analyzed using micro-CT and histology.

Results: Net TRPV6 mediated Ca^{2+} flux across the duodenum was absent in pre-weaned (P14) mice but present post-weaning. In contrast, we found significant transcellular Ca^{2+} absorption in the jejunum at two weeks but not 2 months of age. Net jejunal Ca^{2+} absorption observed at P14 was not present in either *Trpv6* mutant (D541A) mice, nor $Ca_v1.3$ knockout mice. We observed significant nifedipine sensitive transcellular absorption across the ileum at P14 but not 2 months. $Ca_v1.3$ knockout pups exhibited delayed bone mineral accrual, compensatory nifedipine insensitive Ca^{2+} absorption in the ileum and increased expression of renal Ca^{2+} reabsorption mediators at P14. Moreover, weaning pups at 2 weeks reduced jejunal and ileal $Ca_v1.3$ expression.

Conclusions: We have detailed novel pathways contributing to transcellular Ca^{2+} transport across the distal small intestine of mice during development, highlighting the complexity of the multiple mechanisms involved in achieving a positive Ca^{2+} balance early in life.

2.2. Graphical Abstract

Transcellular Intestinal Calcium Absorption
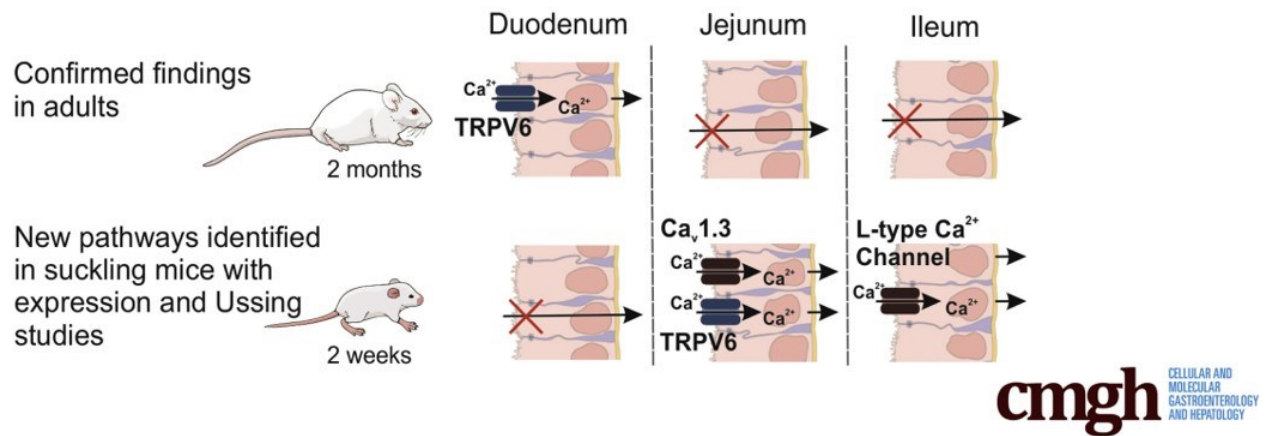
Figure 2.1. Graphical abstract of transcellular calcium absorption pathways of the small intestine of suckling and adult mice.

2.3. Introduction

The greatest net positive calcium (Ca^{2+}) balance occurs in infancy.[190] This process is vital to mineralizing bone throughout development.[70] An estimated 60% of osteoporosis risk can be attributed to a failure to reach optimal peak bone mass density by early adulthood.[7] In women, the incidence of fractures due to osteoporosis is greater than breast cancer and cardiovascular disease combined and represents a major health care burden.[17, 191] Infancy and childhood are thus critical periods for long-term skeletal health.

Bone Ca^{2+} deposition rate is greatest in infancy and is a direct function of intestinal absorption.[31, 190] Unfortunately, studies to date have not fully examined how intestinal absorption is maximized in infants to meet increased demand. Intestinal Ca^{2+} absorption can occur via passive paracellular or active transcellular pathways.[41] The current hypothesized model of transcellular absorption in both humans and rodents consists of apical entry into the enterocyte through the Ca^{2+}-selective channel, transient receptor potential vanilloid 6 (TRPV6), intracellular binding to calbindin-D$_{9k}$, and basolateral extrusion via the plasma membrane Ca^{2+}-ATPase 1 (PMCA1) or sodium-calcium exchanger (NCX).[1, 53, 66] Interestingly, *Trpv6* knockout or mutant mice (*Trpv6 ^{mt}*) do not display a severe Ca^{2+} wasting phenotype, strongly inferring another apical Ca^{2+} entry channel.[50, 51, 53] $Ca_v1.3$ has been proposed as a complementary channel to TRPV6.[56, 57]

Consistent with this, one group has reported that global *Cacna1d* knockout ($Ca_v1.3$ KO) mice have lower weight and decreased bone mineral density at 20 weeks in males, however, others report normal growth.[192, 193] Regardless, the role of $Ca_v1.3$ in intestinal Ca^{2+} absorption has not been directly assessed.

The molecular components of the proposed transcellular absorption pathway are expressed in the duodenum and large intestine of adult animals while paracellular absorption or

secretion predominates in the jejunum and ileum.[39, 59, 108] In contrast, existing evidence suggests that alternative Ca^{2+} absorption mechanisms are present during development compared to older animals.[108, 113, 194] However, the exact molecular details conferring increased intestinal Ca^{2+} absorption and their contribution to bone mineralization early in life have yet to be determined.

We therefore sought to delineate the molecular details of transcellular Ca^{2+} absorption from the small intestine and how they contribute to bone mineralization during early postnatal development. We report net transcellular Ca^{2+} flux prior to weaning across jejunum and ileum but not duodenum at 2 weeks with the opposite pattern present at 2 months. Further, we find that TRPV6 and $Ca_v1.3$ are necessary for this absorption across jejunum and that $Ca_v1.3$ may mediate absorption across ileum although compensation is present in *Cacna1d* KO pups. Furthermore, *Cacna1d* KO pups exhibit delayed bone mineralization and renal compensation to increase Ca^{2+} reabsorption. Together, this work defines the molecular details in mice of how the small intestine facilitates increased demand of Ca^{2+} early in life to meet requirements of growth.

2.4. Materials and Methods

Animals

FVB/N (Taconic labs, North America) and *Trpv6* ^{mt} mice[52] were maintained on a 12-hour light/dark cycle with drinking water and chow ad libitum (Lab Diet Irradiated Rodent Diet 5053 4% fat, 0.81% calcium). Experiments were approved by the University of Alberta animal ethics committee, Health Sciences Section (AUP00000213). Experiments on the *Cacna1d* and HA-tagged *Cacna1d* KO mice[193] were conducted in agreement with the European Communities Council Directive (2010/63/EU) in accordance with the German law on the use of laboratory

animals and approved by the regional board for scientific animal experiments of Saarland. *Trpv6*
mt mice were genotyped by PCR.[52, 195] For the early weaning experiments, half of the mice in a
litter (FVB/N mice) were weaned at P12 to the standard rodent chow diet while the littermates
remained with the dam. After 48 hours, tissue was collected from all pups. Experiments
involving mice include both female and male mice in approximately equal numbers except for
the bone phenotype analysis of P14 *Trpv6* *mt* mice. Individual data points represent biological
replicates from one animal.

Isolation of Tissue

Murine tissue was taken as previously described,[66] snap frozen in liquid nitrogen and stored at -
80°C until use. At each age, the length of the whole small intestine was measured. The
duodenum was defined at the first ninth, the jejunum as the second two-ninths, and ileum as the
remaining two-thirds of the length. For expression studies, tissue was taken from the middle of
these defined sections. For experiments in Ussing chambers at P14, the duodenum was defined
as the first 2 cm, jejunum from 5-7 cm and ileum as 14-16 cm from the pyloric sphincter. For 2-
month-old mice, the duodenum was taken as the first 4.6 cm, jejunum as 10-14.8 cm and ileum
as 22-26.8 cm.

Quantitative real-time PCR

Total RNA was isolated from tissue as described.[196] Briefly, RNA was isolated using the TRIzol
method (Invitrogen, Carlsbad, CA, Cat# 15596026) and treated with DNAse (ThermoScientific,

Vilnius, LT, Cat# EN0521). RNA quality and quantity were measured with a Nanodrop 2000 (Thermo Fisher Scientific, Waltham, MA USA). 5µg of RNA was then reverse transcribed into cDNA (SuperScript II, Invitrogen, Carlsbad, CA, Cat# 18064014). Quantitative real-time PCR was performed in triplicate for each sample using TaqMan Universal Master Mix II (Applied Biosystems, Foster City, CA, Cat# 4440042) and specific primers and probes on a ABI 7900HT Sequence Detection System (Applied Biosystems, Foster City, CA) as previously.[196] Primer and probe sequences for murine *Trpv6*, *S100g*, *Atp2b1*, *Slc8a1*, *Gapdh*, *18s*, and *β-Actin* have been published elsewhere.[66, 196] Sequences for murine *Cacna1d* primers and probe (F: TCCTCTTCCTCTTCACCTACTG, R: AGTCAACCAGATAGCCAACAG, Probe: CCCTTACCCGCCCTGTGATGT) were created using IDT software (Integrated DNA Technologies, San Diego, CA) and specificity was assessed with NCBI Primer-BLAST. Samples were quantified using the standard curve method where the standard curve was made of serial dilutions of cDNA from a positive control or the target tissue. A C_t value greater than 35 was considered negligible.

Immunoblotting

Tissue was lysed in RIPA buffer (50mM Tris, 150mM NaCl, 1mM EDTA, 1% Triton-X, 1% SDS, 1% NP-40, pH 7.4) with (PMSF to 1:1000 concentration (Thermo Scientific, Rockford, IL, Cat# 36978) and protease inhibitor set III to 1:100 concentration (Calbiochem, Cat# 535140) for one hour on ice and then centrifuged for 10 minutes at 14,000 cf at 4°C. The protein content of the supernatant was quantified against a standard curve of serial dilutions of bovine serum

albumin (Sigma, St. Louis, MO, Cat# A-9647) using a Nanodrop 2000 (Thermo Fisher Scientific, Waltham, MA USA).

For immunoblots, 150 µg of protein from total lysate was run on a 15% SDS-PAGE, electrotransferred to 0.45 µM PVDF (Merck Millipore, Cat# IVPH00010) and blocked overnight in TBST with 5% milk. The blot was then incubated overnight at 4°C with either rabbit anti-calbindin-D$_{9k}$ (1:1000, Swant, Switzerland, Cat# CB9) or mouse anti-GAPDH (1:1000, ThermoFisher Scientific, Rockford, IL, Cat# MA5-15738) followed by incubation for 1 hour at room temperature with HRP conjugated donkey anti-rabbit or goat anti-mouse IgG (1:5000, Santa Cruz Biotechnology Inc., Cat# sc-2005, sc-2317) and visualized using Clarity Western ECL (BioRad, USA, Cat# 1705061) and a ChemiDoc Touch imaging system (BioRad, USA). Protein was semi-quantified with ImageJ (U. S. National Institutes of Health, Bethesda, Maryland, USA) and each sample normalized to GAPDH as a loading control and one age group as indicated to enable the combination of results from several blots.

Micro-CT analysis of femora

Femora from P14 *Trpv6* [mt] and *Cacna1d* KO and wild-type mice were scanned by µCT at a resolution of 6.5 µm (Bruker µCT SkyScan 1172). The bones were wrapped into wet paper, placed in a plastic holder and mounted vertically in the sample chamber for scanning. Voltage and current X-rays source were adjusted to 49 kV and 200 µA, respectively, beam hardening was reduced using a 0.5 mm Al filter; the exposure time was 5 s and scanning angular rotation was set to 180° with an increment of 0.4 deg rotation step.[197] NRecon (1.6.10.6) was used to reconstruct and DataViewer (1.5.1.2) and CT Analyser (1.16.4.1+, all from Bruker) were used for bone analysis.

A total number of fifty cross-sections (6.5 µm) exactly in the middle of femoral shaft were analyzed to access the cortical bone volume, endocortical volume, cross-sectional thickness, perimeter and mineral density.

Non-decalcified bone histology

Femurs were fixed in 4%PFA at 4°C and incubated in 30% (w/v) sucrose solution overnight. Samples were then embedded in an anterior, posterior orientation in tissue freezing medium (SCEM; CEM-001, Section-Lab Co Ltd) according to Kawamoto and Shimizu[198] and stored at -80°C until sectioning. Four 6 µm sections per bone were made in an anterior-posterior orientation at two different regions spaced at least 100 µm from each other. Two sections were stained with a modified toluidine blue staining to visualize cartilage. The thickness of the growth plate was determined from the middle of the section. The mean of either two per bone was taken as a single value. Two sections were stained with Alizarin red to visualize calcified bone (red) and to calculate trabecular parameters as previously published.[199]

Immunohistochemistry

Sections of the jejunum were prepared and fixed with Zamboni's fixative solution at 4°C for 12 h and transferred to 30% (w/v) sucrose solution at 4°C for 12 h. Samples were embedded in tissue freezing medium OCT (optical cutting temperature, Leica Microsystems GmbH, Wetzlar, Germany) and cut into 7 µm sagittal sections with a cryostat. Sections were incubated with primary anti-HA antibody overnight (1:1000, clone 3F10 Roche, Switzerland, Cat# 11867431001)

followed by one-hour incubation with a secondary antibody (donkey anti rat-Cy3, JacksonImmuno Research, UK, Cat# 712-165-150) followed by incubation in the presence of 1 μg/mL bisbenzimide (Hoechst 33342, Sigma-Aldrich, Germany) for five minutes. Images were collected on an Axio Scan.Z1 microscope via the Plan-Apoichromat 20x/0.8 M27 objective, equipped with AxioVision 4.7 or Zen 2.3 software (all from Zeiss, Oberkochen, Germany).

Ussing Chamber Studies

Net ^{45}Ca flux (J_{Ca}) was measured essentially as previously.[39] Fresh intestinal tissue was excised from mice, linearized, mounted onto Ussing chamber sliders and placed into the corresponding P2400/P2300 Ussing Chambers connected to a VCC Multichannel Voltage/Current Clamp (Physiologic Instruments, San Diego, USA). For all experiments, whole-thickness intestinal tissue was used, as our previous work found no difference between stripped tissue and full thickness for Ca^{2+} fluxes across all the intestinal segments.[39] A maximum of 4 segments were mounted per tissue and the mean of biological replicates was used for analysis. For experiments using P2407B sliders, the internal resistance offset of the Voltage/Current clamp was increased by the manufacturer to compensate for the artificially increased fluid resistance created by the small aperture of the sliders.

Tissue was bathed on both sides with 4 mL Kreb's Ringer Buffer (140 mM Na, 5.2 mM K, 120 mM Cl, 1.2 mM Mg, 1.2 mM Ca, 2.8 mM PO_4, 2.5 mM HCO_3: pH = 7.4) at 37°C and bubbled with 5% CO_2 (balance O_2).[200] The buffer contained 2 μM Indomethacin (from 10 mM stock solubilized in 100% EtOH) (Sigma, St. Louis, MO, Cat# I7378) bilaterally and 0.1 μM Tetrodotoxin (Alomone Labs, Cat# T-550) basolaterally to inhibit prostaglandin synthesis and

48

neuronal activity.[201] The basolateral side contained 10 mM dextrose and the apical side contained 10 mM mannitol to balance osmolarity.

After 15 minutes under open circuit conditions, 2 mV pulses were applied 3 times across the tissue for 20 seconds and the resulting current was recorded to calculate the resistance of the tissue using Ohm's law. One side of each chamber was then spiked with ^{45}Ca (5 µCi/mL) (PerkinElmer Health Sciences, Cat# NEZ013001MC) and the potential difference clamped to 0 mV across the tissue, and time was set to 0 min. Thereafter, samples of 50 µL were taken in quadruplicate from both sides at 15-minute intervals for four time points. For experiments with ruthenium red (Sigma, Oakville, Canada, Cat# R275-1), a 5 mM stock was added apically to a final concentration 100 µM at time 45 min and, after 20 minutes of incubation, samples were collected for three time points at 15-minute intervals. Where indicated, nifedipine (Sigma, Cat# N7634) was added to a final concentration 10 µM apically.[57] In P14 FVB/N mice (Figure 4H), experiments were performed under vehicle and nifedipine conditions on separate animals. For P14 *Cacna1d* KO mice (Figure 4J), experiments were performed on tissue from the same mouse as above for experiments with ruthenium red. After samples were collected, the tissue was clamped at 2 mV, as described above, to calculate the post-experiment resistance. Data were excluded if the transepithelial resistance changed by more than 40%.[39] To further assess tissue viability, forskolin (LC Laboratories, Woburn, MA, Cat# F-9929) was added to a final concentration of 10 µM bilaterally. The tissue was considered viable if an increase in short circuit current of greater than 50% was observed.[39]

Radioactivity of samples was measured with an LS6500 Multi-Purpose Scintillation Counter (Beckman Coulter, Brea, CA) as an average count per minute (cpm) over three minutes. Ca^{2+} flux (J_{Ca}^{2+}) was calculated as the rate of appearance of $^{45}Ca^{2+}$ in the "cold" chamber (*i.e.* not

spiked with $^{45}Ca^{2+}$) in cpm/h divided by the specific activity of the hot chamber (*i.e.* spiked with

$^{45}Ca^{2+}$) in cpm/mol and normalized to surface area of tissue exposed.[202] Net J_{Ca}^{2+} was calculated

as flux from apical to basolateral side minus flux from basolateral to apical side for tissues with a

difference in resistance less than 25%.[39] As the potential difference across the tissue was

clamped to 0 mV throughout the experiment, and there were equimolar concentrations of Ca^{2+} in

both hemichambers, there was no electrochemical gradient to drive net paracellular diffusion of

Ca^{2+}. Net J_{Ca}^{2+}, therefore, represents transcellular flux and a positive value indicates net

absorption.[39]

Although transcellular Ca^{2+} absorption is known to occur across the duodenum of adult

rodents, previous studies have not consistently found net absorption with protocols similar to

those used in the current study.[1, 39] It is known that TRPV6 is activated under hyperpolarizing

conditions.[56] We, therefore, sought to optimize experimental conditions for absorption in the

duodenum by inducing a hyperpolarized state. Previously, it has been shown that apical

hyperosmolar conditions induce hyperpolarization of the apical membrane of epithelial cells.[203]

We therefore increased the osmolarity of our apical buffer by 100 mOsm (Osmometer Model

3D3, Advanced Instruments, Inc.) with the addition of 100 mM mannitol. Net J_{Ca}^{2+} under apical

hyperosmolar conditions across duodenum of 2-month old FVB/N mice was 42.65 ± 8.7

$nmol \cdot hr^{-1} \cdot cm^{-2}$ compared to 26.26 ± 7.5 $nmol \cdot hr^{-1} \cdot cm^{-2}$ (n = 7/group, *P* = 0.18, two-tailed

Student's t-test). Net J_{Ca}^{2+} across the duodenum of P14 FVB/N mice, under apical hyperosmolar

conditions was not different than under isoosmolar conditions, 18.6 ± 16.0 $nmol \cdot hr^{-1} \cdot cm^{-2}$ vs

5.86 ± 2.85 $nmol \cdot hr^{-1} \cdot cm^{-2}$ (n= 6/group, *P* = 0.45, two-tailed Student's t-test) and not

significantly different from 0 (*P* = 0.3, one sample t-test). Data presented for the net J_{Ca}^{2+} across

duodenum of all mice was obtained under apical hyperosmolar conditions.

Quantification and Statistical Analysis

Statistical analyses were carried out using GraphPad Prism 7.03 (GraphPad Software Inc., San Diego, USA). Groups were compared by unpaired t-test, paired t-test, one-way ANOVA with Dunnett's multiple comparisons test, or Mann-Whitney test as indicated in figure and table legends. All n indicated in figure legends represents samples from independent mice. The Brown-Forsythe test was used to assess equality of group variance. A non-parametric test was performed when variance was significantly different between groups. $P < 0.05$ was considered significant. All authors had access to the study data and had reviewed and approved the final manuscript. Figures were created using CorelDRAW 2017 and the Mind the Graph platform (www.mindthegraph.com).

2.5. Results

2.5.1. Expression of Transcellular Ca^{2+} Absorption Mediators is Absent from the Duodenum of Young Mice

To assess how transcellular Ca^{2+} absorption changes with age, we first examined the expression of known mediators in the duodenum prior to weaning at postnatal day 1 (P1), P7 and P14 and after weaning at 1 - 6 months in wildtype (WT) mice (Figure 2.2). *Trpv6* was undetectable at P1 and increased 6-fold from P14 to 1 month. *Cacna1d,* encoding the L-type Ca^{2+} channel $Ca_v1.3$, was greatest at P7 and 3 months. Expression of *S100g*, encoding calbindin-D_{9k} was very low at P1, P7 and P14, but increased with age. *Atb2b1*, encoding the basolateral PMCA1, followed a similar pattern. *Slc8a1*, encoding NCX1 showed bimodal pattern with greater expression prior to weaning and at 6 months. Calbindin-D_{9k} protein was detectable by immunoblot only at and after

1 month. Together, these results suggest that the transcellular Ca^{2+} absorption pathway is poorly expressed or not present before weaning in the duodenum.

2.5.2. Net Ca^{2+} Absorption Occurs Across the Duodenum at 2 Months and is Mediated by Transient Receptor Potential Vanilloid 6

To functionally validate the expression pattern changes observed with age, we sought to examine Ca^{2+} flux (J_{Ca}^{2+}) across the duodenum of mice at P14 and 2 months. Net J_{Ca}^{2+} from P14 mice was not different from zero, while net J_{Ca}^{2+} from 2-month mice demonstrated absorption (Figure 2.2H). Net J_{Ca}^{2+} was significantly decreased in the presence of 100 µM apical ruthenium red,[204] implicating TRPV6 activity (Figure 2.2I). This experiment was performed with hyperosmolar apical buffer to stimulate Trpv6 activity,[56, 203] however, this decrease was also noted with ruthenium red under isoosmolar conditions (Figure 2.2J). Similarly, net J_{Ca}^{2+} was significantly greater in WT compared to *Trpv6* mutant (*Trpv6 ^{mt}*) littermates expressing a pore mutation (D541A) rendering the channel non-permeable to Ca^{2+}.[52] Further, ruthenium red significantly decreased net J_{Ca}^{2+} in WT but not *Trpv6 ^{mt}* mice (Figure 2.2K). Importantly, the drug had no effect on net J_{Ca}^{2+} in P14 mice (Figure 2.2L). These results demonstrate TRPV6 mediated, transcellular Ca^{2+} absorption across duodenum which develops by 2 months of age.
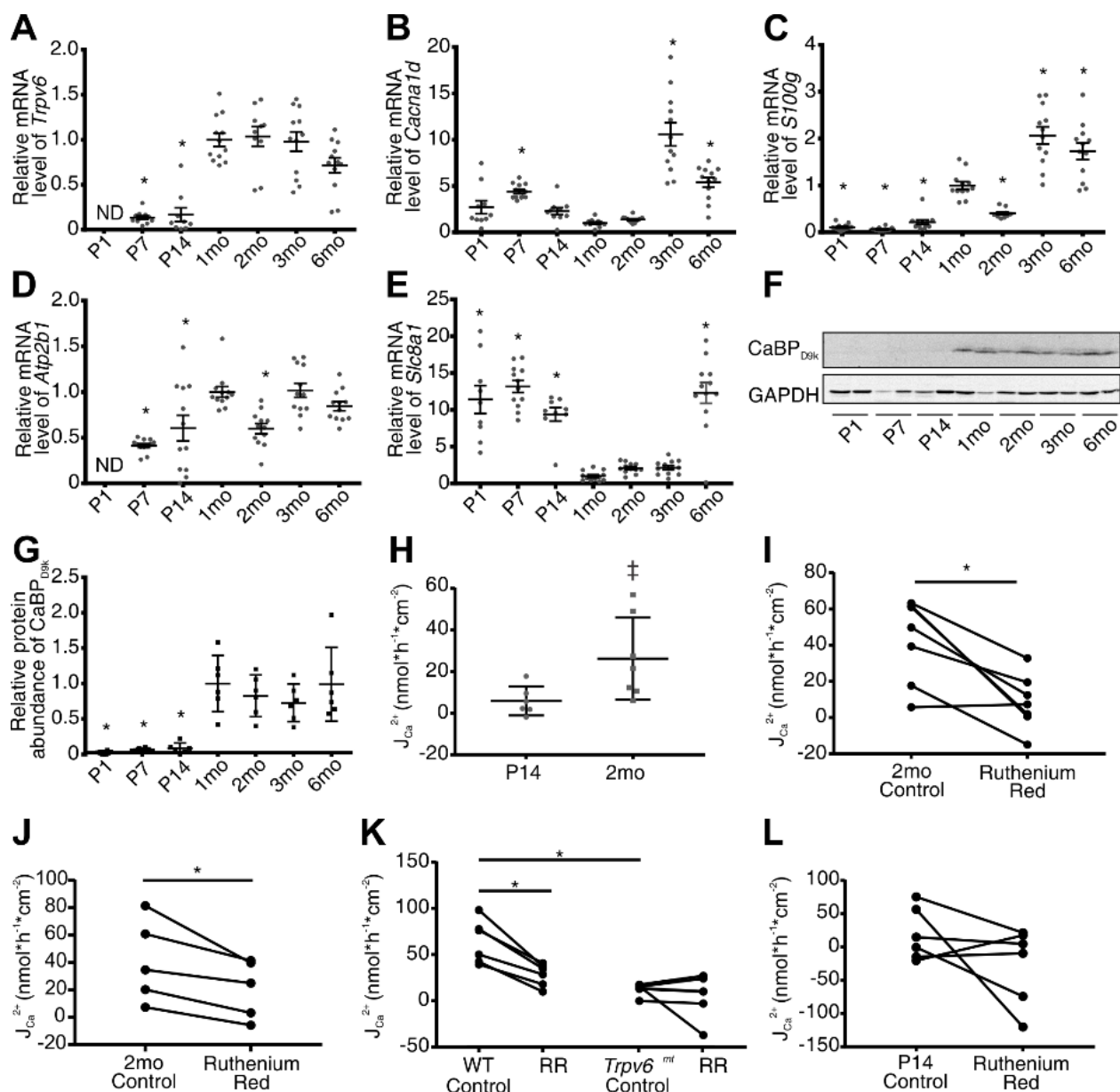
Figure 2.2. Transcellular Ca²⁺ flux across the duodenum is not detectable at P14 but mediated by TRPV6 in 2-month-old mice. Relative expression of (A) *Trpv6* (B) *Cacna1d* (C) *S100g* (D) *Atb2b1* and (E) *Slc8a1* in the duodenum across ages (n = 12/group). Expression is normalized to *Gapdh* and relative to 1-month. (F) Representative immunoblot from three replicates and (G) semi-quantification of calbinidin-D₉ₖ. Protein abundance is normalized to GAPDH and presented relative to the 1-month group (n = 6/group). Groups compared by 1-way ANOVA with Dunnett's multiple comparisons test, *P < 0.05 compared to 1-month group. (H) Net J$_{Ca}$²⁺ across *ex vivo* sections of mouse duodenum is not different from zero in P14 mice (n = 6, P = 0.095) but significantly greater than 0, consistent with absorption, in 2-month mice (n = 7,

‡P = 0.013) (two-tailed, one-sample t-test). Net J_{Ca}^{2+} is significantly reduced in 2-month mice after addition of 100 µM ruthenium red apically under (I) apical hyperosmolar (n = 6, two-tailed, paired t-test *P = 0.006) and (J) isoosmolar conditions (n = 5, two-tailed, paired t-test *P = 0.02). (K) Net J_{Ca}^{2+} is significantly lower in 2-month-old *Trpv6^{mt}* mice compared to WT litter mates (n = 6/group, two-tailed, unpaired t-test *P < 0.001). 100 µM apical ruthenium red significantly decreases net J_{Ca}^{2+} in WT (*P = 0.002) but not *Trpv6^{mt}* mice (P = 0.474) (two-tailed, paired t-test) Both paired experiments were performed under apical hyperosmolar conditions. (L)100 µM ruthenium red did not decrease net J_{Ca}^{2+} in P14 mice (n =6, two-tailed, paired t-test, P = 0.2). Data are presented as mean ± SEM. ND, not detected; mo, month; WT, wildtype; *Trpv6^{mt}*, *Trpv6* mutant; RR, ruthenium red.

2.5.3. Mice Express Transcellular Ca²⁺ Absorption Mediators in the Jejunum Prior to Weaning

We next examined the expression of the transcellular pathway in the jejunum (Figure 2.3). To our surprise, we identified *Trpv6* expression from P1 to P14 A). Minimal expression was detected at 1 month, but not at any older age. *Cacna1d* expression was significantly higher at P1 to P14 relative to 1 month of age. Similarly, expression of *S100g*, *Atp2b1*, and *Slc8a1* were significantly greater from P1 to P14. Calbindin-D$_{9k}$ protein was detected from P1 to 1 month but was nearly undetectable from 2 to 6 months. Ca$_v$1.3 has been identified apically in the jejunum of rats.[57] To determine if we could detect Ca$_v$1.3 protein in the jejunum of P14 pups, we fixed tissue from mice expressing HA-tagged *Cacna1d*.[205] We observed HA immunoreactivity in the jejunum of HA-*Cacna1d* mice but not WT mice (Figure 2.4). Together these results suggest the presence of a transcellular Ca²⁺ absorption pathway in the jejunum in the first 2 weeks of life in mice with apical entry mediated by either TRPV6, Ca$_v$1.3 or both channels.

2.5.4. TRPV6 and Ca$_v$1.3 Are Required for Net Transcellular Ca²⁺ Absorption Across the Jejunum at P14

Given the expression patterns observed, we next sought to measure transcellular J_{Ca}^{2+} across the jejunum. We found net apical to basolateral J_{Ca}^{2+} in P14 but not 2-month mice (Figure 2.3G). To specifically implicate TRPV6 in this process, we repeated the studies using *Trpv6^{mt}* P14 mice. We observed significantly lower net J_{Ca}^{2+} across jejunum of *Trpv6^{mt}* mice compared to WT littermates (Figure 2.3H). Together, these studies infer a role for TRPV6 in Ca²⁺ absorption across the jejunum of pre-weaned mice.

Next, we aimed to determine the potential role of the L-type Ca^{2+} channel $Ca_v1.3$ in net Ca^{2+} absorption across jejunum of P14 mice. We first examined the expression of other, potentially confounding, L-type Ca^{2+} channels, specifically *Cacna1s*, *Cacna1c*, and *Cacna1f*. *Cacna1s* and *Cacna1f* were not detected at P14 or 2 months. However, *Cacna1c*, encoding $Ca_v1.2$, was detected at both ages with 5-fold greater expression at P14 (Figure 2.3I). Importantly, $Ca_v1.2$ is more sensitive than $Ca_v1.3$ to nifedipine so this drug could not be used to specifically implicate $Ca_v1.3$.[206] To specifically implicate $Ca_v1.3$ in net J_{Ca}^{2+} observed at P14, we repeated the Ca^{2+} flux studies in *Cacna1d* KO pups.[193] Net J_{Ca}^{2+} was abolished in *Cacna1d* KO compared to WT animals, indicating that $Ca_v1.3$ is required for Ca^{2+} absorption from the jejunum of P14 mice (Figure 2.3J).
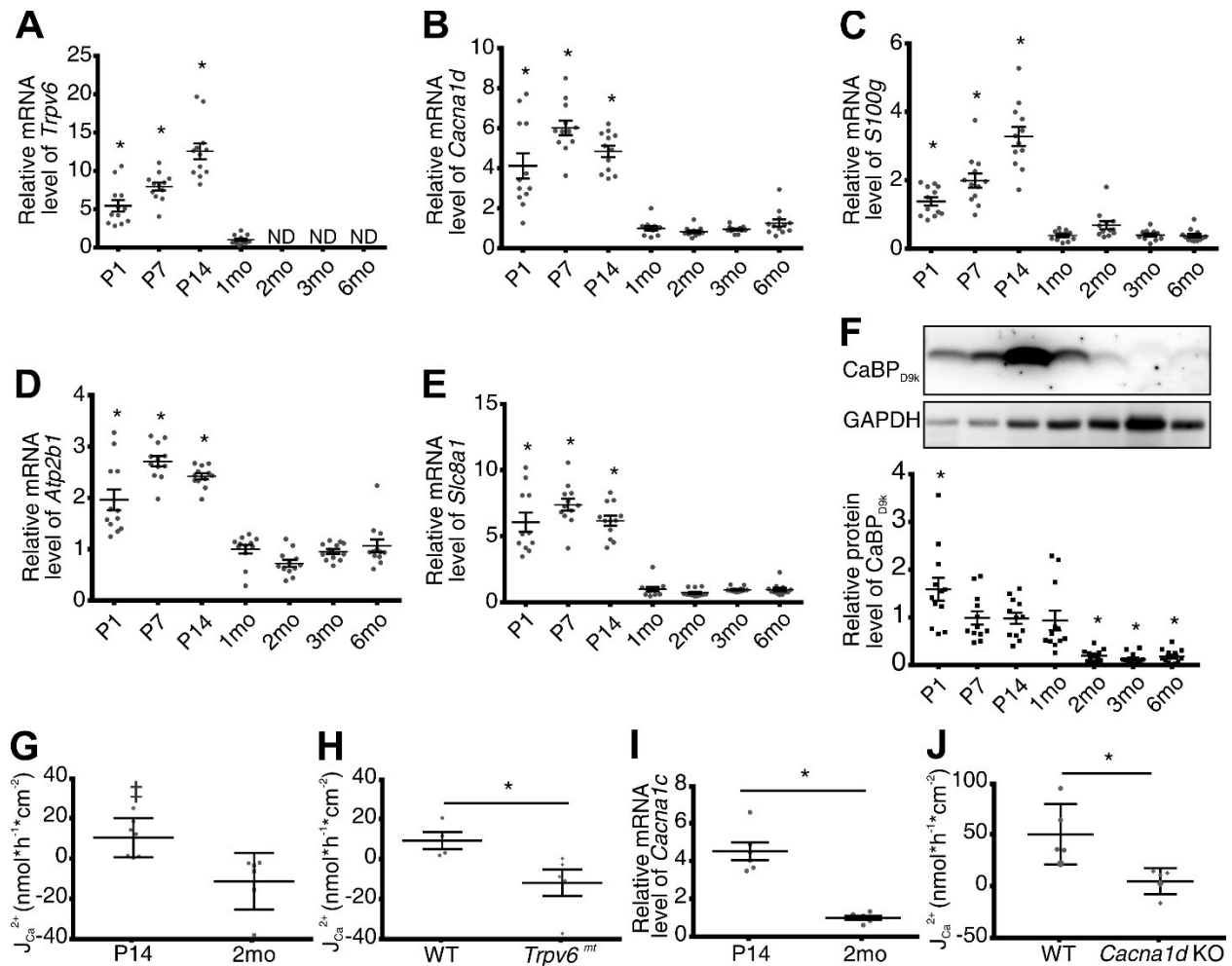
Figure 2.3. Net Ca²⁺ absorption across the jejunum of P14 mice is mediated by TRPV6 and Ca_v1.3 and is not present at 2 months. Relative expression of (A) *Trpv6*, (B) *Cacna1d*, (C) *S100g*, (D) *Atp2b1*, and (E) *Slc8a1* by age (n = 12/group). Expression is normalized to *Gapdh* and relative to 1 month. (F) Representative calbindin-D9k (CaBPD9k) immunoblot of 12 replicates and quantification by age (n = 12/group). Groups compared by 1-way analysis of variance with Dunnett multiple comparisons test. *$P < .05$ compared with 1-month group. (G) Net J_{Ca}^{2+} across *ex vivo* sections of mouse jejunum are greater than 0, indicating absorption at P14 (n = 7; ‡$P = .03$) but not 2-month-old mice (n = 6; $P = .11$; two-tailed, one-sample t test). (H) Net J_{Ca}^{2+} is significantly reduced across the jejunum of P14 *Trpv6*^mt mice compared with WT littermates (n = 4 WT and 5 mt; two-tailed unpaired t test; *$P = .04$). (I) Greater expression of *Cacna1c*, encoding Ca_v1.2, at P14 (n = 6/group; two-tailed unpaired t test; *$P < .0001$) normalized to *Gapdh*. (J) Significantly reduced net J_{Ca}^{2+} across the jejunum of P14 *Cacna1d* KO mice compared with WT mice (n = 5/group; Mann-Whitney test; *$P = .008$). Data are presented as mean ± standard error of the mean. CaBPD9k, calbindin-D9k; ND, not detected; *Trpv6*^mt, *Trpv6* mutant.
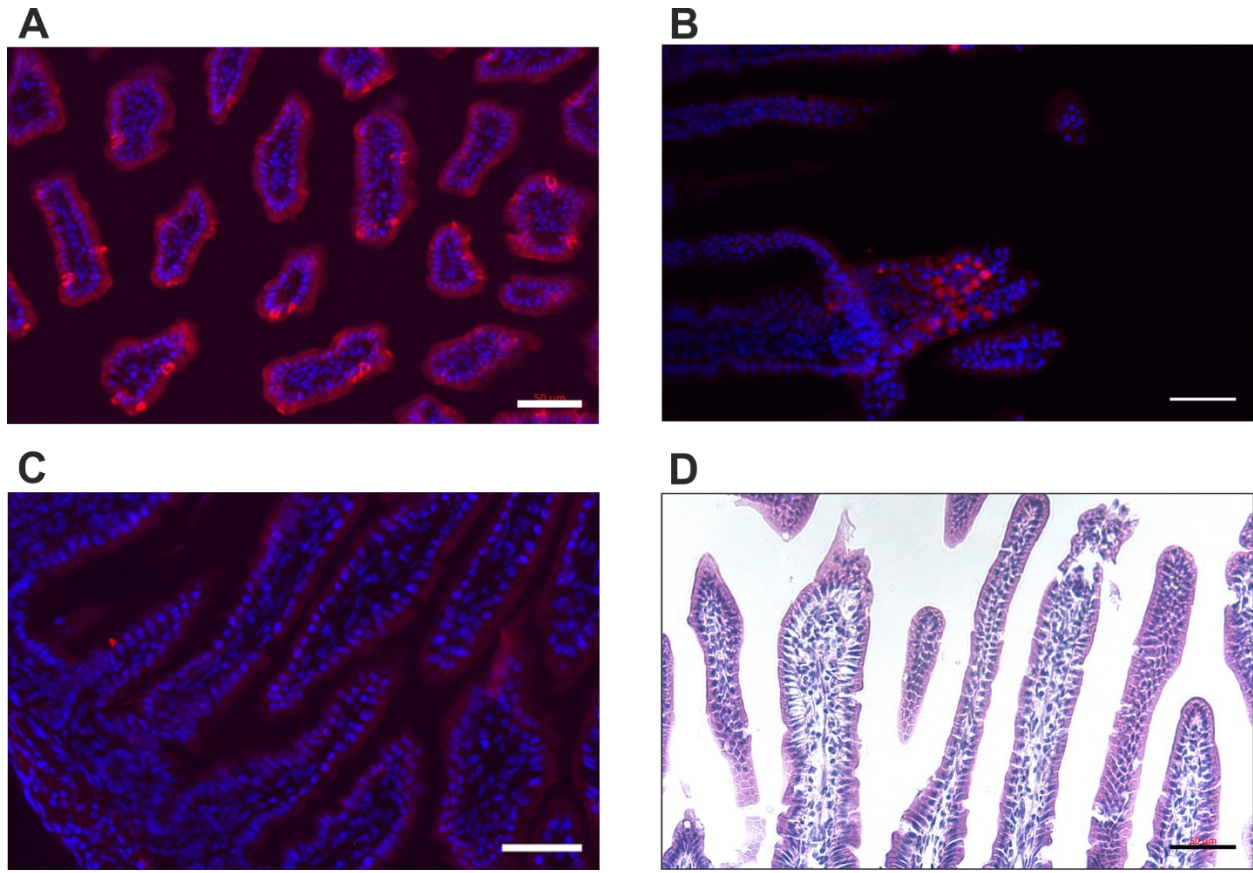
Figure 2.4. Ca$_v$1.3 expression in jejunum of P14 mice. (A and B) Immunoreactivity (red) of HA reveals apical localization of HA-tagged Ca$_v$1.3 on sections (7 µm) of jejunum from P14 mice expressing HA-tagged *Cacna1d*. (C) Section of jejunum from WT mice (control) shows no HA immunoreactivity. Cell nuclei were stained with bisbenzimide (Hoechst 33342) (blue). (D) Hematoxylin-eosin staining of sections of jejunum of Ca$_v$1.3-HA mice. Scale bars: 50 µm.

2.5.5. The Ileum of Younger Animals Expresses Transcellular Ca^{2+} Absorption Mediators

The presence of a transcellular Ca^{2+} absorption pathway in the ileum of mice prior to weaning was also examined. *Trpv6* expression was not detected at any age. *Cacna1d* expression was greater from P1 to P14 compared to 1 to 6-month-old mice (Figure 2.5A). A similar pattern was observed for *S100g*, *Atp2b1* and *Slc8a1* (Figure 2.5B-D). Calbindin-D$_{9k}$ protein expression was detected on immunoblot (Figure 2.5E) with semi-quantification (Figure 2.5F) at P1 - P14 but not at 1 month of age or older. Together, this data infers transcellular Ca^{2+} absorption occurs across the ileum prior to weaning but not after.

2.5.6. Net Transcellular Ca^{2+} Absorption Occurs Across the Ileum at 2 Weeks but not 2 Months

To determine if transcellular Ca^{2+} absorption occurs across the ileum of P14 mice, we measured Ca^{2+} flux across this segment *ex vivo* in Ussing chambers. In FVB/N wild-type mice, net J$_{Ca}$$^{2+}$ was significantly greater than zero in P14 but not 2-month-old mice (Figure 2.5G). As *Trpv6* was not detectable at any age in ileum, we sought to implicate Ca$_v$1.3 in mediating the net absorption. To do so, we repeated the flux studies in P14 mice in the presence of vehicle or 10 µM nifedipine and observed a significant inhibition of net J$_{Ca}$$^{2+}$ (Figure 2.5H). To more specifically implicate Ca$_v$1.3, we repeated the experiments in WT and *Cacna1d* KO mice at P14. We did not, however, observe lower net J$_{Ca}$$^{2+}$ in the KO mice (Figure 2.5I). To determine if another L-type Ca^{2+} channel was compensating for the loss of *Cacna1d*, we repeated net J$_{Ca}$$^{2+}$ studies with 10 µM nifedipine. Again, no difference was observed between groups (Figure 2.5J). This made us examine the results more closely. The transepithelial resistance (TER) was not different across the ileum of WT and *Cacna1d* KO with or without nifedipine (Figure 2.5K). Unidirectional

apical to basolateral $^{45}Ca^{2+}$ flux was slightly increased after addition of nifedipine, however

basolateral to apical $^{45}Ca^{2+}$ flux also increased slightly after nifedipine treatment (Figure 2.5L-

M), likely due to increased tissue permeability over time in this *ex vivo* experiment. Regardless,

together, these results suggest net transcellular Ca^{2+} absorption across the ileum of mice at P14 is

mediated by an L-type Ca^{2+} channel with compensation by a non-L-type Ca^{2+} channel after

genetic deletion of $Ca_v1.3$.
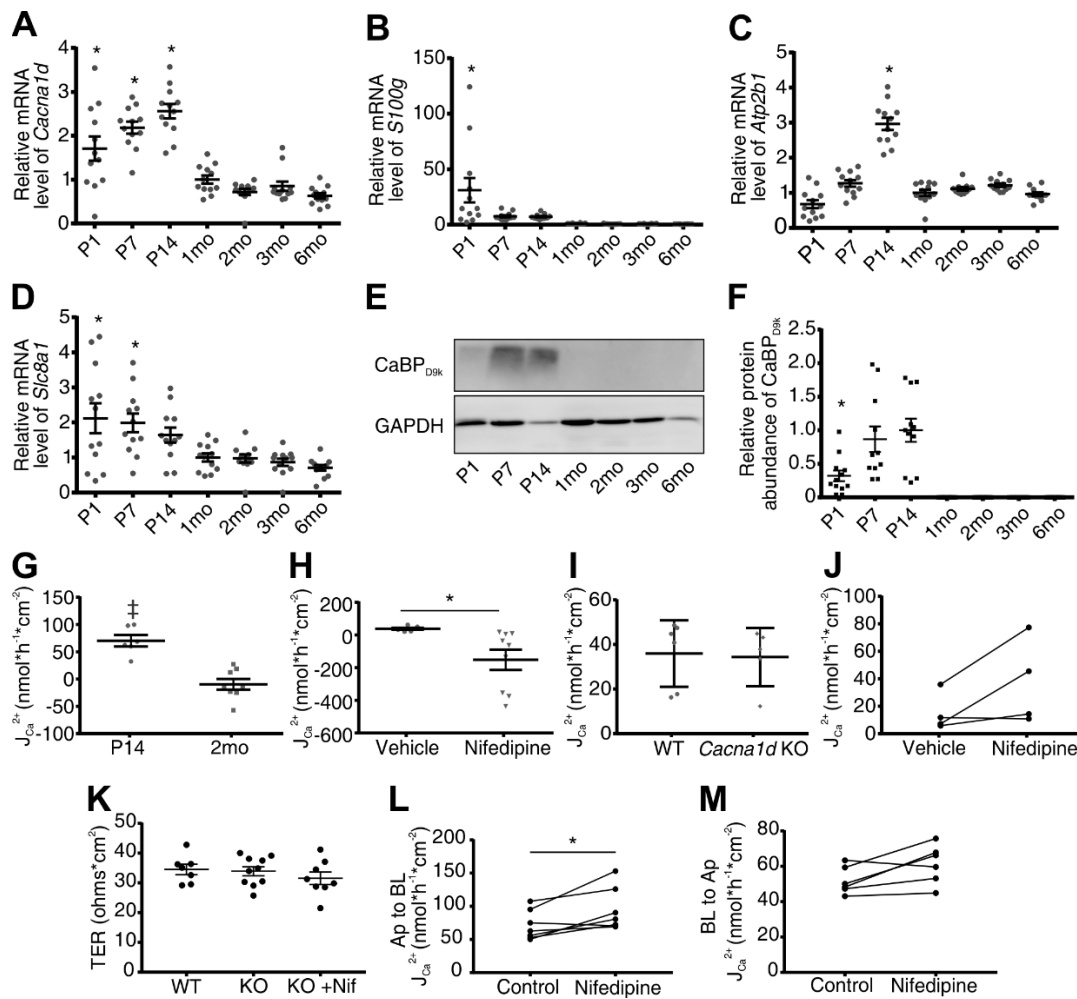
Figure 2.5. P14 but not 2-month-old mice display net apical to basolateral calcium flux across the ileum, mediated by L-type Ca^{2+} channel. Expression of (A) *Cacna1d*, (B) *S100g*, (C) *Atp2b1*, and (D) *Slc8a1* by age (n = 12/group). Expression is normalized to *Gapdh* and relative to 1 month. (E) Representative immunoblot of 12 repeats and (F) semi-quantification of calbindin-D$_{9k}$ (CaBPD$_{9k}$) demonstrates expression in ileum only in younger mice. Results are normalized to GAPDH and displayed relative to P14 age (n = 12/group). Groups are compared by 1-way analysis of variance with Dunnett multiple comparisons test; *P < .05. (G) Net J$_{Ca}$$^{2+}$ across *ex vivo* sections of mouse ileum are greater than 0 at P14 (n = 6; ‡P = .001) but not 2 months (n = 6; P = .359) (two-tailed, one-sample t tests). (H) Ten μmol/L apical nifedipine decreases net J$_{Ca}$$^{2+}$ in P14 mice compared with vehicle (n = 5 vehicle and 9 nifedipine; Mann-Whitney test; *P = .001). (I) No difference in net J$_{Ca}$$^{2+}$ across ileum between WT and *Cacna1d* KO mice at P14 (n = 5 WT and 6 KO; Mann-Whitney test; P = .54). (J) Ten μmol/L apical nifedipine does not decrease net J$_{Ca}$$^{2+}$ in *Cacna1d* KO mice at P14 mice (n = 4; Wilcoxon matched-pairs signed rank test; P = .25). (K) Transepithelial resistance (TER) across the ileum of P14 WT, *Cacna1d* KO, or *Cacna1d* KO with nifedipine (1-way analysis of variance; P = .5) (n = 7–10/group). Unidirectional apical to basolateral (L) and basolateral to apical (M) J$_{Ca}$$^{2+}$ across ileum of P14 *Cacna1d* KO mice before (control) and after apical addition of 10 μmol/L nifedipine (paired t test; *P < .05) (n = 6). Data are presented as mean ± standard error of the mean.

61

2.5.7. Delayed Bone Mineralization in *Cacna1d* KO Pups

We next queried whether the loss of net transcellular Ca^{2+} absorption from the jejunum of *Cacna1d* KO and *Trpv6 ^{mt}* pups altered bone mineralization at P14. Femur growth plate thickness measured on toluidine blue stained sections was greater in *Cacna1d* KO (Figure 2.6A-C and Table 2.1) but not *Trpv6 ^{mt}* (Table 2.2) compared to WT pups. These results suggest delayed bone mineralization in the *Cacna1d* KO mice. No other differences were observed in trabecular bone between WT and *Cacna1d* KO (Table 2.1) or WT and *Trpv6 ^{mt}* (Table 2.2) pups as determined by alizarin red staining (Figure 2.6D). Similarly, no differences were observed for cortical bone parameters as assessed by μCT (Figure 2.6E) for either WT vs *Cacna1d* KO pups (Table 2.1) or WT vs *Trpv6 ^{mt}* pups (Table 2.2). Together, these data suggest that $Ca_v1.3$ contributes to maintaining a positive Ca^{2+} balance during postnatal growth whereas TRPV6 is not critical at this age.
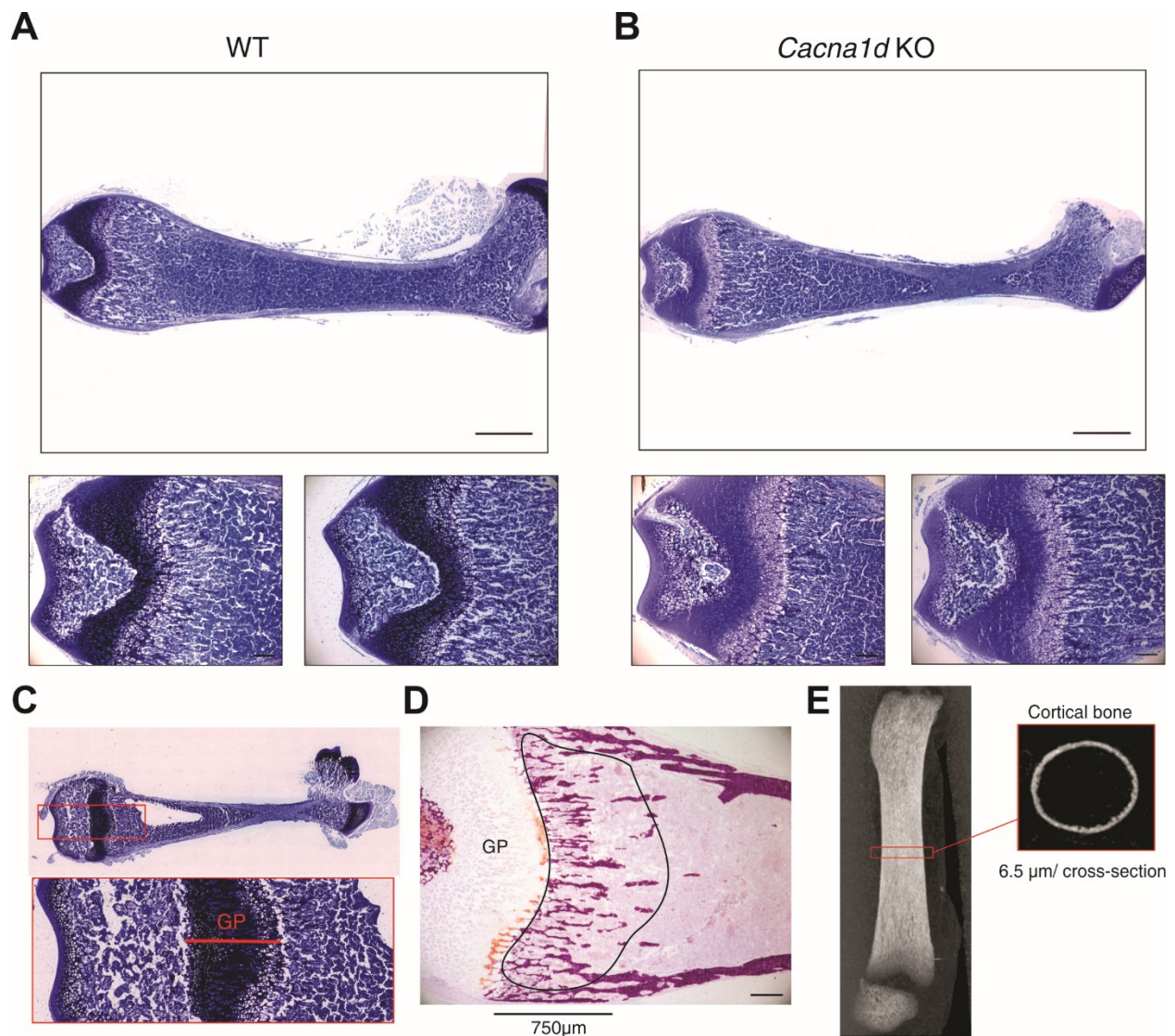
Figure 2.6. Bone phenotype of *Cacna1d* KO pups. Representative toluidine blue–stained sections from fixed non-decalcified femurs of (A) WT and (B) *Cacna1d* KO mice at P14 (P13-P15). The growth plate thickness was measured in middle of the section as indicated below. Scale bar = 1 mm (upper panels) and 0.2 mm (lower panels). (C) Representative toluidine blue–stained sections obtained from non-decalcified femur (top) and enlarged region covering the growth plate (GP) used to determine thickness of growth plate shown in Tables 2.1 and 2.2 . (D) Representative alizarin red stain used to visualize calcified bone (red) and to calculate trabecular parameters shown in Tables 2.1 and 2.2. Region of interest (ROI) starting at growth plate (GP) and covering primary spongiosa over 750 μm is indicated. (E) Lateral scout view of femur indicating midshaft section used to analyze cortical bone.

Table 2.1. Trabecular and cortical bone parameters of P14 WT and *Cacna1d* KO mice

	Male		Female	
	WT	***Cacna1d* KO**	**WT**	***Cacna1d* KO**
Trabecular Bone				
N	6	5	5	6
BV/TV (%)	20.3 ± 0.92	19.2 ± 2.68	20.7 ± 2.1	17.2 ± 1,03
Trabecular Number (1/mm)	0.012 ± 0.001	0.011 ± 0.001	0.013 ± 0.001	0.011 ± 0.001
Trabecular Width (µm)	16.5 ± 0.37	16.6 ± 0.88	16.1 ± 0.35	15.6 ± 0.42
Trabecular Separation (µm)	65.4 ± 3.06	75.0 ± 9.8	64.3 ± 6.63	76.4 ± 5.95
Growth Plate Thickness (µm)	343.4 ± 14.6	426.2 ± 30.9 *	361.1 ± 25.5	484.5 ± 17.2 **
Cortical Bone				
N	6	7	4	9
Bone Volume (mm^3)	0.056 ± 0.003	0.059 ± 0.005	0.061 ± 0.004	0.067 ± 0.003
Endocortical Volume (mm^3)	0.26 ± 0.01	0.25 ± 0.01	0.26 ± 0.01	0.27 ± 0.01
Cross-sectional Thickness (mm)	0.043 ± 0.002	0.045 ± 0.003	0.047 ± 0.002	0.050 ± 0.002
Perimeter (mm)	3.87 ± 0.09	3.76 ± 0.09	3.74 ± 0.07	3.87 ± 0.03
Tissue Mineral Density (g/cm^3)	0.98 ± 0.01	0.98 ± 0.01	0.99 ± 0.01	1.01 ± 0.01

Trabecular bone parameters were calculated from bone sections stained with Alizarin red and cortical bone parameters as measured by µCT. Data is presented as mean ± SEM (unpaired, two-tailed t-test KO vs WT for each sex). BV/TV; bone volume/tissue volume. *$P < 0.05$; **$P < 0.01$

Table 2.2. Trabecular and cortical bone parameters of P14 WT and *Trpv6^{mt}* mice

	N	WT	*Trpv6 ^{mt}*
Trabecular Bone			
BV/TV (%)	3	21.6 ± 1.25	21.4 ± 1.6
Trabecular Number (1/mm)	3	0.013 ± 0.0009	0.013 ± 0.0002
Trabecular Width (μm)	3	17.3 ± 0.44	19.0 ± 1.12
Trabecular Separation (μm)	3	63.3 ± 6.0	60.2 ± 2.1
Growth Plate Thickness (μm)	3	652.5 ± 18.0	630.2 ± 19.6
Cortical Bone			
Femur length (mm)	5	8.26 ± 0.25	8.07 ± 0.14
Bone Volume (mm^3)	5	0.074 ± 0.004	0.078 ± 0.004
Endocortical Volume (mm^3)	5	0.18 ± 0.007	0.19 ± 0.006
Cross-sectional Thickness (mm)	5	0.062 ± 0.002	0.068 ± 0.004
Perimeter (mm)	5	3.37 ± 0.09	3.42 ± 0.05
Tissue Mineral Density (g/cm^3)	5	1.04 ± 0.01	1.05 ± 0.01

Trabecular bone parameters calculated from bone sections stained with Alizarin red and cortical bone parameters as measured by μCT. Data is presented as mean ± SEM (unpaired Student's t-test). BV/TV; bone volume/tissue volume.

2.5.8. Renal and Intestinal Compensation for Loss of Ca$_v$1.3

To understand the lack of a severe bone phenotype in *Cacna1d* KO and *Trpv6 ^{mt}* pups, we examined the expression of genes that might compensate for the loss of jejunal Ca^{2+} absorption in the intestine and kidney. We observed no difference in *Trpv6* nor *S100g* expression along the length of the intestine in *Cacna1d* KO pups (Figure 2.7A, C). We did, however, find a 2-fold increase in *Cacna1c*, encoding Ca$_v$1.2, expression in the ileum but not in other segments (Figure 2.7B). It is unlikely that Ca$_v$1.2 contributes to compensatory increased net J$_{Ca}^{2+}$ in this segment given that we observed nifedipine-insensitive flux in the *Cacna1d* KO pups (Figure 2.7J). In contrast, we observed significant upregulation of mediators of renal Ca^{2+} reabsorption in the proximal tubule and thick ascending limb (TAL), the segments responsible for a combined 90% of renal Ca^{2+} reabsorption.[41] Specifically, the *Cldn2* and *Nhe3* genes that encode a calcium permeable pore and generate the driving force for Ca^{2+} reabsorption from the proximal tubule, respectively were increased in *Cacna1d* KO pups (Figure 2.7D-E).[71, 84, 146] Further, we observed increased expression of *Cldn16* and *Cldn19*, genes that encode the Ca^{2+} permeable pore in the TAL (Figure 2.7F-G).[148] No differences were observed in expression of *Cldn14* which blocks Ca^{2+} reabsorption in the TAL,[150] or *Trpv5* and *Calb1,* which mediate transcellular Ca^{2+} reabsorption in the distal nephron (Figure 2.7H-J).[1] Interestingly, *Trpv6 ^{mt}* pups had significantly decreased expression of *Cacna1d* in the jejunum, ileum and cecum (Figure 2.8A) although no differences were observed in *S100g* expression (Figure 2.8B). Contrary to findings in *Cacna1d* KO pups, renal expression of *Cldn2*, *Nhe3*, *Cldn16*, and *Cldn19* were not different in *Trpv6 ^{mt}* compared to WT mice (Figure 2.8C-F). We did identify a significant decrease in both *Cldn14* and *Trpv5* expression (Figure 2.8G-I). Together these results suggest compensatory increases in renal Ca^{2+} reabsorption in *Cacna1d* KO.
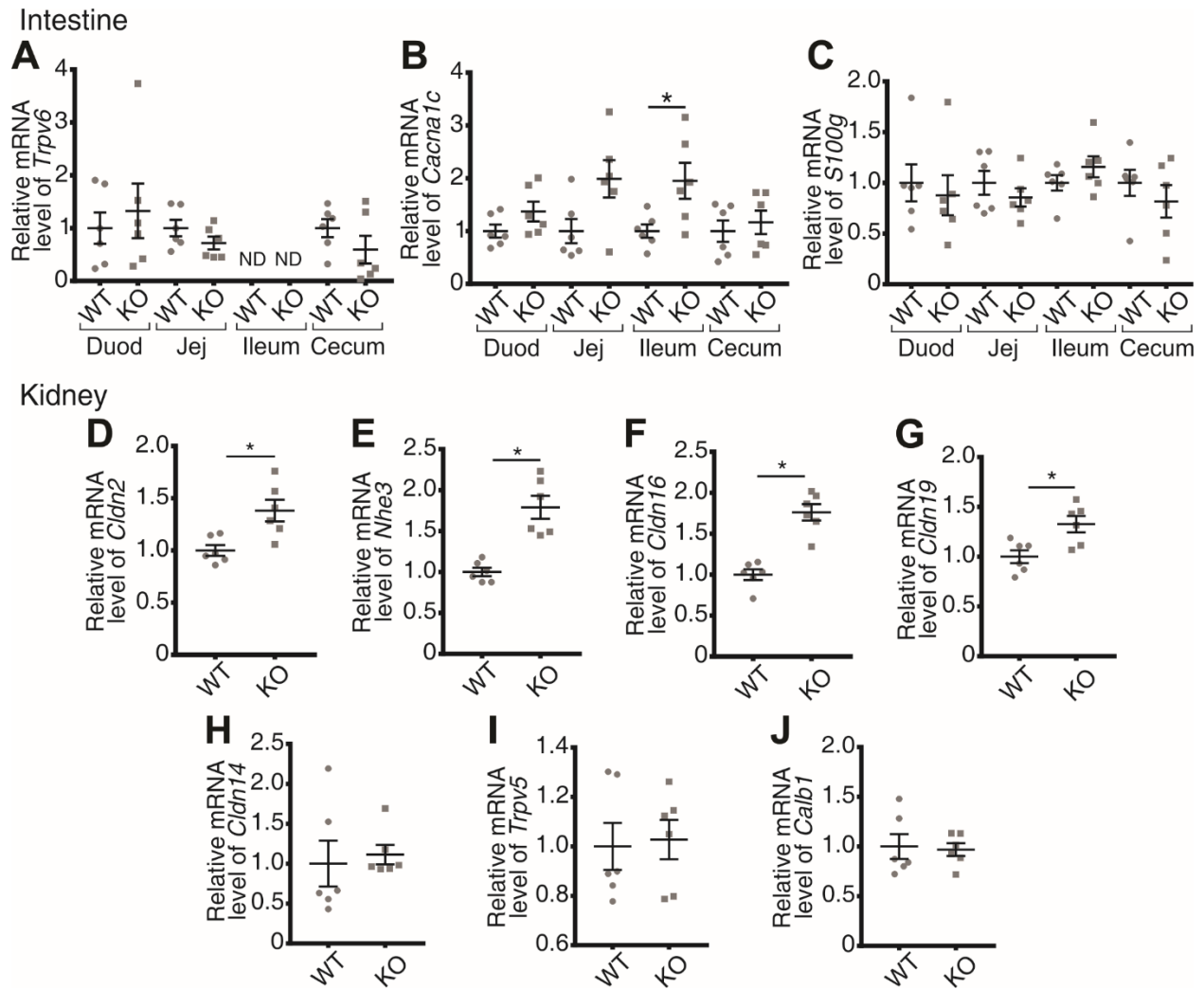
Figure 2.7. Renal compensation in *Cacna1d* KO mice at P14. Quantitative real-time PCR results of (A) *Trpv6*, (B) *Cacna1c* encoding Ca$_v$1.2, and (C) *S100g* along the intestine. Renal expression of (D) *Cldn2*, (E) *Nhe3*, (F) *Cldn16*, (G) *Cldn19*, (H) *Cldn14*, (I) *Trpv5*, and (J) *Calb1* encoding calbindin-D$_{28k}$ reveals compensatory increases in *Cacna1d* KO pups. Small intestine and kidney results are normalized to *Gapdh*; cecum results are normalized to *β-actin*. All expression results are displayed relative to WT group for each tissue. *$P < .05$ vs WT by Mann-Whitney test. (n = 6/group). Data are presented as mean ± standard error of the mean. Duod, duodenum; Jej, jejunum.
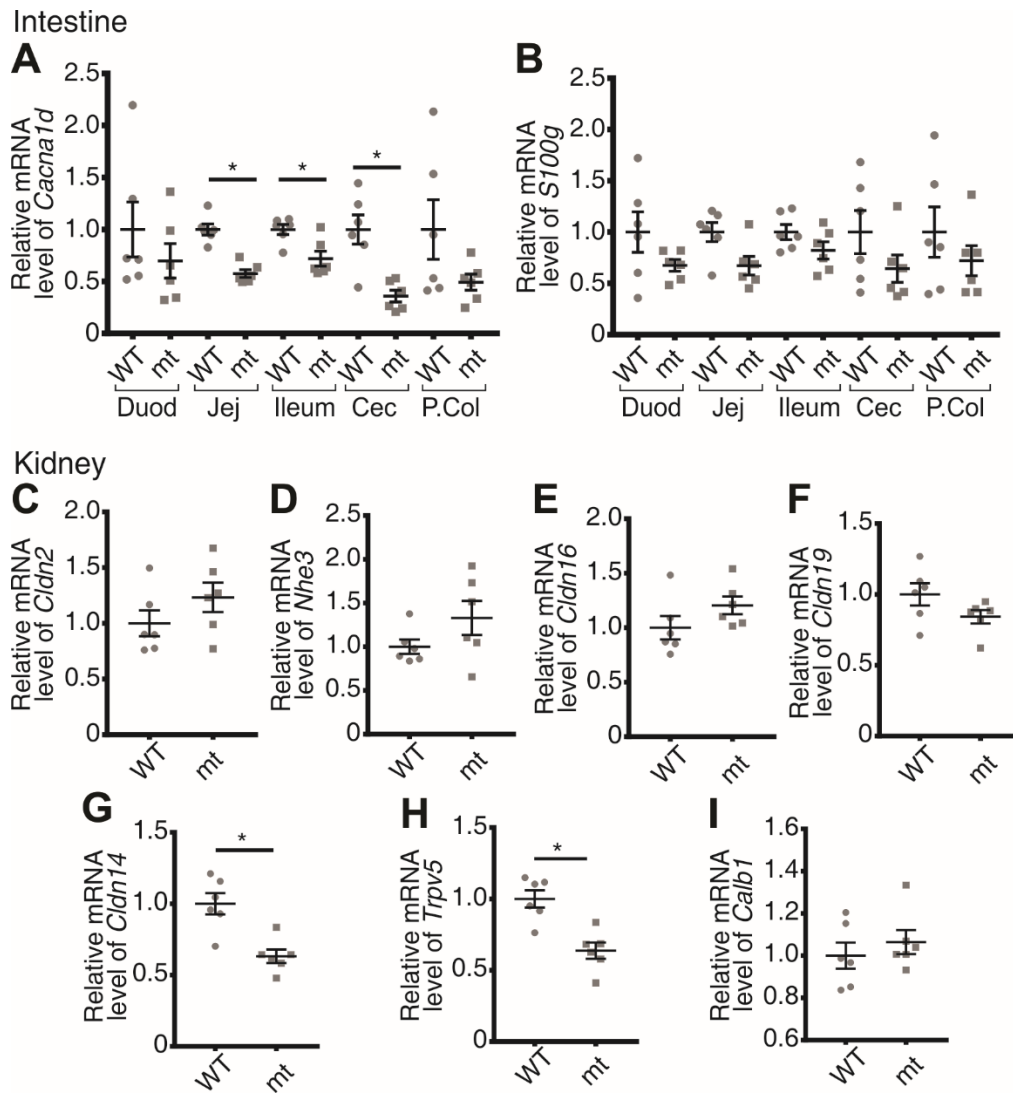
Figure 2.8. Compensatory expression changes in *Trpv6*^{mt} pups. Quantitative real-time PCR results of (A) *Cacna1d* and (B) *S100g* encoding calbindin-D$_{9k}$ along the intestine from *Trpv6*^{mt} pups relative to WT expression in each tissue. Quantitative real-time PCR expression of mediators of renal Ca^{2+} reabsorption, (C) *Cldn2*, (D) *Nhe3*, (E) *Cldn16*, (F) *Cldn19*, (G) *Cldn14*, (H) *Trpv5*, and (I) *Calb1* encoding calbindin-D$_{28k}$ in *Trpv6*^{mt} pups relative to WT. Small intestine and kidney results are normalized to *Gapdh*; cecum and proximal colon (P.Col) results are normalized to *β-actin*. All expression results are relative to WT group for each tissue. *$P < .05$ vs WT by Mann-Whitney test. (n = 6/group). Data presented as mean ± standard error of the mean. Duod, duodenum; Jej, jejunum; mt, mutant.

2.5.9. Early Weaning Alters Expression of *Trpv6*, *Cacna1d*, and *S100g* in the Jejunum and Ileum

To determine if weaning from breastmilk to a regular chow diet results in the changes in expression observed, we weaned pups at P12, roughly 7 days before they are typically weaned, collected tissue 48 hours later and compared gene expression to littermates, which were not weaned early. We observed a 2-fold increase in expression of *Trpv6* and a 1.8-fold increase in *S100g* in the jejunum of pups weaned early. Further, jejunal *Cacna1d* was decreased by 38% in pups weaned early (Figure 2.9A-C). In the ileum, *Cacna1d* expression was also decreased by 66% with early weaning while no difference was observed in *S100g* (Figure 2.9D-E). Together these results suggest that expression of these pathways are regulated by a bioactive compound in breast milk and/or dietary calcium changes.
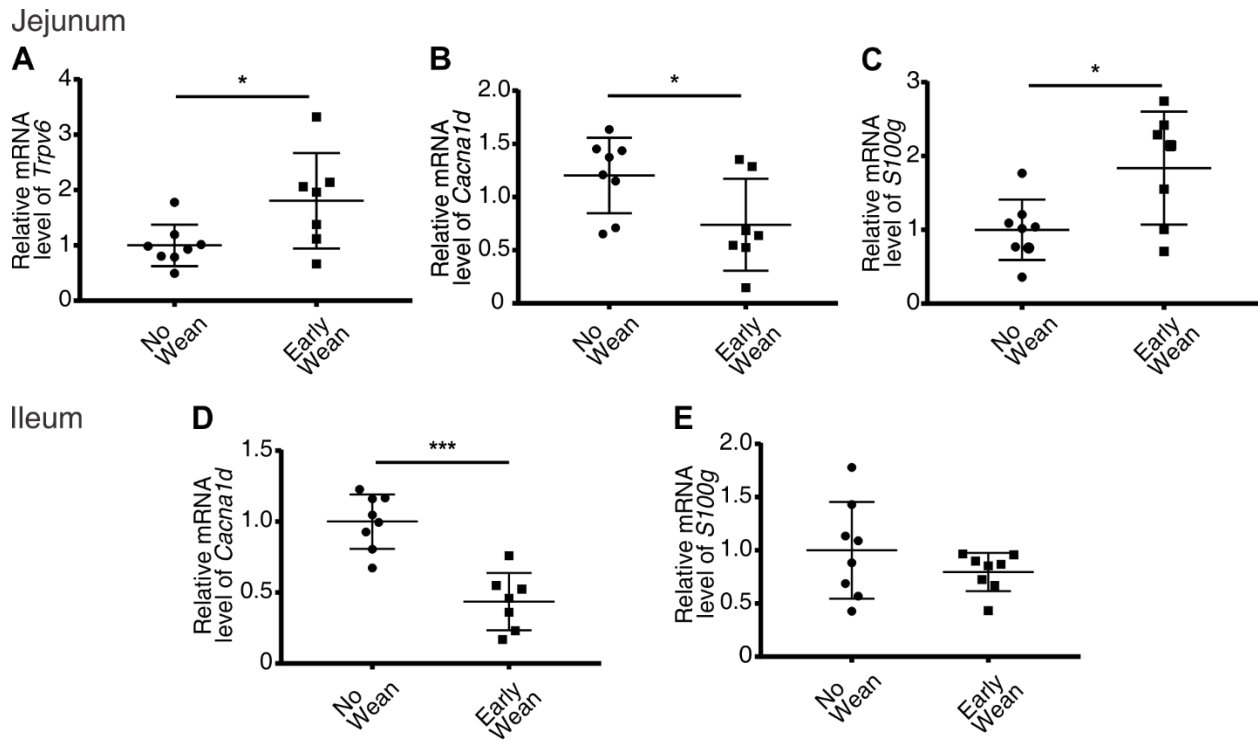
Figure 2.9. Early weaning to rodent chow alters *Trpv6*, *Cacna1d*, and *S100g* expression in jejunum and ileum at P14. Quantitative real-time PCR results of (A) *Trpv6*, (B) *Cacna1d*, and (C) *S100g* in jejunum and (D) *Cacna1d* and (E) *S100g* in ileum. Tissue was taken from mice at P14 after either early weaning to rodent chow at P12 or not. Results are normalized to *β-actin*. *$P < .05$, ***$P < .0001$ vs P14 mice not weaned by Mann-Whitney or unpaired t-test. (n = 7–8/group). Data are presented as mean ± standard error of the mean.

2.6. Discussion

The lifetime osteoporosis risk is independently related to bone mineral content accrued early in life.[207] Infancy and adolescence represent the two periods of greatest Ca^{2+} accretion into bone. When normalized to body weight, the rate of calcium deposition into bone is greatest in the first year of life.[31, 190] A positive calcium balance is necessary for this deposition rate and is a linear function of intestinal absorption. Thus, intestinal absorptive capacity is greatest during infancy.[190] We identify active Ca^{2+} absorption across distal small intestinal segments in mice from 1 day to 6 months of age. Our results failed to identify transcellular Ca^{2+} absorption in the duodenum until after weaning while significant net absorption from the jejunum and ileum occurs only in early postnatal development. Further, TRPV6 and $Ca_v1.3$ mediate this novel absorption pathway identified in the jejunum, while absorption across the ileum is mediated by an L-type Ca^{2+} channel, likely $Ca_v1.3$ (Figure 2.10).
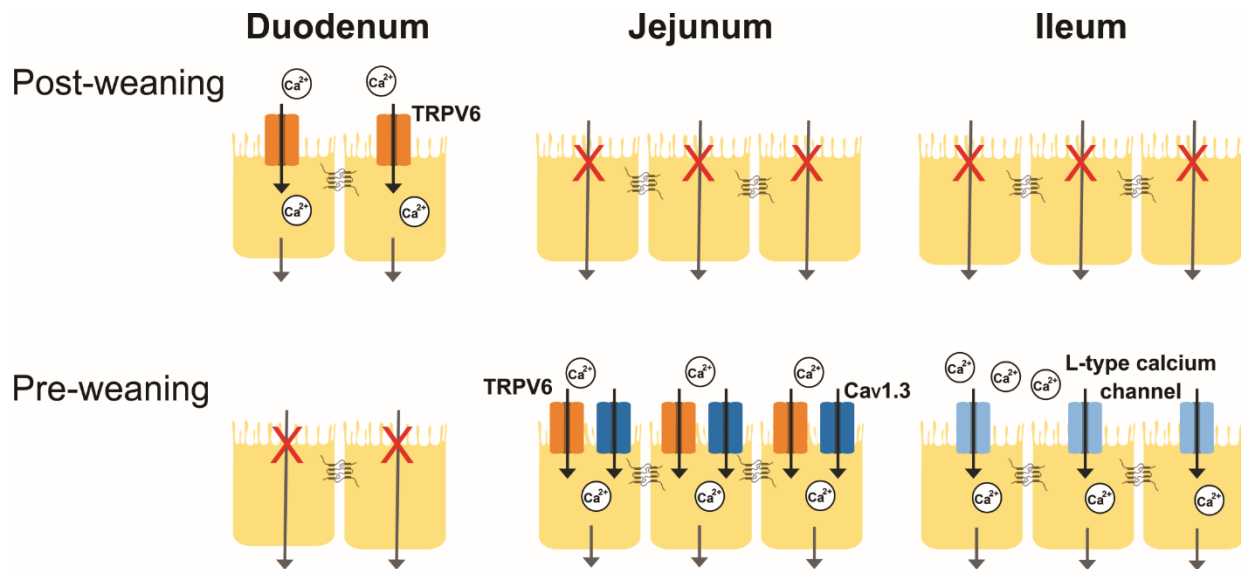
Figure 2.10. Summary of apical entry mechanisms contributing transcellular Ca^{2+} absorption across the small intestine before and after weaning. Significant net transcellular Ca^{2+} absorption across the duodenum is mediated by apical TRPV6 and is present only after weaning. In the jejunum, significant net transcellular Ca^{2+} absorption is present only before weaning and is mediated by apical TRPV6 and Ca$_v$1.3. Similarly, significant net transcellular Ca^{2+} absorption occurs only before weaning across the ileum and is mediated by an L-type calcium channel.

Previous studies have examined expression of the transcellular Ca^{2+} absorption pathway in the duodenum at various ages.[113, 208] TRPV6 and calbindin-D_{9k} were first identified at 1 week in mice, consistent with our findings.[113, 114] We observed *Trpv6* at P7 and P14; however, the expression was far below that of older mice. Similarly, calbindin-D_{9k} was nearly undetectable prior to 1 month. Calbindin-D_{9k} expression is induced by transcellular Ca^{2+} absorption and maintains a low free cytosolic Ca^{2+} concentration.[55] The dramatic shift in expression of the apical entry channel, i.e. TRPV6, and intracellular buffer, i.e. calbindin-D_{9K}, indicate that this pathway is not present in the duodenum of mice before 1 month. Indeed, we observed absorption at 2 months but not P14. This is consistent with previous *in situ* ligated loop studies in rats demonstrating duodenal absorption occurs only via an unsaturable, paracellular process up to P14 with increasing prevalence of a saturable, transcellular process thereafter.[107, 108] We extended this observation and revealed that TRPV6 is essential to net transcellular duodenal Ca^{2+} absorption at 2 months through pharmacological inhibition and a TRPV6 pore mutant. This is consistent with the previous findings that lumen to serum $^{45}Ca^{2+}$ flux after oral gavage of 3 month old *Trpv6* KO mice is reduced by 40-50% compared to WT.[50] Importantly, transcellular Ca^{2+} absorption across the duodenum does not contribute to net absorption prior to weaning. There must, therefore, be other mechanisms mediating Ca^{2+} absorption at a young age.

Previous studies failed to identify transcellular Ca^{2+} absorption in the jejunum and ileum while noting significant paracellular secretion in 9-15 week-old mice.[39, 59] A study employing *in situ* ligated loops in 16-day old rats measured absorption along the length of the small intestine.[104] This technique, however, does not fully capture serosal to lumen recycling and thus cannot definitively demonstrate transcellular absorption. We observed transcellular absorption

across the jejunum and ileum prior to weaning but not thereafter. Additionally, our gene expression profiling supported our functional observations. Importantly, we detected calbindin-D_{9k} protein in mice up to P14. Previous work detected calbindin-D_{9k} in rat ileum at 2 months but at a level less than one fifth of duodenum. However, other work has failed to find expression in mice at 1 month of age.[108, 194] These findings illustrate that active Ca^{2+} uptake from distal small bowel is an alternative pathway to meet the high requirements of infancy.

We further reveal the molecular identity of this developmental Ca^{2+} absorption pathway in the jejunum. Net transcellular Ca^{2+} flux was absent from the jejunum of both *Trpv6^{mt}* and *Cacna1d* KO mice at P14, clearly implicating both channels. Prior work using perfused jejunal loops of adult rats found decreased unidirectional lumen to serosal flux upon apical addition of nifedipine and therefore suggested that $Ca_v1.3$ contributes to intestinal Ca^{2+} absorption at later ages.[209] However, their study has been contradicted by further work in rodents.[59] Collectively, these results illustrate the potential role of $Ca_v1.3$, but not in early postnatal development. Our study clearly illustrates the importance of $Ca_v1.3$ in the jejunum prior to weaning. It is unclear if TRPV6 and $Ca_v1.3$ directly or indirectly interact to mediate Ca^{2+} absorption in this segment; however, both appear to be necessary.

The ileum is the longest intestinal segment with the longest sojourn time and thus could contribute significantly to a positive Ca^{2+} balance early in life.[40] Some authors have speculated the existence of transcellular Ca^{2+} absorption across the ileum of mice and humans.[36, 56, 210] However, prior to the current work, no functional measurements were performed prior to weaning. Morgan et al. observed Ca^{2+} flux that was inhibited by L-type Ca^{2+} channel blockers in the jejunum of older rats. Combined with protein detected in the jejunum and ileum, the authors suggested that $Ca_v1.3$ mediates Ca^{2+} absorption.[57] However, direct functional measurements on

the ileum did not support this. Ussing chambers studies on 9-15-week-old mice did not find net Ca^{2+} flux.[39] Further work employing *in situ* ligated loops in 1-month-old rats, found only passive diffusion without a transcellular component.[108] We, however, found significant net transcellular Ca^{2+} absorption across the ileum of mice at P14 that was not present at 2 months. Further, this net flux was inhibited by nifedipine at a concentration that blocks both $Ca_v1.2$ and $Ca_v1.3$.[209] To specifically implicate $Ca_v1.3$, we repeated the Ca^{2+} flux studies across ileum of *Cacna1d* KO pups. However, these animals did not have decreased net absorption. Interestingly, the net flux observed in the *Cacna1d* KO ileum was no longer inhibited by nifedipine, suggesting that $Ca_v1.3$ mediates flux in WT animals, but that a non- L-type Ca^{2+} channel compensates when $Ca_v1.3$ is knocked out. The identification of this third transcellular Ca^{2+} absorption pathway is the focus of further studies.

To determine if the absence of net transcellular Ca^{2+} absorption across the jejunum of P14 mice negatively impacted the ability to maintain a positive Ca^{2+} balance resulting in poorly mineralized bone, we examined the bone phenotype of *Cacna1d* KO and *Trpv6 ^{mt}* pups. We observed a significantly thicker growth plate in the *Cacna1d* KO pups relative to WT suggesting delayed mineralization of bone in these animals. These findings are consistent with increased growth plate thickness and morphological changes in bones of rabbits treated with nifedipine.[211] Although Platzer et al. reported normal growth, Li et al. found decreased mineral content (BMC) and cross-sectional area of cortical bone of male *Cacna1d* KO mice at 18 weeks of age consistent with our observation.[192, 193] Li et al. attributed the observed bone phenotype to the loss of $Ca_v1.3$ in osteoblasts. Given our findings of a key role of $Ca_v1.3$ in jejunal Ca^{2+} absorption and bone mineralization at P14, it is possible that later BMC differences are the result of reduced

intestinal Ca^{2+} absorption early in life. It is not possible to delineate the effect of bone versus gut with the available global *Cacna1d* KO model.

In a different mutant *Trpv6* mouse strain, a 9.3% reduction in femoral bone mineral density was observed in *Trpv6* KO mice at 3 months of age on a 1% Ca^{2+} diet but not a diet without Ca^{2+}.[50] We did not find altered bone parameters in *Trpv6 ^{mt}* pups, suggesting adequate intestinal Ca^{2+} absorption or renal compensation to mineralize bone. Absorption across the ileum at P14, where *Trpv6* is not expressed, likely compensates for loss of jejunal absorption.[40] Interestingly, infants born with *TRPV6* mutations have skeletal abnormalities detectable *in utero*.[212, 213] This human phenotype is likely the result of decreased placental Ca^{2+} transfer, as has been observed in mice.[214, 215] Since bone mineralization normalizes by two years in these infants, humans also appear to compensate for the loss of *TRPV6* in early development. We should also acknowledge that our work and most previous molecular studies on intestinal calcium absorption has been performed on rodents, and confirmation of these molecular pathways in humans should be done.

The *Cacna1d* KO pups do not have a severe bone phenotype due to two compensatory mechanisms. First, transcellular Ca^{2+} absorption across the ileum of *Cacna1d* KO mice is replaced by nifedipine insensitive flux consistent with the upregulation of a yet unidentified, calcium absorption pathway. Secondly, *Cacna1d* KO mice also display renal compensation in the proximal tubule and thick ascending limb of the nephron to maintain Ca^{2+} balance.[148, 150] These results suggest that increased renal Ca^{2+} reabsorption is necessary to maintain appropriate Ca^{2+} balance, consistent with suboptimal Ca^{2+} absorption across the intestine in the absence of $Ca_v1.3$.

To elucidate whether weaning itself caused the changes in Ca^{2+} absorption observed, we weaned mice early to a regular rodent chow diet. Unexpectedly, we observed an increase in *Trpv6* and *S100g* expression in the jejunum, but not the ileum, in the pups weaned early. *Trpv6* and *S100g* expression are upregulated by hormones found in breast milk including epidermal growth factor and prolactin, which may stimulate expression in suckling pups.[216, 217] However, a change from a high to low calcium diet with early weaning may also lead to activation of vitamin D via parathyroid hormone which, in turn, increases *Trpv6* and *S100g* expression, thus explaining the increased expression observed in the jejunum.[218] There is a paucity of data regarding the free Ca^{2+} concentration available in each segment of the intestine from breast milk or chow diet, which is then available for absorption. It is likely that the post-prandial lumen Ca^{2+} concentrations are in the millimolar range. *Cacna1d* expression was decreased with early weaning similar to our observations with age suggesting its regulation by a bioactive compound in breast milk such as prolactin.[105] Further studies are required to delineate the mechanisms mediating the intestinal Ca^{2+} absorption changes observed at weaning.

In conclusion, we identified pathways mediating active, transcellular Ca^{2+} absorption in the jejunum and ileum early in life. TRPV6 and $Ca_v1.3$ mediate this absorption in the jejunum. Pharmacological blockade of L-type Ca^{2+} channels prevents net absorption in the ileum where TRPV6 is absent. The loss of $Ca_v1.3$ induces a compensatory increase in Ca^{2+} absorption from the ileum and renal Ca^{2+} reabsorption in pre-weaned mice despite delayed bone mineralization. Further, we have demonstrated that a change in diet from breast milk to solid food causes shifts in expression of these pathways in the jejunum and ileum. We have therefore identified molecular details of how active Ca^{2+} uptake from the intestine contributes to the increased demand early in life.

Chapter 3

Paracellular Calcium Absorption Across the Small Intestine

Adapted from: Megan R. Beggs, Kennedi Young, Allen Plain, Ahsan Raza, Justin J. Lee, Matthew Saurette, Petra Weissgerber, Veit Flockerzi, Henrik Dimke, R. Todd Alexander, "Epidermal growth factor in breast milk increases calcium permeability across murine small intestine via claudin-2" prepared for submission.

3.1. Abstract

Background and Aims: Bone mineral deposition is greatest in early life, permitting optimal growth. Optimal bone mineralization also helps prevent osteoporosis later in life, which affects half of adults over 50. Paracellular intestinal calcium absorption is an energetically favorable mechanism enabling maximal calcium (Ca^{2+}) absorption. We aimed to ascertain if suckling animals have increased intestinal Ca^{2+} permeability (P_{Ca}) thereby maximizing absorption.

Methods: Claudin expression was examined by RT-PCR at different ages. P_{Ca} was measured in wildtype, *Cldn12* and *Cldn2* KO mice. CLDN2 expression was also assessed in Caco-2 cells in response to hormones or breast milk added.

Results: P_{Ca} across the jejunum and ileum were 2-fold greater at 2 weeks compared to 2 months ($P = 0.0022$ and $P = 0.0007$). Mice at 2 weeks had greater expression of *Cldn2* and *Cldn12*. *Cldn2* but not *Cldn12* KO mice had decreased P_{Ca} compared to WT ($P < 0.0001$). This translated to decreased bone volume ($P = 0.0343$), cross-sectional thickness ($P < 0.0001$), and tissue mineral density ($P = 0.0228$) of femurs. Weaning from breast milk led to a 50% decrease in *Cldn2* expression in the jejunum ($P = 0.0019$) and ileum ($P = 0.0003$). Epidermal growth factor (EGF) in breast milk specifically increased CLDN2 expression in Caco-2 cells.

Conclusion: Intestinal permeability to Ca^{2+}, conferred by claudin-2, is greater in suckling mice. CLDN2 expression is increased in response to EGF in breast milk. Loss of this pathway leads to suboptimal bone mineralization. EGF mediated increased intestinal claudin-2 expression thus maximizes intestinal Ca^{2+} absorption with therapeutic potential.

3.2. Introduction

Osteoporosis is a disease of compromised bone mineral density which leads to increased risk of debilitating fractures and affects over 200 million people globally.[6, 219] The burden of osteoporosis to the healthcare system amounts to annual costs of $57 billion and €37 billion in the US and Europe, respectively.[220, 221] While this disease is classically considered one of older age, about 60% of the risk of developing osteoporosis can be attributed to suboptimal peak bone mineral density by early adulthood.[7] The rate of mineral accretion into bone is greatest during infancy with a roughly 3-fold decrease by one year of age, and further decline into early adulthood.[4] Thus, understanding the mechanisms underlying maintenance of a positive calcium balance early in life enabling optimal bone mineralization may provide vital insights into preventing or reversing bone loss later in life.

The intestines, via interactions with kidneys and bone, are a major site maintaining calcium (Ca^{2+}) homeostasis. Intestinal absorption occurs via both transcellular and paracellular pathways. We have previously described novel pathways of transcellular absorption that occur only early in infancy.[222] It is not known if the paracellular pathway undergoes similar alterations to facilitate greater permeability and thus paracellular absorption to Ca^{2+} (P_{Ca}) during postnatal development.[194] However, given the high concentration of Ca^{2+} in breast milk, absorption via paracellular diffusion represents an energetically favorable pathway to absorb a greater amount of Ca^{2+} thereby enabling growth.[223]

Claudins are tight junction proteins that interact between epithelial cells to form selective barriers and pores and thus confer the specific permeability properties across epithelial tissue. Of the many isoforms, claudin-2 (gene *CLDN2*) and claudin-12 (gene *CLDN12*) have been implicated in forming Ca^{2+} permeable pores across intestinal and renal epithelia.[78, 84] Global

knockout (KO) of *Cldn2* in mice results in decreased P_{Ca} across the proximal colon.[86] Both

Cldn2 and *Cldn12* are expressed in the renal proximal tubule where *Cldn12* KO mice have

decreased P_{Ca} and *Cldn2* KO have hypercalciuria.[87, 146] In both mice and humans, intestinal

CLDN2 expression is greater early in life.[77, 80, 224] However, previous work has not examined

whether claudin-2 or -12 confer P_{Ca} to the small intestine early in life and if this changes with

age.

We therefore sought to determine if P_{Ca} across the small intestine changes with age and if

claudin-2 or -12 facilitate paracellular Ca^{2+} absorption. We hypothesized that intestinal Ca^{2+}

permeability would be greater early in life to optimize absorption for growth and that claudin-2

or -12 would confer this greater P_{Ca}. Here we show that P_{Ca} across the jejunum and ileum

decreased by half after weaning in mice and that the greater P_{Ca} is conferred by greater *Cldn2*

abundance. Loss of *Cldn2* leads to decreased bone mineralization early in life. Moreover, we

demonstrate that epidermal growth factor (EGF) present in breast milk specifically increases

CLDN2 expression *in vitro*. Thus, claudin-2 in the small intestine facilitates greater uptake of

dietary Ca^{2+} to optimize bone mineralization.

3.3. Materials and Methods

Animals

FVB/N (Taconic labs, North America), global *Cldn2* KO (MMRRC at Univ. of California,

Davis), global *Cldn12* KO[87] and mice with a non-functioning pore mutation in TRPV6

(*Trpv6*[mt])[52] were maintained on a 12-hour light/dark cycle with drinking water and standard

chow (Lab Diet Irradiated Rodent Diet 5053 4.5% fat) available ad libitum. KO and mutant mice were back-crossed to FVB/N for at least 5 generations. The *Cldn2* gene is on the X-chromosome so WT and KO males were bred to heterozygous females. Heterozygous breeding of *Cldn12* mice yielded WT and KO littermates used in experiments. Early weaning experiments were previously described.[222] Briefly, at P13, pups were assessed to ensure eruption of teeth and half of the litter was removed from the dam and given *ad lib* chow and water and monitored to ensure consumption. The other half of the pups remained suckling from the dam. Experiments were approved by the University of Alberta animal ethics committee, Health Sciences Section (AUP00000213). Individual data points from animal experiments represent biological replicates from one animal.

Ca^{2+} flux studies

Fresh tissue was excised, linearized, and mounted into Ussing chambers connected to a VCC multichannel voltage/current clamp (Physiologic Instruments, San Diego, CA).[222] Tissue was bathed bilaterally with 4 mL Kreb's buffer (140 mM Na$^+$, 5.2 mM K$^+$, 120 mM Cl$^-$, 1.2 mM Mg^{2+}, 1.2 mM Ca^{2+}, 2.8 mM PO$_4^-$, 2.5 mM HCO3, pH 7.4) at 37°C and bubbled with 5% CO$_2$ (balance O$_2$). Indomethacin (Sigma-Aldrich Cat# 17378) 2 μM bilaterally and tetrodotoxin (Alomone Labs, Jerusalem, Israel; Cat# T-550) 0.1 μM only basolaterally were added to inhibit prostaglandin synthesis and neuronal activity, respectively. The basolateral buffer contained 10 mM glucose and the apical side 10 mM mannitol to balance osmolarity. Tissue was left to stabilize for 15 minutes and then a 2 mV pulse applied thrice to determine TER (transepithelial resistance) using Ohm's law. One hemichamber was then spiked with 5 mCi/mL ^{45}Ca^{2+}

(PerkinElmer Health Sciences, Waltham, MA). The voltage clamp was then set to 0 mV.

Samples were taken from both chambers at 15-minute intervals for 60 minutes. 2 mV pulses

were then applied to calculate TER and data omitted if TER changed by more than 40%.[39]

Sample radioactivity was measured (LS6500 Multi-Purpose Scintillation Counter, Beckman

Coulter, Brea, CA) and J_{Ca} calculated as the rate of appearance of $^{45}Ca^{2+}$ in cpm/h into the cold

chamber divided by the specific activity of the hot chamber in cpm/mol and normalized to

surface area of tissue exposed. Net J_{Ca}^{2+} was calculated as apical to basolateral J_{Ca}^{2+} minus

basolateral to apical J_{Ca}^{2+} from samples from the same animal and contiguous intestinal segment.

Data for basolateral to apical unidirectional fluxes by age were taken from previously published

net J_{Ca}^{2+} data.[222]

Intestinal permeability to Ca^{2+}

Bi-ionic diffusion potential experiments were performed as described previously.[86] Fresh tissue

was excised and mounted into Ussing chambers (VCC multichannel Voltage/Current Clamp,

Physiologic Instruments, San Diego, CA). Both chambers were then filled with "control" Kreb's-

Ringer buffer (144 mM Na^+, 3.6 mM K^+, 146 mM Cl^-, 1 mM Mg^{2+}, 1.3 mM Ca^{2+}, 2 mM PO_4^-,

pH 7.4) at 37°C and bubbled with 5% CO_2 (balance O_2). Tissue stabilized for 15 minutes and

then 90 µA current pulses were applied to calculate transepithelial resistance (TER) using Ohm's

law. The apical buffer was then changed to low NaCl (30 mM Na^+, 3.6 mM K^+, 32 mM Cl^-, 1

mM Mg^{2+}, 1.3 mM Ca^{2+}, 2 mM PO_4^-, pH 7.4). The resulting peak change in transepithelial

voltage was used to determine the permeability ratio of Na^+ to Cl^- (P_{Na}/P_{Cl}) and absolute

permeability to Na^+ using the Goldman-Hodgkin-Katz and simplified Kimizuka-Koketsu

equations.[152, 225] The apical buffer was then changed to the control buffer and TER measured as above when the potential difference stabilized. To assess P_{Ca}, buffers were exchanged on both the basolateral (140 mM Na^+, 3.6 mM K^+, 146 mM Cl^-, 1 mM Mg^{2+}, 1.3 mM Ca^{2+}, 3 mM HEPES, pH 7.4) and apical sides (3.6 mM K^+, 146 mM Cl^-, 1 mM Mg^{2+}, 70 mM Ca^{2+}, 3 mM HEPES, pH 7.4). Both buffers were finally changed back to the control buffer to measure TER. Tissue viability was considered as a TER change less than 40%.[39] All potential difference measurements were corrected for liquid junction potentials as previously described.[84] All basolateral buffers contained 10 mM dextrose. Osmolarity of all buffers was balanced using mannitol to 291 ±1 mOsm (Advanced Instruments Model 3D3 osmometer).

Quantitative real-time PCR

Quantitative PCR was performed as previously described.[194] Briefly, total RNA was isolated using the TRIzol method (Invitrogen, Carlsbad, CA) according to the manufacturer's instructions with DNAse treatment (ThermoScientific, Vilnius, Lithuania). 5 µg total RNA, quantified with a Nanodrop 2000 (Thermo Fisher Scientific, Waltham, MA) was reverse transcribed (SensiFAST cDNA Synthesis Kit, FroggaBio, CA, USA). Real-time PCR was then performed in triplicate for each cDNA sample (TaqMan Universal Master Mix II, ThermoFischer Scientific) with specific primers and probes (Integrated DNA Technologies) on a QuantStudio 6 Pro Real-Time PCR System (ThermoFisher Scientific). Pooled RNA was used to create a standard mix of cDNA that was serially diluted to generate a standard curve and samples were quantified using the standard curve method. Primer and probe sequences have been previously published.[66, 196, 222] A C_q value of greater than 35 was considered not detectable.

Immunohistochemistry of intestinal tissue

Tissue was embedded in paraffin and stained for EGFR or CLDN2 as previously described.[196] Rehydrated tissue was microwave boiled in Tris-EGTA buffer (TEG, 10 mM Tris, 0.5 mM EGTA, pH 9.0) for antigen retrieval. Free aldehyde groups were blocked in 0.6% H_2O_2 and 50 mM NH_4Cl in PBS. Sections were blocked in 5% milk, probed with primary antibody in 0.1% Triton-X in PBS overnight at 4 °C and then incubated with secondary antibodies. Sections were visualized with DAB$^+$ Substrate Chromogen System (K3467, DakoCytomation) and counterstained with hematoxylin.

Cell Culture

Caco-2 cells (ATCC, Rockville, MD) were grown in DMEM supplemented with 10% FBS and 5% penicillin streptomycin glutamine at 37 °C in 5% CO_2. For immunoblots, cells were seeded onto 100 mm dishes. When cells reached confluence, hormone, human breast milk or erlotinib was added to the media for 48 hours. EGF (Life Technologies Inc., Cat#PHG0311) was added at 100 ng/mL, vitamin D (Sigma-Aldrich, Cat#17936) at 20 nM,[121] prolactin (Sigma-Aldrich, Cat#SRP9000) at 400 ng/mL. Erlotinib (Sigma-Aldrich, Cat#SML2156) was added at 0.1 or 1 µM as indicated. Human milk was obtained as a random sample donated by volunteer participants and stored at -80 °C until used for experiments as approved by the University of Alberta Health Research Ethics Board - Biomedical Panel (Pro00100603). Milk was then added to cell culture media as percent volume as indicated.

Immunoblot

Cells were lysed in RIPA buffer (50 mM Tris, 150 mM NaCl, 1 mM EDTA, 1% Triton-X, 1% SDS, 1% NP-40, pH 7.4) with 1:100 0.1 M PMSF (Thermo Scientific, Rockford, IL), and 1:100 protease inhibitor cocktail (Calbiochem, San Diego, CA). Protein quantity was measured with Pierce 660 nm Protein Assay Reagent (ThermoFisher Scientific). 50 µg of protein was run on a 12% SDS-PAGE gel and electrotransferred to 0.22 µm PVDF (Merck Millipore, Burlington, MA) and blocked overnight with 5% milk in TBST at 4 °C. Blots were incubated with 1:1000 primary antibody in 5% milk in TBST overnight at 4 °C, rinsed in TBST and then incubated for 1 hour at room temperature with secondary antibody. Blots were visualised with Immobilon Crescendo Western HRP substrate (Sigma-Aldrich, Canada) and a ChemiDoc Touch imaging system (Bio-Rad). Protein was semi-quantified using Image Lab 6.0 (Bio-Rad). Primary antibodies were mouse anti-claudin-2 (Cat#32-5600, ThermoFisher Scientific), rabbit anti-claudin-4 (Cat#PA1-37471, ThermoFisher Scientific), rabbit anti-claudin-7 (Cat#34-9100, Invitrogen), rabbit anti-claudin-10 (sc-25710, Santa Cruz Biotechnologies), and mouse anti-β-actin (BA3R, Invitrogen). Secondary antibodies were anti-rabbit (#7074, Cell Signaling, MA, USA) and anti-mouse (#7076, Cell Signaling, MA, USA).

IHC bones

Femurs were fixed in 4% PFA at 4°C and then embedded in tissue freezing medium (simulated colonic environment medium; CEM-001; Section-Lab Co Ltd, Hiroshima, Japan).[198] Four 6-mm sections per bone were made in an anterior-posterior orientation at 2 different regions spaced at

least 100 µm apart. Two sections were stained with a modified toluidine blue staining to visualize cartilage. The thickness of the growth plate was determined from the middle of the section. Two sections were stained with alizarin red to visualize calcified bone (red) and to calculate trabecular parameters as previously published.[199]

microCT analysis of bones

Femora from P14 WT and *Cldn-2* KO mice were scanned with the resolution of 6.5 µm using a high-resolution micro-CT system (Bruker, SkyScan 1172). Bones were wrapped in wet tissue, placed in a plastic holder and mounted vertically in the scanner sample chamber. X-rays source voltage and current were 49 kV and 200 µA respectively. Beam hardening was reduced using a 0.5 mm Al filter. The exposure time was 5 s and scanning angular rotation was set to 180° with an increment of 0.4 deg rotation step.[197] NRecon (1.6.10.6) was used to reconstruct the images and the DataViewer (1.5.1.2) and CT Analyser (1.16.4.1+) from Bruker, MicroCT were used for bone analysis. A total number of fifty cross-sections exactly in the middle of the femoral shaft were analyzed to access cortical bone parameters.

Urine and plasma

Urine electrolytes were measured by ion chromatography (Dionex Aquion Ion Chromatography System, Thermo Fisher Scientific). Samples were diluted 1:50 in ddH$_2$O with eluent of 4.5 mM Na$_2$CO$_3$/1.5 mM NaHCO$_3$ in ddH$_2$O for anions and 20 mM Methanesulfonic acid in ddH$_2$O for cations. Sample results were obtained from serial dilutions of Dionex five anion and six cation-I

standards (Dionex, Thermo Fisher Scientific Inc., Mississauga, ON, Canada). Results were

analyzed using Chromeleon 7 Chromatography Data System software (Thermo Scientific). Urine

creatinine was measured using the Parameter creatinine kit (R&D systems, Minneapolis, USA).

Plasma PTH (Immutopics Mouse Intact PTH 1–84) and 1,25(OH)$_2$-vitamin D

(Immunodiagnostic Systems Limited, Boldon, UK) and FGF23 (Kainos Laboratories, Inc.) and

milk EGF (Quantikine Human EGF Immunoassay, R&D systems) were measured by ELISA.

Statistical analysis

Individual data points in each graph represent data from one animal or experimental repeat. Data

were analysed using GraphPad Prism 9.1.0. The Shapiro-Wilk test was used to evaluate for

normal distribution and F test to compare variances. Data were analyzed and presented as

indicated in figure and table legends. $P < 0.05$ was considered statistically significant.

3.4. Results

3.4.1. Calcium permeability is greater prior to weaning along the small intestine

Previously, we assessed net transcellular $^{45}Ca^{2+}$ flux across all segments of the small

intestine in mice at P14 and 2 months of age.[222] This experiment required us to measure

unidirectional basolateral to apical $^{45}Ca^{2+}$ which can only occur via a paracellular route. Mice at

P14 have increased basolateral to apical $^{45}Ca^{2+}$ flux across the duodenum and jejunum,

suggesting increased Ca^{2+} permeability (P_{Ca}) across these segments Figure 3.1. No difference

was observed across the ileum however, significant apical to basolateral flux occurs across this

segment only in the young mice, which may recycle Ca^{2+} back to the basolateral side and thus mask a true difference in P_{Ca}.[222] Therefore, to directly measure P_{Ca}, bi-ionic diffusion potential experiments were performed. We noted slight, but significantly greater P_{Ca} across the duodenum in mice at P14 than at 2 months (Figure 3.2A). Strikingly, the P_{Ca} across the jejunum and ileum of young mice was doubled that of older animals (Figure 3.2B-C). Transepithelial resistance (TER) and permeability to Na^+ and Cl^- for each tissue are provided in Supplementary Tables 3.1 – 3.3. In the duodenum, P_{Na} is lower while TER and P_{Cl} are not different at P14. In the jejunum, TER is lower, P_{Cl} is greater and P_{Na} are not different at P14. Across the ileum TER and P_{Na} are not different while P_{Cl} is greater at P14. These results demonstrate that the small intestine of younger mice have greater P_{Ca} and thus a greater capacity for Ca^{2+} absorption or secretion.

We performed further experiments to rule out the possibility of the transcellular pathway contributing to the perceived P_{Ca} measured. TRPV6 mediates transcellular Ca^{2+} uptake across the duodenum at 2 months but not 2 weeks.[222] To determine if TRPV6 was contributing Ca^{2+} permeability under our experimental conditions, P_{Ca} was measured across the duodenum of *Trpv6*[mt] mice at 2 month and found no difference when compared to P_{Ca} from WT mice at 2 months (0.917 (0.878 – 1.226) vs 1.133 (0.914 – 1.330), *P* = 0.2229 by Mann-Whitney test). Previous work demonstrated that TRPV6 in the jejunum and $Ca_v1.3$ in the jejunum and ileum mediate net Ca^{2+} absorption at 2 weeks but not 2 months.[222] To test whether these channels were contributing to the greater P_{Ca} observed in younger mice, we repeated the bi-ionic diffusion potential experiments on *Trvp6* WT and *Trpv6*[mt] mice and in the presence of the L-type Ca^{2+} channel blocker, nifedipine. No differences were observed in either tissue (jejunum with nifedipine 1.664 (1.103 – 1.923), *P* = 0.9143; jejunum *Trvp6* WT vs *Trpv6*[mt] (2.009 (1.809 – 2.408) vs. 2.000 (1.614 – 2.335), *P* = 0.5368; ileum with nifedipine 2.171 (1.998 – 2.499), *P* =

89

0.1320 by Mann-Whitney test). Together, this work strongly supports increased intestinal P_{Ca} in the jejunum and ileum of young mice.
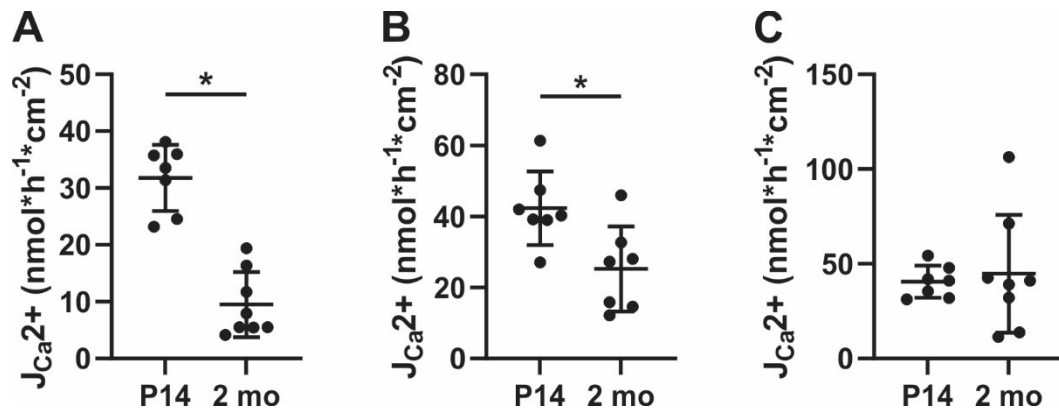
Figure 3.1. Basolateral to apical $^{45}Ca^{2+}$ flux across the small intestine is greater in mice at 2 weeks compared to 2 months. A) duodenum ($P < 0.0001$), B) jejunum ($P = 0.0146$), C) ileum ($P = 0.7351$). Values presented as mean ± SD. Analysis by unpaired t-test.
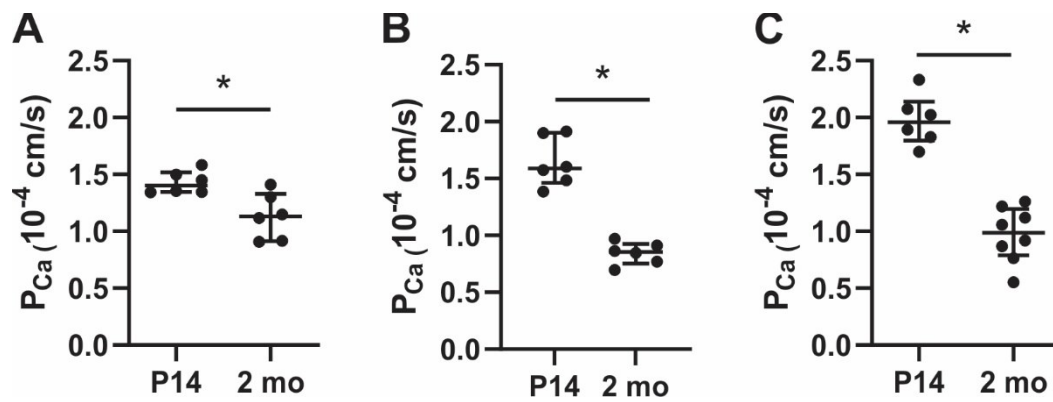
Figure 3.2. Calcium permeability across the small intestine is greater in young mice. A) duodenum ($P = 0.0152$), B) jejunum ($P = 0.0022$), C) ileum ($P = 0.0007$). Values presented as median and interquartile range. Analysis by Mann-Whitney test. P14, 2 weeks old; 2 mo, 2 months old.

Table 3.1. Resistance and ion permeability across the duodenum of 2 week and 2-month-old mice

	P14 (n = 6)	2 months (n = 6)	*P* – value
TER (Ω cm^2)	56.99 (53.6 – 58.1)	52.71 (48.9 – 56.7)	0.3095
P$_{Na}$ (x10^{-4} cm s^{-1})	0.255 (0.243 – 0.277)	0.307 (0.289 – 0.318)	0.0087
P$_{Cl}$ (x10^{-4} cm s^{-1})	0.219 (0.212 – 0.226)	0.203 (0.182 – 0.220)	0.2403
P$_{Na}$/P$_{Cl}$	1.186 (1.103 – 1.289)	1.546 (1.421 – 1.665)	0.0022
P$_{Ca}$/P$_{Na}$	5.523 (5.23 – 5.69)	3.469 (3.27 – 4.32)	0.0022

TER, transepithelial resistance; P$_x$, permeability to ion x. Data presented at median (IQR). *P* – value determined by Mann-Whitney test.

Table 3.2. Resistance and ion permeability across the jejunum of 2 week and 2-month-old mice

	P14 (n = 6)	2 months (n = 6)	*P* – value
TER (Ω cm^2)	44.97 (39.9 – 49.7)	51.74 (50.0 – 63.1)	0.0152
P_{Na} (x10^{-4} cm s^{-1})	0.348 (0.330 – 0.414)	0.380 (0.298 – 0.396)	0.8182
P_{Cl} (x10^{-4} cm s^{-1})	0.232 (0.210 – 0.285)	0.162 (0.142 – 0.172)	0.0022
P_{Na}/P_{Cl}	1.529 (1.425 – 1.648)	2.227 (2.064 – 2.478)	0.0043
P_{Ca}/P_{Na}	4.506 (4.188 – 4.757)	2.366 (2.136 – 2.595)	0.0022

TER, transepithelial resistance; P_x, permeability to ion x. Data presented at median (IQR). *P* – value determined by Mann-Whitney test.

Table 3.3. Resistance and ion permeability across the ileum 2 week and 2-month-old mice

	P14 (n = 6)	2 months (n = 8)	*P* – value
TER (Ω cm^2)	40.35 (37.0 – 42.7)	45.35 (38.7 – 49.4)	0.1812
P_{Na} (x10^{-4} cm s^{-1})	0.432 (0.390 – 0.472)	0.461 (0.397 – 0.531)	0.5728
P_{Cl} (x10^{-4} cm s^{-1})	0.256 (0.234 – 0.271)	0.148 (0.121 – 0.203)	0.0007
P_{Na}/P_{Cl}	1.764 (1.638 – 2.120)	2.839 (2.372 – 3.970)	0.0007
P_{Ca}/P_{Na}	4.696 (4.502 – 4.938)	2.352 (1.960 – 2.456)	0.0007

TER, transepithelial resistance; P_x, permeability to ion x. Data presented at median (IQR). *P* – value determined by Mann-Whitney test.

3.4.2 *Cldn2* expression is greater along the small intestine prior to weaning

Previous *in vitro* and *ex vivo* work demonstrate that claudin-2 and -12 mediate calcium permeability across epithelia.[78, 86, 87] We hypothesized that the expression of one or both of these claudins would therefore be increased in the younger mice who demonstrate greater P_{Ca}. We assessed small intestine tissue from mice aged P1 to 6 months. Indeed, *Cldn2* expression was greater in the jejunum and ileum at P1, P7 and P14 compared to at 1 month, which correspond to ages where the pup is still suckling from the dam. In the duodenum, *Cldn2* expression was greater at P1 and P7 but not P14 relative to 1 month (Figure 3.3A-C). To determine if CLDN2 protein is also more abundant in younger animals we stained fixed sections of intestine (Figure 3.3D-F) and observed diffuse CLDN2 staining throughout the apical membrane along the villi and crypts throughout the small intestine at P14. By 2 months however, CLDN2 expression was less abundant and found only in the crypts (Figure 3.3G-I). *Cldn12* gene expression was greater in the jejunum but not duodenum or ileum of younger mice (Figure 3.3J-L). These results suggest that either or both of claudin-2 and -12 may confer the greater P_{Ca} observed in younger mice.
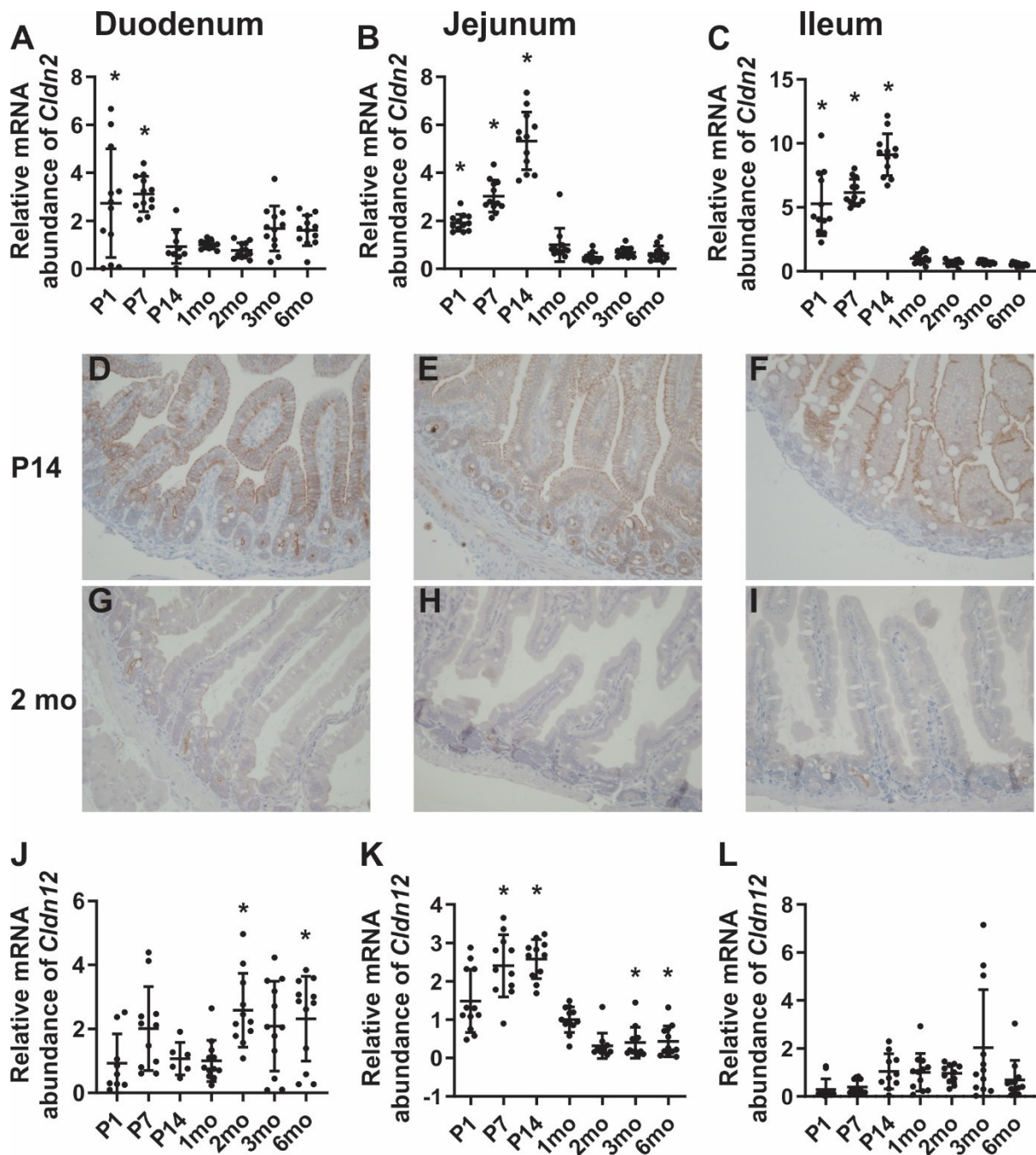
Figure 3.3. *Cldn2* and *Cldn12* expression varies with age along the small intestine. Relative expression of A-C) *Cldn2* and J-L) *Cldn12* from P1 to 6 months of age in the duodenum (A and J), jejunum (B and K), and ileum (C and L). Expression is normalized to *Gapdh* and relative to 1 mo. Data presented as mean ± SD, * $P < 0.05$ vs 1 mo by ANOVA with Dunnett's multiple comparisons test. Immunostaining for CLDN2 along the villi and crypt of segments from D) duodenum, E) jejunum, F) ileum at P14 and localized only to crypt at 2 months (G – I). Images were taken at 20X magnification. Representative images are obtained from evaluation of n = 1-4 mice per group.

3.4.3. *Cldn2* confers the greater Ca²⁺ permeability observed across the jejunum and ileum

Based on the results of the expression studies, we hypothesized that mice with genetic deletion of *Cldn2* would have decreased P_{Ca} across the jejunum and ileum at P14. We repeated bi-ionic dilution potential studies in WT and *Cldn2* KO mice at P14 and 2 months. Indeed, P_{Ca} across the jejunum and ileum was significantly reduced in the P14 *Cldn2* KO mice. Moreover, the P_{Ca} in the *Cldn2* KO P14 mice was no longer different than that at 2 months, consistent with it conferring the increased P_{Ca}. No difference was observed by genotype across the duodenum or in any segment at 2 months (Figure 3.4A-C). Transepithelial resistance (TER) and permeability to Na⁺ and Cl⁻ for each tissue are provided in Tables 3.4 – 3.6.

To determine if claudin-12 confers P_{Ca} across the small intestine, we performed bi-ionic diffusion potential experiments on tissue from WT and *Cldn12* KO mice. Consistent with our previous results, P_{Ca} was significantly greater in younger mice. However, no differences were observed between WT and *Cldn12* KO mice at any age or tissue (Figure 3.4D-F). These results demonstrate the greater P_{Ca} observed across the jejunum and ileum of younger mice can be attributed to claudin-2. Transepithelial resistance (TER) and permeability to Na⁺ and Cl⁻ for each tissue are provided in Tables 3.7 – 3.9.
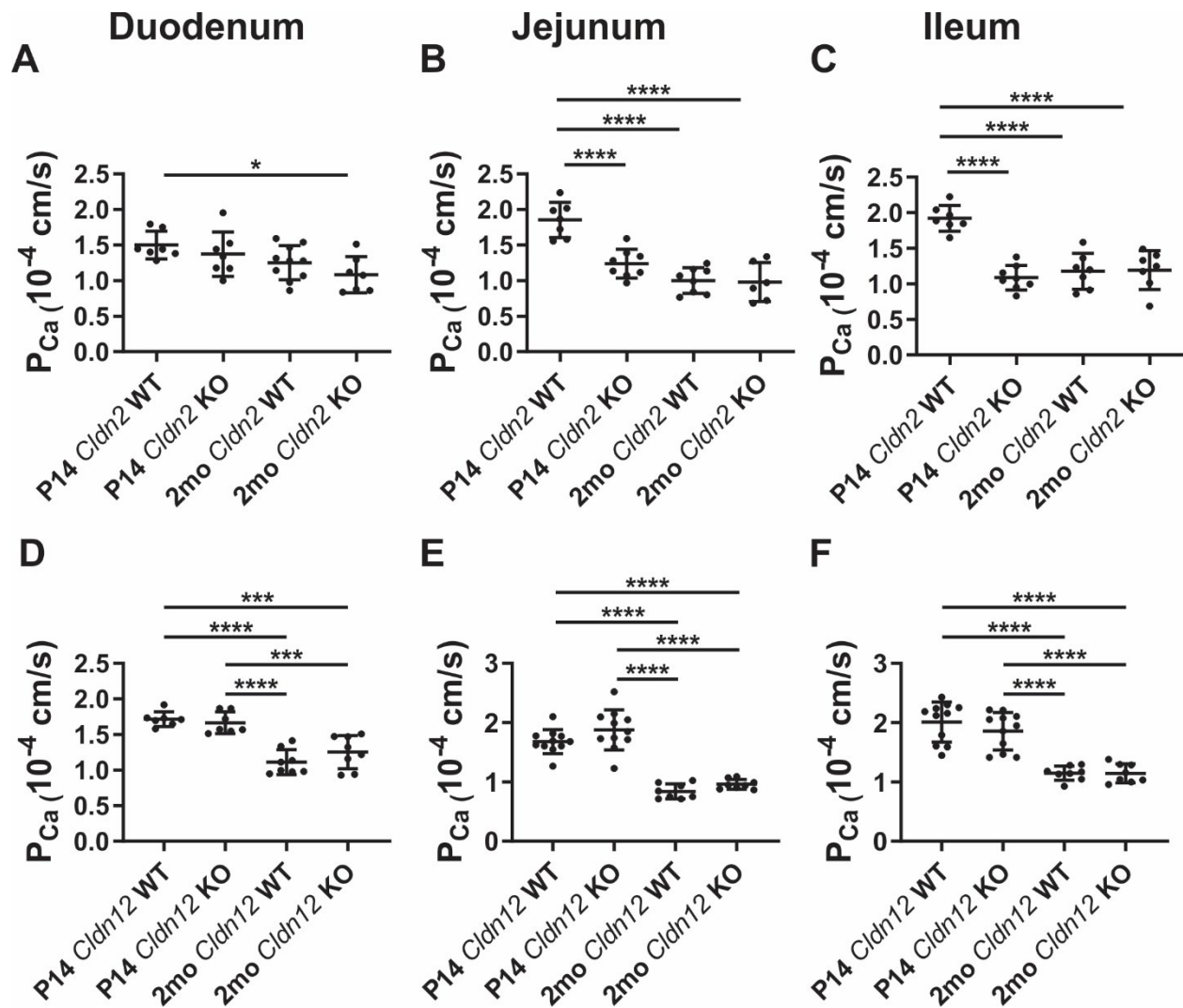
Figure 3.4. Claudin-2 confers increased P_{Ca} across jejunum and ileum in P14 mice. Calcium permeability across the duodenum (A, D), jejunum (B, E), and ileum (C, F) from *Cldn2* (A-C) and *Cldn12* (D-F) WT and KO mice at P14 and 2 months. Data presented as mean ± SD and compared by one-way ANOVA with Tukey's multiple comparisons test, *$P < 0.05$, ***$P < 0.001$, ****$P < 0.0001$.

Table 3.4. Resistance and ion permeability across the duodenum in *Cldn2* KO mice

	P14 WT (n = 7)	P14 *Cldn2* KO (n = 7)	2 months WT (n = 10)	2 months *Cldn2* KO (n = 7)
TER (Ω cm^2)	58.6 ± 6.0	60.7 ± 10.3	59.0 ± 8.5	60.0 ± 10.6
P_{Na} (x10^{-4} cm s^{-1})	0.284 ± 0.028	0.260 ± 0.040	0.288 ± 0.030	0.282 ± 0.032
P_{Cl} (x10^{-4} cm s^{-1})	0.201 ± 0.034	0.208 ± 0.039	0.190 ± 0.033	0.200 ± 0.052
P_{Na}/P_{Cl}	1.44 ± 0.20	1.26 ± 0.11	1.58 ± 0.24	1.50 ± 0.30
P_{Ca}/P_{Na}	5.30 ± 0.43[a]	5.30 ± 0.66[a]	4.34 ± 0.56[b]	3.83 ± 0.63[b]

TER, transepithelial resistance; P_x, permeability to ion x. Data presented as mean $\pm$ SD and compared by one-way ANOVA with Tukey's multiple comparisons test. Different superscript letters denote significant differences between groups ($P < 0.05$).

Table 3.5. Resistance and ion permeability across the jejunum in *Cldn2* KO mice

	P14 WT (n = 7)	P14 *Cldn2* KO (n = 8)	2 months WT (n = 8)	2 months *Cldn2* KO (n = 6)
TER (Ω cm^2)	47.9 ± 3.1^a	59.9 ± 6.9^b	58.5 ± 4.5^b	55.5 ± 9.5^{ab}
P_{Na} (x10^{-4} cm s^{-1})	0.346 ± 0.035^a	0.244 ± 0.025^b	0.316 ± 0.033^a	0.339 ± 0.066^a
P_{Cl} (x10^{-4} cm s^{-1})	0.227 ± 0.035^a	0.210 ± 0.027^{ac}	0.160 ± 0.017^b	0.173 ± 0.030^{bc}
P_{Na}/P_{Cl}	1.55 ± 0.29^a	1.17 ± 0.09^a	2.01 ± 0.27^b	1.99 ± 0.39^b
P_{Ca}/P_{Na}	5.40 ± 0.63^a	5.10 ± 0.61^a	3.18 ± 0.56^b	2.85 ± 0.74^b

TER, transepithelial resistance; P_x, permeability to ion x. Data presented as mean $\pm$ SD and compared by one-way ANOVA with Tukey's multiple comparisons test. Different superscript letters denote significant differences between groups ($P < 0.05$).

Table 3.6. Resistance and ion permeability across the ileum in *Cldn2* KO mice

	P14 WT (n = 7)	P14 *Cldn2* KO (n = 8)	2 months WT (n = 7)	2 months *Cldn2* KO (n = 7)
TER (Ω cm^2)	46.4 ± 4.1^a	70.7 ± 7.6^b	43.1 ± 5.1^{ac}	42.3 ± 10.2^{ac}
P_{Na} (x10^{-4} cm s^{-1})	0.408 ± 0.04^a	0.216 ± 0.038^b	0.418 ± 0.078^a	0.405 ± 0.124^a
P_{Cl} (x10^{-4} cm s^{-1})	0.199 ± 0.026^a	0.189 ± 0.019^a	0.210 ± 0.023^a	0.216 ± 0.029^a
P_{Na}/P_{Cl}	2.06 ± 0.27^a	1.15 ± 0.16^b	2.03 ± 0.48^a	1.88 ± 0.53^a
P_{Ca}/P_{Na}	4.76 ± 0.25^a	5.08 ± 0.59^a	2.98 ± 1.03^b	3.22 ± 1.27^b

TER, transepithelial resistance; P_x, permeability to ion x. Data presented as mean $\pm$ SD and compared by one-way ANOVA with Tukey's multiple comparisons test. Different superscript letters denote significant differences between groups ($P < 0.05$).

Table 3.7. Resistance and ion permeability across the duodenum in *Cldn12* KO mice

	P14 WT (n = 7)	P14 *Cldn2* KO (n = 8)	2 months WT (n = 7)	2 months *Cldn2* KO (n = 7)
TER (Ω cm^2)	51.7 ± 3.8	54.3 ± 3.4	58.9 ± 6.1	54.9 ± 7.8
P_{Na} (x10^{-4} cm s^{-1})	0.304 ± 0.02	0.281 ± 0.021	0.286 ± 0.032	0.305 ± 0.043
P_{Cl} (x10^{-4} cm s^{-1})	0.241 ± 0.018^a	0.236 ± 0.025^a	0.189 ± 0.022^b	0.215 ± 0.034^{ab}
P_{Na}/P_{Cl}	1.27 ± 0.10^{ac}	1.20 ± 0.08^a	1.53 ± 0.18^b	1.43 ± 0.16^{bc}
P_{Ca}/P_{Na}	5.67 ± 0.26^a	5.93 ± 0.47^a	3.91 ± 0.59^b	4.12 ± 0.56^b

TER, transepithelial resistance; P_x, permeability to ion x. Data presented as mean $\pm$ SD and compared by one-way ANOVA with Tukey's multiple comparisons test. Different superscript letters denote significant differences between groups ($P < 0.05$).

Table 3.8. Resistance and ion permeability across the jejunum in *Cldn12* KO mice

	P14 WT (n = 11)	P14 *Cldn2* KO (n = 11)	2 months WT (n = 8)	2 months *Cldn2* KO (n = 8)
TER (Ω cm^2)	46.5 ± 5.6^a	43.1 ± 5.9^a	59.8 ± 5.9^b	55.4 ± 8.5^b
P_{Na} (x10^{-4} cm s^{-1})	0.352 ± 0.07^{ac}	0.401 ± 0.065^a	0.322 ± 0.035^b	0.323 ± 0.06^{bc}
P_{Cl} (x10^{-4} cm s^{-1})	0.232 ± 0.030^a	0.248 ± 0.048^a	0.148 ± 0.017^b	0.163 ± 0.021^b
P_{Na}/P_{Cl}	1.51 ± 0.25^a	1.67 ± 0.37^{ac}	2.19 ± 0.25^b	2.06 ± 0.39^{bc}
P_{Ca}/P_{Na}	4.94 ± 0.68^a	4.74 ± 0.57^a	2.64 ± 0.36^b	3.00 ± 0.53^b

TER, transepithelial resistance; P_x, permeability to ion x. Data presented as mean $\pm$ SD and compared by one-way ANOVA with Tukey's multiple comparisons test. Different superscript letters denote significant differences between groups ($P < 0.05$).

Table 3.9. Resistance and ion permeability across the ileum in *Cldn12* KO mice

	P14 WT (n = 11)	P14 *Cldn2* KO (n = 11)	2 months WT (n = 8)	2 months *Cldn2* KO (n = 8)
TER (Ω cm^2)	38.9 ± 6.3^a	39.5 ± 4.8^a	49.9 ± 4.8^b	47.1 ± 5.8^b
P_{Na} (x10^{-4} cm s^{-1})	0.492 ± 0.080^a	0.427 ± 0.093^a	0.354 ± 0.033^b	0.389 ± 0.060^b
P_{Cl} (x10^{-4} cm s^{-1})	0.224 ± 0.040^a	0.225 ± 0.033^a	0.196 ± 0.021^a	0.203 ± 0.032^a
P_{Na}/P_{Cl}	2.26 ± 0.37^a	2.26 ± 0.51^a	1.84 ± 0.23^a	1.93 ± 0.18^a
P_{Ca}/P_{Na}	$4.15 \pm 0.58^{a,b}$	$3.91 \pm 0.99^{a,b}$	$3.32 \pm 0.50^{b,c}$	2.97 ± 0.24^c

TER, transepithelial resistance; P_x, permeability to ion x. Data presented as mean $\pm$ SD and compared by one-way ANOVA with Tukey's multiple comparisons test. Different superscript letters denote significant differences between groups ($P < 0.05$).

3.4.4. Epidermal growth factor is present in breast milk and increases *Cldn2* expression

We next hypothesized that a bioactive compound present in breast milk mediates the increased P_{Ca} observed via increased Cldn2 expression. To test this hypothesis, half of a litter of pups was weaned early to solid chow while the other half of the litters remained suckling with the dam. In both the jejunum and ileum, *Cldn2* expression was lower by 50% in the mice that were no longer receiving breast milk (Figure 3.5A-B). These results suggest that breast milk indeed contains a bioactive compound that acts to increase *Cldn2* expression. However, early weaning itself may also pose stress to the pups which may then alter intestinal gene expression.[226, 227] To specifically implicate breast milk in regulating claudin-2 expression, we grew Caco-2 cells in the absence or presence of varying concentrations of breast milk from human donors. We observed increased CLDN2 expression by immunoblot when the concentration of milk in the cell culture media was 2-5% (Figure 3.5C-D). Expression of CLDN4, CLDN7 and CLDN10 (Supplementary Figure 3.6A-C) were not altered by breast milk thus suggesting a specific effect on CLDN2.

Vitamin D is known to increase claudin-2 expression although its concentration in breast milk is quite low.[121, 228] Prolactin is also present in breast milk and has been proposed to increase Ca^{2+} absorption via both transcellular and paracellular pathways along the small and large intestine.[229-232] Epidermal growth factor (EGF) has been reported in murine and human breast milk and to be involved in intestinal epithelial proliferation and differentiation.[226] EGF has also previously been reported to alter claudin-2 expression with different effects based on the cell line.[140, 141] Consistent with the literature we found an average of 31.7 ± 23.1 ng/mL EGF in the samples of breast milk collected for this study. This is lower than the published average of 83 ± 14 ng/mL, however, the mothers in the current study were further postpartum than in the

previous published work.[233-235] When grown in media containing vitamin D, CLDN2 expression increased by 2.5-fold ($\pm$ 1.0), consistent with previous findings.[121] When grown with 100 ng/mL EGF, CLDN2 expression was increased by 3.5-fold ($\pm$ 2.1). Furthermore, this increase in expression was specific to CLDN2. Prolactin had no effect on CLDN2 expression in the Caco-2 intestinal epithelial cell model (Figure 3.5E-F and Supplementary Figure 3.6D-F). These results suggest that EGF is present in breast milk and regulates intestinal CLDN2 expression.

To specifically implicate EGF in breast milk in regulating CLDN2 abundance, we cultured Caco-2 cells in the presence of the EGF receptor (EGFR) inhibitor erlotinib with or without media containing 2% breast milk (Figure 3.5G-H). Consistent with the previous experiments, the addition of breast milk increased CLDN2 abundance 2-fold. The addition of 1 µM but not 0.1 µM erlotinib inhibited the milk-induced increase in CLDN2. These results further implicate EGF as the specific bioactive compound present in breastmilk which increases intestinal expression of *Cldn2*.

EGF exerts its actions via the plasma membrane EGF receptor (EGFR). Therefore, if EGF present in breast milk is regulating intestinal expression of *Cldn2*, the EGFR must be expressed in these intestinal cells. Indeed, *Egfr* is expressed in all segments of the small intestine and proximal colon of *Cldn2* WT and KO mice at P14 although no differences were found between genotypes (Figure 3.5I). Through histochemical staining, we also found EGFR in the jejunum and ileum of mice at both P14 and 6 weeks old (Figure 3.5J-M). We observed however more EGFR staining in older mice, likely due to upregulation from the lower exposure to EGF at this age.
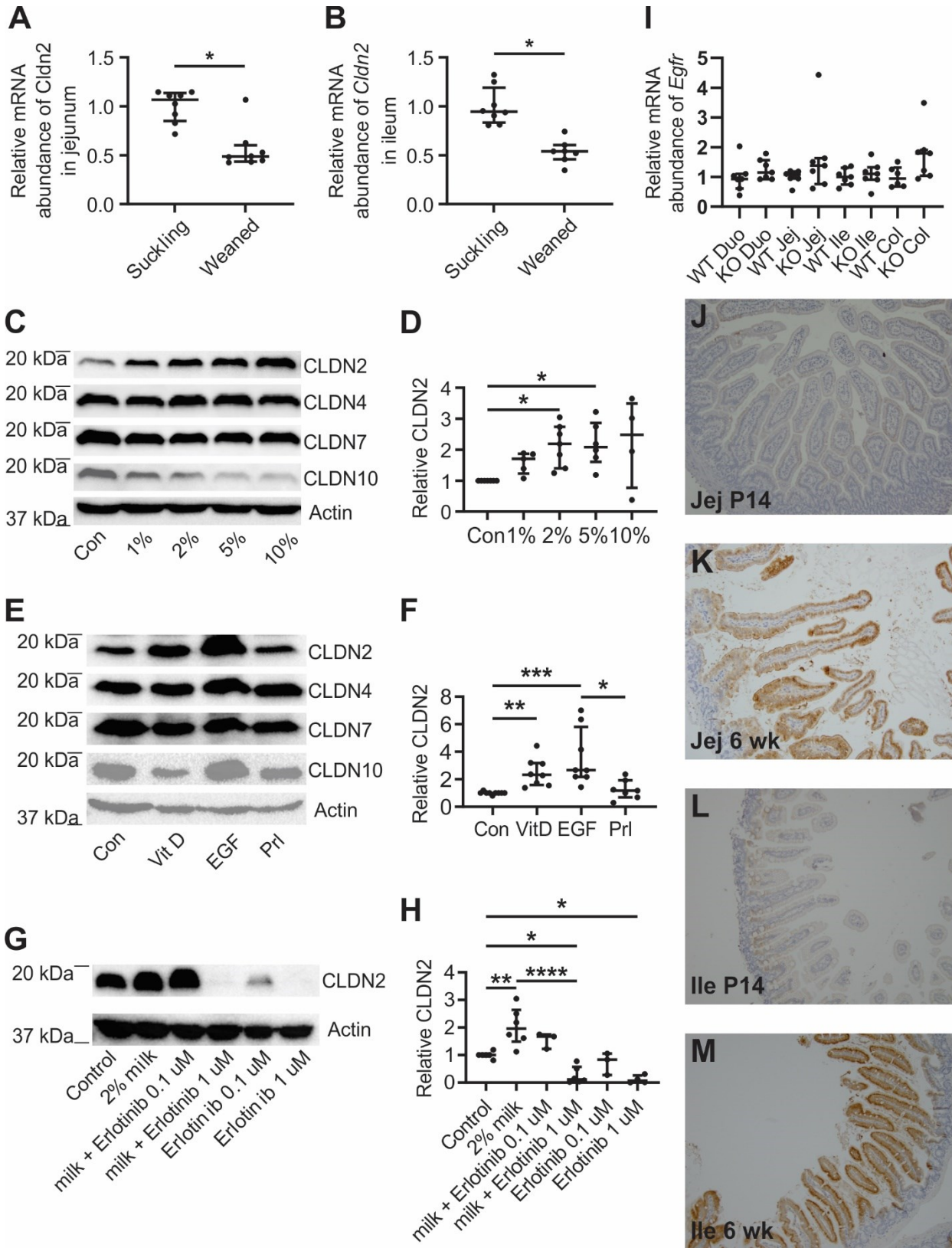
Figure 3.5. EGF is present in breastmilk and increases claudin-2 expression. mRNA abundance of *Cldn2* in the A) jejunum ($P = 0.0019$) and B) ileum ($P = 0.0003$) of mice at P15 who remain with the dam (suckling) or who were weaned to solid chow at P12 (weaned). Expression is normalized to *β-Actin* and presented as relative to suckling group. C) Representative blots from 4 – 7 independent experiments of Caco-2 cells grown in media for 48 hours with increasing concentration as percent by volume of human breast milk. D) Semi-quantification of CLDN2 abundance from panel C. E) Representative blots from 4 – 8 independent experiments of Caco-2 cells grown in media with additional hormones vitamin D 20 nM, EGF 100 ng/mL, and prolactin 400 ng/mL for 48 hours. F) Semi-quantification of CLDN2 abundance from panel E. G) Representative blots from 3 – 6 independent experiments of Caco-2 cells grown with or without human breast milk and the EGFR inhibitor erlotinib at the concentration indicated for 48 hours. H) Semi-quantification of CLDN2 abundance from panel G. I) Expression of *Egfr* encoding EGF receptor in the small and large intestine of *Cldn2* WT and *Cldn2* KO mice at P14. J-M) Histochemical staining for EGFR in jejunum and ileum of mice at P14 and 6 weeks old. Images were taken at 20X magnification. Representative images are obtained from evaluation of N = 4-6 mice per group. Data presented as median ± IQR and compared by Mann-Whitney test or Kruskal-Wallis test. *$P < 0.05$, **$P < 0.01$, ***$P < 0.001$, ****$P < 0.0001$. Con, control; VitD, calcitriol; EGF, epidermal growth factor; Prl, prolactin; milk, breast milk; Duo, duodenum; Jej, jejunum; Ile, ileum; Col, colon.
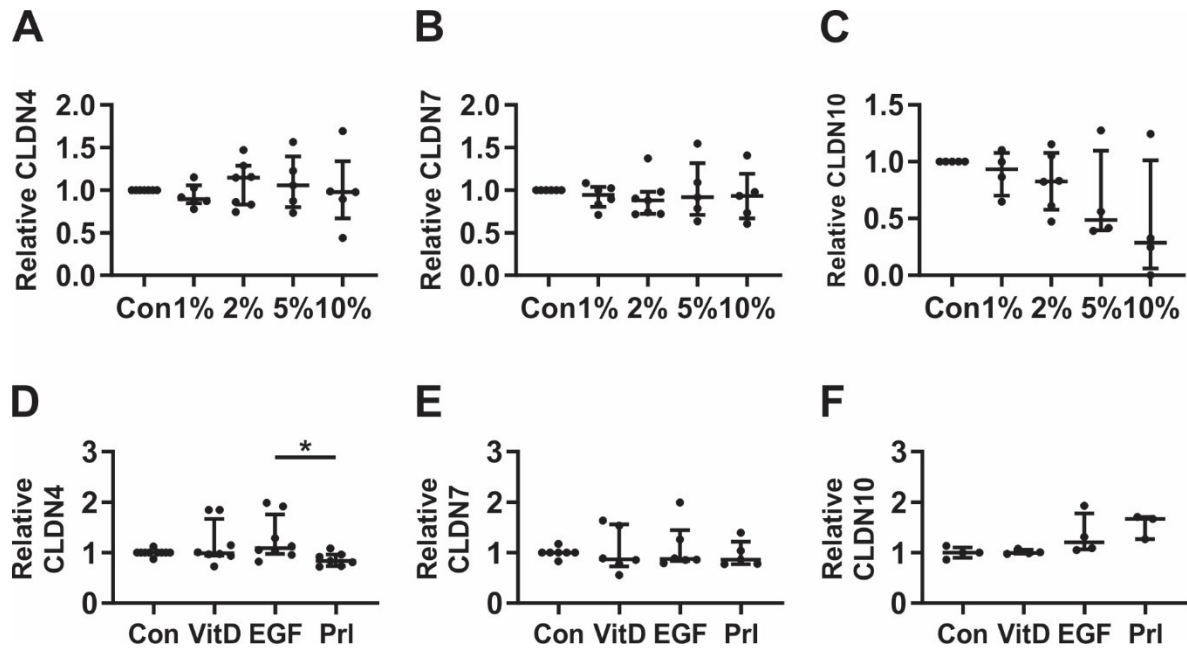
Figure 3.6. Breast milk and EGF have do not increase expression of CLDN4, CLDN7 and CLDN10. Semi-quantification of A) CLDN4, B) CLDN7, and C) CLDN10 from blots depicted in Figure 3.5C and semi-quantification of D) CLDN4, E) CLDN7, and F) CLDN10 from blots depicted in Figure 3.5E.

3.4.5. *Cldn2* KO mice have impaired bone mineralization at 2 weeks

We hypothesized that the loss of *Cldn2* mediated intestinal absorption and renal reabsorption of Ca^{2+} would lead to an overall inability to maintain an optimal Ca^{2+} balance for bone mineralization during growth. We, therefore, examined the microarchitecture of femurs from *Cldn2* WT and KO mice at P14 (Table 3.10). We observed significant decreases in bone volume, cross-sectional thickness, and tissue mineral density in the *Cldn2* KO mice. No significant differences were observed in the parameters of trabecular bone. These results suggest that the greater P_{Ca} across the small intestine early in life conferred by claudin-2 is necessary to attain a positive Ca^{2+} to facilitate peak bone mineralization during this critical period of growth.

Table 3.10. Microarchitecture of femurs from *Cldn2* WT and KO mice at 2 weeks.

	WT	*Cldn2* KO	*P* – value
Cortical Bone			
N	7	6	
Tissue Volume (mm^3)	0.322 ± 0.020	0.328 ± 0.016	0.819
Bone Volume (mm^3)	0.101 ± 0.005	0.085 ± 0.003	0.034
Endocortical Volume (mm^3)	0.221 ± 0.015	0.243 ± 0.013	0.312
Cross-sectional Thickness (mm)	0.081 ± 0.001	0.070 ± 0.001	< 0.001
Perimeter (mm)	3.72 ± 0.11	3.76 ± 0.10	0.813
Femur Length (mm)	9.07 ± 0.26	9.17 ± 0.19	0.754
Tissue Mineral Density (g/cm^3)	1.11 ± 0.01	1.07 ± 0.01	0.023
Trabecular Bone			
N	6	6	
BV/TV (%)	24.6 ± 1.1	26.7 ± 1.3	0.2487
Trabecular Number (1/mm)	0.014 ± 0.0003	0.015 ± 0.0004	0.0802
Trabecular Width (µm)	17.9 ± 0.04	18.1 ± 0.6	0.8686
Trabecular Separation (µm)	55.5 ± 2.2	50.0 ± 2.4	0.1175
Growth Plate Thickness (µm)	388. ± 18	396 ± 32	0.8482

BV/TV, bone volume / tissue volume. Data presented as mean ± SD and compared by unpaired t-test.

3.4.6. Two-week-old *Cldn2* KO mice have a compensatory reduction in urinary Ca²⁺ excretion and increased net transcellular absorption across the jejunum

Given that claudin-2 mediates increased small intestine P_{Ca} at P14, we hypothesized that *Cldn2* KO mice at this age would display intestinal and renal alterations to compensate for the loss of paracellular Ca²⁺ absorption. Indeed, urinary Ca²⁺ excretion normalized to creatinine was more than 2-fold lower in the *Cldn2* KO mice relative to WT (Table 3.11). This is particularly significant given that *Cldn2 KO* mice at 8 weeks have a 3-fold increase in fractional Ca²⁺ excretion.[146] We next examined the expression of genes involved in renal Ca²⁺ reabsorption and found greater expression of *Trpv5*, *Calb1*, and *Atp2b1* which together mediate transcellular Ca²⁺ reabsorption in the distal renal tubule (Supplementary Figure 3.7). Thus, our results suggest compensatory increased Ca²⁺ reabsorption in this segment of *Cldn2* KO pups leading to decreased urinary excretion. Interestingly, we also noted decreased urinary phosphate, magnesium, and chloride excretion in the P14 *Cldn2* KO mice (Table 3.11).

Serum Ca²⁺ is tightly regulated. Decreased plasma Ca²⁺ results in increased plasma active vitamin D (calcitriol) via parathyroid hormone (PTH) signaling to increase intestinal Ca²⁺ absorption.[236, 237] Plasma PTH was slightly higher in the *Cldn2* KO mice although not statistically different than WT (Table 3.11). However, plasma calcitriol was almost 1.6-fold greater in the *Cldn2* KO mice. FGF-23 was not different between groups.

We next hypothesized that the increased plasma calcitriol would lead to increased transcellular Ca²⁺ absorption across the intestine of P14 *Cldn2* KO mice. We examined expression of apical Ca²⁺ channels *Trpv6, Cacna1d* encoding Ca_v1.3, and *Trpm7* across all segments of the small intestine and proximal colon (Figure 3.8A-C). The only significant difference noted was a 1.3-fold increase in *Trpm7* expression in the duodenum of *Cldn2* KO

113

pups (P = 0.0262). Of note, we observed a 2.3-fold greater expression of *S100g*, which encodes

the intracellular binding protein calbindin-D$_{9k}$ (P = 0.0221) across the jejunum of the *Cldn2* KO

mice (Figure 3.8D). No differences were observed in the expression of the basolateral Ca^{2+}

extrusion proteins *Atp2b1* encoding PMCA1b, and *Slc8a1*, encoding NCX1 (Figure 3.8E-F).

Increased *S100g* expression suggests greater influx of Ca^{2+} into the enterocyte.[55] Accordingly,

we measured net apical to basolateral flux of $^{45}Ca^{2+}$ across *ex vivo* sections of jejunum. Indeed,

the *Cldn2* KO mice at P14 had greater net absorption across this segment than WT littermates

(Figure 3.8G).

Table 3.11. Urine biochemistries and plasma calciotropic hormones at P14

Urine	N	WT	N	*Cldn2* KO	*P* - value
Ca^{2+}/Creatinine	8	0.84 ± 0.44	8	0.38 ± 0.11	0.011
Na^+/Creatinine	8	28.2 ± 20.4	8	19.0 ± 10.0	0.273
K^+/Creatinine	8	122 ± 44	8	96.1 ± 30.1	0.189
Mg^{2+}/Creatinine	8	20.3 ± 6.0	8	11.7 ± 2.1	0.002
PO_4^{3-}/Creatinine	8	98.4 ± 29.1	8	65.3 ± 22.0	0.0226
Cl^-/Creatinine	8	91.4 ± 38.4	8	53.9 ± 29.2	0.0453
Plasma					
PTH (pg/mL)	8	110.7 ± 51.5	8	168.2 ± 99.3	0.1680
Calcitriol (pmol/L)	6	128.2 ± 65.7	5	210.3 ± 33.0	0.0323
FGF-23 (pg/mL)	7	457.0 ± 121.6	8	407.9 ± 70.6	0.3480

PTH, parathyroid hormone; FGF-23, fibroblast growth factor. Values presented as mean $\pm$ SD and compared by unpaired t-test.
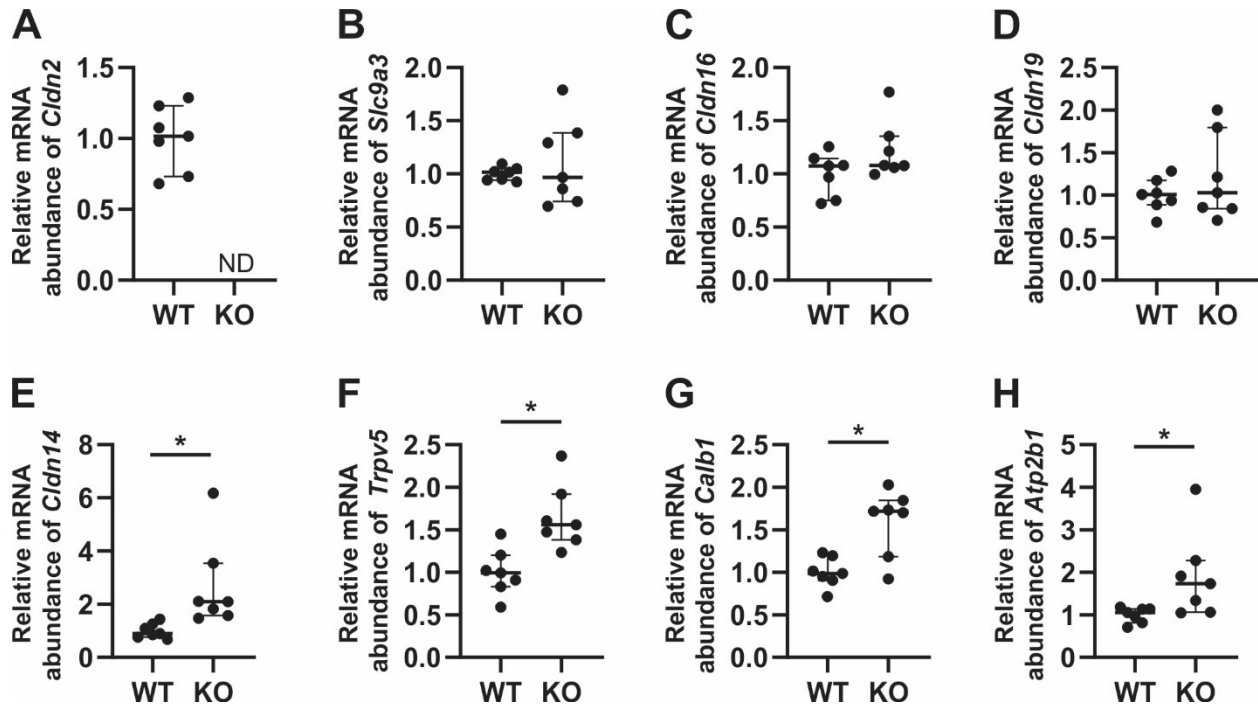
Figure 3.7. Compensatory increase in genes mediating renal Ca^{2+} reabsorption in *Cldn2* KO mice at 2 weeks. A) Confirmation that no *Cldn2* expression is detectable in the *Cldn2* KO mouse. Renal expression of B) *Slc9a3* encoding NHE3 ($P > 0.9999$), C) *Cldn16* ($P = 0.2593$), D) *Cldn19* ($P = 0.7104$), E) *Cldn14* ($P = 0.0006$), F) *Trpv5* ($P = 0.0023$), G) *Calb1* encoding calbindin-D$_{28k}$ ($P = 0.0262$), and H) *Atp2b1* encoding PMCA1b ($P = 0.0262$) in *Cldn2* WT and *Cldn2* KO mice at P14. Expression is normalized to *Gapdh* and presented as relative to WT. Data presented at median ± IQR. WT and KO compared by Mann-Whitney test. ND, not detected.
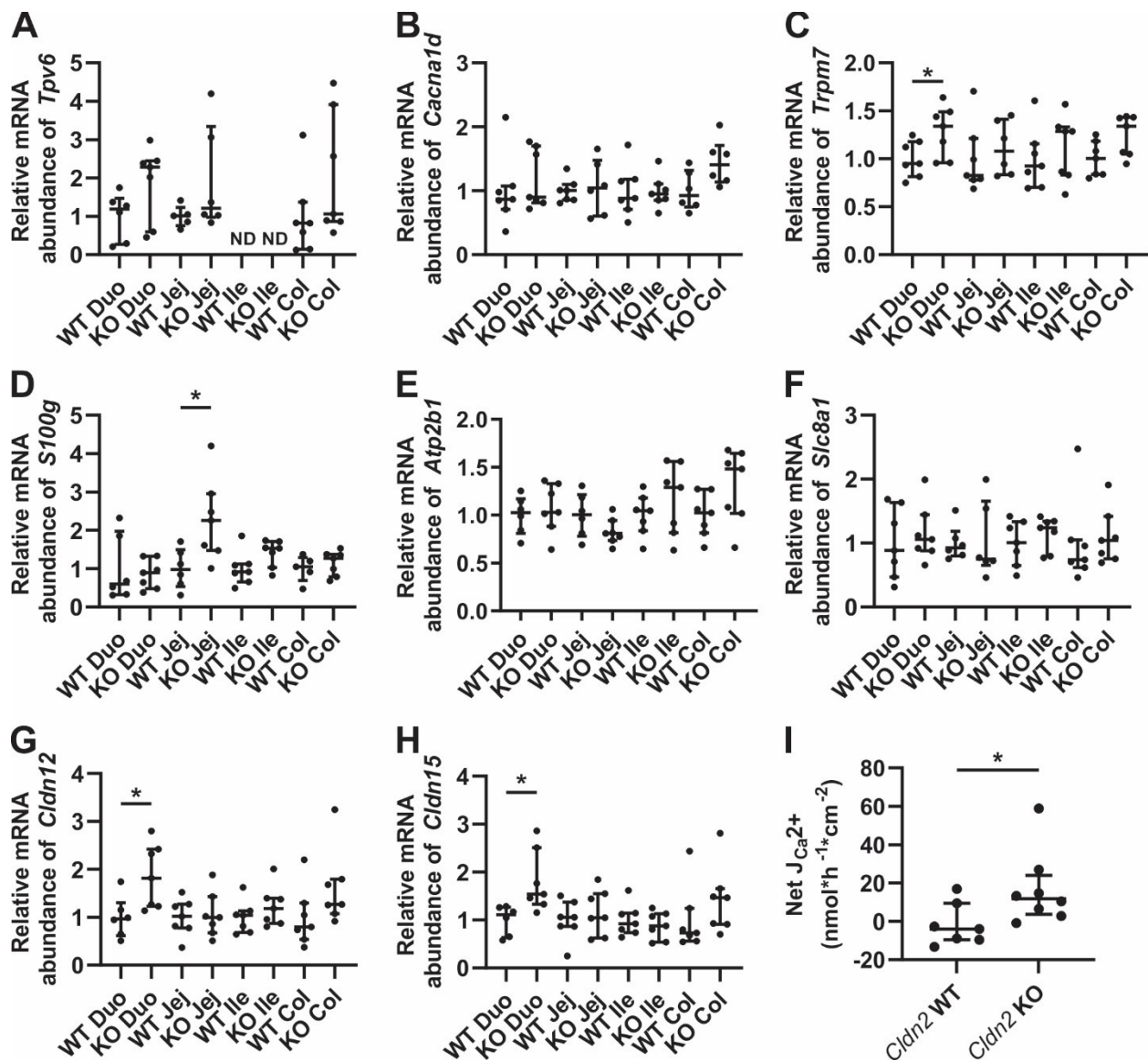
Figure 3.8. *Cldn2* KO pups at P14 display a compensatory increase in jejunal transcellular Ca^{2+} absorption. Relative abundance of genes encoding A) TRPV6, B) Ca$_v$1.3, C) TRPM7, D) calbindin-D$_{9k}$, E) PMCA1b, F) NCX1 G) claudin-12, and H) claudin-15 in the intestine of WT and *Cldn2* KO mice at P14. Expression normalized to *β-Actin* and expressed relative to WT for each intestinal segment. I) Net apical to basolateral ^{45}Ca^{2+} flux across *ex vivo* segments of jejunum from P14 mice (P = 0.0289). Each data point per segment represents an individual animal. Data presented as median ± IQR. Comparison of KO to WT for each intestinal segment by Mann-Whitney test. *$P < 0.05$. Duo, duodenum; Jej, jejunum; Ile, ileum; Col, colon. ND = not detected.

3.5 Discussion

We found greater P_{Ca} across the jejunum and ileum of suckling compared to older mice. Younger mice, therefore, likely have greater capacity for intestinal Ca^{2+} absorption via the paracellular pathway. Moreover, given the high Ca^{2+} concentration in breast milk (~5.5 mM) relative to plasma (~1.2 mM) providing a favourable electrochemical gradient, the paracellular pathway likely predominates during suckling .[238] Using genetic knockout mouse models, we were able to attribute the greater P_{Ca} in young animals to increased claudin-2 expression. Loss of *Cldn2* results in decreased bone mineralization at 2 weeks, despite compensatory increased transcellular intestinal Ca^{2+} absorption and renal reabsorption. Using an intestinal epithelial cell model, increased *Cldn2* expression was found to be mediated by EGF in breast milk, as incubating cells with breast milk increased claudin-2 an expression that was abolished by coincubation with the EGF receptor antagonist erlotinib. Thus, EGF is a bioactive compound in breast milk that increases intestinal paracellular Ca^{2+} absorption from the small intestine to meet the high demands of this mineral required for optimal growth.

The current work contributes significant evidence that reduced paracellular Ca^{2+} absorption across the small intestine results in decreased bone mineralization. Failure to reach optimal peak bone mass by early adulthood has life-long consequences, increasing osteoporosis risk. In 2010, an estimated 54% of adults over 50 years of age in the US had osteoporosis or low bone mass and this is projected to increase to over 70% prevalence by 2030.[239] Between 3 and 11 weeks of age in rats, intestinal Ca^{2+} absorption is equivalent to whole body Ca^{2+} retention and therefore, bone mineralization.[102] Similarly, in humans, Ca^{2+} retention and intestinal absorption are greatest during infancy and adolescence.[190] Previous studies in rats at 2, 3, and 6 weeks of

age and as adults suggests that the paracellular absorption pathway predominates early in life and decreases with age but remains important for overall net absorption across the small intestine.[35, 111] Still, both transcellular and paracellular pathways of intestinal Ca^{2+} absorption contribute to overall Ca^{2+} retention enabling growth and maintenance of bone mineral density.[222]

Physiologically, the paracellular pathway is energetically favorable because, unlike the transcellular pathway, it does not directly consume ATP.[223] In particular, diffusion down a concentration gradient is favourable under conditions of relatively high dietary Ca^{2+} intake such as occurs in breast milk. Dietary intake may explain why net absorption is observed across the small intestine of suckling rodents while net secretion is observed across the jejunum and ileum of adult mice consuming chow.[39, 42, 43, 104] Importantly, diffusion through the paracellular pore is driven by an electrochemical gradient.[41] Thus, this pathway is more beneficial under conditions of high dietary intake and thus increased luminal concentration of Ca^{2+} but may permit Ca^{2+} secretion and loss under conditions of lower Ca^{2+} intake.[70, 86] It is, furthermore, intriguing to consider the forms of Ca^{2+} in breast milk and standard rodent chow in the context of the current study. In breast milk, Ca^{2+} is bound as calcium phosphate within a casein micelle and as calcium citrate.[240-242] In rodent chow, Ca^{2+} is present in the form of salts including phosphate, carbonate, and iodate. How this translates into the food matrix in each intestinal lumen segment is not known.

In this study we highlight the vital of role of intestinal claudin-2 for overall Ca^{2+} balance prior to weaning. Claudin-2 has previously been implicated in mediating Ca^{2+} permeability across intestinal and renal epithelia in adults.[78, 84, 86] Consistent with our results, loss of *Cldn2* in mice decreased cation permeability (P_{Na}) across the small intestine of mice that were 2 and 8 weeks of age.[77] The current and previous works demonstrate greater claudin-2 expression in

suckling animals.[80] In humans, children have a 3.3-fold greater claudin-2 abundance than adults in the duodenum. The authors of this work state that claudin-2 expression changes with age are independent of weaning although the pediatric population examined was 1-5 years old and the age of weaning was not specifically stated.[224] It is possible that expression was even greater during infancy or that the jejunum and ileum are tissues of greater significance. Nonetheless, the current work provides the possibility that regulation of intestinal claudin-2 abundance presents a potential therapeutic target to maximize Ca^{2+} absorption for those with poor bone mineralization.

EGF has long been recognized as a bioactive compound in breast milk, which is also present in saliva at all ages.[132-135] EGF in amniotic fluid and breast milk has a strong trophic effect on infant intestines and is associated with a decreased risk of necrotizing enterocolitis (NEC) in premature infants.[243, 244] In mice weaned early, EGF administration increases weight gain, villous height, crypt depth, and enterocyte proliferation.[226] EGF is critical for epithelial proliferation and repair throughout life and lower salivary levels are associated with small intestine ulcers.[244] The current work demonstrates that EGF increases CLDN2 abundance in Caco-2 human colon epithelial cells. Similarly, previous work has shown that addition of EGFR ligands to growth media increases CLDN2 in these cells.[139] Consistent with an effect of EGF on breast milk mediating increased claudin-2 expression, we found that weaning from breast milk leads to decreased *Cldn2* expression in infant mice. Therefore, in addition to previous investigations of EGF as a therapeutic for intestinal conditions, we present evidence for the potential of EGF as a target to modulate intestinal Ca^{2+} absorption.

Claudin-2 has also been proposed as a therapeutic target for inflammatory bowel disease (IBD) where expression increases in the duodenum and sigmoid colon but not ileum.[82, 224, 245] Transgenic overexpression of *Cldn2* under a villin promoter leads to expression beyond the

crypts into the surface epithelium and led to exacerbated disease severity in an IBD model. In contrast, *Cldn2* KO mice have a delayed onset of and reduced severity of immune-mediated colitis, but a greater mortality due to intestinal obstruction.[246] Both chemical and infectious models of IBD suggest that claudin-2 may be protective.[247] However, claudin-2 expression is upregulated via EGFR activation in colon cancer, a process that correlates with disease progression.[248, 249] These results suggest a critical balance of inflammation and proliferation of intestinal epithelia mediated by claudin-2.[247] This balance must further consider a vital role for claudin-2 in early life Ca^{2+} balance that must be considered when developing potential therapies for IBD.

A potential limitation of the current study is the lack of investigation of the large intestine. Previous work by our group found that, at three months, *Cldn2* KO mice have decreased P_{Ca} across the proximal colon.[86] The colon is a major site of net Ca^{2+} absorption in adult humans and rodents, a process that may be mediated in some part by the microbiome.[38, 39, 250-253] However, only net secretion has been observed in suckling mammals.[104] Therefore, it seems unlikely that the colon contributes to net Ca^{2+} absorption in young mammals although further research is required to test this hypothesis.

In conclusion, we demonstrate that small intestine permeability to Ca^{2+} is 2-fold greater in suckling versus adult mice. This greater capacity for paracellular Ca^{2+} absorption is conferred by increased claudin-2 expression induced by EGF in breast milk. Loss of this absorption pathway results in suboptimal bone mineralization during this critical period of growth. This research illustrates a vital pathway to maximizing intestinal Ca^{2+} absorption and highlights a potential therapeutic target to maximize bone mineralization.

Chapter 4

Claudin-2 or claudin-12 in the colon is required to maintain calcium homeostasis

Adapted from: Megan R. Beggs, Kennedi Young, Wanling Pan, Debbie O'Neill, Matthew Saurette, Allein Plain, Juraj Rievaj, Michael R. Doschak, Emmanuelle Cordat, Henrik Dimke, R. Todd Alexander, "Claudin-2 or claudin -12 is required to maintain calcium homeostasis" prepared for submission.

4.1. Abstract

Calcium (Ca^{2+}) is a mineral vital for a myriad of physiological functions. Ca^{2+} homeostasis is maintained by interactions between intestinal absorption, renal reabsorption and bone remodelling. Intestinal and renal (re)absorption occurs via transcellular and paracellular pathways where the paracellular route is hypothesized to predominate. Claudins are tight junction proteins that confer paracellular permeability properties to epithelia. Claudins (*Cldn*)-2 or -12 contribute calcium permeability across the intestine and renal tubule. However, loss of either claudin in a mouse model does not result in a negative Ca^{2+} balance or compensatory changes, suggesting the absence of one compensates for the other. To test whether CLDN2 and CLDN12 contribute to Ca^{2+} homeostasis by forming independent pores, we generated a double knockout mouse model (DKO). DKO mice at 2 months displayed reduced intestinal absorption and increased urinary losses of Ca^{2+}, leading to hypocalcemia and markedly impaired bone mineralization. DKO mice have decreased Ca^{2+} permeability across the colon but not small intestine. Consistent with each claudin forming an independent Ca^{2+} pore, claudin-2 and claudin-12 did not physically interact in cell culture and PCa is increased in cell models expressing both claudins compared to just one. Together this data is consistent with claudin-2 and -12 independently mediating paracellular intestinal Ca^{2+} absorption and renal reabsorption; processes critical for maintaining Ca^{2+} homeostasis.

4.2. Introduction

Calcium (Ca^{2+}) is an essential mineral vital to physiological processes including cell signaling, muscle contraction and bone mineralization. Serum Ca^{2+} is tightly regulated within a narrow range and homeostasis is maintained by interactions between the intestines, kidneys, and

bones.[1] Suboptimal Ca^{2+} handling in one or more of these organs will elicit compensation from the other systems. For example, if intestinal Ca^{2+} absorption or renal reabsorption is suboptimal, mineralization of bones can be compromised to maintain serum Ca^{2+} levels.

Intestinal absorption occurs via either a transcellular pathway or a paracellular route through the tight junction. TRPV6 constitutes the apical component of transcellular absorption in the duodenum and colon, while $Ca_v1.3$ likely contributes apical entry into enterocytes in the small intestine, although this has been disputed and may be age-dependent.[50, 53, 57, 59, 222, 250, 254] Ca^{2+} is shuttled across the epithelial cell by calbindin-D_{9k}, and basolateral extrusion occurs via the plasma membrane calcium ATPase (PCMA1b) and the sodium/calcium exchanger (NCX1).[1, 66, 69]

Tight junction proteins called claudins determine the paracellular permeability characteristics of epithelial layers. This pathway is postulated to contribute the majority of Ca^{2+} absorption from the distal small intestine, although the role of the large intestine has not been thoroughly investigated.[86, 237] Both claudin-2 and claudin-12 are expressed throughout intestinal epithelia and studies on human Caco-2 cells found both to contribute P_{Ca}, implicating them in paracellular Ca^{2+} absorption and secretion along the intestine.[78] Claudin-2 (*Cldn2*) knockout mice at 3 months have decreased Ca^{2+} permeability (P_{Ca}) in the proximal colon, but not small intestine and overall decreased fecal Ca^{2+} excretion although no changes in bone mineral content or serum Ca^{2+}.[86, 146] The intestinal phenotype of adult claudin-12 (*Cldn12*) KO mice has not been fully described, although fecal Ca^{2+} and serum Ca^{2+} are not different than WT.[87] Ca^{2+} absorption via the paracellular pathway, including from the colon is proposed to predominate under conditions of adequate to high dietary Ca^{2+}.[40, 237, 255] However, whether CLDN2 and CLDN12 form

independent pores and contribute different paracellular pathways of Ca^{2+} transport has not been established.

Claudin-2 and Claudin-12 are both expressed in the renal proximal tubule (PT), where two-thirds of filtered Ca^{2+} is reabsorbed.[87] Loss of *Cldn2* reduces paracellular ion permeability in the proximal tubule and leads to hypercalciuria and nephrocalcinosis, while *Cldn12* deletion results in decreased P_{Ca} in the proximal tubule without altered urinary Ca^{2+} excretion.[86, 87] *Cldn2* KO mice display normal plasma Ca^{2+} levels and bone mineral content, likely due to decreased paracellular secretion across the colon.[86] Interestingly, neither *Cldn2* KO nor *Cldn*12 KO animals have increased parathyroid hormone (PTH) or calcitriol ($1,25(OH)_2$-vitamin D) levels.[86, 87] It might be due to compensation by one protein for the loss of the other, although this has not been investigated.

We hypothesized that claudin-2 and claudin-12 form independent cation permeable pores in intestinal and renal epithelia, thereby contributing to paracellular Ca^{2+} transport and maintenance of Ca^{2+} homeostasis. To test this hypothesis, we generated *Cldn2* and *Cldn12* double knockout (DKO) mice. The DKO animals had decreased P_{Ca} across the colon but not small intestine which, in contrast to the single knockout animals, reduced net intestinal Ca^{2+} absorption. DKO mice also displayed increased urinary Ca^{2+} excretion (even greater than the single *Cldn2 KO* animals), hypocalcemia, and markedly decreased bone mineral density without an increase in serum calcitriol. Further, in cell culture, we found that claudin-2 and -12 do not physically interact and expression of each claudin has an additive effect on P_{Ca}. These results suggest that claudin-2 and -12 mediate paracellular Ca^{2+} absorption and reabsorption independently and one is sufficient to maintain normal Ca^{2+} balance.

4.3. Materials and Methods

Ethics Approval

Experiments were approved by the University of Alberta Research Ethics Board animal ethics committee, Health Sciences Section (AUP00000213).

Animals and husbandry

Mice were housed on a 12-hour light/dark cycle with drinking water and chow *ad libitum* (Lab Diet Irradiated Rodent Diet 5053, 4% fat, 0.81% calcium). For all experiments, male and female mice were used. Data presented includes equal numbers of both males and females as sex-specific differences were not found in any analysis. For animal experiments, individual data points represent biological replicates from one animal. FVB/N were obtained from Taconic Biosciences, Rensselaer, NY). *Cldn2* global KO mice were from MMRRC at Univ. of California, Davis. *Cldn12* global KO mice were described previously.[87]

We generated a *Cldn2* and *Cldn12* global double knockout strain (*Cldn2/12* DKO) by crossbreeding *Cldn2* with *Cldn12* KO animals. DKO genotyping was confirmed by real-time PCR as described below using kidney and intestinal tissue. *Cldn2* and *Cldn12* gene expression was detected in WT and not DKO animals whereas β-galactosidase was detected in tissue of DKO animals only, N.B. *Cldn12* KO animals were generated by homologous recombination of exon 4 of the *Cldn12* gene with the β-galactosidase coding sequence from *E. coli* and therefore, this gene will only be detected in mice carrying the mutant form of this gene.[87]

Metabolic cage studies

WT and *Cldn2/12* DKO mice aged 2-3 months, with approximate equal numbers of both genders were placed in metabolic cages for 72 hours as previously described.[71, 150] Water and chow (0.6% Calcium) were available *ad libitum*. For experiments with low calcium diet, mice were housed in metabolic cages for 24 hours with standard rodent chow and then switched to low calcium (0.01%) diet. Bodyweight was determined at time 0 h. Urine, feces, body weight, chow and water consumed were monitored every 24 hours at the same time each morning. After 72 hours, mice were euthanized with a lethal dose of sodium pentobarbital. Blood was collected in lithium heparin coated tubes and centrifuged at 3500 rpm for 20 minutes at 4°C to collect serum which was then stored at -80°C. Tissues were excised, rinsed in PBS and stored at -80°C. A very low calcium diet was employed to ensure the mice would be in a deficient state and thus whether they could compensate for this.

For experiments with calcitriol administration, mice were housed in metabolic cages as above for 24 hours and then given intraperitoneal injection of 500 pg/g body weight $1,25(OH)_2D_3$ diluted in 5% PBS each morning at the same time for three days and euthanized 24 hours after the final dose.[150] Samples were collected as above.

Urine and serum analysis

Freshly collected blood was analyzed for electrolytes, ionized calcium (iCa), glucose, urea nitrogen (BUN), hematocrit (Hct) and hemoglobin (Hgb) using an i-STAT1 Analyzer (Abaxis, Union City, CA, USA) with a CHEM8+ cartridge. Serum creatinine was measured with Diazyme creatinine kit (Diazyme Laboratories, CA, USA). Urine creatinine was measured with Parameter

creatinine kit (R&D systems, Minneapolis, USA). Urine electrolytes were measured by ion chromatography (Dionex Aquion Ion Chromatography System, Thermo Fisher Scientific Inc., Mississauga, ON, Canada) with autosampler. Samples were diluted 1:100 in ddH$_2$O and carried in 4.5 mM Na$_2$CO$_3$/1.5 mM NaHCO$_3$ in ddH$_2$O for anion eluent, 20 mM Methanesulfonic acid in ddH$_2$O for cation eluent. Calibration curves were created with serial dilutions of Dionex five anion and six cation-I standards (Dionex, Thermo Fisher Scientific Inc., Mississauga, ON, Canada). Results were analyzed using Chromeleon 7 Chromatography Data System software (Thermo Scientific). Urine cations were normalized to urine creatinine concentration. FECa was calculated as (urine Ca^{2+} * serum creatinine) / (serum iCa^{2+} * urine creatinine). Ca^{2+} balance was calculated as: mg ingested – mg Ca^{2+} in feces – mg Ca^{2+} in urine. PTH (Immutopics Mouse Intact PTH 1–84) and 1,25(OH)$_2$-vitamin D were measured by ELISA (Immunodiagnostic Systems Limited, Boldon, UK).

Net Ca^{2+} absorption

Net Ca^{2+} absorption was calculated as previously described.[87] Feces was collected from metabolic cage studies and dried at 55°C for 72 hours (Imperial III Incubator, Labline, Mumbai, India). Dried pellets were then ground with mortar and pestle. After mixing the powder, 50 mg was taken and solubilized in 1 ml 0.6 M HCl and rotated for 72 hours. A 1 mL aliquot was diluted 1:50 and total Ca^{2+} measured using ion chromatography as above. Bioavailability is presented as the percentage of Ca^{2+} consumed in the chow ((mg of Ca^{2+} consumed – mg of Ca^{2+} in feces) / mg of Ca^{2+} consumed *100).

Real-time PCR

Quantitative real-time PCR was performed as previously described.[222] Total RNA was isolated

from frozen tissues using the TRIzol method (Invitrogen, Carlsbad, CA) according to the

manufacturer's instructions and treated with DNAse (ThermoScientific, Vilnius, Lithuania).

RNA purity and quantity were measured using a Nanodrop 2000 (Thermo Fisher Scientific,

Waltham, MA). Five micrograms of RNA were then reverse transcribed using reverse

transcriptase (SensiFAST cDNA Synthesis Kit, FroggaBio, CA, USA). A pooled sample of RNA

was used to create cDNA with serial dilutions for the standard curve. Quantitative RT-PCR was

performed in triplicate on each sample using TaqMan Universal Master Mix II (ThermoFischer

Scientific) with specific primers and probes on a QuantStudio 6 Pro Real Time PCR System

(ThermoFisher Scientific). Sequences for murine *Trpv6*, *Trpv5*, *Cacna1d*, *Calb1*, *S100g*, *Atp2b1*,

Slc8a1, *Cldn2*, *Cldn3*, *Cldn4*, *Cldn14*, *Cldn15*, *Cldn16*, *Cldn19*, *Cyp27b1*, *Cyp24a1*, *Gapdh*, *18s*,

and *β-actin* have been published elsewhere.[66, 71, 87, 150, 196, 222] Specificity of primer sequences was

assessed with NCBI Primer-BLAST. Samples were quantified using the standard curve method.

A C_q value of greater than 35 was considered negligible.

Measurement of Ca^{2+} permeability

Paracellular Ca^{2+} permeability of intestinal segments *ex vivo* in Ussing chambers was determined

by imposing a bi-ionic diffusion potential as previously described.[86] Fresh intestinal tissue was

excised from euthanized mice, rinsed in Kreb's ringer buffer (KRB), linearized, and mounted

onto P2407B sliders in P2400 Ussing chambers connected to a VCC multichannel

voltage/current clamp (Physiologic Instruments, San Diego, CA). Small intestine segments were

delineated as previous.[222] A 1.2 cm long section of tissue immediately distal to the cecum from

each animal was excised and cut into four sections to represent proximal colon. One mouse was

used for each experiment and represents one data point. Full-thickness tissue was used as

previous work has not found a difference in TER to tissue stripped of the seromuscular layer in

colon.[86] A bi-ionic dilution potential was then determined as previously described.[86] Tissue was

bathed in KRB as above as a "control" buffer (144 mM Na^+, 1 mM Mg^{2+}, 1.3 mM Ca^{2+}, 2 mM

PO_4^-, 3.6 mM K^+, 146 mM Cl^-, pH 7.4). After 15 minutes, a 90 µA current was applied and the

recorded voltage change used to determine TER with Ohm's law. The apical buffer was then

changed to a low-NaCl isotonic buffer (30 mM Na^+, 1 mM Mg^{2+}, 1.3 mM Ca^{2+}, 2 mM PO^{4-}, 3.6

mM K^+, 32 mM Cl^-, 227 mM mannitol, pH 7.4). The resulting peak change in transepithelial

voltage was used to determine the permeability ratio of Na^+ to Cl^- (P_{Na} /P_{Cl}) and absolute

permeability to Na^+ and Cl^- using the Goldman-Hodgkin-Katz and simplified Kimizuka-Koketsu

equations.[152, 225] The apical solution was then changed back to the control solution until the

potential difference stabilized again and TER was again measured. The basolateral buffer was

then changed to a phosphate-free isotonic control (140 mM Na^+, 1 mM Mg^{2+}, 1.3 mM Ca^{2+}, 3.6

mM K^+, 146 mM Cl^-, 5 mM mannitol, 3 mM HEPES, pH 7.4) and the apical to a high Ca^{2+}

isotonic buffer (1 mM Mg^{2+}, 70 mM Ca^{2+}, 2 mM PO_4^-, 3.6 mM K^+, 146 mM Cl^-, 3 mM HEPES,

pH 7.4) and the peak change in potential difference was again measured and used to calculate

P_{Ca}/P_{Na} and $P_{Ca}{}^{2+}$. Buffers were then changed to the control in both chambers and TER measured

as above. Data were excluded if TER decreased more than 40%.[39] To further assess tissue

viability, forskolin (LC Laboratories, Woburn, MA) was added at 10 µM bilaterally. Data were

included if a change in potential difference of at least 50% was observed.[39] All changes in

potential difference were corrected for liquid junction potentials as previously described.[84]

Permeability to calcium across epithelial monolayers was performed as above on OK cells expressing empty vector or CLDN2 in pcDNA3.1+ (Invitrogen) as previously described.[256] Briefly, $1x10^5$ cells were seeded onto 1.12 cm^2 Transwell inserts (Corning, NY) in DMEM/F-12 medium, supplemented with 10% FBS and 5% penicillin streptomycin glutamine. After 7 days, P_{Ca} was determined as above. After each experiment, cells were removed from the membrane with trypsin and the experiment repeated on the empty filter and these values were subtracted from results with cells. Caco-2 cells were cultured in DMEM medium, supplemented with 10% FBS and 5% penicillin streptomycin glutamine.

Murine claudin-12 (pMCV6 entry vector, Origene) was subcloned into pTRE2hyg vector and then transfected with FuGene HD (Promega) into Caco-2 cells stably expressing pTet-Off (Clontech) under double selection with hygromycin and G418 (Invitrogen) per manufacturer instructions. Transwells were seeded with $1x10^7$ cells as previous and grown for 20 days before P_{Ca} was determined as above.[257]

Micro-Computed Tomography

Micro-computed tomography (µ-CT) experiments were performed on tibia of WT and Cldn2/12 DKO mice essentially as previously described.[71] Bones were fixed in 4% PFA and stored at 4°C prior to analysis. The right tibial metaphasis was scanned at a resolution of 18 µm using a Skyscan 1176 micro-computed tomography (µCT) imager (Skyscan NV, Kontich, Belgium). Voltage was set to 45 kV, current was set to 555 µA, and low photon energies reduced using a 0.5 mm Al filter, at a 0.5° rotation step. The origin of trabecular bone was taken as the bridging of the metaphyseal growth plate. The region of interest spanned 100 slices starting 20 slices

below the landmark. Analysis was conducted using CT-analyser (version 1.14.4.1, Bruker). Representative images were reconstructed using CTVol (Bruker).

Immunoblot

Tissue or cells were lysed in RIPA buffer (50 mM Tris, 150 mM NaCl, 1 mM EDTA, 1% Triton-X, 1% SDS, 1% NP-40, pH 7.4) with 1:100 0.1 M PMSF (Thermo Scientific, Rockford, IL), and 1:100 protease inhibitor cocktail (Calbiochem, San Diego, CA). Protein content was measured using Pierce 660 nm Protein Assay Reagent (ThermoFisher Scientific). 150 µg of tissue protein or 50 µg protein from cell culture was run on 10% SDS-PAGE, electrotransferred to PVDF (Merck Millipore, Burlington, MA) and blocked overnight in TBST with 5% milk. The blots were probed with primary antibody overnight at 4 °C then secondary antibody for 1 hour at room temperature and visualised using Immobilon Crescendo Western HRP substrate (Sigma-Aldrich, Canada) and a ChemiDoc Touch imaging system (Bio-Rad). Protein was semi-quantified using Image Lab 6.0 (Bio-Rad), normalized to β-actin as a loading control and presented as relative to WT. Primary antibodies were rabbit anti-Calbindin$_{D28k}$ (CB-38a, Swant, Switzerland), mouse anti-claudin-2 (12H12, ThermoFisher Scientific), rat anti-HA (3F10, Roche), and mouse anti-β-actin (BA3R, Invitrogen, USA).

Co-immunoprecipitation

HEK 293 cells (ATCC, Rockville, MD, USA) were transiently transfected with pTRE2hyg vector expressing HA-tagged claudin-12, pTRE2hyg vector expressing myc tagged claudin-2, pcDNA 3.1 vector expressing HA-tagged claudin-2 and/or empty pTRE2hyg vector as described

in the figure legend. Cells were lysed in IPEB buffer (10 mM Tris-HCl, 1% NP-40, 5 mM EDTA, 0.15 M NaCl, pH 7.5) containing 1:100 0.1 M PMSF in 100% ethanol (Thermo Scientific, Rockford, IL), and 1:100 protease inhibitor cocktail (Calbiochem, San Diego, CA) and an aliquot was saved. The remaining cell lysate was incubated with mouse anti-myc antibody (ThermoFisher, cat# MAI-21316) and precipitated with Dynabeads with protein G (magnetic beads, Invitrogen) overnight at 4 °C. Protein was eluted with Laemmli buffer and detected by immunoblot as above with rat anti-HA (Roche Cat# 11867423001) or rabbit anti-myc (Covance Cat# PRB-150P) antibodies.

Immunohistochemistry and X-gal staining

Sections of colon tissue were fixed in 4% PFA and stained for X-gal as previously described.[87] Briefly, sections were incubated for 3 h in 1:40 X-gal solution in 4% DMSO (Sigma-Aldrich) with potassium ferricyanide crystalline 5 mM, potassium ferricyanide trihydrate 5 mM, MgCl2 2 mM, and PBS 100 mM. Tissue was stained for CLDN2 as previously described.[196] Rehydrated tissue was microwave boiled in Tris-EGTA buffer (TEG, 10 mM Tris, 0.5 mM EGTA, pH 9.0) for antigen retrieval. Free aldehyde groups were blocked in 0.6% H_2O_2 and 50 mM NH_4Cl in PBS. Sections were blocked in 5% milk, probed with primary antibody in 0.1% Triton-X in PBS overnight at 4 °C and then incubated with secondary antibodies. Sections were visualized with DAB$^+$ Substrate Chromogen System (K3467, DakoCytomation).

Statistics

Data were analyzed using GraphPad Prism 9.0. The Shapiro-Wilk test was used to evaluate for normal distribution and F-test to compare variances. Data were analyzed and presented as indicated in figure and table legends. $P < 0.05$ was considered statistically significant.

4.4. Results

4.4.1. Claudin-2 and claudin-12 contribute paracellular Ca^{2+} permeability to the proximal colon

The paracellular pathway is proposed to contribute significant calcium absorption from the small intestine. However, prior work found no difference in P_{Ca} between *Cldn2* KO and WT mice across the small but not the large intestine [86]. Therefore, we first performed Ussing chamber bi-ionic diffusion potential studies along all sections of the small intestine of DKO mice. The only difference observed was an increase in relative cation permeability across the jejunum relative to WT (Figure 4.1), suggesting either that CLDN2 and CLDN12 do not contribute significant Ca^{2+} paracellular permeability to the small intestine or their contribution is to more distal segments.

We previously reported decreased P_{Ca} across the colon of adult *Cldn2* KO mice by measuring bi-ionic diffusion potentials in Ussing chambers.[86] First, we confirmed these results (Figure 4.2A), and then using the same methodology, we observed a significant decrease in $P_{Ca^{2+}}$ across the colon of *Cldn12* KO mice compared to WT littermates (Figure 4.2B). These results are consistent with both claudin-2 and claudin-12 conferring $P_{Ca^{2+}}$ to the proximal colon. To determine if the loss of both claudins further decreases colonic $P_{Ca^{2+}}$, we generated a global *Cldn2* and *Cldn12*

double knockout mouse (DKO) and assessed P_{Ca}^{2+} in Ussing chambers *ex vivo*. P_{Ca}^{2+} was significantly reduced in the DKO mice (Figure 4.2C). Transepithelial resistance was increased while P_{Na} and P_{Cl} were reduced in the single *Cldn12* KO and DKO mice, but not the single *Cldn2* KO mice (Tables 4.1, 4.2, 4.3). To determine if the loss of both *Cldn2* and *Cldn12* in the DKO mice results in an additive loss of P_{Ca}^{2+}, we analyzed the results of each KO or DKO relative to their respective WT littermates. Because the DKO and single KO are not littermates, this method normalizes to any potential differences that arise from background differences between colonies. P_{Ca}^{2+} across the colon of *Cldn2* KO animals was 16.9% (± 9.1%) lower than WT, *Cldn12* KO animals had a 16.7% (± 9.0%) lower P_{Ca}^{2+} than WT and DKO was 31.4% (± 11.8%) lower than WT (Figure 4.2D). These results suggest that both claudin-2 and claudin-12 contribute P_{Ca}^{2+} across the colon, and the loss of both proteins results in an even greater loss of P_{Ca}^{2+}.

To determine localization of claudin-12 expression in the mouse colon we performed X-gal staining on fixed tissue sections. The *Cldn12* KO mouse was created with β-galactosidase inserted into the *Cldn12* coding sequence.[87] X-gal staining is present in the tissue from the seromuscular layer and crypts of *Cldn12* heterozygous mice but not WT mice (Figure 4.2E-F). Co-staining for claudin-2 reveals both proteins are present in the crypts (Figure 4.2G).
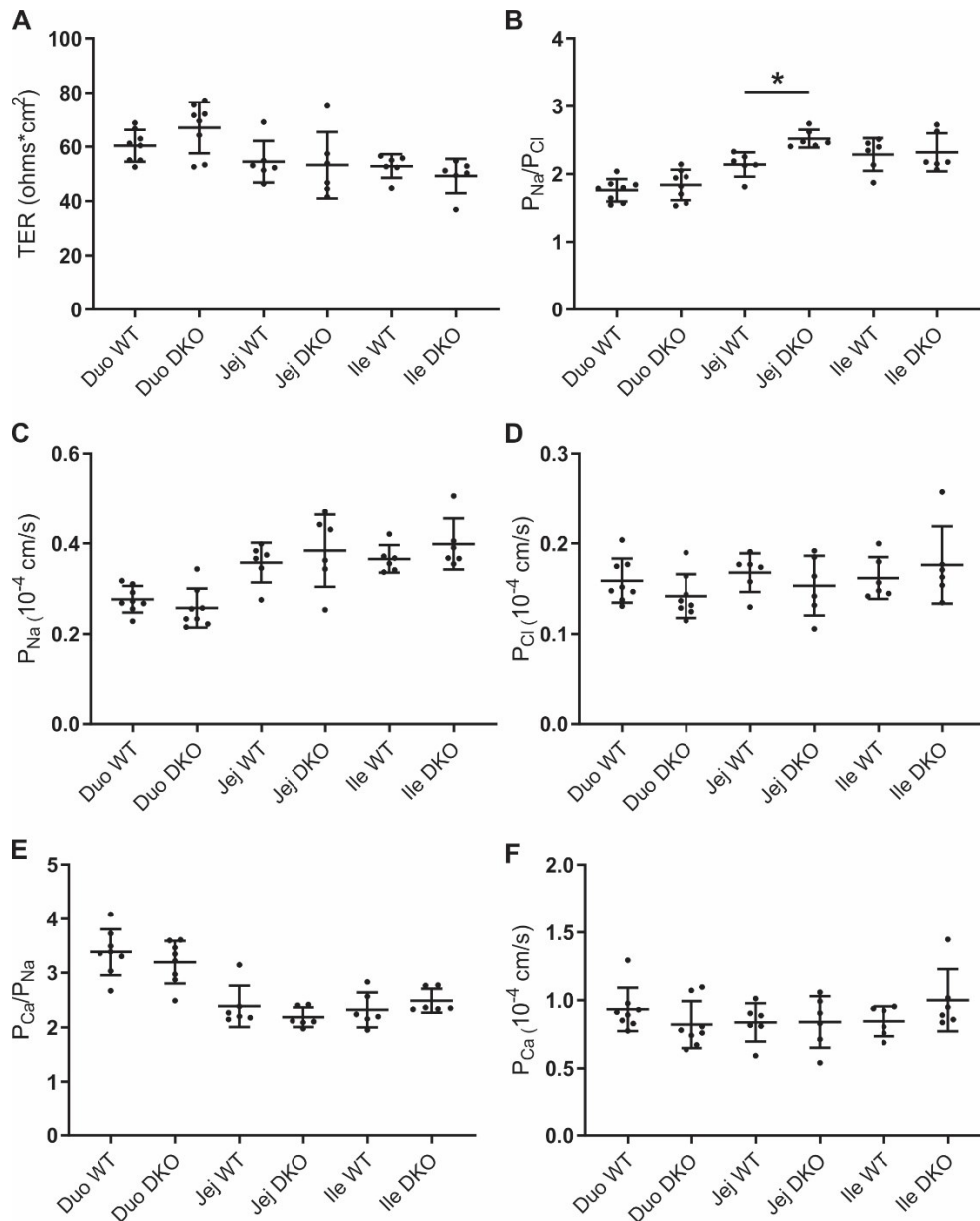
Figure 4.1. Calcium permeability is not different from wild-type animals along the small intestine of *Cldn2/12* DKO mice. A) Transepithelial resistance, B and E) permeability ratios, C, D, F) absolute ion permeability of *Cldn2/12* DKO mice vs WT for each intestinal segment. Duo, duodenum; Jej, jejunum; Ile, ileum. N = 8 per group for Duo and 6 per group for Jej and Ile. Data presented as mean ± SD, comparisons by unpaired t-test * P < 0.05.
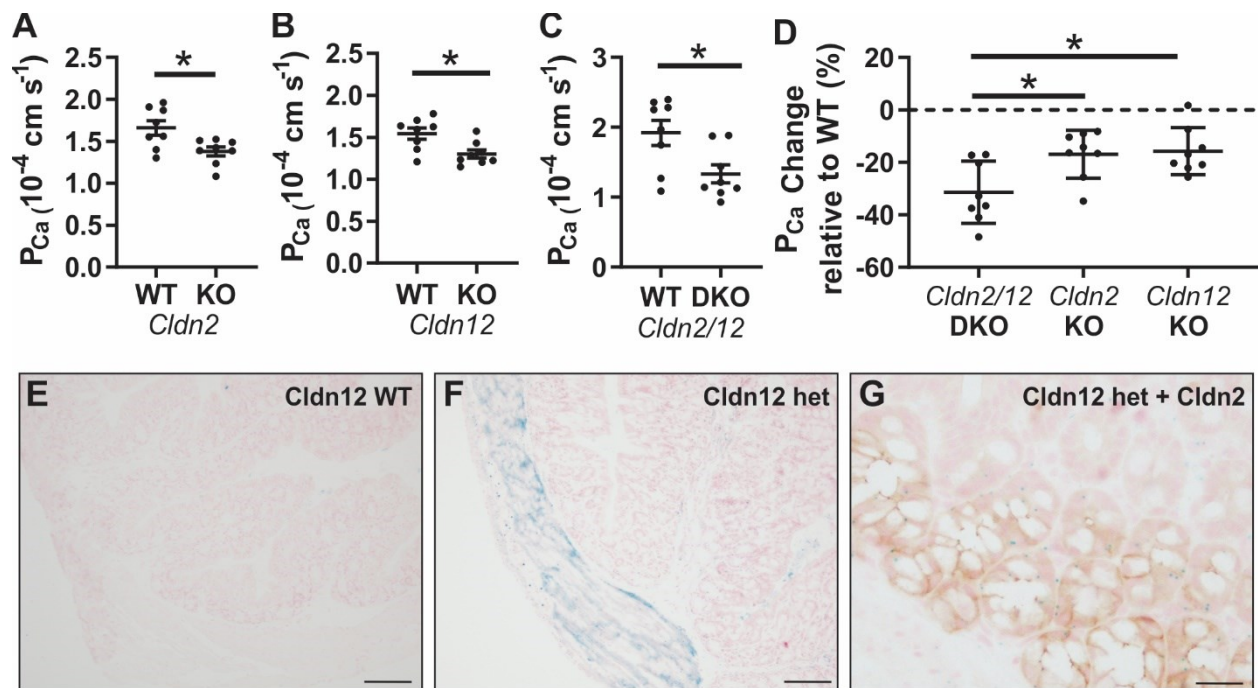
Figure 4.2. Claudin-2 and claudin-12 confer independent Ca^{2+} permeability to the proximal colon. P_{Ca} measured *ex vivo* in Ussing's chambers across the proximal colon compared to WT of A) *Cldn2* KO (n = 8 each group, $P = 0.0155$); B) *Cldn12* KO (n = 8 each group, $P = 0.0115$); C) *Cldn2/12* DKO (n = 8 each group, $P = 0.0191$). Full results of bi-ionic diffusion potential experiments on colon are presented in Tables 4.1 – 4.3. Means compared by Student's t-test. D) Data from A-C expressed as the percentage change in P_{Ca} relative to WT for each genotype. Data presented as mean ± SD. One-way ANOVA with Dunnett correction for multiple comparisons to compare mean from DKO mice to *Cldn2* KO ($P = 0.0168$) and *Cldn12* KO ($P = 0.0100$). E-F) X-gal staining on colon sections from *Cldn12* WT and *Cldn12* heterozygous mice showing staining of claudin-12 in the heterozygous mouse. Scale bars = 200 µm. G) X-gal staining and immunohistochemical staining for claudin-2 in colon slice from *Cldn12* heterozygous mouse. Scale bars = 25 µm.

Table 4.1. Proximal colon resistance and ion permeability of WT and *Cldn2/12* DKO mice

	WT (n = 8)	*Cldn2/12* DKO (n = 8)	*P* – value
TER (Ω cm^2)	44.0 (12.3)	61.1 (17.4)	0.0392
P_{Na} (x10^{-4} cm s^{-1})	0.307 (0.055)	0.249 (0.049)	0.0427
P_{Cl} (x10^{-4} cm s^{-1})	0.338 (0.082)	0.239 (0.065)	0.0182
P_{Na}/P_{Cl}	0.923 (0.071)	1.06 (0.150)	0.0330
P_{Ca}/P_{Na}	6.17 (0.676)	5.37 (0.864)	0.0692

TER, transepithelial resistance; P_x, permeability to ion x. Data presented at mean (SD). *P* – value determined by unpaired t-test.

Table 4.2. Proximal colon resistance and ion permeability of WT and *Cldn2* KO mice

	WT (n = 8)	*Cldn2* KO (n = 8)	*P* – value
TER (Ω cm^2)	55.4 (7.20)	59.5 (5.83)	0.2377
P_{Na} (x10^{-4} cm s^{-1})	0.261 (0.031)	0.243 (0.027)	0.2581
P_{Cl} (x10^{-4} cm s^{-1})	0.232 (0.037)	0.212 (0.022)	0.2143
P_{Na}/P_{Cl}	1.14 (0.11)	1.16 (0.13)	0.7605
P_{Ca}/P_{Na}	6.36 (0.403)	5.68 (0.353)	0.0029

TER, transepithelial resistance; P_x, permeability to ion x. Data presented at mean (SD). *P* – value determined by unpaired t-test.

Table 4.3. Proximal colon resistance and ion permeability of WT and *Cldn12* KO mice

	WT (n = 8)	*Cldn12* KO (n = 8)	*P* – value
TER (Ω cm^2)	52.4 (5.29)	62.1 (5.84)	0.0035
P_{Na} (x10^{-4} cm s^{-1})	0.267 (0.023)	0.232 (0.022)	0.0075
P_{Cl} (x10^{-4} cm s^{-1})	0.253 (0.033)	0.203 (0.024)	0.0040
P_{Na}/P_{Cl}	1.07 (0.07)	1.14 (0.06)	0.0308
P_{Ca}/P_{Na}	5.77 (0.417)	5.65 (0.474)	0.6053

TER, transepithelial resistance; P_x, permeability to ion x. Data presented at mean (SD). *P* – value determined by unpaired t-test.

4.4.2. Claudin-2 and claudin-12 DKO mice have hypocalcemia, hypercalciuria and decreased Ca^{2+} balance

We next sought to ascertain whether *Cldn2/12* DKO mice displayed a phenotype consistent with altered Ca^{2+} homeostasis. To this end, mice were housed in metabolic cages for three days. Male DKO mice had a lower body weight than male WT, but no difference was observed in females (Table 4.4). Water and chow consumption, urine volume and fecal mass were not different between genotypes. Blood analysis revealed a significantly decreased ionized calcium (iCa^{2+}) in DKO animals (DKO median 1.04 (0.96 – 1.07) vs. WT 1.11 (1.08 – 1.15)) (Fig. 4.2A). DKO mice had slightly increased blood sodium which is not likely to be physiologically relevant. No differences in other chemistry, hematology, nor blood gas parameters were noted (Table 4.5). These results suggest that the DKO mice have a selective Ca^{2+} phenotype that is not compensated.

We measured fecal Ca^{2+} excretion to assess intestinal Ca^{2+} absorption as a percentage of Ca^{2+} consumed. DKO mice had decreased net absorption of Ca^{2+}, $23 \pm 11\%$ compared to $34 \pm 9\%$ in WT animals (Figure 4.3B). As the only intestinal segment displaying altered P_{Ca}^{2+} was the colon, this suggests decreased paracellular Ca^{2+} absorption from the colon of the DKO mice. We then determined urinary ion excretion. While no differences were observed for Na^+, K^+, PO_4^{3-}, Cl^- or Mg^{2+}, we found an almost three-fold increase in Ca^{2+} excretion in the DKO vs WT mice (Table 4.5). To account for potential differences in glomerular filtration rate, and the difference in plasma $Ca^{2+,}$ we calculated fractional excretion of Ca^{2+} (FECa). Relative to WT mice, the FECa in DKO mice was 4.3-fold greater (Fig. 4.3 C). Thus, *Cldn2/12* DKO mice have marked hypercalciuria in addition to decreased net intestinal Ca^{2+} absorption.

Cldn2 KO mice are known to display hypercalciuria, while *Cldn12* KO mice do not have altered urinary Ca^{2+} excretion at adult ages.[87, 146] To determine if the DKO mice had increased urinary Ca^{2+} excretion that was greater than single *Cldn2* KO animals, we compared urinary Ca^{2+} excretion to their respective wild-type littermates as above. This demonstrated further increased urinary Ca^{2+} excretion in the DKO mice relative to single *Cldn2* KO animals (Figure 4.3C). Given the increased urinary excretion and decreased intestinal absorption in DKO animals, we assessed the overall Ca^{2+} balance of DKO mice. We observed a decreased, yet positive, overall Ca^{2+} balance in the DKO mice (Figure 4.3D).

The DKO mice had reduced serum ionized Ca^{2+}, which should increase serum parathyroid hormone (PTH) and consequently, calcitriol levels. As expected, the hypocalcemia observed in DKO mice resulted in increased serum PTH (Figure 4.3E). However, despite a decrease in serum iCa^{2+} and increased PTH, DKO mice did not have a statistically significant increase in serum calcitriol levels (Figure 4.3F).

To sought to determine if mice the DKO could respond to exogenous calcitriol administration. To this end, we injected mice with calcitriol daily for three days and housed them in metabolic cages.[150] Indeed, serum iCa^{2+} normalized in DKO mice with calcitriol (median (IQR), 1.12 (1.08 – 1.21) mM) suggesting that they respond to the hormone (Mann-Whitney test with Bonferroni correction of serum iCa^{2+} after three days of calcitriol compared to serum iCa^{2+} from original metabolic cage experiments, $P = 0.0024$) (Figure 4.4A). However, the serum iCa^{2+} was still significantly greater in WT mice. While intestinal bioavailability did not appear to change, urine Ca^{2+} excretion significantly increased with calcitriol after just one dose in DKO mice (Figure 4.4B-C). These results suggest that the DKO mice are able to respond to exogenous calcitriol although the response appears to be attenuated.

We then asked if DKO mice can increase serum calcitriol in response to a low Ca^{2+} diet. Indeed, serum calcitriol was elevated in DKO mice and even greater than WT mice after three days on a low Ca^{2+} diet although serum iCa^{2+} was still significantly lower in the DKO mice (Figure 4.4A, D). Interestingly, urine Ca^{2+} increased in response to the diet where WT mice did not have a change. Both genotypes responded to the diet with significantly decreased fecal Ca^{2+} excretion (Figure 4.4E-F). These results suggest that DKO mice can increase serum calcitriol but the response to it is attenuated.
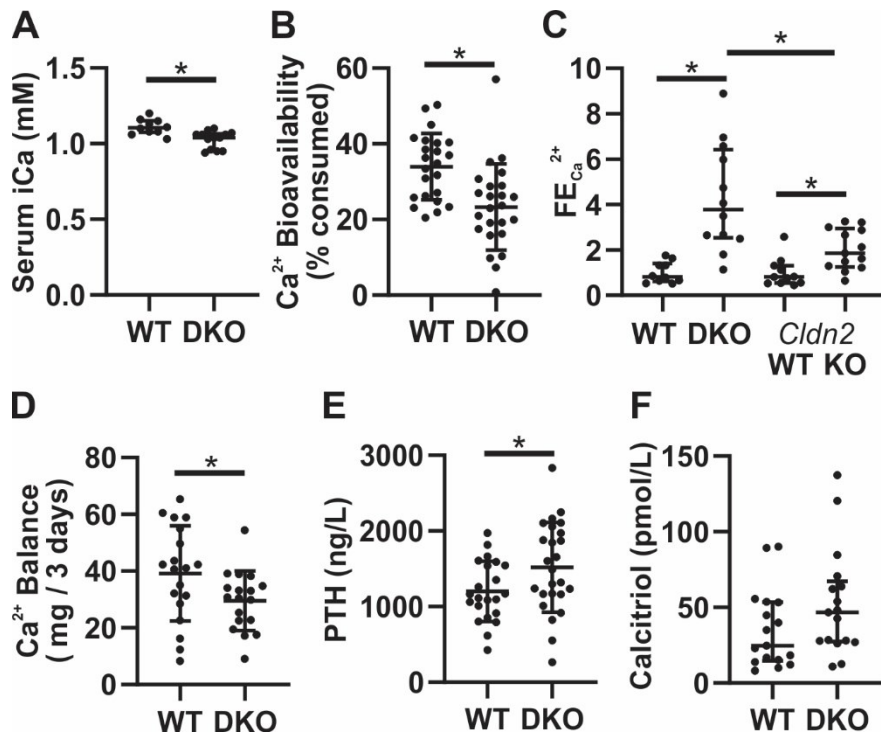
Figure 4.3. *Cldn2/12* **DKO mice display hypocalcemia, hypercalciuria, and decreased intestinal Ca^{2+} absorption.** A) Serum ionized Ca^{2+} (median ± IQR, n = 10 WT, 13 DKO, Mann Whitney Test $P = 0.0020$); B) Ca^{2+} bioavailability as a % of Ca^{2+} consumed (mean ± SD, n = 23 WT and 24 DKO, student's t-test $P = 0.0008$); C) Fractional excretion of urinary Ca^{2+} normalized to WT for each genotype (median ± IQR, n = 10 WT, 12 DKO, 11 *Cldn2* WT, 13 *Cldn2* KO, Mann Whitney, $P < 0.0001$ WT vs DKO, $P = 0.0031$ *Cldn2* WT vs KO, $P = 0.0114$ DKO vs *Cldn2* KO); D) net 3 day Ca^{2+} balance (mean ± SD, n = 19 WT and 18 DKO, student's t-test $P = 0.0431$); E) serum parathyroid hormone levels (mean ± SD, n = 22 WT and 25 DKO, student's t-test $P = 0.0392$); F) serum calcitriol (median ± IQR, n=17 WT and 17 DKO, Mann Whitney Test $P = 0.0987$).

Table 4.4. Metabolic cage data

	Male			Female		
	WT	**DKO**	***P-*value**	**WT**	**DKO**	***P-*value**
N	15	19		19	18	
Body Weight (g)	31.3 ± 4.52	28.5 ± 2.73	0.0346	25.4 ± 3.48	24.3 ± 2.88	0.2925
Chow eaten (g/g body weight)	0.12 ± 0.05	0.14 ± 0.05	0.2146	0.17 ± 0.05	0.17 ± 0.05	0.8337
Water intake (mL/24 hour/g body weight)	0.16 ± 0.08	0.15 ± 0.04	0.8252	0.15 ± 0.04	0.16 ± 0.04	0.2801
Urine volume (mL/24 hour/g body weight)	0.074 ± 0.047	0.080 ± 0.026	0.6673	0.043 ± 0.016	0.060 ± 0.039	0.0878
Fecal excretion, wet (g/24 hour/g body weight)	0.012 ± 0.004	0.015 ± 0.006	0.2459	0.017 ± 0.005	0.018 ± 0.005	0.5585

Data presented as mean ± SD compared by unpaired t-test.

Table 4.5. Serum and urine biochemistries

	N	WT	N	*Cldn2/12* DKO	*P*-value
Serum					
Sodium (mM)	34	146 (144 – 148)	37	147 (146 – 149)	0.0201
Potassium (mM)	34	4.8 (4.5 – 5.2)	37	4.7 (4.3 – 5.1)	0.2689
Chloride (mM)	34	116 (113.8 – 119)	37	116 (114 – 119.5)	0.7411
TCO_2 (mM)	34	22.7 ± 3.1	37	22.8 ± 2.4	0.8766
BUN (mM)	34	24.6 ± 5.9	37	27.4 ± 6.2	0.0543
Glucose (mM)	34	10.2 ± 2.2	37	10.0 ± 1.7	0.5846
Hct (%PCV)	34	41.0 (39.0 – 42.0)	37	41.0 (39.5 – 43.0)	0.2146
Hgb (g/L)	34	139 (133 – 143)	37	139 (134 – 146)	0.2146
pH	24	7.28 ± 0.05	24	7.30 ± 0.03	0.0509
pCO_2 (mmHg)	24	47.0 ± 5.6	24	45.6 ± 3.4	0.3045
HCO_3 (mM)	24	22.0 ± 2.7	24	22.6 ± 1.8	0.4982
BE (mM)	24	-5 ± 3	24	-4 ± 2	0.2148
Anion Gap (mM)	34	13.3 ± 3.0	37	13.9 ± 2.4	0.3190
Urine (/Creatinine)					
Ca^{2+}	24	0.91 (0.50 – 1.63)	24	2.67 (1.65 – 4.23)	< 0.0001
Cl^-	24	102 (80 – 133)	24	121 (82 – 141)	0.4284
PO_4^{3-}	24	106 (85 – 149)	24	131 (98 – 156)	0.2912
Mg^{2+}	24	3.8 (2.8 – 5.6)	24	4.4 (3.6 – 5.5)	0.3152
K^+	24	179 (156 – 230)	24	223 (171 – 271)	0.1065
Na^+	24	131 (109 – 151)	24	152 (111 – 192)	0.3203

Data presented as mean ± SD compared by unpaired t-test, or as median (IQR) compared by Mann-Whitney test. TCO_2, total carbon dioxide; BUN, blood urea nitrogen; Hct, hematocrit; Hgb, hemoglobin; pCO_2, partial pressure of carbon dioxide; HCO_3, bicarbonate; BE, base excess.
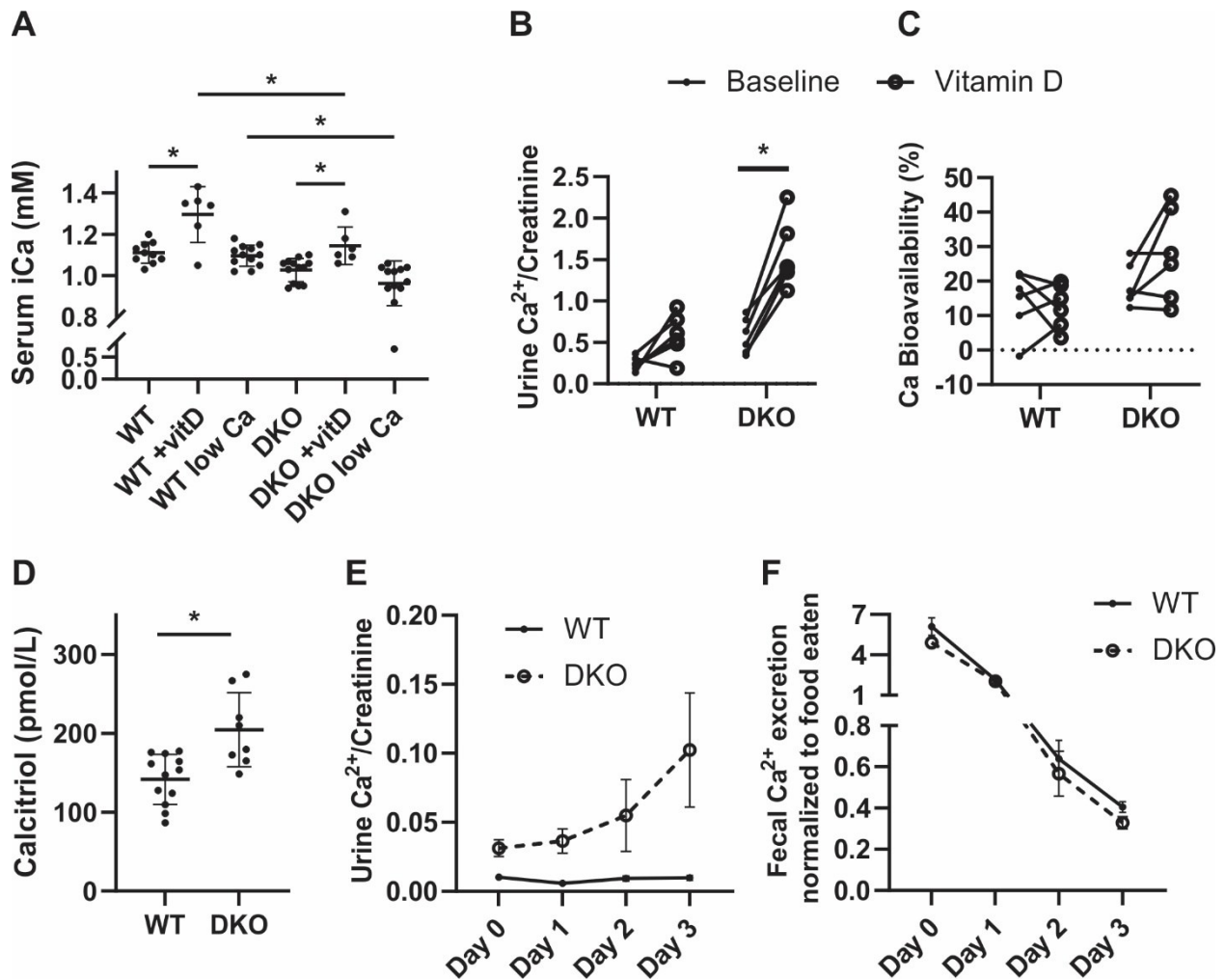
Figure 4.4. *Cldn2/12* **DKO mice respond to exogenous calcitriol and increase serum calcitriol in response to a low Ca^{2+} diet.** A) Serum ionized Ca^{2+} in WT and DKO mice in response to intraperitoneal calcitriol or a low calcium diet (0.01%). Data presented as individual animals and mean ± SD and compared by one-way ANOVA with Bonferroni correction for multiple corrections. B) Urine Ca^{2+} excretion normalized to urine creatinine (WT $P > 0.9999$, DKO $P = 0.2538$) and C) intestinal Ca^{2+} bioavailability (WT $P = 0.0720$, DKO $P = 0.0015$) in WT and DKO mice for 24 hours following intraperitoneal injection of calcitriol. Each data point represents an individual animal and compared by paired t-test with Bonferroni correction. D) Serum calcitriol in WT and DKO mice in response to a low Ca^{2+} diet. Data presented as individual animals and mean ± SD and compared by t-test ($P = 0.0021$). E) Urine Ca^{2+} excretion normalized to urine creatinine is not altered in WT (WT $P > 0.9999$) mice but increases in DKO mice ($P = 0.0199$) after 3 days on a low Ca^{2+} diet and is greater in DKO mice vs. WT ($P = 0.0040$) compared with a mixed-effects analysis with Bonferroni correction. F) Fecal Ca^{2+} excretion significantly decreases daily in WT and DKO mice ($P < 0.0001$) on a low Ca^{2+} diet. Data presented as mean ± SEM and compared with a mixed-effects analysis with Bonferroni correction.

4.4.3. Renal and intestinal gene expression suggests compensatory changes in DKO mice

To determine if there were compensatory renal or intestinal alterations in the DKO mice, we examined expression of genes mediating Ca^{2+} transport across these epithelia. We observed increased expression of both *Cldn14* and *Cldn16* in kidneys of DKO mice. *Cldn14 and Cldn16* are known to block and permit Ca^{2+} reabsorption in the thick ascending limb of the nephron, respectively (Figure 4.5A-C).[148, 150] Expression of genes contributing to transcellular reabsorption from the distal nephron, specifically *Trpv5*, *Calb1*, and *Slc8a1*, were also increased in DKO mice including increased protein abundance of calbindin-D$_{28k}$ (Figure 4.5D – I). In addition, we examined the expression of *Cyp27b1* and *Cyp24a1* in the kidney, genes coding for enzymes that activate and deactivate vitamin D, respectively. Consistent with the serum calcitriol results, we were not able to detect significant differences in expression of *Cyp27b1* and *Cyp24a1* in DKO kidneys (Figure 4.5J, K).

We also examined gene expression in the duodenum and colon. In the colon, the expression of the apical calcium channels *Trpv6* and *Cacna1d* were not changed, however, expression of the intracellular Ca^{2+} binding protein *S100g* and basolateral extrusion pump *Atp2b1* were increased by 5-fold and 0.5-fold, respectively. We observed no changes in *Cldn3* or *Cldn4* expression but did see a slight decrease in *Cldn15* expression, a gene which encodes a cation permeable pore.[77] No changes were observed in the duodenum (Figure 4.6). These results suggest that the DKO mice have compensatory increased transcellular Ca^{2+} absorption from the colon, which is not calcitriol stimulated. The intestinal expression of potential compensatory genes has not been previously described in the single *Cldn12* KO mouse. Figure 4.7 illustrates that the only difference observed in these mice is a two-fold increase in *S100g* in the colon.

Taken together, the above results indicate that DKO mice have impaired intestinal Ca^{2+} absorption and renal reabsorption with suboptimal compensation to maintain serum iCa^{2+}.
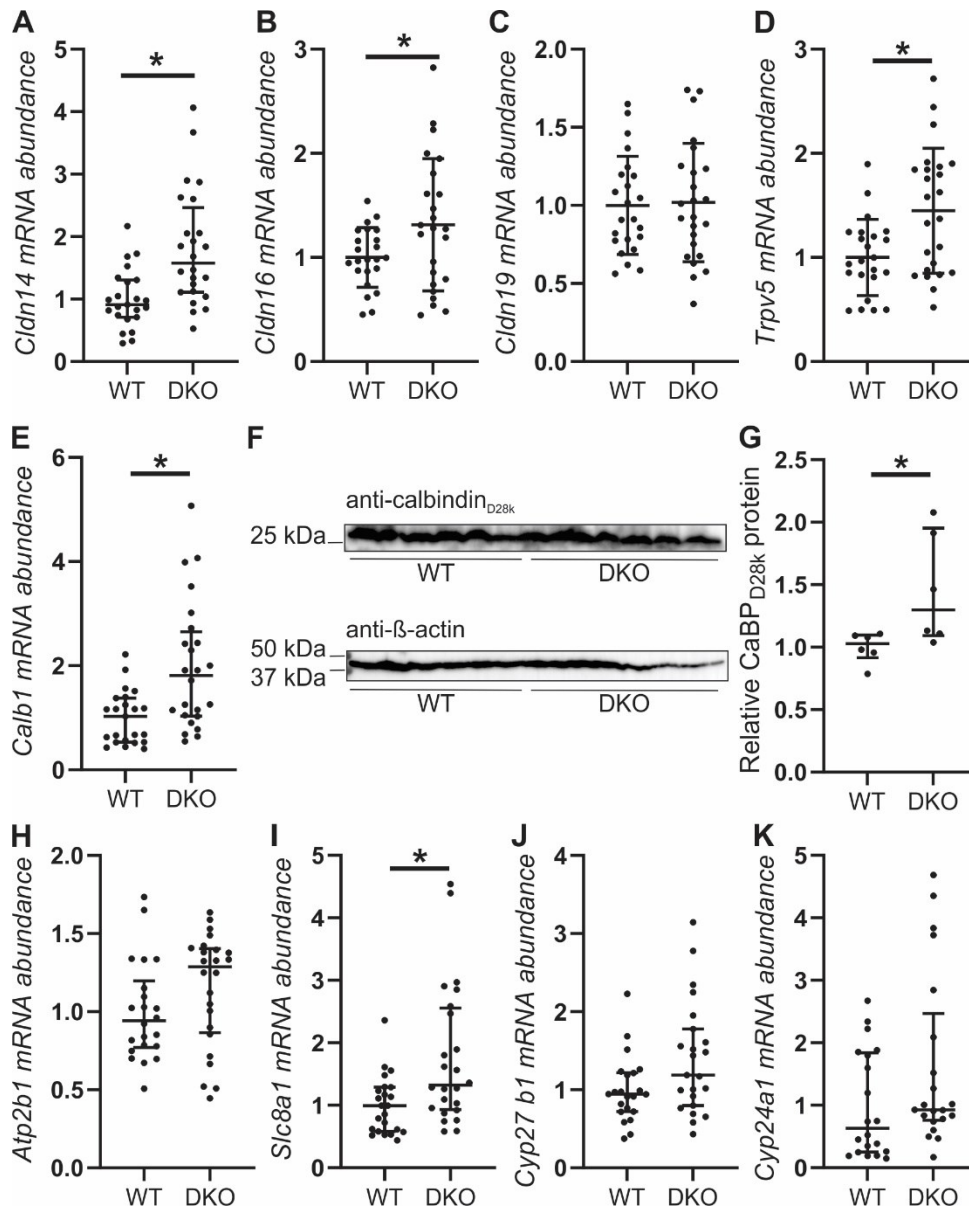
Figure 4.5. *Cldn2/12* **DKO renal gene expression suggests compensatory increased Ca^{2+} reabsorption from the distal nephron.** mRNA abundance of renal genes expressing A) claudin-14 ($P = 0.0003$), B) claudin-16 ($P = 0.0354$), C) claudin-19 ($P = 0.8567$), D) TRPV5 ($P = 0.0035$), E) calbindin-D$_{28k}$ ($P = 0.0016$). F) Representative immunoblots from kidney of WT and DKO mice probed with anti-calbindin$_{D28k}$ and β-actin and G) semi-quantification of results immunoblot ($P = 0.0152$, N = 6 each group). mRNA abundance of genes encoding H) PMCA1b ($P = 0.1218$), I) NCX1 ($P = 0.0051$), J) 1α-hydroxylase ($P = 0.0516$), and K) 24-hydroxylase ($P = 0.0782$) in the kidney of WT and *Cldn2/12* DKO mice. Results are normalized to *β-Actin* and expressed relative to WT. Data presented as median ± IQR and compared using Mann-Whitney test (A, E – I), data presented as mean ± SD and compared by Welch's t-test (B – D). n = 23 WT and 24 DKO.
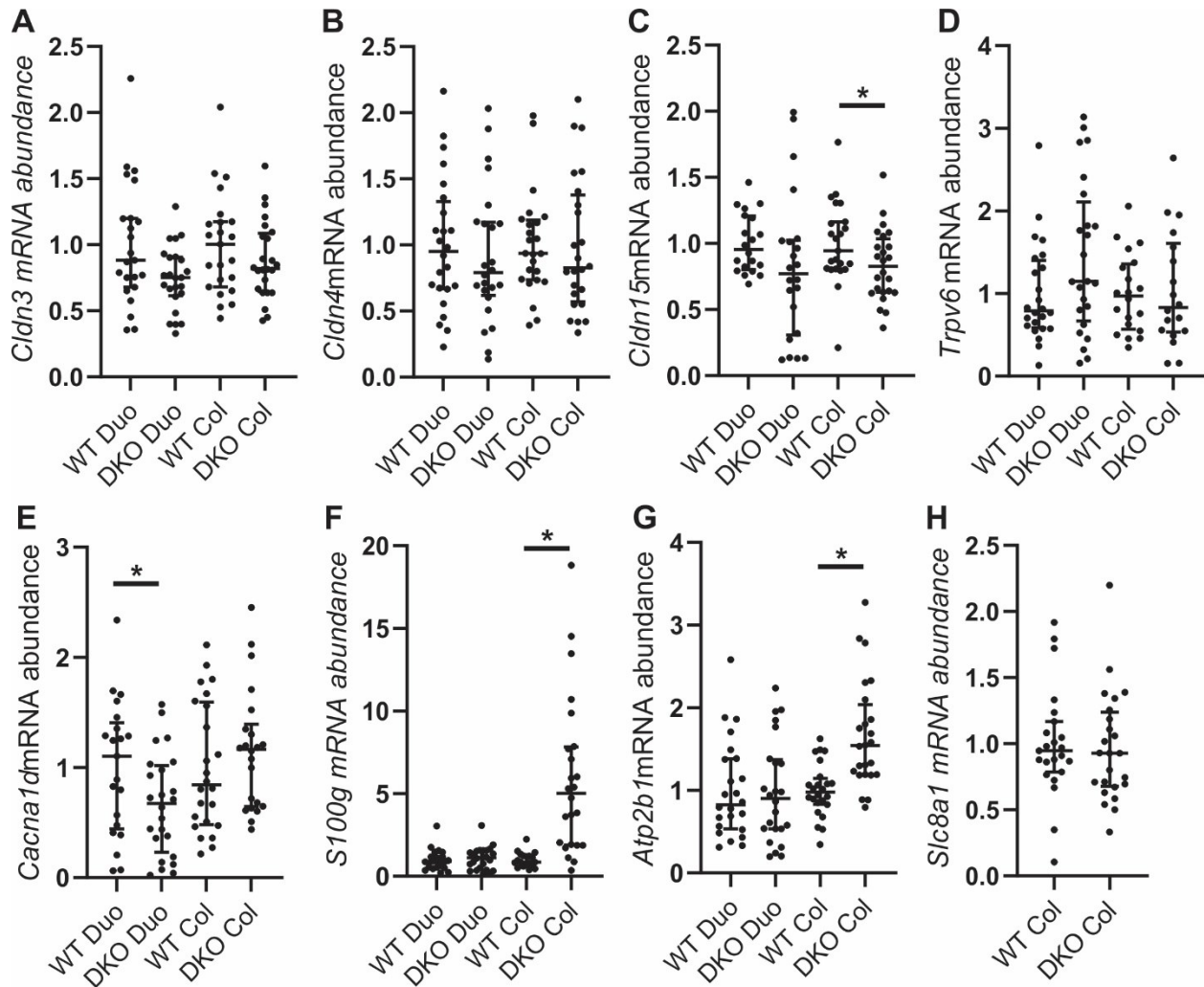
Figure 4.6. *Cldn2/12* **DKO intestinal gene expression suggests compensatory increases in transcellular Ca^{2+} from the proximal colon.** mRNA abundance of genes encoding A) claudin-3, B) claudin-4, C) claudin-15, D) TRPV6, E) Ca$_v$1.3, F) calbindin-D$_{9k}$, G) PMCA1b, H) NCX1 in the intestine of WT and *Cldn2/12* DKO mice. Expression normalized to *β-actin* and expressed relative to WT for each intestinal segment. Duo, duodenum; Col, colon. n = 23 WT and 24 DKO. Data presented as median ± IQR. Comparison of DKO to WT for each intestinal segment by Mann-Whitney test. *P < 0.05
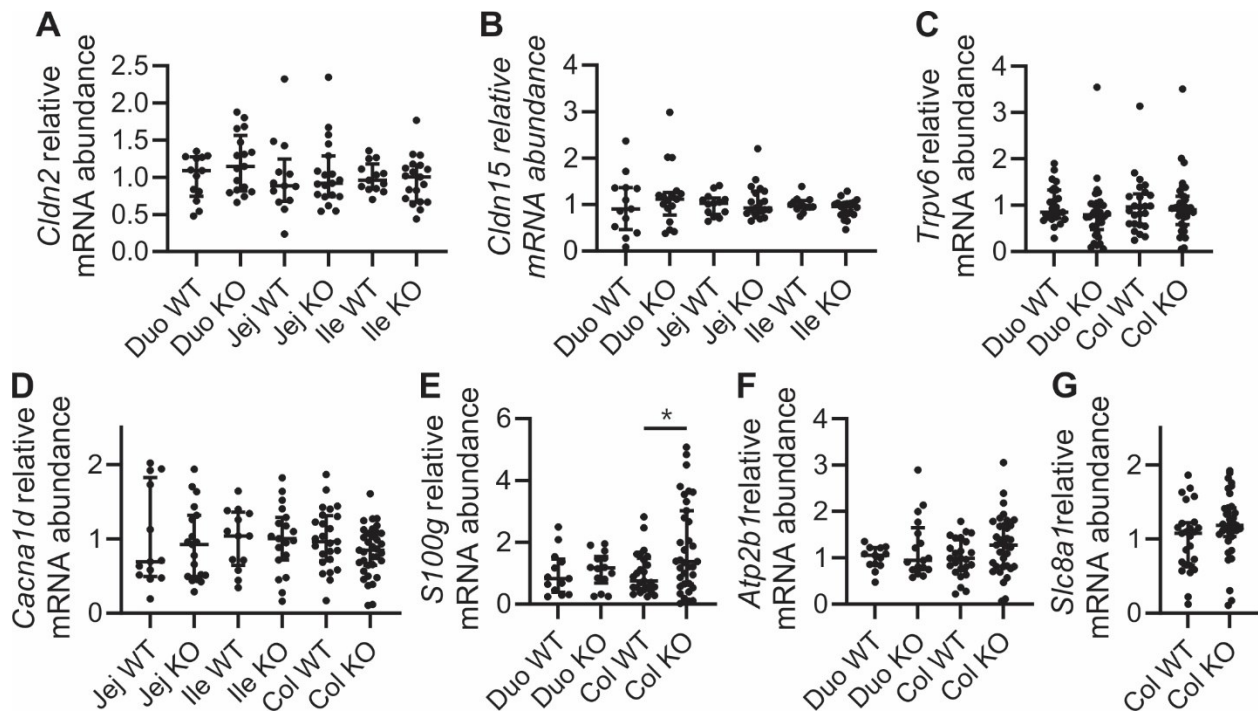
Figure 4.7. Gene expression in *Cldn12* KO intestine. mRNA abundance of genes expressing A) claudin-2, B) claudin-15, C) TRPV6, D) Ca$_v$1.3, E) calbindin-D$_{9k}$, F) PMCA1b, G) NCX1 in the intestine of WT and *Cldn12* KO mice. Expression normalized to *Gapdh* (Duo, Jej, Ile) or *18S* (Col) and expressed as relative to WT for each intestinal segment. Duo, duodenum; Jej, jejunum; Ile, ileum; Col, colon. n = 23 WT and 24 DKO. Data presented as median ± IQR. Comparison of KO to WT for each intestinal segment by Mann-Whitney test. *$P < 0.05$

4.4.4. Claudin-2 and claudin-12 DKO mice display reduced bone mineralization

It has been previously established that *Cldn2* KO mice have bone mineralization that is not different than WT littermates.[86] However, whether *Cldn12* KO mice have a normal bone phenotype is not known. We, therefore, performed μCT studies on *Cldn12* KO mice at 3 and 6 months of age. No differences compared to WT mice were observed in either trabecular or cortical bone (Tables 4.6 and 4.7). In contrast to the single *Cldn2* or *Cldn12* KO animal, the DKO mice displayed reduced plasma iCa^{2+}, reduced intestinal Ca^{2+} absorption and more marked renal Ca^{2+} wasting. We, therefore, hypothesized that DKO mice would have altered microarchitecture and mineral density of tibia. Consistent with this, we observed a greater than 4-fold decrease in trabecular bone mineral density in DKO mice compared to WT. Further, trabecular thickness and number were significantly decreased in DKO mice. Similarly, we found decreased bone volume, thickness, and tissue mineral density in cortical bone of DKO mice (Figure 4.8). These results are consistent with DKO mice having reduced bone mineralization due to the loss of both claudins. Further, it suggests that either claudin can compensate for the loss of the other alone.

Table 4.6. Trabecular and cortical bone parameters of 3-month-old *Cldn12* KO vs. WT mice

	Male			Female		
	WT	*Cldn12* KO	P- value	WT	*Cldn12* KO	P- value
N	8	7		7	9	
Trabecular Bone						
Bone Mineral Density (g/cm^3)	0.193 ± 0.041	0.223 ± 0.069	0.3076	0.200 ± 0.024	0.197 ± 0.060	0.9027
BV/TV (%)	11.38 ± 4.20	17.10 ± 9.55	0.1805	11.13 ± 3.00	11.97 ± 8.56	0.7891
Trabecular Thickness (mm)	0.066 ± 0.006	0.075 ± 0.012	0.0769	0.079 ± 0.006	0.078 ± 0.020	0.9242
Trabecular Separation (mm)	0.403 ± 0.124	0.331 ± 0.159	0.3385	0.520 ± 0.126	0.457 ± 0.136	0.5197
Trabecular Number (1/mm)	1.68 ± 0.539	2.16 ± 1.04	0.2745	1.40 ± 0.344	1.48 ± 0.852	0.7943
Cortical Bone						
Bone Volume (mm^3)	1.87 ± 0.210	1.96 ± 0.262	0.4492	1.98 ± 0.100	1.89 ± 0.203	0.2874
Cortical Thickness (mm)	0.195 ± 0.010	0.201 ± 0.028	0.5978	0.231 ± 0.015	0.223 ± 0.013	0.2986
Tissue Mineral Density (g/cm^3)	0.830 ± 0.057	0.817 ± 0.057	0.6724	0.907 ± 0.038	0.924 ± 0.048	0.4463

Data is presented as mean ± SD (unpaired t-test KO vs WT for each sex). BV/TV; bone volume/tissue volume.

Table 4.7. Trabecular and cortical bone parameters of 6-month-old *Cldn12* KO vs. WT mice

	Male			Female		
	WT	*Cldn12* KO	P- value	WT	*Cldn12* KO	P- value
N	6	6		6	6	
Trabecular Bone						
Bone Mineral Density (g/cm^3)	0.112 ± 0.020	0.158 ± 0.048	0.0931	0.096 ± 0.001	0.103 ± 0.014	0.3159
BV/TV (%)	6.95 ± 2.09	11.14 ± 6.39	0.1763	4.27 ± 1.03	4.51 ± 1.38	0.7422
Trabecular Thickness (mm)	0.063 ± 0.002	0.068 ± 0.009	0.1967	0.046 ± 0.010	0.045 ± 0.010	0.8432
Trabecular Separation (mm)	0.463 ± 0.151	0.318 ± 0.064	0.0566	0.667 ± 0.136	0.572 ± 0.085	0.1759
Trabecular Number (1/mm)	1.10 ± 0.306	1.57 ± 0.731	0.1729	0.976 ± 0.356	1.02 ± 0.318	0.8428
Cortical Bone						
Bone Volume (mm^3)	1.87 ± 0.189	2.07 ± 0.105	0.0452	1.98 ± 0.202	1.86 ± 0.276	0.4222
Cortical Thickness (mm)	0.199 ± 0.014	0.205 ± 0.012	0.4790	0.230 ± 0.022	0.214 ± 0.017	0.1859
Tissue Mineral Density (g/cm^3)	0.894 ± 0.035	0.905 ± 0.026	0.5787	0.949 ± 0.008	0.950 ± 0.043	0.9549

Data is presented as mean ± SD (unpaired t-test KO vs WT for each sex). BV/TV; bone volume/tissue volume.
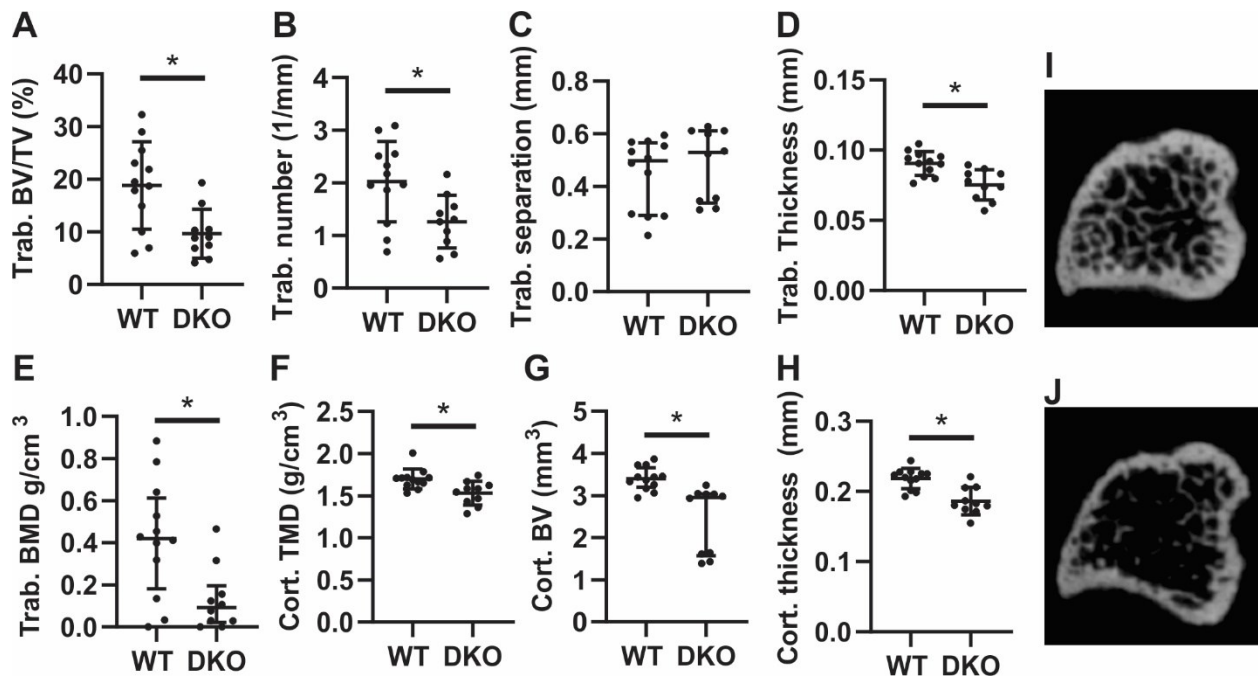
Figure 4.8. *Cldn2/12* DKO mice have altered bone morphometry at 3 months. Micro-CT analysis of tibia in WT and DKO mice to examine A) trabecular bone volume/ tissue volume (P = 0.0058), B) trabecular number (P = 0.0139), C) trabecular separation (P = 0.2276), D) trabecular thickness (P = 0.0014), E) trabecular bone mineral density (P = 0.0137), F) cortical tissue mineral density (P = 0.0063), G) cortical bone volume (P = 0.0001), H) cortical thickness (P = 0.0003). Microarchitecture of trabecular (trab) (A-E) and cortical (cort) (F-H) bone in tibia of WT and *Cldn2/12* DKO mice analysed by micro-CT. Representative micro-CT images of the tibial metaphyses shown at 40 slices from growth plate from I) WT and J) DKO mice. Data presented as mean ± SD compared by unpaired t-test (A, B, D, G, H) or as median (IQR) compared by Mann-Whitney test (C, E, F).

4.4.5. Claudin-2 and -12 physically do not interact when expressed *in vitro*

Given that claudin-2 and -12 have an additive effect on P_{Ca} and urinary Ca^{2+} excretion, we hypothesized that these proteins form Ca^{2+} pores physically independent of each other. To assess this, we performed co-immunoprecipitation on HEK cells expressing epitope-tagged claudin-2 and claudin-12. As a positive control, we found that myc-tagged claudin-2 was able to immunoprecipitate HA-tagged claudin-2. However, myc-tagged claudin-2 was unable to immunoprecipitate HA-tagged claudin-12 (Figure 4.9A-B). The immunoprecipitation with no cell lysate as a negative control identifies the IgG light chain band at 25 kDa. Together, these results are consistent with claudin-2 and claudin-12 not physically interacting to create a pore, and instead forming redundant, separate Ca^{2+} permeable pores.

If claudin-2 and claudin-12 form separate Ca^{2+} permeable pores in renal and intestinal epithelia, P_{Ca} should be greater with both proteins present than with only one. We established a Caco-2 cell line that stably expressed CLDN12 under a tet-off system. CLDN2 is endogenously present in these cells (Figure 4.9C). CLDN12 is present in the cells before doxycycline treatment and, after 40 hours of treatment, most of the CLDN12 was only very faintly detected (Figure 4.9C). Cells expressing both CLDN2 and CLDN12 had higher P_{Ca} than cells only expressing CLDN2 (Figure 4.9D). Similarly, we employed OK cells endogenously expressing CLDN12 with empty vector or also overexpressing CLDN2 (Figure 4.9E). Cells expressing both CLDN2 and CLDN12 had significantly higher P_{Ca} than cells only expressing CLDN12 (Figure 4.9F). These results indicate that claudin-2 and claudin-12 form separate Ca^{2+} permeable pores.
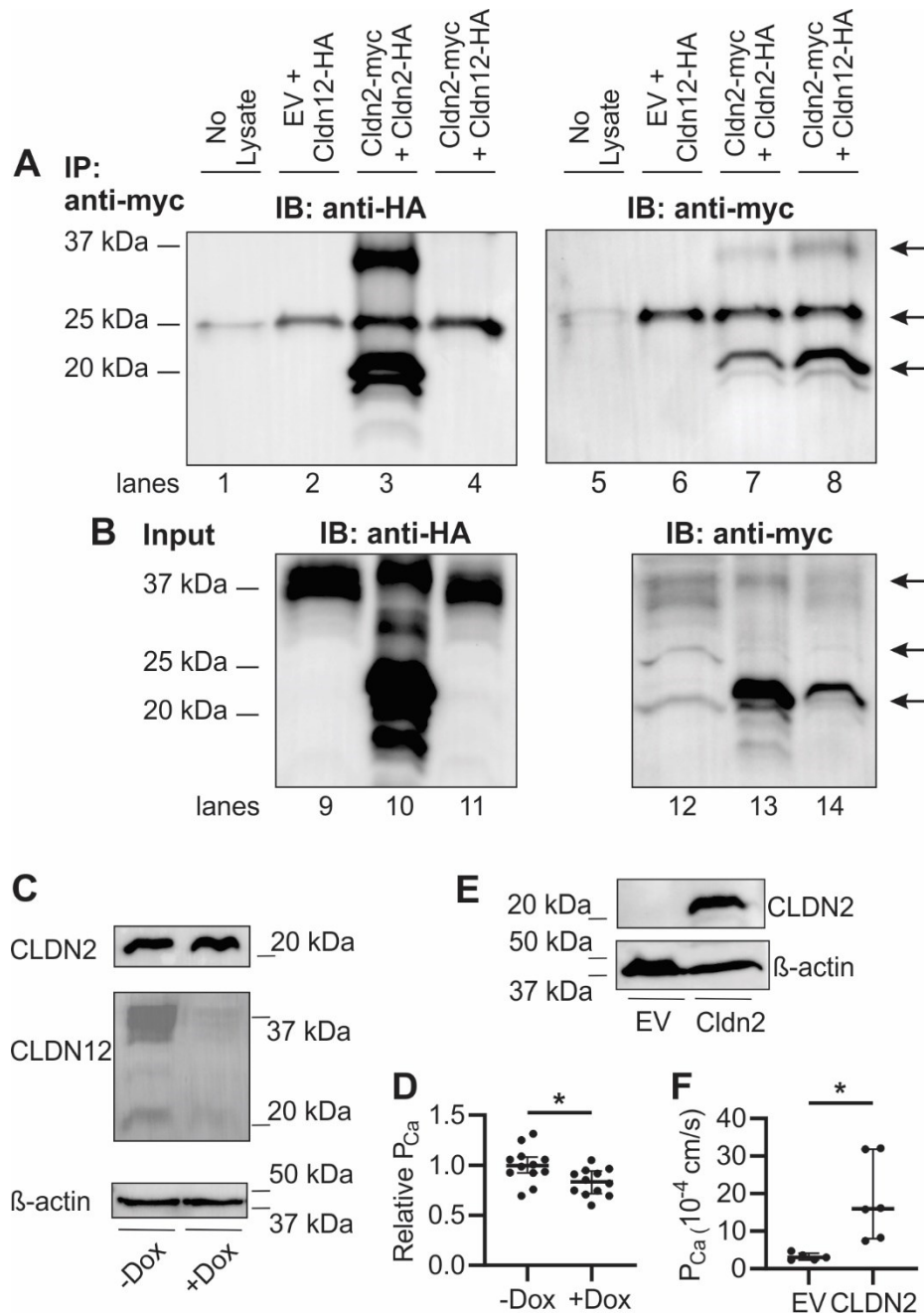
Figure 4.9. Claudin-2 and claudin-12 form separate Ca²⁺ permeable pores. HEK cells transfected as indicated were lysed or buffer without cell lysate as control (no lysate lane) and proteins A) immunoprecipitated (IP) with antibodies to myc before SDS-PAGE. Proteins were electrotransferred and blotted with anti-HA antibody (lanes 1 – 4) and then stripped and re-probed with anti-myc antibody (lanes 5 -8). B) protein from HEK cells above directly resolved on SDS-PAGE (Input) and blotted with anti-HA (lanes 9 - 11) and then anti-myc (lanes 12 - 14). Claudin dimers (37 kDa) and monomers (20 kDa) are highlighted by arrows. The arrow at 25

kDa illustrates IgG light chain in the IP samples as seen in the lane with no cell lysate added. EV, empty vector. Representative blot of 2 repeats. C) Caco-2 cells endogenously express CLDN2 and express CLDN12 under a tet-off system at 20 days in culture. D) Caco-2 cells expressing CLDN2 and CLDN12 (-Dox) have greater P_{Ca} than cells expressing only CLDN2 (+Dox) ($P = 0.0142$, t-test) at 20 days in culture. E) OK cells endogenously expressing CLDN12 and expressing either empty vector (EV) or CLDN2. F) OK cells expressing CLDN2 and CLDN12 (CLDN2) have greater P_{Ca} than cells expressing only CLDN12 (EV) ($P = 0.0183$, Welch's t-test).

4.5. Discussion

Employing murine models, detailed balance studies, *ex vivo* and *in vitro* techniques, we provide evidence that claudin-2 or claudin-12 are necessary to maintain Ca^{2+} homeostasis and optimal bone mineralization. This conclusion is supported by *Cldn2/Cldn12* DKO mice having decreased P_{Ca}^{2+} across the colon, contributing to decreased net intestinal Ca^{2+} absorption. Further, the DKO mice have even greater hypercalciuria than the single *Cldn2* KO animals, suggesting non-redundant functions in the proximal tubule. Intestinal and renal compensatory mechanisms in the DKO mice are inadequate to maintain a normal serum ionized Ca^{2+} which may be due to an inability to increase serum calcitriol levels. Ultimately, loss of both proteins results in decreased bone mineral density compared to WT mice. Moreover, we demonstrate that claudin-2 and -12 do not physically interact, consistent with the additive effects of their deletion on colonic P_{Ca} and urinary Ca^{2+} excretion, suggesting they encode independent Ca^{2+} pores in the proximal colon and renal proximal tubule.

Paracellular intestinal Ca^{2+} absorption is proposed as the predominant pathway when dietary Ca^{2+} is adequate or high.[237] However, this has never been directly tested. Claudins-2 and -12 have been implicated in mediating paracellular Ca^{2+} diffusion between epithelial cells.[78, 84, 87] Herein, we describe a genetic model where these two tight junction proteins conferring P_{Ca} to intestinal epithelium are deleted. The DKO mice display decreased intestinal Ca^{2+} absorption when fed an adequate Ca^{2+} containing diet. Further, when intestinal P_{Ca} was measured *ex vivo*, the DKO mice displayed reduced colonic Ca^{2+} permeability. Previous work has clearly demonstrated that Ca^{2+} can be absorbed across the large intestine under adequate and high dietary Ca^{2+} conditions via the paracellular pathway.[40, 255, 258] However, this paracellular pathway mediates bidirectional diffusion of Ca^{2+}.[258, 259] Therefore, depending on the electrochemical

properties across the tissue, net secretion or absorption may occur. Previous work has shown that the loss of *Cldn2* leads to increased net Ca^{2+} absorption, possibly due to reduced colonic Ca^{2+} secretion.[86] Despite reduced colonic P_{Ca}, *Cldn12* KO mice do not have altered net intestinal Ca^{2+} absorption.[87] In contrast to the single KO animals, we observe decreased net Ca^{2+} absorption in DKO mice. Moreover, again in contrast to the single KO mice, the DKO animals demonstrate reduced plasma Ca^{2+} levels and reduced bone mineralization. In *Cldn2* KO mice, we observed only changes in P_{Ca} across the colon. However, in DKO and *Cldn12* KO mice, TER was increased, absolute P_{Na}, P_{Cl} and relative cation permeability were decreased. These alterations may contribute to an altered electrochemical driving force across the colon and thus explain the differences observed between *Cldn2* KO and DKO mice. While this work has provided evidence in support of a significant role for paracellular intestinal Ca^{2+} absorption to the maintenance of Ca^{2+} homeostasis further research is required to examine the differences between the reported phenotype of *Cldn2* KO and DKO mice observed here.

The contribution of the colon to net Ca^{2+} absorption has been argued to be negligible.[4] However, in studies of patients with bowel resection, individuals with a functional colon absorb significantly more Ca^{2+} than those with an ileostomy.[251, 252] Furthermore, the longer transit time in the colon of approximately 39 hours compared to 3.9 hours in the small intestine permits a greater absorption capacity.[260] Our work reveals that a loss of the paracellular pathway across the colon results in a reduced net Ca^{2+} absorption and overall balance, inferring an important role for this segment. Indeed, the large intestine may be a major site of systemically and acutely regulated Ca^{2+} absorption.[250, 261, 262] This is consistent with the colon being a site of absorption of other nutrients.[254, 263, 264] These studies suggest a "fine-tuning" role of the colon in regulating total body Ca^{2+} balance. The colon might be best thought of in analogy to the distal

convolution/connecting tubule in the nephron. Loss of Ca^{2+} reabsorption from the distal nephron, which accounts for roughly 10% of total Ca^{2+} reabsorption, leads to reduced bone mineralization since there is no distal segment to compensate.[158]

PTH and calcitriol are central hormones regulating Ca^{2+} homeostasis. Low serum Ca^{2+} triggers PTH release from the parathyroid, which then acts on the proximal tubule to upregulate transcription of 1α-hydroxylase which catalyzes the synthesis of active vitamin D, calcitriol.[236] This hormone, in turn, increases intestinal Ca^{2+} absorption and bone resorption to maintain serum Ca^{2+} in a narrow range.[1, 237] In the current study, DKO mice had lower serum Ca^{2+} than WT mice with the expected increase in PTH. However, serum calcitriol was not significantly increased nor was the renal expression of *Cyp27b1,* the enzyme responsible for its activation. *Cldn2*, *Cldn12*, and *Cyp27b1* are expressed in the proximal tubule.[1, 87, 146, 184, 265] When calcitriol was administered to DKO mice, they were able to increase serum iCa^{2+} although still to a level less than the WT mice. Similarly, on a low Ca^{2+} diet, DKO mice increased serum calcitriol but still had lower serum iCa than WT mice. It is recognized that claudins, including claudin-2, have permeability-independent functions in cell signaling and gene transcription.[141, 266] However, more work is required to explore a possible role for claudin-2 or claudin-12 in regulating vitamin D metabolism.

Without increased active vitamin D, targets of its regulation including *Trpv6* were also not increased in the duodenum or colon.[261] However, increased *S100g* expression was observed in the colon of DKO mice, suggesting increased compensatory transcellular Ca^{2+} transport in this segment, as *S100g* expression appears to be regulated by increased cellular Ca^{2+}.[55] Transcellular transport from the colon may still be mediated by *Trpv6* as previous work has shown that the colon can directly sense low extracellular Ca^{2+} concentrations through the calcium sensing

receptor and increase TRPV6 mediated transcellular Ca^{2+} absorption in the absence of changes in expression.[262]

The DKO phenotype observed does not appear to be due only to the loss of calcitriol dependent transcellular absorption across the intestine. Mice lacking functional TRPV6 channels have decreased transcellular Ca^{2+} absorption across the duodenum under conditions of low intake.[50, 53, 267] However, unlike the lower serum iCa^{2+} in DKO mice, *Trpv6* KO mice do not have decreased serum Ca^{2+}, although overall net Ca^{2+} balance has not been described.[50, 51, 53] *Trpv6* KO mice do have decreased bone mineral density.[50, 268] However, *Trpv6* is expressed on the cell membrane of osteoclasts where it functions to negatively regulate bone resorption.[268, 269] Therefore, rather than decreased bone mineralization due to decreased Ca^{2+} balance, changes in bone architecture may be caused by alterations in osteoclast function. Claudin expression has been described in osteoblasts, although their function is yet to be fully determined.[270, 271] Still, if our observed phenotype was due only to action in bone, it is likely we would observe greater intestinal Ca^{2+} absorption or renal reabsorption for compensation rather than the decreases described. $Ca_v1.3$ has also been posited to mediate Ca^{2+} homeostasis via transcellular intestinal Ca^{2+} uptake,[56, 57, 192, 222] although conflicting results have been reported.[59, 193] However, *Cacna1d* expression is not regulated by calcitriol.[261] Therefore, our results cannot be explained only by loss of calcitriol mediated pathways. Rather, these studies and our work support a significant role for the paracellular pathway in intestinal Ca^{2+} absorption under adequate dietary intake.

The DKO mice display marked hypercalciuria. Both claudin-2 and claudin-12 contribute P_{Ca} to the proximal tubule.[86, 87] Perfused proximal tubules from *Cldn12* KO mice have a decrease in both P_{Na} and P_{Ca} with no change in P_{Cl}.[87] Moreover, both *Cldn2* KO and *Cldn12* KO proximal tubules are anion-selective in contrast to proximal tubules from WT mice that are cation-

selective.[87, 146] However, *Cldn12* KO mice do not have increased urinary Ca^{2+} excretion perhaps due to compensation.[87, 150] Conversely, *Cldn2* KO mice have a 3-fold increase in fractional Ca^{2+} excretion compared to WT.[146] However, this can be partly explained by decreased colonic Ca^{2+} secretion contributing increased net intestinal absorption, increased Ca^{2+} filtered at the glomerulus and increased urinary excretion, notably without increased serum Ca^{2+}.[86] In contrast, DKO mice have decreased net intestinal absorption and greater renal Ca^{2+} wasting. Therefore, the loss of claudin-2 and claudin-12 likely leads to markedly inadequate Ca^{2+} reabsorption across the proximal tubule that overwhelms the compensatory capacity of the more distal segments.

In summary, we present a murine model of disturbed Ca^{2+} homeostasis whereby loss of paracellular Ca^{2+} permeability across the colon and proximal tubule leads to a decreased net balance, decreased bone mineralization, and inability to maintain serum Ca^{2+} levels. Our work supports two independent, redundant, paracellular pathways mediated by either claudin-2 or claudin-12. Overall, we highlight the critical role of claudins-2 and -12 in maintaining Ca^{2+} balance.

Chapter 5

Final Discussion

The overall aim of this thesis was to delineate molecular mechanisms mediating a positive calcium balance during early postnatal development. Significant evidence indicates that intestinal absorption is the main contributor to overall balance where the absorption mirrors bone accretion throughout development.[31, 102, 103] Therefore, mechanisms mediating intestinal calcium absorption are the focus of this thesis. To our knowledge, this is the most comprehensive study to date of pathways of postnatal intestinal calcium absorption.

5.1. Summary of Results

Previous studies suggested that significant alterations in intestinal calcium absorption occur around the time of weaning. These studies were completed largely before the molecular details of calcium absorption were determined and, therefore, functionally characterized the pathways as saturable or unsaturable, referring to transcellular and paracellular calcium absorption, respectively. Consistent with findings of a transition from predominantly paracellular to having significant transcellular pathways present after weaning, we found that net transcellular uptake is mediated by TRPV6 and only appears after weaning in the duodenum. Despite being the predominant pathway, P_{Ca} across the duodenum is not greater at two weeks than two months in this segment.

Of particular interest are our observations in the jejunum and ileum. We noted net absorption via a transcellular pathway across the jejunum and ileum in sucking mice that was not present in the two-month-old mice. This pathway is mediated by TRPV6 and $Ca_v1.3$ in the jejunum and is inhibitable by nifedipine in the ileum, inferring the function of a voltage gated calcium channel. However, this pathway remained active in *Cacna1d* (encoding $Ca_v1.3$) KO mice, therefore implicating the presence of another channel. Loss of $Ca_v1.3$ led to delayed bone

mineralization at two weeks while loss of functional TRPV6 did not. In addition, we observed 2-fold increased permeability to calcium across the jejunum and ileum at two weeks of age relative to at 2 months consistent with a greater capacity for paracellular calcium absorption in suckling animals. The greater permeability is mediated by increased claudin-2 in the younger animals. When removed from breast milk feeding, *Cldn2* expression decreased to adult levels. Using an *in vitro* model we determined that EGF in breastmilk increases claudin-2 expression. Therefore, our results are consistent with breast milk regulating increased absorptive capacity of the small intestine during the suckling period.

Very early studies in humans and rats recognized the colon as a site of absorption or secretion, dependent on the amount of calcium in the diet.[272] This includes work done in the Alexander lab demonstrating local regulation of TRPV6 mediated flux.[273] Recent work has begun to revisit the colon as a site of significant regulated calcium absorption and secretion including a collaboration of the Alexander lab demonstrating decreased calcium permeability across the colon of *Cldn2* KO mice at 3 months.[86, 250] Preliminary work demonstrates that neither claudin-2 or claudin-12 contribute calcium permeability across the colon at 2 weeks (Appendix A). However, we observed that global loss of both claudin-2 and claudin-12 (DKO) lead to decreased calcium permeability across only the colon at 2 months which then resulted in decreased net intestinal absorption and decreased serum ionized calcium. These mice also had increased urinary excretion of calcium, greater than that observed in *Cldn2* single KO mice which contributed to reduced net balance. The decreased trabecular and cortical bone mineralization in the DKO mice was significant and appreciable on μCT images. Thus, we propose that the colon is a site of significant calcium absorption contributing to overall homeostasis. Some of our results are presented in updated Table 5.1 and Figure 5.1.

167

Table 5.1. Expression of molecules implicated in intestinal calcium absorption throughout development – updated with results of current thesis.

	Duodenum			Jejunum			Ileum			Cecum			Colon			
Age (weeks)	< 3	3-8	> 8	< 3	3-8	> 8	< 3	3-8	> 8	< 3	3-8	> 8	< 3	3-8	> 8	Ref
Transcellular																
Trpv6	No	Yes	Yes*	Yes	No	No	No	No	No	ND	ND	Yes	ND	ND	Yes	37, 40, 71, 104, 105, 222
Cav1.3	Yes	Yes	Yes	Yes	Yes	Yes	Yes	Yes	Yes	ND	ND	No	Yes	ND	No	56, 222
CaBP9K	No	Yes	Yes*	Yes	Yes	No	Yes	No	No	ND	Yes	Yes	Yes	ND	Yes	37, 40, 62, 63, 71, 104, 105, 222
Pmca1	Yes	Yes	Yes*	Yes	Yes	Yes	Yes	ND	Yes*	ND	ND	Yes	ND	ND	Yes*	37, 40, 65, 66, 69, 71, 104, 222
Pmca4	ND	ND	Yes	ND	ND	Yes	Yes	Yes	Yes	ND	ND	Yes	ND	ND	Yes	66
Ncx1	ND	ND	Yes	Yes	Yes	Yes	Yes	Yes	Yes	ND	ND	Yes	ND	ND	Yes	37, 222
Paracellular																
Cldn2	ND	Yes	Yes*	Yes	Yes	Yes	ND	ND	Yes*	ND	ND	Yes*	ND	ND	Yes*	37, 69, 71, 80, 86
Cldn12	ND	ND	Yes*	Yes	Yes	Yes	ND	ND	Yes*	ND	ND	Yes*	ND	ND	Yes*	37, 69, 71, 80
Cldn15	ND	ND	Yes*	Yes	Yes	Yes	ND	ND	Yes*	ND	ND	Yes*	ND	ND	Yes*	37, 69, 71, 80
Cldn19	ND	ND	No	Yes	ND	No	ND	ND	No	ND	ND	No	ND	ND	No	80
Nhe3	ND	ND	Yes	ND	ND	Yes	ND	ND	Yes	ND	ND	Yes	ND	ND	Yes	37

Note: Ages refer to age of rodent animal models. ND, no data.

*Expression in adult human and rodent samples.

Figure 5.1. Net calcium absorption and secretion by intestinal section during suckling and after weaning. A pictorial representation of evidence updated to include data from this thesis. Absorption is represented by a downward arrow indicating net movement of calcium from lumen to serosa. When both transcellular and paracellular pathways are present in a segment, a larger arrow indicates the predominant pathway. Note that the transcellular pathway in the duodenum pre-weaning occurs after 1–2 weeks of age in rodents. The dashed line indicates that evidence supporting the pathway is limited. Evidence for calcium absorption in the cecum is from animal models only. Weaning is at 21 days in rodents. ND: no data.

5.2. Significance of Results and General Discussion

5.2.1. Calcium absorption across the small intestine in postnatal development

The current thesis work has contributed several insights to the field of intestinal calcium transport, but also physiology and nutrition more broadly. Early studies debated whether calcium transport across the small intestine occurred via a passive, diffusive process or an active carrier mediated process.[274, 275] We now have evidence that both pathways exist, although contribution to net absorption depends on dietary intake and by intestinal segment. In addition, a few studies suggested marked alterations in the pathway in early life, particularly around the time of weaning.[104, 107-112, 276, 277] The current thesis builds on this foundation of evidence and provides a more comprehensive understanding of the molecular pathways mediating intestinal calcium absorption in early postnatal life.

The apical entry channel, TRPV6 was first cloned in 1999.[45] This channel was found to be highly selective for calcium, did not permit magnesium conductance and was unaffected by iron, manganese and zinc ions.[45] These properties and its expression in the rat duodenum, proximal jejunum, cecum and colon is consistent with it being a major mediator of net intestinal calcium absorption.[45] *Trpv6* KO mice do not display a drastic phenotype.[50, 51, 53, 54] However a transgenic mouse model expressing *TRPV6* under a villin promoter hyperabsorbed calcium and rescued the hypocalcemic phenotype of the *Vdr* KO mice.[55] Our findings that TRPV6 mediates flux across the jejunum early in life build on this earlier research. The Michaelis constant of TRPV6 is 0.44 mM.[45] Therefore, in older mice, this channel is more critical under conditions of low lumen calcium or low dietary intake. In infants, TRPV6 likely has a role in maximizing absorption as the calcium concentration of breast milk is relatively high at approximately 5.5

mM.[238] Thus, breastmilk ingestion contributes a significant driving force for paracellular absorption across the proximal small intestine. As lumen concentration declines, transcellular absorption in the jejunum and ileum, including by TRPV6, would ensure optimal absorption.

When pups were weaned early from breast milk to a solid chow diet, we observed an increase in *Trpv6* expression in the jejunum. It may be that the switch from a diet of breast milk high in calcium to one low in calcium caused this change. *TRPV6* mutations have been identified as a cause of transient neonatal hyperparathyroidism where infants are born with hypomineralized skeletons.[213, 278] In one of these cases, serum calcium was low at birth and normalized by 2 weeks, serum PTH normalized by 3 months and skeletal findings normalized at 18 months.[278] The delay in normalizing serum calcium and PTH suggests a role for TRPV6 in optimizing intestinal absorption. However, based on the results of this thesis, it is likely that another transcellular pathway is present and that paracellular absorption was also a major pathway contributing intestinal calcium absorption. This report did not state whether the infant received breast milk or formula. To date, research into human TRPV6 mutations have not determined if they pose an increased risk for osteoporosis later in life.[279]

In addition to the TRPV6 mediated flux occurring in the jejunum, we described a transcellular flux across the ileum only present before weaning. This flux was inhibited by nifedipine but was unaltered when $Ca_v1.3$ was knocked out. One previous study demonstrates consistent findings. *Ex vivo* evidence in rats suggested increased calcium uptake into cells of the ileum prior to weaning.[112] The ileum is the longest segment of the small intestine with the greatest sojourn time.[40] Therefore, this pathway may be a major contributor of net calcium absorption in early life. *Trpv6* KO mice did not have altered bone size, structure or density, while *Cacna1d* KO mice had a delay in bone mineralization. Indeed, when taken together, all evidence

to date into intestinal transcellular calcium absorption is suggestive of another carrier that has yet to be identified. After our study was published, work on another TRP channel, TRPM7, proposed this as the gatekeeper of intestinal calcium absorption in postnatal development.[280] However, the *in vitro* and *in vivo* data did not support a direct role for TRPM7 mediating entry of calcium into the cell.[280] Rather, it is more likely that this channel mediates magnesium and zinc absorption. Together, these micronutrients are cofactors for hundreds of enzymes, including being vital for functioning Mg-ATP complex.[281] Hence, the unidentified calcium carrier remains elusive. Our work on the ileum of young mice can be used to identify this apical channel.

Our finding of a vital role of claudin-2 early in life is intriguing. Claudin-2 was first identified in 1998 and the first evidence of this protein forming a calcium permeable pore came from *in vitro* studies a decade later.[78, 84, 282] The first direct evidence of claudin-2 mediating intestinal calcium permeability came via a collaboration which occurred in conjunction with this thesis, where we showed that claudin-2 contributes calcium permeability to the colon of adult mice.[86] The work of the current thesis is the first to investigate the molecular details of intestinal calcium permeability in postnatal development. Of note, a recent study found that iron deficiency in male rats aged 5 – 6 weeks upregulated claudin-2 expression and consequently, calcium absorption across the duodenum.[283] *Cldn2* KO mice were previously shown to have decreased sodium permeability across the small intestine at two weeks of age, but calcium was not investigated.[77] Studies in the *Cldn2* KO mice indicate that these animals are largely phenotypically normal however, they consume significantly more oxygen in the kidney.[85] This is due to a compensatory increase in active reabsorption pathways because of the loss of the passive, paracellular pathways. Therefore, the paracellular pathway of ion transport represents an energy efficient evolutionary advantage.[223] This is consistent with our findings. As stated above,

the calcium concentration in breast milk is approximately 5.5 mM.[238] This far surpasses the calculated requirement of 1.74 mM calcium to overcome an estimated transepithelial potential difference of lumen negative 5 mV and serum ionized calcium of 1.2 mM.[41] Therefore, our results describe a mechanisms by which infants maximize calcium absorption across the small intestine to meet requirements for growth in an energy efficient manner.

In addition to describing claudin-2 facilitating greater intestinal calcium permeability in suckling mice, we attribute this increased expression to EGF found in breast milk.[132] To our knowledge, this is this second study to investigate adding human breast milk directly to cell culture media and the first to propose a role for increasing intestinal calcium absorption.[132] EGF is found in breast milk but also saliva and amniotic fluid.[135] Others have posited a potential benefit to adding EGF to infant formula to prevent life-threatening NEC in preterm infants.[244] Our results indicate that this addition may also increase calcium absorption. Previous work has demonstrated that the percentage of calcium absorption is greater in infants receiving human milk or fortified human milk relative to formula.[32] This is especially intriguing given that the calcium concentration in formula is 2.5-fold greater than in breast milk. Therefore, our results suggest that this phenomenon may be due, at least in part, to the lack of EGF in formula.

Based on these observations that claudin-2 is regulated by EGF, we may now propose specific therapeutic options for premature and term infants and potentially the millions of people suffering from osteoporosis. In addition, claudin-2 is known to have a complex role in inflammatory bowel disease.[72, 224] It must, however, be appreciated that the health-related impact of this research is built on a foundation of fundamental science and a curiosity for physiology and nutrition knowledge. It is impossible to know if early scientists were thinking of specific

therapeutics related to this work however, the intended purpose of the research was not stated as such in the publications.

5.2.1. Claudin-2 and claudin-12 mediated calcium absorption across the colon

Vitamin D is known to increase transcellular calcium absorption. Variants in the *VDR* gene associate with BMD and calcium absorption at low dietary intake but this effect is reduced at high dietary intakes, thus highlighting the important role of the paracellular pathway under conditions of adequate intake.[284, 285] These studies were carried out in adults or postmenopausal women. Consistent with the epidemiological data, we observed that alterations in calcium permeability across the colon by genetic loss of claudin-2 and -12 resulted in drastic reductions in bone mineralization and microarchitecture of mice at 2 – 3 months.

Further to the importance of the paracellular pathway is the role this pathway plays in the colon of adult mice. Preserving half the colon versus none in adult patients with short bowel syndrome (SBS) allowed the patient to remain in a neutral calcium balance while others had to be supplemented.[286] In another study of SBS patients, all the patients not requiring total parenteral nutrition (TPN), a marker of adequate intestinal nutrient absorption, had an intact colon whereas any patient without a colon required TPN.[287] In a separate study, parental infusion of calcium increased fecal calcium without changing the endogenous loss into feces in people with intact colon but not in people with jejunostomy.[288] These studies are small but suggest that the colon is an important site to the maintenance of calcium homeostasis.

Many early studies on rodent colon have indicated the presence of both a transcellular pathway and a paracellular pathway using methods of everted sacs, *in vivo* perfusion or Ussing

chambers.[36, 38, 289-295] Observations that the net absorption across the colon may be saturable and vitamin D-dependent have led to the conclusion that this flux is predominantly via a transcellular pathway while secretion is via a passive paracellular process.[292, 294, 296] Our results are the first to implicate claudin-2 and claudin-12 independently conferring paracellular calcium permeability to the colon which results in net absorption. These results question previous assertions that net absorption from the colon occurs via the transcellular pathway only because both claudin-2 and claudin-12 have been demonstrated to be regulated by vitamin-D.[78, 121, 297] Furthermore, claudin-2 is demonstrated to be gated in a symmetrical and reversible manner.[298] Thus, the role of this paracellular pathway across the colon was likely overlooked in early kinetic studies. Results from this thesis work, along with a collaboration stemming from it, have highlighted a significant pathway in the colon contributing to overall calcium homeostasis.[86]

5.2.1. Regulation of calcium homeostasis

One finding of particular interest is the inability of the *Cldn2/12* DKO mice to adequately upregulate serum calcitriol in response to low serum calcium. The DKO mice appear to respond appropriately to exogenously delivered calcitriol and increase serum calcitriol in response to a low calcium diet. Indeed, the response of the DKO mice was similar to previous reports of wildtype mice on a 0.125% versus 1% calcium diet increasing *Cyp27b1* expression three-fold and serum calcitriol 5-fold (40 – 200 pM).[299] Claudin-2 and -12 are both expressed in the proximal tubule where *Cyp27b1* is expressed. This gene encodes 1α-hydroxylase which activates vitamin D. A link between claudins and PTH or vitamin D signaling in the kidney has not been previously described. It may be that there is some type of serum calcium threshold for signaling that is altered in the DKO mice leaving them unable to appropriately respond to decreased serum

calcium on a standard chow diet while still responding moderately to a low calcium diet. Bolstering this hypothesis is that claudin-2 has been recognized as regulating permeability-independent processes including cell proliferation, cell migration.[141] Much of this work has been completed relatively recently and many questions remain.

5.3. Future Directions

Research provides answers but also generates more questions. The current thesis has established a model of normal physiology of intestinal calcium absorption during postnatal development. Future work can apply these results to study pathophysiology of intestinal diseases linked to poor calcium balance and bone mineralization. For example, SBS is a risk factor for osteoporosis/osteopenia.[23] In one study, almost 90% of adult subjects with SBS had osteoporosis or osteopenia.[300] Pediatric populations with SBS also have short stature and low bone mineral content.[24] Furthermore, epithelial barrier disruption or poor bone mineralization has been recognized in inflammatory bowel disease, celiac disease, irritable bowel syndrome, necrotizing enterocolitis, sepsis, and prematurity.

While much of the early work on the pathways of intestinal calcium absorption were performed on rodent duodenum, the evidence to date, including this thesis, questions the physiological significance of this short segment of the intestine. Certainly, the lower pH in this segment lends to a greater proportion of soluble calcium available for diffusion or enterocyte entry but the quick transit time calls into question the relevance.[40] Future work is required to understand transit time, pH and soluble calcium concentration in this segment in postnatal development. It may also be hypothesized that a mechanism of calcium sensing and feedback to

more distal segments exists to sample the calcium delivered from a meal and respond appropriately. Future work could consider this type of inter-segment regulation.

In the literature, there are conflicting reports regarding expression of *Trpv6* in the proximal jejunum of adult models.[39, 45] Whether the extent of expression can be upregulated as a protective adaptation to a low calcium is diet is not known. Given that global intakes of calcium are highly variable by country, it would be interesting to see if polymorphisms in the TRPV6 gene are associated with adaptations to high or low dietary calcium.[301] As an analogy, polymorphisms in genes related to choline metabolism may alter the requirements for this nutrient during pregnancy and lactation.[302] Still, a meta-analysis supports the use of a calcium and vitamin D supplement to decrease total fracture risk by 15% so that any adaptation may have a threshold of protection.[303]

Certainly, future work should investigate the protein mediating apical entry of calcium into ileal epithelial cells early in life. This work may include an extension of current studies by investigating upregulated genes in the ileum of *Trpv6/Cldn2* DKO mice at P14. For example, this could be completed by RNA sequencing with the hypothesis that the gene should be upregulated in the DKO pups. The nifedipine blocks the net absorption in this segment suggests a voltage-gated calcium channel. However, nifedipine is known to block other channels.[304]

The hypothesis of an evolutionary advantage to utilizing passive diffusion to absorb calcium early in life via claudin-2 could be further explored. For example, do *Cldn2* KO mice early in life have increased oxygen requirements? It might also be hypothesized that *CLDN2* polymorphisms could be associated with less resistance to high altitude or low oxygen environments in humans or other animals.

The current thesis has explored paracellular calcium permeability across the colon in an adult model. Previous work in the lab has explored regulation of the transcellular path at this age. However, the role of the colon in calcium balance during postnatal development has not been fully explored. Preliminary work on this subject has begun and is depicted in (Appendix A). The work to date suggests that the transcellular flux is not greater at a young age and may even be less than in the adult. However, further research is required to fully delineate this pathway. Of interest, excoriated epithelial cells in feces have previously been used to interrogate gene expression in colonocytes of infants.[305] This method can help the translation of basic rodent work to humans. It may also be that the microbiome of the colon contributes to the development of calcium absorption pathways or availability in the lumen.

How the loss of claudin-2 and claudin-12 renders the mouse unable to appropriately regulate serum calcium and vitamin D signaling remains to be fully investigated. It appears that there is altered signaling from PTH to transcription of *Cyp27b1* but this remains to be fully examined with *in vitro* models. This phenomenon appears to only occur in the DKO mice but not the single KO mice. This suggests that one claudin may compensate for the other. However, whether there are interactions with other claudins which mediate signaling is not known.

Recent work has begun to understand the mosaic of homomers and heteromers that claudins can form and alter permeability properties of the tight junction.[306] However, this work has been specific to the renal proximal tubule and thick ascending limb.[307] Similar investigations using co-immunoprecipitations or imaging techniques should also be performed in segments of the intestine and at different ages. Understanding how claudins interact in wild-type and KO mice and disease models will provide insight into normal development and pathophysiology. In addition, this type of work will provide insight into how loss of claudin-2 in the colon results in

net increased intestinal absorption while loss of both claudin-2 and claudin-12 in the colon results in net decreased intestinal absorption.

The focus of this thesis work has been on intestinal transport physiology. In a similar manner to the present studies, future work can investigate postnatal changes in renal physiology. This may have important implications for treating pediatric patients including those with renal disease, gastrointestinal disease, or cardiac disease. Furthermore, it has been recognized that many proteins identified as forming pathways of intestinal calcium absorption are also expressed in bone cells. One study investigated the role of TRPV6 in bone cells in vivo and in vitro and concluded that this protein is not necessary for normal bone mineralization.[54] Both claudin-2 and claudin-12 are expressed in osteoblasts.[271] However, the function of these proteins has yet to be delineated.[270] Certainly, their function with age also merits investigation.

Examination of the role of the food matrix in the intestinal lumen is also warranted. In particular, this will aid in translation of results from rodent models to clinical models. As a first step, mice could be fed diets made of food products instead of rodent chow. This would create a more realistic delivery of nutrients into the intestinal lumen of the animal.

Finally, infancy is an age where the greatest rate of bone deposition of mineral occurs. This offers an intriguing age to study the maximal uptake of calcium from the diet. However, children and adolescents continue to build bone. Understanding the physiology at these ages can have important benefits for long term public health guidance.

5.4. Limitations

Certainly, the largest limitation to the current work is the use of an animal model. This calls into question how translatable the results are to humans. Development of the small intestine occurs in three stages: 1) cell proliferation, 2) cell differentiation, and 3) functional maturation.[308] After birth, the intestine of both humans and rodents continues to mature and develop with regard to gene expression, protein localization, enzyme secretion and villi length leading to altered nutrient absorption.[309] At birth, the murine intestine is more immature than the human intestine, although the trends of development over time are remarkably similar.[308-310] For example, mice at birth have a relatively greater expression of claudin-1, occludin, and EGF receptor than human infants.[310] However, the relative number of Paneth, goblet, and enteroendocrine cells are not different between mice and human infants.[310] Overall, the patterns of development for and between each species vary with particular enzymes and genes examined. Future work can overcome these limitations by confirming gene expression patterns observed or functional alterations noted in mice in healthy tissue taken from biopsies or intraoperatively from human infants. Mice age at a faster rate than humans as well. This makes it difficult to translate the age of a mouse at weaning to that of a human. It is reasonable, however, to think of an infant at weaning from 6 months to 18 months of age.

The use of suckling mice in our studies limited some methodology. We did not have a metabolic cage apparatus that could accommodate a separated dam and pups during suckling. Therefore, we were unable to perform balance studies on young mice.

Another limitation of the current work is the use of global knockout models. Our proteins of interest are not only expressed in the intestine. This makes it difficult to directly assert observed results to being a consequence of altered intestinal transport. However, the use of *ex*

vivo tissue sections combined with expression studies for compensation as well as metabolic cage studies to look at fecal and urinary parameters provide us with confidence to assign our whole-body observations to changes observed in the intestines.

5.5. Conclusions

Overall, this thesis has highlighted novel pathways of intestinal calcium absorption during postnatal development when requirements for this mineral are greatest. Furthermore, we implicate EGF in breastmilk in the regulation of this absorption. Findings of this thesis work highlights the importance of considering age, and young age in particular, to understanding physiology and mechanisms of nutrient balance. Mechanisms understood in adult models cannot be extrapolated to infants and potentially not to children or adolescents either. Highlighting the significant contributions of our work to the field, an editorial written about our work on the transcellular pathway has suggested that our "results will no doubt spur further research into the absorption mechanisms of other essential trace elements, which are required for infant development".[311] The therapeutic implications of our work also has the potential to benefit care of infants and adults.

We have also implicated an important role of paracellular calcium absorption across the colon to net balance in an adult model. While historically considered insignificant to the regulation of many nutrients, recent results including those presented here are illustrating how underappreciated this organ has been. In addition, we have implicated a role for claudins-2 and -12 in the regulation of vitamin D metabolism. Certainly, further work in these areas is warranted. Results of this research will make significant contributions to the field and has the potential for broad health benefits.

Chapter 6

Works Cited

1. Hoenderop JGJ, Nilius B, Bindels RJM. Calcium absorption across epithelia. Physiological Reviews 2005;85:373-422.
2. Kopic S, Geibel JP. Gastric acid, calcium absorption, and their impact on bone health. Physiol Rev 2013;93:189-268.
3. Kovacs CS. Bone development in the fetus and neonate: role of the calciotropic hormones. Current osteoporosis reports 2011;9:274-283.
4. Bronner F, Pansu D. Nutritional aspects of calcium absorption. Journal of nutrition 1999;129:9-12.
5. Golden NH, Abrams SA. Optimizing Bone Health in Children and Adolescents. Pediatrics 2014;134:e1229-e1243.
6. Klibanski A, Adams-Campbell L, Bassford T, Blair SN, Boden SD, Dickersin K, Gifford DR, Glasse L, Goldring SR, Hruska K. Osteoporosis prevention, diagnosis, and therapy. Journal of the American Medical Association 2001;285:785-795.
7. Bachrach LK, Levine MA, Cowell CT, Shaw NJ. Clinical Indications for the Use of DXA in Pediatrics. In: Sawyer AJ, L.K. B, E.B. F, eds. Current Clinical Practice: Bone Densitometry in Growing Patients: Guidelines for Clinical Practice. Totowa, NJ: Humana Press, 2007:59-72.
8. Kent G, Price R, Gutteridge D, Allen J, Rosman K, Smith M, Bhagat C, Wilson S, Retallack R. Effect of pregnancy and lactation on maternal bone mass and calcium metabolism. Osteoporosis International 1993;3:44-47.
9. Møller U, Við Streym S, Mosekilde L, Rejnmark L. Changes in bone mineral density and body composition during pregnancy and postpartum. A controlled cohort study. Osteoporosis International 2012;23:1213-1223.
10. Grizzo FMF, Alarcão ACJ, Dell' Agnolo CM, Pedroso RB, Santos TS, Vissoci JRN, Pinheiro MM, Carvalho MDB, Pelloso SM. How does women's bone health recover after lactation? A systematic review and meta-analysis.
11. Cai G, Tian J, Winzenberg T, Wu F. Calcium supplementation for improving bone density in lactating women: a systematic review and meta-analysis of randomized controlled trials. Am J Clin Nutr 2020;112:48-56.
12. Institute of Medicine. Dietary reference intakes for calcium and vitamin D, 2011.
13. Brannon PM, Picciano MF. Vitamin D in Pregnancy and Lactation in Humans. Annual Review of Nutrition 2011;31:89-115.
14. Cullers A, King JC, Van Loan M, Gildengorin G, Fung EB. Effect of prenatal calcium supplementation on bone during pregnancy and 1 y postpartum. The American Journal of Clinical Nutrition 2019;109:197-206.
15. Kovacs CS. Maternal Mineral and Bone Metabolism During Pregnancy, Lactation, and Post-Weaning Recovery. Physiol Rev 2016;96:449-547.
16. Public Health Agency of Canada. Osteoporosis and Related Fractures in Canada Report from the Canadian Chronic Disease Surveillance System, 2020.
17. Cauley J, Wampler N, Barnhart J, Wu L, Allison M, Chen Z, Hendrix S, Robbins J, Jackson R. Incidence of fractures compared to cardiovascular disease and breast cancer: the Women's Health Initiative Observational Study. Osteoporosis international 2008;19:1717.

18. Rashki Kemmak A, Rezapour A, Jahangiri R, Nikjoo S, Farabi H, Soleimanpour S. Economic burden of osteoporosis in the world: A systematic review. Medical journal of the Islamic Republic of Iran 2020;34:154-154.

19. Goulding A, Jones Ie Fau - Taylor RW, Taylor Rw Fau - Manning PJ, Manning Pj Fau - Williams SM, Williams SM. More broken bones: a 4-year double cohort study of young girls with and without distal forearm fractures.

20. Clark EM, Tobias JH, Ness AR. Association between bone density and fractures in children: a systematic review and meta-analysis. Pediatrics 2006;117:e291-7.

21. Clark EM. The epidemiology of fractures in otherwise healthy children. Curr Osteoporos Rep 2014;12:272-8.

22. Escott BG, To T, Beaton DE, Howard AW. Risk of Recurrent Fracture: A Population-Based Study. Pediatrics 2019;144:e20172552.

23. Johnson E, Vu L, Matarese LE. Bacteria, Bones, and Stones: Managing Complications of Short Bowel Syndrome. Nutr Clin Pract 2018;33:454-466.

24. Olieman JF, Penning C, Spoel M, Ijsselstijn H, van den Hoonaard TL, Escher JC, Bax NM, Tibboel D. Long-term impact of infantile short bowel syndrome on nutritional status and growth. Br J Nutr 2012;107:1489-97.

25. Carroll WF, Fabres J, Nagy TR, Frazier M, Roane C, Pohlandt F, Carlo WA, Thome UH. Results of extremely low birth weight infants randomized to receive extra enteral calcium supply. Journal of pediatric gastroenterology and nutrition 2011;53:339.

26. Wesseling K, Bakkaloglu S, Salusky I. Chronic kidney disease mineral and bone disorder in children. Pediatric Nephrology 2008;23:195-207.

27. Birge SJ, Peck WA, Berman M, Whedon GD. Study of Calcium Absorption in Man: A Kinetic Analysis and Physiologic Model. J Clin Invest 1969;48:1705-13.

28. Norman DA, Fordtran JS, Brinkley LJ, Zerwekh JE, Nicar MJ, Strowig SM, Pak CYC. Jejunal and ileal adaptation to alterations in dietary calcium: changes in calcium and magnesium absorption and pathogenetic role of parathyroid hormone and 1,25-dihydroxyvitamin D. Journal of Clinical Investigation 1981;67:1599-1603.

29. Sandstrom B, Cederbiad A, Kivistoo B, Stenquist B, Andersson H. Retention of zinc and calcium from the human colon. American Journal of Clinical Nutrition 1986;44:501-504.

30. Grinstead WC, Pak CYC, Krejs GJ. Effect of 1,25-dihydroxyvitamin D3 on calcium absorption in the colon of healthy humans. American Journal of Physiology: Gastrointestinal and Liver Physiology 1984;247:G189-G192.

31. Abrams SA, Esteban NV, Vieira NE, Yergey AL. Calcium Absorption and Endogenous Fecal Excretion in Low Birth Weight Infants. Pediatric Research 1991;29:615-618.

32. Hillman LS, Johnson LS, Lee DZ, Vieira NE, Yergey AL. Measurement of true absorption, endogenous fecal excretion, urinary excretion, and retention of calcium in term infants by using a dual-tracer, stable-isotope method. Journal of Pediatrics 1993;123:444-56.

33. Richard A. Ehrenkranz BAA, Catherine M. Nelli, Morteza Janghorbani. Absorption of Calcium in Premature Infants as Measured With a Stable Isotope 46Ca Extrinsic Tag. Pediatric Research 1985;19:178-184.

34. Karbach U, Schmitt A, Saner FH. Different mechanism of magnesium and calcium transport across rat duodenum. Digestive diseases and sciences 1991;36:1611-1618.

35. Karbach U. Paracellular Calcium Transport Across the Small Intestine. Journal of nutrition 1992;122:672-677.

36. Favus MJ. Factors that influence absorption and secretion of calcium in the small intestine and colon. American journal of physiology 1985;248:G147-G157.

37. Nellans HN, Kimberg DV. Cellular and paracellular calcium transport in rat ileum: effects of dietary calcium. American Journal of Physiology-Endocrinology And Metabolism 1978;235:E726.

38. Karbach U, Feldmeier H. The cecum is the site with the highest calcium absorption in rat intestine. Digestive diseases and sciences 1993;38:1815-1824.

39. Rievaj J, Pan W, Cordat E, Alexander RT. The Na^+/H^+ exchanger isoform 3 is required for active paracellular and transcellular Ca^{2+} transport across murine cecum. American Journal of Physiology: Gastrointestinal and Liver Physiology 2013;305:G303-13.

40. Duflos C, Bellaton C, Pansu D, Bronner F. Calcium solubility, intestinal sojourn time and paracellular permeability codetermine passive calcium absorption in rats. Journal of nutrition 1995;125:2348-2355.

41. Alexander RT, Rievaj J, Dimke H. Paracellular calcium transport across renal and intestinal epithelia. Biochemistry and Cell Biology 2014;92:467-480.

42. Karbach U. Segmental heterogeneity of cellular and paracellular calcium transport across the rat duodenum and jejunum. Gastroenterology 1991;100:47-58.

43. Karbach U. Paracellular calcium transport across the small intestine. The Journal of nutrition 1992;122:672-677.

44. Hoenderop JGJ, Bindels RJM. Epithelial Ca2+ and Mg2+ channels in health and disease. Journal of the American Society of Nephrology 2005;16:15-26.

45. Peng J-B, Chen X-Z, Berger UV, Vassilev PM, Tsukaguchi H, Brown EM, Hediger MA. Molecular cloning and characterization of a channel-like transporter mediating intestinal calcium absorption. Journal of Biological Chemistry 1999;274:22739-22746.

46. Lameris AL, Nevalainen PI, Reijnen D, Simons E, Eygensteyn J, Monnens L, Bindels RJ, Hoenderop JG. Segmental transport of Ca^{2+} and Mg^{2+} along the gastrointestinal tract. Am J Physiol Gastrointest Liver Physiol 2015;308:G206-16.

47. Hoenderop JG, Hartog A, Stuiver M, Doucet A, Willems PH, Bindels RJ. Localization of the epithelial Ca^{2+} channel in rabbit kidney and intestine. Journal of the American Society of Nephrology 2000;11:1171-8.

48. Walters JR, Balesaria S, Chavele KM, Taylor V, Berry JL, Khair U, Barley NF, van Heel DA, Field J, Hayat JO, Bhattacharjee A, Jeffery R, Poulsom R. Calcium channel TRPV6 expression in human duodenum: different relationships to the vitamin D system and aging in men and women. J Bone Miner Res 2006;21:1770-7.

49. Zhuang L, Peng J-B, Tou L, Takanaga H, Adam RM, Hediger MA, Freeman MR. Calcium-Selective Ion Channel, CaT1, Is Apically Localized in Gastrointestinal Tract Epithelia and Is Aberrantly Expressed in Human Malignancies. Laboratory Investigation 2002;82:1755-1764.

50. Bianco SDC, Peng JB, Takanaga H, Suzuki Y, Crescenzi A, Kos CH, Zhuang L, Freeman MR, Gouveia CHA, Wu J. Marked disturbance of calcium homeostasis in mice with targeted disruption of the Trpv6 calcium channel gene. Journal of Bone and Mineral Research 2007;22:274-285.

51. Benn BS, Ajibade D, Porta A, Dhawan P, Hediger M, Peng J-B, Jiang Y, Oh GT, Jeung E-B, Lieben L. Active intestinal calcium transport in the absence of transient receptor potential vanilloid type 6 and calbindin-D9k. Endocrinology 2008;149:3196-3205.

52. Weissgerber P, Kriebs U, Tsvilovskyy V, Olausson J, Kretz O, Stoerger C, Vennekens R, Wissenbach U, Middendorff R, Flockerzi V. Male fertility depends on Ca^{2+} absorption by TRPV6 in epididymal epithelia. Science signaling 2011;4:ra27.

53. Woudenberg-Vrenken TE, Lameris AL, Weissgerber P, Olausson J, Flockerzi V, Bindels RJ, Freichel M, Hoenderop JG. Functional TRPV6 channels are crucial for transepithelial Ca^{2+} absorption. Am J Physiol Gastrointest Liver Physiol 2012;303:G879-85.

54. van der Eerden BC, Weissgerber P, Fratzl-Zelman N, Olausson J, Hoenderop JG, Schreuders-Koedam M, Eijken M, Roschger P, de Vries TJ, Chiba H, Klaushofer K, Flockerzi V, Bindels RJ, Freichel M, van Leeuwen JP. The transient receptor potential channel TRPV6 is dynamically expressed in bone cells but is not crucial for bone mineralization in mice. J Cell Physiol 2012;227:1951-1959.

55. Cui M, Li Q, Johnson R, Fleet JC. Villin promoter-mediated transgenic expression of transient receptor potential cation channel, subfamily V, member 6 (TRPV6) increases intestinal calcium absorption in wild-type and vitamin D receptor knockout mice. J Bone Miner Res 2012;27:2097-107.

56. Kellett GL. Alternative perspective on intestinal calcium absorption: proposed complementary actions of $Ca_v1.3$ and TRPV6. Nutrition Reviews 2011;69:347-370.

57. Morgan EL, Mace OJ, Helliwell PA, Affleck J, Kellett GL. A role for $Ca_v1.3$ in rat intestinal calcium absorption. Biochemical and Biophysical Research Communications 2003;312:487-493.

58. Thongon N, Nakkrasae L-i, Thongbunchoo J, Krishnamra N, Charoenphandhu. Enhancement of calcium transport in Caco-2 monolayer through PKCzeta-dependent Cav1.3-mediated transcellular and rectifying paracellular pathways by prolactin. American journal of physiology: Cell physiology 2009;296:C1373-82.

59. Reyes-Fernandez PC, Fleet JC. Luminal glucose does not enhance active intestinal calcium absorption in mice: evidence against a role for Ca(v)1.3 as a mediator of calcium uptake during absorption. Nutr Res 2015;35:1009-15.

60. Schachter D, Rosen SM. Active transport of Ca45 by the small intestine and its dependence on vitamin D. American Journal of Physiology-Legacy Content 1959;196:357-362.

61. Ernesto Carajoli. INTRACELLULAR CALCIUM HOMEOSTASIS. Annual review of biochemistry 1987:395-433.

62. Bronner F, Pansu D, Stein W. An analysis of intestinal calcium transport across the rat intestine. American Journal of Physiology-Gastrointestinal and Liver Physiology 1986;250:G561-G569.

63. Barley NF, Radhika Prathalingam S, Zhi P, Legon S, Howard A, Walters JRF. Factors involved in the duodenal expression of the human calbindin-D9k gene. Biochem. J 1999;341:491-500.

64. Balesaria S, Sangha S, Walters JRF. Human duodenum responses to vitamin D metabolites of TRPV6 and other genes involved in calcium absorption. American Journal of Physiology-Gastrointestinal and Liver Physiology 2009;297:G1193-G1197.

65. Akhter S, Kutuzova GD, Christakos S, Deluca HF. Calbindin D 9k is not required for 1,25-dihydroxyvitamin D3 -mediated Ca^{2+} absorption in small intestine. Archives of Biochemistry and Biophysics 2007;460:227-232.

66. Alexander RT, Beggs MR, Zamani R, Marcussen N, Frische S, Dimke H. Ultrastructural and immunohistochemical localization of plasma membrane Ca^{2+}-ATPase 4 in Ca^{2+}-

transporting epithelia. American Journal of Physiology: Renal Physiology 2015;309:F604-F616.

67.   Howard A, Legon S, Walters J. Human and rat intestinal plasma membrane calcium pump isoforms. American Journal of Physiology-Gastrointestinal and Liver Physiology 1993;265:G917-G925.

68.   Hildmann B, Schmidt A, Murer H. Ca++-transport across basal-lateral plasma membranes from rat small intestinal epithelial cells. The Journal of membrane biology 1982;65:55-62.

69.   Ryan ZC, Craig TA, Filoteo AG, Westendorf JJ, Cartwright EJ, Neyses L, Strehler EE, Kumar R. Deletion of the intestinal plasma membrane calcium pump, isoform 1, Atp2b1, in mice is associated with decreased bone mineral density and impaired responsiveness to 1, 25-dihydroxyvitamin D 3. Biochemical and Biophysical Research Communications 2015;467:152-156.

70.   Bronner F. Recent developments in intestinal calcium absorption. Nutrition reviews 2009;67:109-113.

71.   Pan W, Borovac J, Spicer Z, Hoenderop JG, Bindels RJ, Shull GE, Doschak MR, Cordat E, Alexander RT. The epithelial sodium/proton exchanger, NHE3, is necessary for renal and intestinal calcium (re) absorption. American Journal of Physiology: Renal Physiology 2012;302:F943-F956.

72.   Turner JR. Intestinal mucosal barrier function in health and disease. Nat Rev Immunol 2009;9:799-809.

73.   Kubota K, Furuse M, Sasaki H, Sonoda N, Fujita K, Nagafuchi A, Tsukita S. Ca(2+)-independent cell-adhesion activity of claudins, a family of integral membrane proteins localized at tight junctions. Curr Biol 1999;9:1035-8.

74.   Suzuki H, Nishizawa T, Tani K, Yamazaki Y, Tamura A, Ishitani R, Dohmae N, Tsukita S, Nureki O, Fujiyoshi Y. Crystal structure of a claudin provides insight into the architecture of tight junctions. Science 2014;344:304-7.

75.   Gunzel D, Yu AS. Claudins and the modulation of tight junction permeability. Physiol Rev 2013;93:525-69.

76.   Fuladi S, Jannat RW, Shen L, Weber CR, Khalili-Araghi F. Computational Modeling of Claudin Structure and Function. Int J Mol Sci 2020;21.

77.   Tamura A, Hayashi H, Imasato M, Yamazaki Y, Hagiwara A, Wada M, Noda T, Watanabe M, Suzuki Y, Tsukita S. Loss of claudin-15, but not claudin-2, causes Na+ deficiency and glucose malabsorption in mouse small intestine. Gastroenterology 2011;140:913-923.

78.   Fujita H, Sugimoto K, Inatomi S, Maeda T, Osanai M, Uchiyama Y, Yamamoto Y, Wada T, Kojima T, Yokozaki H. Tight junction proteins claudin-2 and-12 are critical for vitamin D-dependent Ca2+ absorption between enterocytes. Molecular biology of the cell 2008;19:1912-1921.

79.   Lei Z, Maeda T, Tamura A, Nakamura T, Yamazaki Y, Shiratori H, Yashiro K, Tsukita S, Hamada H. EpCAM contributes to formation of functional tight junction in the intestinal epithelium by recruiting claudin proteins. Developmental Biology 2012;371:136-145.

80.   Holmes JL, Van Itallie CM, Rasmussen JE, Anderson JM. Claudin profiling in the mouse during postnatal intestinal development and along the gastrointestinal tract reveals complex expression patterns. Gene Expression Patterns 2006;6:581-588.

81. Fujita H, Chiba H, Yokozaki H, Sakai N, Sugimoto K, Wada T, Kojima T, Yamashita T, Sawada N. Differential expression and subcellular localization of claudin-7,− 8,− 12,− 13, and− 15 along the mouse intestine. Journal of Histochemistry & Cytochemistry 2006;54:933-944.

82. Lameris AL, Huybers S, Kaukinen K, Mäkelä TH, Bindels RJ, Hoenderop JG, Nevalainen PI. Expression profiling of claudins in the human gastrointestinal tract in health and during inflammatory bowel disease. Scandinavian Journal of Gastroenterology 2013;48:58-69.

83. Amasheh S, Meiri N, Gitter AH, Schöneberg T, Mankertz J, Schulzke JD, Fromm M. Claudin-2 expression induces cation-selective channels in tight junctions of epithelial cells. Journal of cell science 2002;115:4969-76.

84. Yu AS, Cheng MH, Angelow S, Gunzel D, Kanzawa SA, Schneeberger EE, Fromm M, Coalson RD. Molecular basis for cation selectivity in claudin-2-based paracellular pores: identification of an electrostatic interaction site. J Gen Physiol 2009;133:111-27.

85. Pei L, Solis G, Nguyen MTX, Kamat N, Magenheimer L, Zhuo M, Li J, Curry J, McDonough AA, Fields TA, Welch WJ, Yu ASL. Paracellular epithelial sodium transport maximizes energy efficiency in the kidney. The Journal of Clinical Investigation 2016;126:2509-2518.

86. Curry JN, Saurette M, Askari M, Pei L, Filla MB, Beggs MR, Rowe PS, Fields T, Sommer AJ, Tanikawa C, Kamatani Y, Evan AP, Totonchi M, Alexander RT, Matsuda K, Yu AS. Claudin-2 deficiency associates with hypercalciuria in mice and human kidney stone disease. J Clin Invest 2020;130:1948-1960.

87. Plain A, Pan W, O'Neill D, Ure M, Beggs MR, Farhan M, Dimke H, Cordat E, Alexander RT. Claudin-12 Knockout Mice Demonstrate Reduced Proximal Tubule Calcium Permeability. Int J Mol Sci 2020;21.

88. Hwang I, Yang H, Kang HS, Ahn C, Hong EJ, An BS, Jeung EB. Alteration of tight junction gene expression by calcium- and vitamin D-deficient diet in the duodenum of calbindin-null mice. Int J Mol Sci 2013;14:22997-23010.

89. Chin AM, Hill DR, Aurora M, Spence JR. Morphogenesis and maturation of the embryonic and postnatal intestine. Semin Cell Dev Biol 2017;66:81-93.

90. Cummins A, Thompson F. Effect of breast milk and weaning on epithelial growth of the small intestine in humans. Gut 2002;51:748-754.

91. Aust G, Kerner C, Gonsior S, Sittig D, Schneider H, Buske P, Scholz M, Dietrich N, Oldenburg S, Karpus ON, Galle J, Amasheh S, Hamann J. Mice overexpressing CD97 in intestinal epithelial cells provide a unique model for mammalian postnatal intestinal cylindrical growth. Molecular Biology of the Cell 2013;24:2256-2268.

92. Walthall K, Cappon GD, Hurtt ME, Zoetis T. Postnatal development of the gastrointestinal system: a species comparison. Birth Defects Res B Dev Reprod Toxicol 2005;74:132-56.

93. Wołczuk K, Wilczyńska B, Jaroszewska M, Kobak J. Morphometric characteristics of the small and large intestines of Mus musculus during postnatal development. Folia Morphol (Warsz) 2011;70:252-9.

94. Sumigray KD, Terwilliger M, Lechler T. Morphogenesis and Compartmentalization of the Intestinal Crypt. Developmental cell 2018;45:183-197.e5.

95. Commare CE, Tappenden KA. Development of the infant intestine: implications for nutrition support. Nutrition in Clinical Practice 2007;22:159-173.

96. Xu RJ, Mellor DJ, Tungthanathanich P, Birtles MJ, Reynolds GW, Simpson HV. Growth and morphological changes in the small and the large intestine in piglets during the first three days after birth. J Dev Physiol 1992;18:161-72.

97. Buddington RK, Malo C, Sangild PT, Elnif J. Intestinal transport of monosaccharides and amino acids during postnatal development of mink. American Journal of Physiology-Regulatory, Integrative and Comparative Physiology 2000;279:R2287-R2296.

98. Leitch GJ. Regional variations in the composition of purified brush borders isolated from infant and adult rabbit small intestine. Archives internationales de physiologie et de biochimie 1971;79:279-286.

99. Bronner F, Salle BL, Putet G, Rigo J, Senterre J. Net calcium absorption in premature infants: results of 103 metabolic balance studies. The American journal of clinical nutrition 1992;56:1037-1044.

100. Pansu D, Bellaton C, Bronner F. Effect of Ca intake on saturable and nonsaturable components of duodenal Ca transport. American Journal of Physiology-Gastrointestinal and Liver Physiology 1981;240:G32-G37.

101. Alevizaki CC, Ikkos DG, Singhelakis P. Progressive decrease of true intestinal calcium absorption with age in normal man. Journal of nuclear medicine 1973;14:760-2.

102. Piyabhan P, Krishnamra N, Limlomwongse L. Changes in the regulation of calcium metabolism and bone calcium content during growth in the absence of endogenous prolactin and during hyperprolactinemia: a longitudinal study in male and female Wistar rats. Canadian journal of physiology and pharmacology 2000;78:757-765.

103. Pugsley LI, Collip JB. The effect of parathyroid hormone upon the serum calcium and calcium excretion of normal and adrenalectomized rats. Biochem J 1936;30:1274-9.

104. Amnattanakul S, Charoenphandhu N, Limlomwongse L, Krishnamra N. Endogenous prolactin modulated the calcium absorption in the jejunum of suckling rats. Canadian journal of physiology and pharmacology 2005;83:595-604.

105. Dorkkam N, Wongdee K, Suntornsaratoon P, Krishnamra N, Charoenphandhu N. Prolactin stimulates the L-type calcium channel-mediated transepithelial calcium transport in the duodenum of male rats. Biochem Biophys Res Commun 2013;430:711-716.

106. Krishnamra N, Lotinun S, Limlomwongse L. Acute effect and mechanism of action of prolactin on the in situ passive calcium absorption in rat. Bone and mineral 1993;23:253-266.

107. Pansu D, Bellaton C, Bronner F. Developmental changes in the mechanisms of duodenal calcium transport in the rat. Am. J. Physiol 1983;244:G20-G26.

108. Toverud SU, Dostal LA. Calcium absorption during development: experimental studies of the rat small intestine. Journal of pediatric gastroenterology and nutrition 1986;5:688-695.

109. Armbrecht HJ, Zenser TV, Bruns ME, Davis BB. Effect of age on intestinal calcium absorption and adaptation to dietary calcium. American Journal of Physiology: Endocrinology and Metabolism 1979;236:E769-E774.

110. Horst RL, Deluca HF, Jorgensen NA. The effect of age on calcium absorption and accumulation of 1,25-hydroxyvitamin D3 in intestinal mucosa of rats. Metabolic Bone Disease and Related Research 1978;1:29-33.

111. Ghishan FK, Parker P, Nichols S, Hoyumpa A. Kinetics of intestinal calcium transport during maturation in rats. Pediatric research 1984;18:235-239.

112. Batt E, Schachter D. Developmental pattern of some intestinal transport mechanisms in newborns rats and mice. American Journal of Physiology-Legacy Content 1969;216:1064-1068.

113. Song Y, Peng X, Porta A, Takanaga H, Peng J-B, Hediger MA, Fleet JC, Christakos S. Calcium transporter 1 and epithelial calcium channel messenger ribonucleic acid are differentially regulated by 1, 25 dihydroxyvitamin D3 in the intestine and kidney of mice. Endocrinology 2003;144:3885-3894.

114. Lee G-S, Lee K-Y, Choi K-C, Ryu Y-H, Paik SG, Oh GT, Jeung E-B. Phenotype of a Calbindin-D9k Gene Knockout Is Compensated for by the Induction of Other Calcium Transporter Genes in a Mouse Model. Journal of Bone and Mineral Research 2007;22:1968-1978.

115. Christakos S, Dhawan P, Porta A, Mady LJ, Seth T. Vitamin D and intestinal calcium absorption. Molecular and cellular endocrinology 2011;347:25-29.

116. Yoshizawa T, Handa Y, Uematsu Y, Takeda S, Sekine K, Yoshihara Y, Kawakami T, Arioka K, Sato H, Uchiyama Y, Masushige S, Fukamizu A, Matsumoto T, Kato S. Mice lacking the vitamin D receptor exhibit impaired bone formation, uterine hypoplasia and growth retardation after weaning. Nature genetics 1997;16:391-6.

117. Van Cromphaut SJ, Dewerchin M, Hoenderop JG, Stockmans I, Van Herck E, Kato S, Bindels RJ, Collen D, Carmeliet P, Bouillon R. Duodenal calcium absorption in vitamin D receptor–knockout mice: functional and molecular aspects. Proceedings of the National Academy of Sciences 2001;98:13324-13329.

118. Kovacs CS. Bone Development and Mineral Homeostasis in the Fetus and Neonate: Roles of the Calciotropic and Phosphotropic Hormones. Physiological Reviews 2014;94:1143-1218.

119. Dostal LA, Toverud SU. Effect of vitamin D3 on duodenal calcium absorption in vivo during early development. American Journal of Physiology: Gastrointestinal and Liver Physiology 1984;246:G528-G534.

120. Halloran BP, DeLuca HF. Calcium transport in small intestine during pregnancy and lactation. American Journal of Physiology: Endocrinology and Metabolism 1980;239:E64-E68.

121. Zhang Y-g, Wu S, Lu R, Zhou D, Zhou J, Carmeliet G, Petrof E, Claud EC, Sun J. Tight junction CLDN2 gene is a direct target of the vitamin D receptor. Scientific reports 2015;5:10642.

122. Aydemir Y, Erdogan B, Türkeli A. Vitamin D deficiency negatively affects both the intestinal epithelial integrity and bone metabolism in children with Celiac disease. Clin Res Hepatol Gastroenterol 2020:101523.

123. Kutuzova GD, DeLuca HF. Gene expression profiles in rat intestine identify pathways for 1,25-dihydroxyvitamin D3 stimulated calcium absorption and clarify its immunomodulatory properties. Archives of Biochemistry and Biophysics 2004;432:152-166.

124. Allen LH. Calcium bioavailability and absorption: a review. The American journal of clinical nutrition 1982;35:783-808.

125. Sato R, Noguchi T, Naito H. Effect of lactose on calcium absorption from the rat small intestine with a non-flushed ligated loop. Journal of nutritional science and vitaminology 1983;29:365-373.

126. Song Y, Kato S, Fleet JC. Vitamin D receptor (VDR) knockout mice reveal VDR-independent regulation of intestinal calcium absorption and ECaC2 and calbindin D9k mRNA. The Journal of nutrition 2003;133:374-380.

127. Cox DB, Owens RA, Hartmann PE. Blood and milk prolactin and the rate of milk synthesis in women. Experimental Physiology 1996;81:1007-1020.

128. Ellis LA, Mastro AM, Picciano MF. Milk-borne prolactin and neonatal development. J Mammary Gland Biol Neoplasia 1996;1:259-269.

129. Freeman ME, Kanyicska B, Lerant A, Nagy G. Prolactin: structure, function, and regulation of secretion. Physiol Rev 2000;80:1523-1631.

130. Nagano M, Chastre E, Choquet A, Bara J, Gespach C, Kelly PA. Expression of prolactin and growth hormone receptor genes and their isoforms in the gastrointestinal tract. Am J Physiol 1995;268:G431-42.

131. Wongdee K, Teerapornpuntakit J, Sripong C, Longkunan A, Chankamngoen W, Keadsai C, Kraidith K, Krishnamra N, Charoenphandhu N. Intestinal mucosal changes and upregulated calcium transporter and FGF-23 expression during lactation: Contribution of lactogenic hormone prolactin. Arch Biochem Biophys 2016;590:109-117.

132. Carpenter G. Epidermal growth factor is a major growth-promoting agent in human milk. Science 1980;210:198-199.

133. Gómez-Rial J, Curras-Tuala MJ, Talavero-González C, Rodríguez-Tenreiro C, Vilanova-Trillo L, Gómez-Carballa A, Rivero-Calle I, Justicia-Grande A, Pardo-Seco J, Redondo-Collazo L, Salas A, Martinón-Torres F. Salivary epidermal growth factor correlates with hospitalization length in rotavirus infection. BMC Infectious Diseases 2017;17:370.

134. Dagogo-Jack S. Epidermal growth factor EGF in human saliva: effect of age, sex, race, pregnancy and sialogogue. Scand J Gastroenterol Suppl 1986;124:47-54.

135. Dvorak B. Milk Epidermal Growth Factor and Gut Protection. The Journal of Pediatrics 2010;156:S31-S35.

136. Puccio F, Lehy T. Oral administration of epidermal growth factor in suckling rats stimulates cell DNA synthesis in fundic and antral gastric mucosae as well as in intestinal mucosa and pancreas. Regul Pept 1988;20:53-64.

137. Shen WH, Xu RJ. Stability and distribution of orally administered epidermal growth factor in neonatal pigs. Life Sci 1998;63:809-20.

138. Goelz R, Hihn E, Hamprecht K, Dietz K, Jahn G, Poets C, Elmlinger M. Effects of Different CMV-Heat-Inactivation-Methods on Growth Factors in Human Breast Milk. Pediatric Research 2009;65:458-461.

139. Kim TI, Poulin EJ, Blask E, Bukhalid R, Whitehead RH, Franklin JL, Coffey RJ. Myofibroblast keratinocyte growth factor reduces tight junctional integrity and increases claudin-2 levels in polarized Caco-2 cells. Growth factors (Chur, Switzerland) 2012;30:320-332.

140. Ikari A, Sato T, Watanabe R, Yamazaki Y, Sugatani J. Increase in claudin-2 expression by an EGFR/MEK/ERK/c-Fos pathway in lung adenocarcinoma A549 cells. Biochim Biophys Acta 2012;1823:1110-8.

141. Venugopal S, Anwer S, Szászi K. Claudin-2: roles beyond permeability functions. International journal of molecular sciences 2019;20:5655.

142. Bardanzellu F, Peroni DG, Fanos V. Human Breast Milk: Bioactive Components, from Stem Cells to Health Outcomes. Curr Nutr Rep 2020;9:1-13.

143. Lonnerdal B. Bioactive proteins in breast milk. J Paediatr Child Health 2013;49 Suppl 1:1-7.
144. Dimke H, Hoenderop JGJ, Bindels RJM. Molecular basis of epithelial Ca^{2+} and Mg^{2+} transport: insights from the TRP channel family. Journal of physiology 2011;589:1535-1542.
145. Dimke H, Hoenderop JG, Bindels RJ. Hereditary tubular transport disorders: implications for renal handling of Ca^{2+} and Mg^{2+}. Clin Sci (Lond) 2010;118:1-18.
146. Muto S, Hata M, Taniguchi J, Tsuruoka S, Moriwaki K, Saitou M, Furuse K, Sasaki H, Fujimura A, Imai M, Kusano E, Tsukita S, Furuse M. Claudin-2 - deficient mice are defective in the leaky and cation-selective paracellular permeability properties of renal proximal tubules. Proceedings of the National Academy of Sciences of the United States of America 2010;107:8011-8016.
147. Schnermann J, Huang Y, Mizel D. Fluid reabsorption in proximal convoluted tubules of mice with gene deletions of claudin-2 and/or aquaporin1. American journal of physiology: Renal physiology 2013;305:F1352-64.
148. Hou J, Renigunta A, Gomes AS, Hou M, Paul DL, Waldegger S, Goodenough DA. Claudin-16 and claudin-19 interaction is required for their assembly into tight junctions and for renal reabsorption of magnesium. Proc Natl Acad Sci U S A 2009;106:15350-15355.
149. Claverie-Martín F, García-Nieto V, Loris C, Ariceta G, Nadal I, Espinosa L, Fernández-Maseda Á, Antón-Gamero M, Avila Á, Madrid Á, González-Acosta H, Córdoba-Lanus E, Santos F, Gil-Calvo M, Espino M, García-Martinez E, Sanchez A, Muley R. Claudin-19 Mutations and Clinical Phenotype in Spanish Patients with Familial Hypomagnesemia with Hypercalciuria and Nephrocalcinosis. PLOS ONE 2013;8:e53151.
150. Dimke H, Desai P, Borovac J, Lau A, Pan W, Alexander RT. Activation of the Ca^{2+}-sensing receptor increases renal claudin-14 expression and urinary Ca^{2+} excretion. American Journal of Physiology: Renal Physiology 2013;304:F761-F769.
151. Gong Y, Renigunta V, Himmerkus N, Zhang J, Renigunta A, Bleich M, Hou J. Claudin-14 regulates renal Ca^{++} transport in response to CaSR signalling via a novel microRNA pathway. The EMBO Journal 2012;31:1999-2012.
152. Plain A, Wulfmeyer VC, Milatz S, Klietz A, Hou J, Bleich M, Himmerkus N. Corticomedullary difference in the effects of dietary Ca^{2+} on tight junction properties in thick ascending limbs of Henle's loop. Pflügers Archiv 2016;468:293-303.
153. Gong Y, Himmerkus N, Plain A, Bleich M, Hou J. Epigenetic regulation of microRNAs controlling CLDN14 expression as a mechanism for renal calcium handling. J Am Soc Nephrol 2015;26:663-76.
154. Mayr B, Schnabel D, Dorr HG, Schofl C. Gain and loss of function mutations of the calcium-sensing receptor and associated proteins: current treatment concepts. Eur J Endocrinol 2016;174:R189-208.
155. Pollak MR, Brown EM, Chou Y-HW, Hebert SC, Marx SJ, Stelnmann B, Levi T, Seidman CE, Seidman JG. Mutations in the human Ca2+-sensing receptor gene cause familial hypocalciuric hypercalcemia and neonatal severe hyperparathyroidism. Cell 1993;75:1297-1303.
156. Hoenderop JG, Müller D, Van Der Kemp AW, Hartog A, Suzuki M, Ishibashi K, Imai M, Sweep F, Willems PH, Van Os CH, Bindels RJ. Calcitriol controls the epithelial calcium channel in kidney. Journal of the American Society of Nephrology 2001;12:1342-9.

157. Lambers TT, Mahieu F, Oancea E, Hoofd L, de Lange F, Mensenkamp AR, Voets T, Nilius B, Clapham DE, Hoenderop JG, Bindels RJ. Calbindin-D28K dynamically controls TRPV5-mediated Ca^{2+} transport. EMBO Journal 2006;25:2978-2988.

158. Hoenderop JG, van Leeuwen JP, van der Eerden BC, Kersten FF, van der Kemp AW, Mérillat AM, Waarsing JH, Rossier BC, Vallon V, Hummler E, Bindels RJ. Renal Ca2+ wasting, hyperabsorption, and reduced bone thickness in mice lacking TRPV5. J Clin Invest 2003;112:1906-14.

159. Gkika D, Hsu Y-J, Van Der Kemp AW, Christakos S, Bindels RJ, Hoenderop JG. Critical Role of the Epithelial Ca^{2+} Channel TRPV5 in Active Ca^{2+} Reabsorption as Revealed by TRPV5/Calbindin-D 28K Knockout Mice. J Am Soc Nephrol 2006;17:3020-3027.

160. Airaksinen MS, Eilers J, Garaschuk O, Thoenen H, Konnerth A, Meyer M. Ataxia and altered dendritic calcium signaling in mice carrying a targeted null mutation of the calbindin D28k gene. Proceedings of the National Academy of Sciences 1997;94:1488-1493.

161. Zheng W, Xie Y, Li G, Kong J, Feng JQ, Li YC. Critical Role of Calbindin-D28k in Calcium Homeostasis Revealed by Mice Lacking Both Vitamin D Receptor and Calbindin-D28k. Journal of Biological Chemistry 2004;279:52406-52413.

162. van Loon EPM, Little R, Prehar S, Bindels RJM, Cartwright EJ, Hoenderop JGJ. Calcium Extrusion Pump PMCA4: A New Player in Renal Calcium Handling? PLOS ONE 2016;11.

163. Koushik SV, Wang J, Rogers R, Moskophidis D, Lambert NA, Creazzo TL, Conway SJ. Targeted inactivation of the sodium-calcium exchanger (Ncx1) results in the lack of a heartbeat and abnormal myofibrillar organization. FASEB journal 2001;15:1209-11.

164. Bindels RJ, Ramakers PL, Dempster JA, Hartog A, van Os CH. Role of Na^+/Ca^{2+} exchange in transcellular Ca^{2+} transport across primary cultures of rabbit kidney collecting system. Pflugers Archiv 1992;420:566-72.

165. Jacinto JS, Modanlou HD, Crade M, Strauss AA, Bosu SK. Renal Calcification Incidence in Very Low Birth Weight Infants. PEDIATRICS;81:31-35.

166. Matos V, van Melle G, Boulat O, Markert M, Bachmann C, Guignard J-P. Urinary phosphate/creatinine, calcium/creatinine, and magnesium/creatinine ratios in a healthy pediatric population. Journal of Pediatrics 1997;131:252-257.

167. Esbjorner E, Jones I. Urinary calcium excretion in Swedish children. Acta Paediatrica 1995;84:156-159.

168. Abuazza G, Becker A, Williams SS, Chakravarty S, Truong H-T, Lin F, Baum M. Claudins 6, 9, and 13 are developmentally expressed renal tight junction proteins. American journal of physiology: Renal physiology 2006;291:F1132-41.

169. van Abel M, Huybers S, Hoenderop JGJ, van der Kemp AWCM, van Leeuwen JPTM, Bindels RJM. Age-dependent alterations in Ca^{2+} homeostasis: role of TRPV5 and TRPV6. American Journal of Physiology: Renal Physiology 2006;291:F1177-F1183.

170. Cheng Z, Liang N, Chen T-H, Li A, Santa Maria C, You M, Ho H, Song F, Bikle D, Tu C, Shoback D, Chang W. Sex and age modify biochemical and skeletal manifestations of chronic hyperparathyroidism by altering target organ responses to Ca^{2+} and parathyroid hormone in mice. Journal of Bone and Mineral Research 2013;28:1087-1100.

171. Sas D, Hu M, Moe OW, Baum M. Effect of claudins 6 and 9 on paracellular permeability in MDCK II cells. American journal of physiology: Regulatory, integrative and comparative physiology 2008;295:R1713-9.

172. Patterson SW. A Contribution to the Study of Calcium Metabolism. Biochem J 1908;3:39-54.

173. Collip JB. THE EXTRACTION OF A PARATHYROID HORMONE WHICH WILL PREVENT OR CONTROL PARATHYROID TETANY AND WHICH REGULATES THE LEVEL OF BLOOD CALCIUM. Journal of Biological Chemistry 1925;63:395-438.

174. Copp DH, Cheney B. Calcitonin-a hormone from the parathyroid which lowers the calcium-level of the blood. Nature 1962;193:381-2.

175. Juhlin C, Holmdahl R, Johansson H, Rastad J, Akerström G, Klareskog L. Monoclonal antibodies with exclusive reactivity against parathyroid cells and tubule cells of the kidney. Proc Natl Acad Sci U S A 1987;84:2990-4.

176. Akerström G, Rastad J, Ljunghall S, Ridefelt P, Juhlin C, Gylfe E. Cellular physiology and pathophysiology of the parathyroid glands. World J Surg 1991;15:672-80.

177. Brown EM, Gamba G, Riccardi D, Lombardi M, Butters R, Kifor O, Sun A, Hediger MA, Lytton J, Hebert SC. Cloning and characterization of an extracellular Ca(2+)-sensing receptor from bovine parathyroid. Nature 1993;366:575-80.

178. Hannan FM, Babinsky VN, Thakker RV. Disorders of the calcium-sensing receptor and partner proteins: insights into the molecular basis of calcium homeostasis. J Mol Endocrinol 2016;57:R127-42.

179. Juppner H, Abou-Samra A-B, Freeman M, Kong XF, Schipani E, Richards J, Kolakowski LF, Hock J, Potts JT, Kronenberg HM. A G protein-linked receptor for parathyroid hormone and parathyroid hormone-related peptide. Science 1991;254:1024-1026.

180. Sutkeviciute I, Clark LJ, White AD, Gardella TJ, Vilardaga J-P. PTH/PTHrP Receptor Signaling, Allostery, and Structures. Trends in endocrinology and metabolism: TEM 2019;30:860-874.

181. Silva BC, Bilezikian JP. Parathyroid hormone: anabolic and catabolic actions on the skeleton. Current opinion in pharmacology 2015;22:41-50.

182. Raisz LG. Stimulation of bone resorption by parathyroid hormone in tissue culture. Nature 1963;197:1015-6.

183. Garabedian M, Holick M, DeLuca H, Boyle I. Control of 25-hydroxycholecalciferol metabolism by parathyroid glands. Proceedings of the National Academy of Sciences 1972;69:1673-1676.

184. Fraser D, Kodicek E. Unique biosynthesis by kidney of a biologically active vitamin D metabolite. Nature 1970;228:764-766.

185. Kremer R, Goltzman D. PARATHYROID HORMONE STIMULATES MAMMALIAN RENAL 25-HYDROXYVITAMIN D3-1α-HYDROXYLASE IN VITRO. Endocrinology 1982;110:294-296.

186. Meyer MB, Benkusky NA, Kaufmann M, Lee SM, Onal M, Jones G, Pike JW. A kidney-specific genetic control module in mice governs endocrine regulation of the cytochrome P450 gene Cyp27b1 essential for vitamin D3 activation. Journal of Biological Chemistry 2017;292:17541-17558.

187. Christakos S, Dhawan P, Verstuyf A, Verlinden L, Carmeliet G. Vitamin D: Metabolism, Molecular Mechanism of Action, and Pleiotropic Effects. Physiological Reviews 2015;96:365-408.

188. Veldurthy V, Wei R, Oz L, Dhawan P, Jeon YH, Christakos S. Vitamin D, calcium homeostasis and aging. Bone research 2016;4:16041.

189. Peacock M. Calcium metabolism in health and disease. Clinical journal of the American Society of Nephrology 2010;5:S23-30.
190. Matkovic V. Calcium metabolism and calcium requirements during skeletal modeling and consolidation of bone mass. The American journal of clinical nutrition 1991;54:245S-260S.
191. Tarride JE, Guo N, Hopkins R, Leslie WD, Morin S, Adachi JD, Papaioannou A, Bessette L, Brown JP, Goeree R. The burden of illness of osteoporosis in Canadian men. Journal of Bone and Mineral Research 2012;27:1830-1838.
192. Li J, Zhao L, Ferries IK, Jiang L, Desta MZ, Yu X, Yang Z, Duncan RL, Turner CH. Skeletal phenotype of mice with a null mutation in Cav 1.3 L-type calcium channel. J Musculoskelet Neuronal Interact 2010;10:180-7.
193. Platzer J, Engel J, Schrott-Fischer A, Stephan K, Bova S, Chen H, Zheng H, Striessnig J. Congenital deafness and sinoatrial node dysfunction in mice lacking class D L-type Ca^{2+} channels. Cell 2000;102:89-97.
194. Beggs MR, Alexander RT. Intestinal absorption and renal reabsorption of calcium throughout postnatal development. Experimental Biology and Medicine 2017;242:840-849.
195. Weissgerber P, Kriebs U, Tsvilovskyy V, Olausson J, Kretz O, Stoerger C, Mannebach S, Wissenbach U, Vennekens R, Middendorff R, Flockerzi V, Freichel M. Excision of Trpv6 gene leads to severe defects in epididymal Ca2+ absorption and male fertility much like single D541A pore mutation. The Journal of biological chemistry 2012;287:17930-41.
196. Beggs MR, Appel I, Svenningsen P, Skjødt K, Alexander RT, Dimke H. Expression of transcellular and paracellular calcium and magnesium transport proteins in renal and intestinal epithelia during lactation. American Journal of Physiology: Renal Physiology 2017;313:F629-F640.
197. Bouxsein ML, Boyd SK, Christiansen BA, Guldberg RE, Jepsen KJ, Muller R. Guidelines for assessment of bone microstructure in rodents using micro-computed tomography. J Bone Miner Res 2010;25:1468-86.
198. Kawamoto T, Shimizu M. A method for preparing 2- to 50-micron-thick fresh-frozen sections of large samples and undecalcified hard tissues. Histochem Cell Biol 2000;113:331-9.
199. Dempster DW, Compston JE, Drezner MK, Glorieux FH, Kanis JA, Malluche H, Meunier PJ, Ott SM, Recker RR, Parfitt AM. Standardized nomenclature, symbols, and units for bone histomorphometry: a 2012 update of the report of the ASBMR Histomorphometry Nomenclature Committee. J Bone Miner Res 2013;28:2-17.
200. Grubb BR. Bioelectric measurement of CFTR function in mice. Methods Mol Med 2002;70:525-35.
201. Clarke LL. A guide to Ussing chamber studies of mouse intestine. American Journal of Physiology: Gastrointestinal and Liver Physiology 2009;296:G1151-G1166.
202. Charoenphandhu N, Tudpor K, Pulsook N, Krishnamra N. Chronic metabolic acidosis stimulated transcellular and solvent drag-induced calcium transport in the duodenum of female rats. American journal of physiology: Gastrointestinal and liver physiology 2006.
203. Mukoh S, Kawasaki K, Yonemura D, Tanabe J. Hyperosmolarity-induced hyperpolarization of the membrane potential of the retinal pigment epithelium. Documenta ophthalmologica 1985;60:369-374.

204. Hoenderop JGJ, Vennekens R, Müller D, Prenen J, Droogmans G, Bindels RJM, Nilius B. Function and expression of the epithelial Ca2+ channel family: comparison of mammalian ECaC1 and 2. The Journal of physiology 2001;537:747-761.

205. Scharinger A, Eckrich S, Vandael DH, Schönig K, Koschak A, Hecker D, Kaur G, Lee A, Sah A, Bartsch D. Cell-type-specific tuning of Cav1. 3 Ca2+-channels by a C-terminal automodulatory domain. Frontiers in cellular neuroscience 2015;9:309.

206. Xu W, Lipscombe D. Neuronal CaV1. 3α1 L-type channels activate at relatively hyperpolarized membrane potentials and are incompletely inhibited by dihydropyridines. Journal of Neuroscience 2001;21:5944-5951.

207. Heaney RP, Abrams S, Dawson-Hughes B, Looker A, Marcus R, Matkovic V, Weaver C. Peak bone mass. Osteoporos Int 2000;11:985-1009.

208. Lee G-S, Jung E-M, Choi K-C, Oh GT, Jeung E-B. Compensatory induction of the TRPV6 channel in a calbindin-D9k knockout mouse: Its regulation by 1,25-hydroxyvitamin D. Journal of Cellular Biochemistry 2009;108:1175-1183.

209. Morgan EL, Mace OJ, Affleck J, Kellett GL. Apical GLUT2 and Cav1.3: regulation of rat intestinal glucose and calcium absorption. The Journal of physiology 2007;580:593-604.

210. Wasserman RH. Vitamin D and the dual processes of intestinal calcium absorption. The Journal of nutrition 2004;134:3137-3139.

211. Duriez J, Flautre B, Blary M, Hardouin P. Effects of the calcium channel blocker nifedipine on epiphyseal growth plate and bone turnover: a study in rabbit. Calcified tissue international 1993;52:120-124.

212. Burren CP, Caswell R, Castle B, Welch CR, Hilliard TN, Smithson SF, Ellard S. TRPV6 compound heterozygous variants result in impaired placental calcium transport and severe undermineralization and dysplasia of the fetal skeleton. Am J Med Genet A 2018;176:1950-1955.

213. Suzuki Y, Chitayat D, Sawada H, Deardorff MA, McLaughlin HM, Begtrup A, Millar K, Harrington J, Chong K, Roifman M, Grand K, Tominaga M, Takada F, Shuster S, Obara M, Mutoh H, Kushima R, Nishimura G. TRPV6 Variants Interfere with Maternal-Fetal Calcium Transport through the Placenta and Cause Transient Neonatal Hyperparathyroidism. Am J Hum Genet 2018;102:1104-1114.

214. Suzuki Y, Kovacs CS, Takanaga H, Peng JB, Landowski CP, Hediger MA. Calcium channel TRPV6 is involved in murine maternal-fetal calcium transport. J Bone Miner Res 2008;23:1249-56.

215. Fecher-Trost C, Lux F, Busch KM, Raza A, Winter M, Hielscher F, Belkacemi T, van der Eerden B, Boehm U, Freichel M, Weissgerber P. Maternal Transient Receptor Potential Vanilloid 6 (Trpv6) Is Involved In Offspring Bone Development. J Bone Miner Res 2019:e3646.

216. Wang L, Zhu F, Yang H, Li J, Li Y, Ding X, Xiong X, Yin Y. Effects of dietary supplementation with epidermal growth factor on nutrient digestibility, intestinal development and expression of nutrient transporters in early-weaned piglets. Journal of animal physiology and animal nutrition 2019.

217. Ajibade DV, Dhawan P, Fechner AJ, Meyer MB, Pike JW, Christakos S. Evidence for a role of prolactin in calcium homeostasis: regulation of intestinal transient receptor potential vanilloid type 6, intestinal calcium absorption, and the 25-hydroxyvitamin D3 1α hydroxylase gene by prolactin. Endocrinology 2010;151:2974-2984.

218. Christakos S. Mechanism of action of 1, 25-dihydroxyvitamin D3 on intestinal calcium absorption. Reviews in Endocrine and Metabolic Disorders 2012;13:39-44.
219. Reginster J-Y, Burlet N. Osteoporosis: A still increasing prevalence. Bone 2006;38:4-9.
220. Clynes MA, Harvey NC, Curtis EM, Fuggle NR, Dennison EM, Cooper C. The epidemiology of osteoporosis. British medical bulletin 2020;133:105-117.
221. Lewiecki EM, Ortendahl JD, Vanderpuye-Orgle J, Grauer A, Arellano J, Lemay J, Harmon AL, Broder MS, Singer AJ. Healthcare Policy Changes in Osteoporosis Can Improve Outcomes and Reduce Costs in the United States. JBMR Plus 2019;3:e10192.
222. Beggs MR, Lee JJ, Busch K, Raza A, Dimke H, Weissgerber P, Engel J, Flockerzi V, Alexander RT. TRPV6 and Cav1.3 Mediate Distal Small Intestine Calcium Absorption Before Weaning. Cell Mol Gastroenterol Hepatol 2019;8:625-642.
223. Yu ASL. Paracellular transport as a strategy for energy conservation by multicellular organisms? Tissue Barriers 2017;5:e1301852.
224. Ong MLDM, Yeruva S, Sailer A, Nilsen SP, Turner JR. Differential regulation of claudin-2 and claudin-15 expression in children and adults with malabsorptive disease. Laboratory Investigation 2020;100:483-490.
225. Günzel D, Stuiver M, Kausalya PJ, Haisch L, Krug SM, Rosenthal R, Meij IC, Hunziker W, Fromm M, Müller D. Claudin-10 exists in six alternatively spliced isoforms that exhibit distinct localization and function. Journal of cell science 2009;122:1507-1517.
226. Cheung QC, Yuan Z, Dyce PW, Wu D, DeLange K, Li J. Generation of epidermal growth factor–expressing Lactococcus lactis and its enhancement on intestinal development and growth of early-weaned mice. The American journal of clinical nutrition 2009;89:871-879.
227. Hu C, Xiao K, Luan Z, Song J. Early weaning increases intestinal permeability, alters expression of cytokine and tight junction proteins, and activates mitogen-activated protein kinases in pigs. Journal of Animal Science 2013;91:1094-1101.
228. Stoutjesdijk E, Schaafsma A, Nhien NV, Khor GL, Kema IP, Hollis BW, Dijck-Brouwer DAJ, Muskiet FAJ. Milk vitamin D in relation to the 'adequate intake' for 0–6-month-old infants: a study in lactating women with different cultural backgrounds, living at different latitudes. British Journal of Nutrition 2017;118:804-812.
229. Kraidith K, Jantarajit W, Teerapornpuntakit J, Nakkrasae L-i, Krishnamra N, Charoenphandhu N. Direct stimulation of the transcellular and paracellular calcium transport in the rat cecum by prolactin. Pflügers Archiv-European Journal of Physiology 2009;458:993-1005.
230. Tanrattana C, Charoenphandhu N, Limlomwongse L, Krishnamra N. Prolactin directly stimulated the solvent drag-induced calcium transport in the duodenum of female rats. Biochimica et Biophysica Acta (BBA)-Biomembranes 2004;1665:81-91.
231. Charoenphandhu N, Limlomwongse L, Krishnamra N. Prolactin directly stimulates transcellular active calcium transport in the duodenum of female rats. Canadian journal of physiology and pharmacology 2001;79:430-438.
232. Vass RA, Kiss G, Bell EF, Roghair RD, Miseta A, Bódis J, Funke S, Ertl T. Breast Milk for Term and Preterm Infants-Own Mother's Milk or Donor Milk? Nutrients 2021;13.
233. Moran JR, Courtney ME, Orth DN, Vaughan R, Coy S, Mount CD, Sherrell BJ, Greene HL. Epidermal growth factor in human milk: Daily production and diurnal variation during early lactation in mothers delivering at term and at premature gestation. The Journal of Pediatrics 1983;103:402-405.

234. Dvorak B, Fituch CC, Williams CS, Hurst NM, Schanler RJ. Increased Epidermal Growth Factor Levels in Human Milk of Mothers with Extremely Premature Infants. Pediatric Research 2003;54:15-19.

235. Commare CE, Tappenden KA. Development of the Infant Intestine: Implications for Nutrition Support. Nutrition in Clinical Practice 2007;22:159-173.

236. Brenza HL, Kimmel-Jehan C, Jehan F, Shinki T, Wakino S, Anazawa H, Suda T, DeLuca HF. Parathyroid hormone activation of the 25-hydroxyvitamin D3-1alpha-hydroxylase gene promoter. Proceedings of the National Academy of Sciences of the United States of America 1998;95:1387-1391.

237. Christakos S, Li S, De La Cruz J, Shroyer NF, Criss ZK, Verzi MP, Fleet JC. Vitamin D and the intestine: Review and update. The Journal of Steroid Biochemistry and Molecular Biology 2020;196:105501.

238. Perrin MT, Belfort MB, Hagadorn JI, McGrath JM, Taylor SN, Tosi LM, Brownell EA. The Nutritional Composition and Energy Content of Donor Human Milk: A Systematic Review. Advances in Nutrition 2020;11:960-970.

239. Wright NC, Looker AC, Saag KG, Curtis JR, Delzell ES, Randall S, Dawson-Hughes B. The recent prevalence of osteoporosis and low bone mass in the United States based on bone mineral density at the femoral neck or lumbar spine. J Bone Miner Res 2014;29:2520-6.

240. Dror DK, Allen LH. Overview of Nutrients in Human Milk. Advances in Nutrition 2018;9:278S-294S.

241. Kent JC, Arthur PG, Mitoulas LR, Hartmann PE. Why calcium in breastmilk is independent of maternal dietary calcium and vitamin D. Breastfeeding review 2009;17:5-11.

242. Neville MC, Keller RP, Casey C, Allen JC. Calcium partitioning in human and bovine milk. Journal of dairy science 1994;77:1964-1975.

243. Hirai C, Ichiba H, Saito M, Shintaku H, Yamano T, Kusuda S. Trophic effect of multiple growth factors in amniotic fluid or human milk on cultured human fetal small intestinal cells. J Pediatr Gastroenterol Nutr 2002;34:524-8.

244. Rowland KJ, Choi PM, Warner BW. The role of growth factors in intestinal regeneration and repair in necrotizing enterocolitis. Seminars in pediatric surgery 2013;22:101-111.

245. Zeissig S, Bürgel N, Günzel D, Richter J, Mankertz J, Wahnschaffe U, Kroesen AJ, Zeitz M, Fromm M, Schulzke JD. Changes in expression and distribution of claudin 2, 5 and 8 lead to discontinuous tight junctions and barrier dysfunction in active Crohn's disease. Gut 2007;56:61-72.

246. Raju P, Shashikanth N, Tsai P-Y, Pongkorpsakol P, Chanez-Paredes S, Steinhagen PR, Kuo W-T, Singh G, Tsukita S, Turner JR. Inactivation of paracellular cation-selective claudin-2 channels attenuates immune-mediated experimental colitis in mice. The Journal of Clinical Investigation 2020;130:5197-5208.

247. Ahmad R, Chaturvedi R, Olivares-Villagómez D, Habib T, Asim M, Shivesh P, Polk D, Wilson KT, Washington MK, Van Kaer L. Targeted colonic claudin-2 expression renders resistance to epithelial injury, induces immune suppression, and protects from colitis. Mucosal immunology 2014;7:1340-1353.

248. Dhawan P, Ahmad R, Chaturvedi R, Smith JJ, Midha R, Mittal MK, Krishnan M, Chen X, Eschrich S, Yeatman TJ, Harris RC, Washington MK, Wilson KT, Beauchamp RD,

Singh AB. Claudin-2 expression increases tumorigenicity of colon cancer cells: role of epidermal growth factor receptor activation. Oncogene 2011;30:3234-3247.

249. Paquet-Fifield S, Koh SL, Cheng L, Beyit LM, Shembrey C, Moelck C, Behrenbruch C, Papin M, Gironella M, Guelfi S. Tight junction protein claudin-2 promotes self-renewal of human colorectal cancer stem-like cells. Cancer research 2018;78:2925-2938.

250. Jiang H, Horst RL, Koszewski NJ, Goff JP, Christakos S, Fleet JC. Targeting 1,25(OH)2D-mediated calcium absorption machinery in proximal colon with calcitriol glycosides and glucuronides. The Journal of Steroid Biochemistry and Molecular Biology 2020;198:105574.

251. Hylander E, Ladefoged K, Jarnum S. The importance of the colon in calcium absorption following small-intestinal resection. Scandinavian journal of gastroenterology 1980;15:55-60.

252. Hylander E, Ladefoged K, Jarnum S. Calcium Absorption after Intestinal Resection: The Importance of a Preserved Colon. Scandinavian Journal of Gastroenterology 1990;25:705-710.

253. Raveschot C, Coutte F, Frémont M, Vaeremans M, Dugersuren J, Demberel S, Drider D, Dhulster P, Flahaut C, Cudennec B. Probiotic Lactobacillus strains from Mongolia improve calcium transport and uptake by intestinal cells in vitro. Food Research International 2020;133:109201.

254. Aufreiter S, Gregory JF, 3rd, Pfeiffer CM, Fazili Z, Kim YI, Marcon N, Kamalaporn P, Pencharz PB, O'Connor DL. Folate is absorbed across the colon of adults: evidence from cecal infusion of (13)C-labeled [6S]-5-formyltetrahydrofolic acid. Am J Clin Nutr 2009;90:116-23.

255. Mineo H, Hara H, Tomita F. Short-chain fatty acids enhance diffusional ca transport in the epithelium of the rat cecum and colon. Life Sci 2001;69:517-26.

256. Borovac J, Barker RS, Rievaj J, Rasmussen A, Pan W, Wevrick R, Alexander RT. Claudin-4 forms a paracellular barrier, revealing the interdependence of claudin expression in the loose epithelial cell culture model opossum kidney cells. Am J Physiol Cell Physiol 2012;303:C1278-91.

257. Pongkorpsakol P., Turner J. R., L. Z. Culture of intestinal epithelial cell monolayers and their use in multiplex macromolecular permeability assays for in vitro analysis of tight junction size selectivity. Current Protocols in Immunology 2020;131:e112.

258. Karbach U, Rummel W. Calcium transport across the colon ascendens and the influence of 1,25-dihydroxyvitamin D3 and dexamethasone. Eur J Clin Invest 1987;17:368-74.

259. Karbach U, Bridges R, Rummel W. The role of the paracellular pathway in the net transport of calcium across the colonic muscosa. Naunyn-Schmiedeberg's archives of pharmacology 1986;334:525-530.

260. Parkman HP, Sharkey E, McCallum RW, Hasler WL, Koch KL, Sarosiek I, Abell TL, Kuo B, Shulman R, Grover M, Farrugia G, Schey R, Tonascia J, Hamilton F, Pasricha PJ. Constipation in Patients with Symptoms of Gastroparesis: Analysis of Symptoms and Gastrointestinal Transit. Clin Gastroenterol Hepatol 2020.

261. Li S, De La Cruz J, Hutchens S, Mukhopadhyay S, Criss ZK, Aita R, Pellon-Cardenas O, Hur J, Soteropoulos P, Husain S, Dhawan P, Verlinden L, Carmeliet G, Fleet JC, Shroyer NF, Verzi MP, Christakos S. Analysis of 1,25-Dihydroxyvitamin D3 Genomic Action Reveals Calcium-Regulating and Calcium-Independent Effects in Mouse Intestine and Human Enteroids. Molecular and Cellular Biology 2020;41:e00372-20.

262. Lee JJ, Liu X, O'Neill D, Beggs MR, Weissgerber P, Flockerzi V, Chen XZ, Dimke H, Alexander RT. Activation of the calcium sensing receptor attenuates TRPV6-dependent intestinal calcium absorption. JCI Insight 2019;5.

263. Wang Y, Song W, Wang J, Wang T, Xiong X, Qi Z, Fu W, Yang X, Chen YG. Single-cell transcriptome analysis reveals differential nutrient absorption functions in human intestine. J Exp Med 2020;217.

264. Kiela PR, Ghishan FK. Physiology of Intestinal Absorption and Secretion. Best Pract Res Clin Gastroenterol 2016;30:145-59.

265. Enck AH, Berger UV, Yu AS. Claudin-2 is selectively expressed in proximal nephron in mouse kidney. Am J Physiol Renal Physiol 2001;281:F966-74.

266. Xing T, Benderman LJ, Sabu S, Parker J, Yang J, Lu Q, Ding L, Chen YH. Tight Junction Protein Claudin-7 Is Essential for Intestinal Epithelial Stem Cell Self-Renewal and Differentiation. Cell Mol Gastroenterol Hepatol 2020;9:641-659.

267. Lieben L, Benn BS, Ajibade D, Stockmans I, Moermans K, Hediger MA, Peng JB, Christakos S, Bouillon R, Carmeliet G. Trpv6 mediates intestinal calcium absorption during calcium restriction and contributes to bone homeostasis. Bone 2010;47:301-308.

268. Chen F, Ni B, Yang YO, Ye T, Chen A. Knockout of TRPV6 causes osteopenia in mice by increasing osteoclastic differentiation and activity. Cell Physiol Biochem 2014;33:796-809.

269. Ma J, Zhu L, Zhou Z, Song T, Yang L, Yan X, Chen A, Ye TW. The calcium channel TRPV6 is a novel regulator of RANKL-induced osteoclastic differentiation and bone absorption activity through the IGF-PI3K-AKT pathway. Cell Prolif 2020:e12955.

270. Alshbool FZ, Mohan S. Emerging multifunctional roles of Claudin tight junction proteins in bone. Endocrinology 2014;155:2363-2376.

271. Wongdee K, Pandaranandaka J, Teerapornpuntakit J, Tudpor K, Thongbunchoo J, Thongon N, Jantarajit W, Krishnamra N, Charoenphandhu N. Osteoblasts express claudins and tight junction-associated proteins. Histochem Cell Biol 2008;130:79-90.

272. Petith MM, Schedl HP. Intestinal adaptation to dietary calcium restriction: in vivo cecal and colonic calcium transport in the rat. Gastroenterology 1976;71:1039-1042.

273. Lee JJ, Liu X, O'Neill D, Beggs MR, Weissgerber P, Flockerzi V, Chen X-Z, Dimke H, Alexander RT. Activation of the calcium sensing receptor attenuates TRPV6-dependent intestinal calcium absorption. JCI insight 2019;5:e128013.

274. Helbock HJ, Forte JG, Saltman P. The mechanism of calcium transport by rat intestine. Biochimica et Biophysica Acta (BBA) - Biophysics including Photosynthesis 1966;126:81-93.

275. Walling MW, Rothman SS. Phosphate-independent, carrier-mediated active transport of calcium by rat intestine. American Journal of Physiology-Legacy Content 1969;217:1144-1148.

276. Krishnamra N, Wirunrattanakij Y, Limlomwongse L. Acute effects of prolactin on passive calcium absorption in the small intestine by in vivo perfusion technique. Canadian journal of physiology and pharmacology 1998;76:161-168.

277. Ghishan FK, Jenkins JT, Younoszai MK. Maturation of calcium transport in the rat small and large intestine. The Journal of nutrition 1980;110:1622-1628.

278. Yamashita S, Mizumoto H, Sawada H, Suzuki Y, Hata D. TRPV6 Gene Mutation in a Dizygous Twin With Transient Neonatal Hyperparathyroidism. Journal of the Endocrine Society 2019;3:602-606.

279. Nett V, Erhardt N, Wyatt A, Wissenbach U. Human TRPV6-pathies caused by gene mutations. Biochimica et Biophysica Acta (BBA) - General Subjects 2021;1865:129873.

280. Mittermeier L, Demirkhanyan L, Stadlbauer B, Breit A, Recordati C, Hilgendorff A, Matsushita M, Braun A, Simmons DG, Zakharian E, Gudermann T, Chubanov V. TRPM7 is the central gatekeeper of intestinal mineral absorption essential for postnatal survival. Proc Natl Acad Sci U S A 2019;116:4706-4715.

281. de Baaij JH, Hoenderop JG, Bindels RJ. Magnesium in man: implications for health and disease. Physiol Rev 2015;95:1-46.

282. Furuse M, Fujita K, Hiiragi T, Fujimoto K, Tsukita S. Claudin-1 and -2: novel integral membrane proteins localizing at tight junctions with no sequence similarity to occludin. J Cell Biol 1998;141:1539-50.

283. Asowata EO, Olusanya O, Abaakil K, Chichger H, Srai SKS, Unwin RJ, Marks J. Diet-induced iron deficiency in rats impacts small intestinal calcium and phosphate absorption. Acta Physiol (Oxf) 2021:e13650.

284. Dawson-Hughes B, Harris SS, Finneran S. Calcium absorption on high and low calcium intakes in relation to vitamin D receptor genotype. J Clin Endocrinol Metab 1995;80:3657-61.

285. Cooper GS, Umbach DM. Are vitamin D receptor polymorphisms associated with bone mineral density? A meta-analysis. J Bone Miner Res 1996;11:1841-9.

286. Ladefoged K, Nicolaidou P, Jarnum S. Calcium, phosphorus, magnesium, zinc, and nitrogen balance in patients with severe short bowel syndrome. The American Journal of Clinical Nutrition 1980;33:2137-2144.

287. Gouttebel MC, Saint Aubert B Fau - Colette C, Colette C Fau - Astre C, Astre C Fau - Monnier LH, Monnier Lh Fau - Joyeux H, Joyeux H. Intestinal adaptation in patients with short bowel syndrome. Measurement by calcium absorption.

288. Ladefoged K. Intestinal and renal loss of infused minerals in patients with severe short bowel syndrome. The American Journal of Clinical Nutrition 1982;36:59-67.

289. Yeh JK, Aloia JF. Influence of Glucocorticoids on Calcium Absorption in Different Segments of the Rat Intestine. Calcified Tissue International 1986;38:282-288.

290. Favus MJ, Langman CB. Effects of 1,25-dihydroxyvitamin D3 on colonic calcium transport in vitamin D-deficient and normal rats. Am J Physiol 1984;246:G268-73.

291. Hendrix ZJ, Alcock NW, Archibald RM. COMPETITION BETWEEN CALCIUM, STRONTIUM, AND MAGNESIUM FOR ABSORPTION IN THE ISOLATED RAT INTESTINE. Clin Chem 1963;12:734-44.

292. Harrison HC, Harrison HE. Calcium transport by rat colon in vitro. Am J Physiol 1969;217:121-5.

293. Bogdal J, Jedrychowski A, Tarnawski A, Dura K, Marszalek Z. Effect of glucagon and radiocalcium excretion by the colon in rats after intracardial administration of 45Ca. Can J Physiol Pharmacol 1974;52:1230-2.

294. Petith MM, Wilson HD, Schedl HP. Vitamin D dependence of in vivo calcium transport and mucosal calcium binding protein in rat large intestine. Gastroenterology 1979;76:99-104.

295. Favus MJ, Kathpalia SC, Coe FL. Kinetic characteristics of calcium absorption and secretion by rat colon. AMERICAN JOURNAL OF PHYSIOLOGY-GASTROINTESTINAL AND LIVER PHYSIOLOGY 1981;240:G350-G354.

296. Favus MJ, Kathpalia SC, Coe FL, Mond AE. Effects of diet calcium and 1, 25-dihydroxyvitamin D3 on colon calcium active transport. AMERICAN JOURNAL OF PHYSIOLOGY-GASTROINTESTINAL AND LIVER PHYSIOLOGY 1980;238:G75-G78.

297. Lee DB, Walling MW, Gafter U, Silis V, Coburn JW. Calcium and inorganic phosphate transport in rat colon: dissociated response to 1,25-dihydroxyvitamin D3. J Clin Invest 1980;65:1326-31.

298. Weber CR, Liang GH, Wang Y, Das S, Shen L, Alan S, Nelson DJ, Turner JR. Claudin-2-dependent paracellular channels are dynamically gated. Elife 2015;4:e09906.

299. Reyes-Fernandez PC, Fleet JC. Compensatory Changes in Calcium Metabolism Accompany the Loss of Vitamin D Receptor (VDR) From the Distal Intestine and Kidney of Mice. J Bone Miner Res 2016;31:143-51.

300. Nygaard L, Skallerup A, Olesen SS, Køhler M, Vinter-Jensen L, Kruse C, Vestergaard P, Rasmussen HH. Osteoporosis in patients with intestinal insufficiency and intestinal failure: prevalence and clinical risk factors. Clinical Nutrition 2018;37:1654-1660.

301. Balk EM, Adam GP, Langberg VN, Earley A, Clark P, Ebeling PR, Mithal A, Rizzoli R, Zerbini CAF, Pierroz DD, Dawson-Hughes B, International Osteoporosis Foundation Calcium Steering C. Global dietary calcium intake among adults: a systematic review. Osteoporosis international : a journal established as result of cooperation between the European Foundation for Osteoporosis and the National Osteoporosis Foundation of the USA 2017;28:3315-3324.

302. Fischer LM, da Costa KA, Galanko J, Sha W, Stephenson B, Vick J, Zeisel SH. Choline intake and genetic polymorphisms influence choline metabolite concentrations in human breast milk and plasma. The American journal of clinical nutrition 2010;92:336-346.

303. Weaver CM, Alexander DD, Boushey CJ, Dawson-Hughes B, Lappe JM, LeBoff MS, Liu S, Looker AC, Wallace TC, Wang DD. Calcium plus vitamin D supplementation and risk of fractures: an updated meta-analysis from the National Osteoporosis Foundation. Osteoporos Int 2016;27:367-76.

304. Li XT, Li XQ, Hu XM, Qiu XY. The Inhibitory Effects of Ca2+ Channel Blocker Nifedipine on Rat Kv2.1 Potassium Channels. PLoS One 2015;10:e0124602.

305. Parra-Llorca A, Gormaz M, Lorente-Pozo S, Cernada M, García-Robles A, Torres-Cuevas I, Kuligoswki J, Collado MC, Serna E, Vento M. Impact of Donor Human Milk in the Preterm Very Low Birth Weight Gut Transcriptome Profile by Use of Exfoliated Intestinal Cells. Nutrients 2019;11:2677.

306. Curry JN, Tokuda S, McAnulty P, Yu AS. Combinatorial expression of claudins in the proximal renal tubule and its functional consequences. American Journal of Physiology-Renal Physiology 2020;318:F1138-F1146.

307. Milatz S, Himmerkus N, Wulfmeyer VC, Drewell H, Mutig K, Hou J, Breiderhoff T, Müller D, Fromm M, Bleich M, Günzel D. Mosaic expression of claudins in thick ascending limbs of Henle results in spatial separation of paracellular Na$^+$ and Mg^{2+} transport. Proceedings of the National Academy of Sciences 2017;114:E219.

308. Drozdowski LA, Clandinin T, Thomson ABR. Ontogeny, growth and development of the small intestine: Understanding pediatric gastroenterology. World journal of gastroenterology 2010;16:787-799.

309. Guilloteau P, Zabielski R, Hammon HM, Metges CC. Nutritional programming of gastrointestinal tract development. Is the pig a good model for man? Nutr Res Rev 2010;23:4-22.

310. Stanford AH, Gong H, Noonan M, Lewis AN, Gong Q, Lanik WE, Hsieh JJ, Lueschow SR, Frey MR, Good M, McElroy SJ. A direct comparison of mouse and human intestinal development using epithelial gene expression patterns. Pediatric Research 2020;88:66-76.

311. Kaji I. Dynamics of Intestinal Calcium Absorption in Neonates. Cellular and Molecular Gastroenterology and Hepatology 2019;8:647-648.

Chapter 7

Appendix

7.1. Appendix A

2 week and 2-month mice demonstrate net Calcium flux from the colon

We examined expression of genes mediated transcellular calcium absorption across the proximal colon in mice from P7 – 6 months old. We found significantly greater expression of *Trpv6* and *S100g* prior to weaning. Thus, we hypothesized that mice prior to weaning would have greater net transcellular absorption across the proximal colon. We measured net J_{Ca} across proximal colon in mice at P14 and 2 months. A net positive apical to basolateral Ca^{2+} absorption was observed at both ages. However, no difference was observed between ages. Previous work has identified TRPV6 as the apical entry channel for Ca^{2+} in mice at 3 months. We therefore interrogated this pathway at P14 by measuring net J_{Ca} in WT and *Trpv6*^{mt} mice. No difference was observed between the genotypes suggesting that TRPV6 does not mediate this pathway. Our previous work has demonstrated transcellular absorption via an apical L-type calcium channel across the ileum at P14. We therefore repeated the net J_{Ca} studies in WT and Trpv6mt at P14 without and then with the addition of apical nifedipine, an L-type calcium channel blocker. No change in net flux was observed with the addition of the blocker suggesting that an L-type calcium channel does not facilitate apical entry of calcium into the cell. Data shown in Figure 7.1.

2-week-old mice demonstrate increased colonic paracellular permeability, that is not mediated by claudin-2 or claudin-12

We next aimed to determine if younger mice would display greater absorptive capacity across the colon via the paracellular pathway. Indeed, P_{Ca} was 20% greater in mice at P14 compared to those at 2 months. Claudin-2, -12, and -15 have been implicated as forming cation permeable pores across intestinal epithelia. We, therefore, assessed expression of these genes from P7 to 6 months in mice. Expression was significantly greater after weaning for all the genes compared to prior to weaning. Claudin-2 and -12 have been implicated as forming Ca^{2+} permeable pores. We therefore sought to determine if these claudins would confer P_{Ca} across the colon at P14 or 2 months. In mice at P14, we did not observe a difference in P_{Ca} between *Cldn2* KO or *Cldn12* KO compared to WT littermates. This suggests that these claudins do not confer P_{Ca} across the colon at this age. Data shown in Figure 7.2.
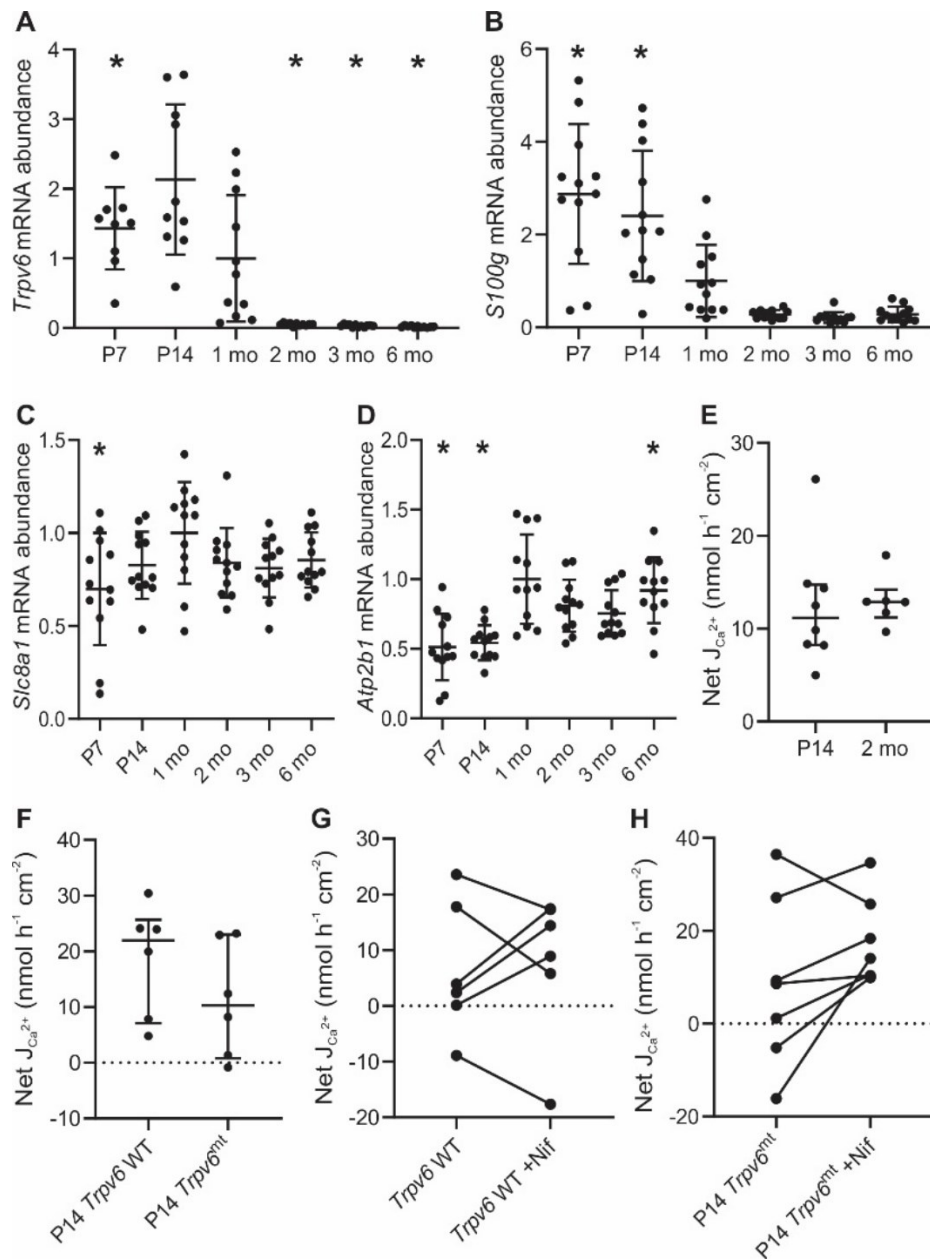
Figure 7.1. Net transcellular calcium flux across the proximal colon in mice at P14 and 2 months. mRNA abundance of A) *Trpv6*, B) *S100g*, C) *Slc8a1*, and D) *Atp2b1* from colon of mice aged P7 to 6 months. Data presented as individual mice with mean ± SD. *$P < 0.05$ compared to 1 mo group by one-way ANOVA. Net apical to basolateral transcellular flux across colon in E) wildtype mice at P14 and 2 months, F) *Trpv6* WT and mutant mice at P14, G) *Trpv6* WT mice without or with nifedipine, and H) *Trpv6* WT mice without or with nifedipine. Data presented as individual mice with mean ± SD or median ± IQR as appropriate. Data compared by t-test or Mann-Whitney test as appropriate.
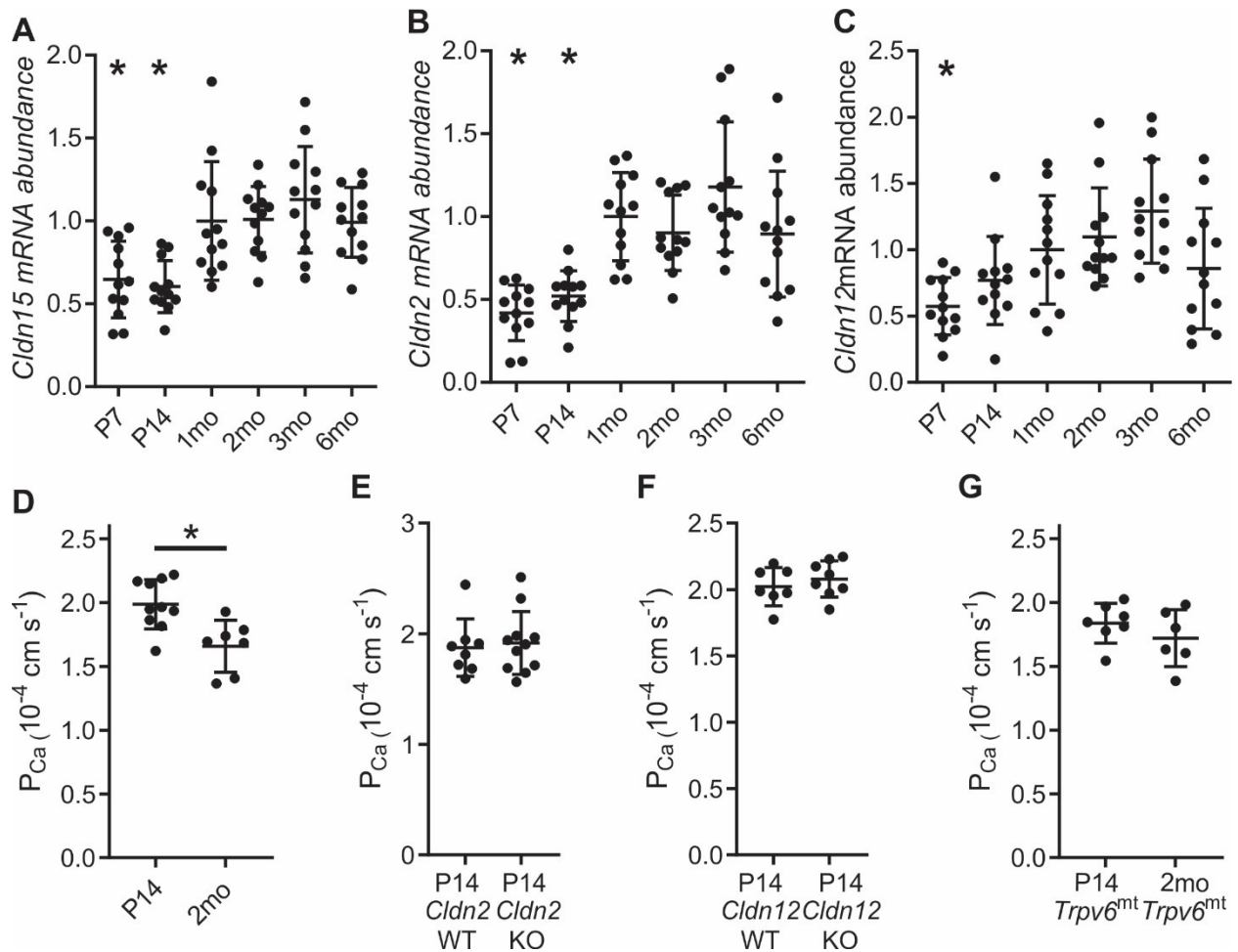
Figure 7.2. Calcium permeability across the proximal colon in mice at P14 and 2 months.
mRNA abundance of A) *Cldn15*, B) *Cldn2*, C) *Cldn12* from colon of mice aged P7 to 6 months.
Data presented as individual mice with mean ± SD. *$P < 0.05$ compared to 1 mo group by one-
way ANOVA. Permeability to calcium across colon in D) wildtype mice at P14 and 2 months, E)
WT and *Cldn2* KO mice at P14, F) WT and *Cldn12* KO mice at P14, G) *Trpv6^mt* mice at P14 and
2 months. Data presented as individual mice with mean ± SD. Data compared by t-test, *$P <$
0.05.